

Journal of SciTech-ASEAN

ISSN 3088-2575 (ONLINE)

Volume 6 Number 2 (July – December 2026)

เจ้าของ	คณะศิลปศาสตร์และวิทยาศาสตร์ มหาวิทยาลัยราชภัฏศรีสะเกษ	
บรรณาธิการ	รองศาสตราจารย์ ดร.เตชภณ ทองเติม	คณะศิลปศาสตร์และวิทยาศาสตร์ มหาวิทยาลัยราชภัฏศรีสะเกษ
กองบรรณาธิการ	รองศาสตราจารย์ ดร.พัชรวรรณ สิทธิศาสตร์	คณะศิลปศาสตร์และวิทยาศาสตร์
	รองศาสตราจารย์ ดร.สิริพร ยศแสน	คณะศิลปศาสตร์และวิทยาศาสตร์
	ผู้ช่วยศาสตราจารย์ ดร.กนิษฐา อินธิชิต	คณะศิลปศาสตร์และวิทยาศาสตร์
	ผู้ช่วยศาสตราจารย์ ดร.จิรนันต์ รัตสีวอ	คณะศิลปศาสตร์และวิทยาศาสตร์
	ผู้ช่วยศาสตราจารย์ ดร.กนกกาญจน์ จิรศิริเลิศ	คณะศิลปศาสตร์และวิทยาศาสตร์
	ผู้ช่วยศาสตราจารย์ ดร.ทัย กาบบัว	คณะศิลปศาสตร์และวิทยาศาสตร์
	ผู้ช่วยศาสตราจารย์ ทิพย์สุดา กุมผัน	คณะศิลปศาสตร์และวิทยาศาสตร์
	อาจารย์ ดร.ภาคภูมิ ชินพฤทธิวงศ์	คณะศิลปศาสตร์และวิทยาศาสตร์
	นางอำพร ไรกลาง	คณะศิลปศาสตร์และวิทยาศาสตร์ มหาวิทยาลัยราชภัฏศรีสะเกษ
รายนามผู้ทรงคุณวุฒิประจำฉบับ	รองศาสตราจารย์ ดร.ถนัดกิจ ศรีโชค	มหาวิทยาลัยอุบลราชธานี
	รองศาสตราจารย์ ดร.เฉลิมชาติ ธีระวิริยะ	มหาวิทยาลัยนครพนม
	รองศาสตราจารย์ ดร.ชัยยุทธ มีงาม	มหาวิทยาลัยราชภัฏสงขลา
	รองศาสตราจารย์ ดร.ไชยวัฒน์ นามบุญลือ	มหาวิทยาลัยราชภัฏอุบลราชธานี
	รองศาสตราจารย์ ดร.ยรรยงค์ พานเพ็ง	มหาวิทยาลัยราชภัฏเลย
	รองศาสตราจารย์ ดร.พัชรวรรณ สิทธิศาสตร์	มหาวิทยาลัยราชภัฏศรีสะเกษ
	รองศาสตราจารย์ ดร.วรพจน์ ศิริรักษ์	มหาวิทยาลัยเทคโนโลยีราชมงคลล้านนา เชียงราย
	รองศาสตราจารย์ ดร.นิรุตติ์ สุขดี	มหาวิทยาลัยการกีฬาแห่งชาติ วิทยาเขตอุดรธานี
	ผู้ช่วยศาสตราจารย์ ดร.วิวัฒน์ เหล่าชัย	จุฬาลงกรณ์มหาวิทยาลัย
	ผู้ช่วยศาสตราจารย์ ดร.นวดนย์ คุณเลิศกิจ	มหาวิทยาลัยเชียงใหม่
	ผู้ช่วยศาสตราจารย์ ดร.ศศิน จันทร์พวงทอง	มหาวิทยาลัยเชียงใหม่
	ผู้ช่วยศาสตราจารย์ ดร.สันติ โพธิ์ศรี	มหาวิทยาลัยบูรพา
	ผู้ช่วยศาสตราจารย์ ดร.อารีรัตน์ เจียมประเสริฐบุญ	มหาวิทยาลัยวลัยลักษณ์
	ผู้ช่วยศาสตราจารย์ ดร.รัชชานันท์ ศรีสุภักดิ์	มหาวิทยาลัยราชภัฏมหาสารคาม
	ผู้ช่วยศาสตราจารย์ ดร.จิตตะวัน กุโบลา	มหาวิทยาลัยราชภับุรีรัมย์
	ผู้ช่วยศาสตราจารย์ ดร.วีรศักดิ์ ฟองเงิน	มหาวิทยาลัยราชภัฏลำปาง
	ผู้ช่วยศาสตราจารย์ ดร.จุฑามาศ แก้วจันดี	มหาวิทยาลัยราชภัฏศรีสะเกษ
	ผู้ช่วยศาสตราจารย์ ดร.เจษฎา โพนแก้ว	มหาวิทยาลัยราชภัฏศรีสะเกษ
	ผู้ช่วยศาสตราจารย์ ดร.ทัย กาบบัว	มหาวิทยาลัยราชภัฏศรีสะเกษ
	ผู้ช่วยศาสตราจารย์ ดร.ไมยรา เศรษฐมาศ	มหาวิทยาลัยราชภัฏศรีสะเกษ
	ผู้ช่วยศาสตราจารย์ ดร.ศุภัคษร มาแสวง	มหาวิทยาลัยเทคโนโลยีราชมงคลพระนคร ศูนย์เทเวศร์
	ผู้ช่วยศาสตราจารย์ ดร.รุ่งวสันต์ ไกรกลาง	มหาวิทยาลัยเทคโนโลยีราชมงคลอีสาน นครราชสีมา
	ผู้ช่วยศาสตราจารย์ ดร.จิรายุส วรรัตน์โภคา	มหาวิทยาลัยเทคโนโลยีราชมงคลอีสาน นครราชสีมา
	ผู้ช่วยศาสตราจารย์จิรายุ มุสิกา	มหาวิทยาลัยอุบลราชธานี
	ผู้ช่วยศาสตราจารย์กษิรา นิติธนนันต์	มหาวิทยาลัยราชภัฏกาญจนบุรี
	ผู้ช่วยศาสตราจารย์รัชนี จูมจี	มหาวิทยาลัยราชภัฏอุบลราชธานี
	ผู้ช่วยศาสตราจารย์พิศาล สุขขี	มหาวิทยาลัยราชภัฏศรีสะเกษ
	อาจารย์ ดร.กัญจน์ จันทร์ศรีสุคต	มหาวิทยาลัยแม่โจ้

อาจารย์ ดร.จีรนันท์ แก้วมา	มหาวิทยาลัยศรีนครินทรวิโรฒ
อาจารย์ ดร.ณัฐวุฒิ โอสระคู	มหาวิทยาลัยเทคโนโลยีสุรนารี
อาจารย์ ดร.ฐาปนวัฒน์ สุขปาละ	มหาวิทยาลัยราชภัฏสงขลา
อาจารย์ ดร.ณพรรธนนท์ ทองปาน	มหาวิทยาลัยราชภัฏมหาสารคาม
อาจารย์ ดร.เบญจวรรณ ดุนขุนทด	มหาวิทยาลัยราชภัฏเพชรบุรี
อาจารย์ ดร.พีรศุษย์ บุญมาธรรม	มหาวิทยาลัยราชภัฏเพชรบุรี
อาจารย์ ดร.ไอยย์ศรัย พีรภาพรกุล	มหาวิทยาลัยราชภัฏจันทรเกษม
อาจารย์ ดร.มัสติกา เรืองอุดมสกุล	มหาวิทยาลัยราชภัฏศรีสะเกษ
อาจารย์ ดร.วิพา ชุปวา	มหาวิทยาลัยราชภัฏศรีสะเกษ
อาจารย์ ดร.กิติยา สุเหม	มหาวิทยาลัยราชมงคลรัตนโกสินทร์
อาจารย์ ดร.หทัยรัตน์ หอมไกรลาส	มหาวิทยาลัยเทคโนโลยีราชมงคลวิทยาเขตสกลนคร

วัตถุประสงค์

Journal of SciTech-ASEAN (JSTA) มีวัตถุประสงค์เพื่อเป็นพื้นที่ทางวิชาการสำหรับเผยแพร่บทความวิจัยและบทความวิชาการคุณภาพสูงด้านวิทยาศาสตร์ประยุกต์ เทคโนโลยี และนวัตกรรม ที่มีฐานคิดทางวิชาการชัดเจน มีความเข้มแข็งด้านระเบียบวิธีวิจัยหรือการวิเคราะห์เชิงวิชาการ มีความใหม่หรือคุณูปการต่อองค์ความรู้ และสามารถนำไปใช้ประโยชน์ในการแก้ปัญหาเชิงปฏิบัติหรือสนับสนุนการพัฒนาในบริบทของประเทศไทยและภูมิภาคอาเซียน โดยครอบคลุมประเด็นด้านสุขภาพ สุขภาวะ และสมรรถนะมนุษย์ เทคโนโลยีดิจิทัลและระบบอัจฉริยะ เกษตร อาหาร สิ่งแวดล้อม และทรัพยากรชีวภาพ อุตสาหกรรม โลจิสติกส์ และวิศวกรรมประยุกต์ ตลอดจนการบูรณาการวิทยาศาสตร์และเทคโนโลยีเพื่อการพัฒนาชุมชนท้องถิ่นอย่างยั่งยืน

ขอบเขตการรับบทความ

Journal of SciTech-ASEAN (JSTA) รับพิจารณาบทความวิจัยและบทความวิชาการด้านวิทยาศาสตร์ประยุกต์ เทคโนโลยี และนวัตกรรม โดยมีขอบเขตครอบคลุมประเด็นหลัก ดังนี้

1) สุขภาพ สุขภาวะ และสมรรถนะมนุษย์ ครอบคลุมวิทยาศาสตร์สุขภาพ สาธารณสุข อาชีวอนามัยและความปลอดภัย วิทยาศาสตร์การกีฬา กิจกรรมทางกาย นันทนาการ สังคมสูงวัย สุขภาพชุมชน และคุณภาพชีวิต

2) เทคโนโลยีดิจิทัลและระบบอัจฉริยะ ครอบคลุมปัญญาประดิษฐ์ วิทยาการข้อมูล ระบบสารสนเทศ การพัฒนาซอฟต์แวร์ อินเทอร์เน็ตของสรรพสิ่ง บล็อกเชน แบบจำลองเชิงคำนวณ และระบบสนับสนุนการตัดสินใจ

3) เกษตร อาหาร สิ่งแวดล้อม และทรัพยากรชีวภาพ ครอบคลุมวิทยาศาสตร์และเทคโนโลยีการเกษตร วิทยาศาสตร์และเทคโนโลยีการอาหาร ทรัพยากรชีวภาพ สารออกฤทธิ์ทางชีวภาพ วิทยาศาสตร์สิ่งแวดล้อม การจัดการทรัพยากร การควบคุมมลพิษ และระบบการผลิตที่ยั่งยืน

4) อุตสาหกรรม โลจิสติกส์ และวิศวกรรมประยุกต์ ครอบคลุมเทคโนโลยีอุตสาหกรรม วิศวกรรมประยุกต์ การออกแบบและพัฒนาผลิตภัณฑ์ การปรับปรุงกระบวนการ ระบบการผลิต ระบบคุณภาพ ความปลอดภัยในงานอุตสาหกรรม โลจิสติกส์ ห่วงโซ่อุปทาน การขนส่ง และการจัดการการดำเนินงาน

5) การบูรณาการวิทยาศาสตร์และเทคโนโลยีเพื่อการพัฒนาชุมชนท้องถิ่น ครอบคลุมงานวิจัยและบทความวิชาการที่ประยุกต์ใช้วิทยาศาสตร์ เทคโนโลยี หรือนวัตกรรมในการแก้ปัญหาเชิงพื้นที่ การยกระดับคุณภาพชีวิต การเพิ่มมูลค่าทรัพยากรท้องถิ่น การพัฒนาระบบบริการ หรือการส่งเสริมความยั่งยืนของชุมชน โดยต้องมีฐานคิด วิธีการศึกษา หรือหลักฐานเชิงวิชาการที่ชัดเจน

นโยบายการใช้เทคโนโลยีปัญญาประดิษฐ์ (AI)

Journal of SciTech-ASEAN (JSTA) อนุญาตให้ผู้เขียนใช้เครื่องมือปัญญาประดิษฐ์หรือเทคโนโลยีที่มีปัญญาประดิษฐ์ช่วยสนับสนุนในการเตรียมต้นฉบับได้อย่างเหมาะสม เช่น การตรวจสอบภาษา การปรับปรุงความชัดเจนของข้อความ การแปลเบื้องต้น การจัดโครงสร้างเนื้อหา หรือการสนับสนุนการวิเคราะห์ข้อมูล ทั้งนี้ เครื่องมือปัญญาประดิษฐ์ไม่สามารถระบุเป็นผู้แต่งหรือผู้มีส่วนร่วมในบทความได้ และผู้เขียนต้องรับผิดชอบต่อความถูกต้อง ความน่าเชื่อถือ ความเป็นต้นฉบับ จริยธรรมการวิจัย และเนื้อหาทางวิชาการทั้งหมดของบทความ

ผู้เขียนที่ใช้เครื่องมือปัญญาประดิษฐ์ในการเตรียมต้นฉบับต้องเปิดเผยการใช้งานอย่างชัดเจน โดยระบุชื่อเครื่องมือ วัตถุประสงค์ และขอบเขตของการใช้ในต้นฉบับ วารสารไม่อนุญาตให้ใช้ปัญญาประดิษฐ์เพื่อสร้างข้อมูล ผลการวิจัย ภาพ ตาราง หรือเอกสารอ้างอิงที่ไม่มีอยู่จริง บิดเบือนข้อมูล คัดลอกผลงานผู้อื่น หรือแทนที่การวิเคราะห์และการตัดสินใจทางวิชาการของผู้เขียน หากพบการใช้ปัญญาประดิษฐ์โดยไม่เปิดเผยหรือใช้ในลักษณะที่กระทบต่อความถูกต้องและจริยธรรมการตีพิมพ์ วารสารอาจพิจารณาปฏิเสธบทความหรือดำเนินการตามหลักจริยธรรมการตีพิมพ์ทางวิชาการ

ลิขสิทธิ์

กองบรรณาธิการวารสาร จะไม่รับพิจารณาบทความที่เป็นการละเมิดลิขสิทธิ์ ในกรณีที่มีการละเมิดลิขสิทธิ์ขึ้น ทางผู้เขียนเป็นผู้รับผิดชอบแต่เพียงฝ่ายเดียว

หมายเหตุ

วารสารเผยแพร่ทุก 6 เดือน (ฉบับต้นปี มกราคม - มิถุนายน และฉบับปลายปี กรกฎาคม - ธันวาคม ของทุกปี) บทความที่ตีพิมพ์ในวารสารเป็นทัศนะ ลิขสิทธิ์ และความรับผิดชอบของผู้เขียนเจ้าของผลงาน

บทบรรณาธิการ

Journal of SciTech-ASEAN (JSTA) ปีที่ 6 ฉบับที่ 2 (กรกฎาคม–ธันวาคม 2569) เป็นฉบับส่งท้ายปีที่นำเสนอบทความวิจัยจำนวน 15 เรื่อง โดยเผยแพร่พร้อมรหัสบทความ (Article Number) เพื่อความสะดวกในการสืบค้นและอ้างอิง ผลงานในฉบับนี้ครอบคลุมองค์ความรู้ด้านวิทยาศาสตร์สุขภาพและสมรรถภาพทางกาย เทคโนโลยีดิจิทัลและอินเทอร์เน็ตของสรรพสิ่ง สิ่งแวดล้อม เกษตรและอาหาร ตลอดจนการจัดการอุตสาหกรรมและการพัฒนาชุมชน แม้แต่ละเรื่องจะมีประเด็นศึกษาและวิธีดำเนินการที่แตกต่างกัน แต่ล้วนสะท้อนความสำคัญของการนำองค์ความรู้ทางวิทยาศาสตร์และเทคโนโลยีมาใช้ในการศึกษาปัญหา พัฒนากระบวนการทำงาน และแสวงหาแนวทางที่เป็นประโยชน์ต่อสังคม ความหลากหลายดังกล่าวสอดคล้องกับเจตนารมณ์ของวารสารที่มุ่งเป็นพื้นที่เผยแพร่และแลกเปลี่ยนองค์ความรู้ข้ามศาสตร์ เพื่อสนับสนุนการพัฒนาประเทศไทยและภูมิภาคอาเซียนอย่างต่อเนื่อง

การพัฒนาคุณภาพวารสารวิชาการในปัจจุบันมิได้พิจารณาเพียงคุณภาพของบทความที่ตีพิมพ์เท่านั้น แต่ยังให้ความสำคัญกับความโปร่งใส ความรับผิดชอบ และมาตรฐานของกระบวนการเผยแพร่ผลงานทางวิชาการ ดังสะท้อนจากการอบรมหลักสูตร TCI Editor Training Program A2: Professional Level ซึ่งจัดโดยศูนย์ดัชนีการอ้างอิงวารสารไทย (TCI) ในระหว่างวันที่ 29–30 ตุลาคม 2569 โดยมีประเด็นสำคัญเกี่ยวกับการจัดการแก้ไขและถอนบทความ การระบุบทบาทของผู้นิพนธ์ การกำหนดนโยบายการใช้ปัญญาประดิษฐ์เชิงสร้างสรรค์อย่างรับผิดชอบ ตลอดจนการใช้ DOI และรหัสบทความให้สอดคล้องกับมาตรฐานการเผยแพร่ในระดับสากล ประเด็นเหล่านี้มิใช่เพียงข้อกำหนดที่วารสารควรประกาศไว้ แต่ต้องนำไปสู่แนวปฏิบัติที่ชัดเจนและตรวจสอบได้ กองบรรณาธิการ JSTA จึงมุ่งทบทวนและพัฒนาการดำเนินงานให้สอดคล้องกับแนวทางดังกล่าว ควบคู่กับการรักษามาตรฐานการประเมินบทความแบบผู้ประเมินและผู้นิพนธ์ไม่ทราบชื่อกันและกัน (Double-blind peer review) โดยผู้ทรงคุณวุฒิจำนวน 3 ท่านต่อบทความ เพื่อธำรงคุณภาพของวารสารในฐานข้อมูล TCI กลุ่มที่ 1 และวางรากฐานสำหรับการพัฒนาสู่มาตรฐานนานาชาติในระยะต่อไป

ในโอกาสส่งท้ายปีพุทธศักราช 2569 และต้อนรับปีใหม่ 2570 ข้าพเจ้าขอถือโอกาสนี้แจ้งการเปลี่ยนผ่านหน้าที่บรรณาธิการวารสาร โดยจะส่งมอบหน้าที่ให้แก่ ผู้ช่วยศาสตราจารย์ ดร.กนิษฐา อินธิชิต ตั้งแต่วันที่ 1 มกราคม พ.ศ. 2570 เป็นต้นไป เพื่อให้ข้าพเจ้าได้มุ่งพัฒนางานวิชาการในด้านอื่น ๆ ต่อไป ทั้งนี้ ผู้ช่วยศาสตราจารย์ ดร.กนิษฐา อินธิชิต ได้มีส่วนร่วมในการดำเนินงานของวารสารในฐานะกองบรรณาธิการมาอย่างต่อเนื่อง ข้าพเจ้าจึงเชื่อมั่นว่าการเปลี่ยนผ่านครั้งนี้จะเป็นไปอย่างราบรื่น สามารถรักษามาตรฐานทางวิชาการที่วารสารยึดถือมาโดยตลอด และต่อยอดการพัฒนาวารสารให้ก้าวสู่ระดับนานาชาติได้อย่างมั่นคง ตลอดระยะเวลาที่ปฏิบัติหน้าที่บรรณาธิการ ข้าพเจ้าขอขอบคุณผู้นิพนธ์ที่ไว้วางใจส่งผลงานมายังวารสาร ผู้ทรงคุณวุฒิที่สละเวลาและความเชี่ยวชาญในการประเมินบทความ ตลอดจนกองบรรณาธิการและผู้มีส่วนเกี่ยวข้องทุกฝ่ายที่ร่วมกันขับเคลื่อนวารสารด้วยดีเสมอมา ท้ายที่สุดนี้ ขอส่งความปรารถนาดีเนื่องในวาระดิถีขึ้นปีใหม่พุทธศักราช 2570 ให้ทุกท่านมีสุขภาพแข็งแรง ประสบความสุข ความสำเร็จ และความก้าวหน้าในการดำเนินชีวิตและการทำงานทางวิชาการตลอดปีและตลอดไป



(ผู้ช่วยศาสตราจารย์ ดร.เตชภณ ทองเติม)
บรรณาธิการวารสาร

สารบัญ

	รหัสบทความ
ผลของการนวดแบบมวยไทย การยืดเหยียดกล้ามเนื้อ และการนั่งพักที่มีต่อการฟื้นสภาพของอัตราการเต้นของหัวใจ ความแข็งแรงของขา และความอ่อนตัวในนักกีฬาเชปักตะกร้อชายมหาวิทยาลัยราชภัฏสุรินทร์ ภัทรพล ทองนำ	e262001
ปัจจัยที่มีความสัมพันธ์กับความสุขและการเตรียมความพร้อมเข้าสู่วัยสูงอายุของบุคคลที่มีความหลากหลายทางเพศในชุมชนชนบท เตชภณ ทองเติม และจีรนันท์ แก้วมา	e262002
การกำกับติดตามการบังคับใช้กฎหมายสิ่งแวดล้อมทางทะเล กรณีน้ำมันรั่วไหลจากเรือเดินสมุทรในท่าเรือหลักของไทย สิรภูมิ กระต่ายทอง นันท์นภัสร อินยิ้ม เสรีย์ ตู้ประกาย และปิยะรัตน์ ปรีย์มาโนช	e262003
ผลของการออกกำลังกายด้วย TRX แบบหนักสลับเบาความเข้มข้นสูงที่มีผลต่อองค์ประกอบของร่างกาย พลังของกล้ามเนื้อ และความแข็งแรงของกล้ามเนื้อในนักศึกษา เศวตฉัตร วันนา ธีร์ธานิศ พันธ์นิกุล และช่อนภา สิทธิ์ธัง	e262004
การพัฒนารูปแบบการพยาบาลผู้ป่วยผ่าตัดหัวใจแบบเปิดโดยใช้กรอบแนวคิด ASPIRE โรงพยาบาลศรีสะเกษ ธันยมัย ปุรินัย และจันทร์ทิรา เจียรณัย	e262005
การพัฒนาระบบตรวจวัดคุณภาพอากาศและแจ้งเตือนฝุ่น PM2.5 แบบเรียลไทม์โดยประยุกต์ใช้เทคโนโลยีอินเทอร์เน็ตของสรรพสิ่ง สุกัญชลิกา บุญมาธรรม พีรศุษย์ บุญมาธรรม ปราโมทย์ ตงฉิน และศิริพร อ่วมศิริ	e262006
ผลของการฝึกความเร็วอดทนโดยใช้แรงต้านแบบยางยืดเปรียบเทียบกับการฝึกแบบการวิ่งต่อสมรรถภาพแอโรบิกและแอนแอโรบิกในนักกีฬาฟุตซอลเยาวชน ธนัมพร ทองลอง สุทธิรักษ์ นาโสม สุภาวดี กสิกรรม อิศวรา จันทร์สมคอย และวารุณี กิจรักษา	e262007
การพัฒนาและประเมินประสิทธิภาพระบบเฝ้าระวังดัชนีความร้อนและแจ้งเตือนแบบเรียลไทมด้วยเทคโนโลยีอินเทอร์เน็ตของสรรพสิ่งสำหรับการฝึกทหาร: กรณีศึกษากองพันทหารสื่อสาร กรมการสื่อสารทหาร กองบัญชาการกองทัพไทย อติกานต์ ม่วงเงิน นัฐพงศ์ ส่งเนียม และอชิตะ พ่วงตรง	e262008
การพัฒนากระบวนการวางแผนการขายและการดำเนินการเพื่อเพิ่มความแม่นยำการพยากรณ์และลดระดับสินค้าคงคลัง: กรณีศึกษาโรงงานแปรรูปสินค้าเกษตร คลอเคลีย วจนะวิชากร และธารชุดา พันธ์นิกุล	e262009

สารบัญ

	รหัสบทความ
ผลของสารผสมล่วงหน้าประเภทวิตามินและแร่ธาตุผสมโพรไบโอติก (Pro Max Plus) ต่อสมรรถภาพการเจริญเติบโตและตอบสนองทางระบบภูมิคุ้มกันปลานิล ฐปนขจร ปันแจ่ม สุดาพร ตงศิริ จงกล พรมยะ Ricardo A. De Guzman และชนกันต์ จิตมนัส	e262010
การเพิ่มประสิทธิภาพตัวจำแนกการยกเลิกบริการในแพลตฟอร์มวิดีโอออนไลน์แบบมีค่าใช้จ่ายด้วยการผสมผสานโมเดลการเรียนรู้แบบรวม จักรินทร์ สันติรัตนภักดี	e262011
การประยุกต์ใช้การประเมินผลกระทบด้านสุขภาพโดยชุมชนเพื่อการพัฒนาศักยภาพในการรองรับผลกระทบต่อความมั่นคงทางอาหาร ก่อนดำเนินกิจการโรงงานแปรรูปยางพารา พื้นที่ตำบลห้วยยาง อำเภอคอนสาร จังหวัดชัยภูมิ วลัญช์ชยา เขตบำรุง และจิราภรณ์ ประธรรมโย	e262012
ผลของการเตรียมเบื้องต้นด้วยสารละลายแมกนีเซียมซัลเฟตต่อฤทธิ์ต้านอนุมูลอิสระและปริมาณคลอโรฟิลล์ของผำอบแห้ง ปภากร ศรีสอน พีรรัตน์ ดวงติ๊บ และกานต์รวี ฮั่นสกุล	e262013
การพัฒนากระบวนการทางชีวภาพสำหรับการผลิตและคุณลักษณะเฉพาะของไฮโดรไลเสตคอลลาเจนเพพไทด์ที่มีคุณสมบัติต้านอนุมูลอิสระจากกระดูกปลากดคัง วุฒิศักดิ์ คุณุ พิบูรณ์ เหง้าณี สรพงษ์ ภวสุปรีย์ และสุภาวดี ปาทาธนานนท์	e262014
การพัฒนาและประเมินคุณภาพเครื่องดื่มเยลลี่ว่านหางจระเข้ผสมน้ำผลไม้สูตรลดพลังงาน อมรรัตน์ สีสุกอง วีรชน ภูหินกอง ฤทธิพันธ์ รุ่งเรือง มณชัย เดชสังกรานนท์ วิสาขา เทียมลม และขวัญจิต อิสระสุข	e262015

ผลของการนวดแบบมวยไทย การยืดเหยียดกล้ามเนื้อ และการนั่งพักที่มีต่อการฟื้นสภาพของอัตราการเต้นของหัวใจ ความแข็งแรงของขา และความอ่อนตัว ในนักกีฬาเซปักตะกร้อชายมหาวิทยาลัยราชภัฏสุรินทร์

Effects of Muaythai Massage, Stretching and Sitting on Recovery Rest of Resting Heart Rate, Legs Strength and Flexibility between Set in Male's Sepak Takraw Player Surindra Rajabhat University

ภัทรพล ทองนำ[1*]

Pattarapol Thongnum[1*]

[1]คณะครุศาสตร์ มหาวิทยาลัยราชภัฏสุรินทร์ จังหวัดสุรินทร์

[1]Faculty of Education, Surindra Rajabhat University, Surin Province

*Corresponding Author: jeffyswucukku@srru.ac.th

Received: December 29, 2026 **Revised:** January 29, 2026 **Accepted:** February 15, 2026

บทคัดย่อ

การวิจัยครั้งนี้มีวัตถุประสงค์เพื่อศึกษาผลของการนวดแบบมวยไทย การยืดเหยียดกล้ามเนื้อ และการนั่งพักที่มีต่ออัตราการเต้นของหัวใจ ความแข็งแรงของขา และความอ่อนตัว ในนักกีฬาเซปักตะกร้อชาย มหาวิทยาลัยราชภัฏสุรินทร์ กลุ่มตัวอย่างที่ใช้เป็นนักกีฬาเซปักตะกร้อชายมหาวิทยาลัยราชภัฏสุรินทร์ จำนวน 12 คน แบ่งออกเป็น 3 กลุ่มเท่า ๆ กัน ด้วยการสุ่มอย่างง่าย แบบจับฉลาก ศึกษาการฟื้นสภาพระหว่างการพักระหว่างเซต 3 รูปแบบ ประกอบด้วยการนวดแบบมวยไทย การยืดเหยียดกล้ามเนื้อ และการนั่งพัก กลุ่มตัวอย่างชุดเดียวกัน ปฏิบัติการทดลองทั้ง 3 รูปแบบ และการทดลองแต่ละครั้งเว้นระยะห่างกันเป็นเวลา 1 สัปดาห์ ทดสอบอัตราการเต้นของหัวใจ ความแข็งแรงของขา และความอ่อนตัว หลังการฝึกแต่ละครั้ง วิเคราะห์ข้อมูลโดยใช้ค่าเฉลี่ย ส่วนเบี่ยงเบนมาตรฐาน วิเคราะห์ความแปรปรวนทางเดียวแบบวัดซ้ำ เปรียบเทียบความแตกต่างเป็นรายคู่ เมื่อพบความแตกต่างจะใช้การวิเคราะห์เป็นรายคู่ด้วยวิธีของตูกี กำหนดนัยสำคัญทางสถิติที่ระดับ 0.05 ผลการวิจัยพบว่าการฟื้นสภาพด้วยการนวดแบบมวยไทย การยืดเหยียดกล้ามเนื้อ และการนั่งพักสามารถช่วยลดอัตราการเต้นของหัวใจขณะพักได้ ไม่พบความแตกต่างในความแข็งแรงของขา และความอ่อนตัวอย่างมีนัยสำคัญทางสถิติที่ระดับ 0.05 โค้ชสามารถนำรูปแบบการฟื้นสภาพดังกล่าวไปใช้กับกีฬาเซปักตะกร้อเพื่อช่วยลดอัตราการเต้นของหัวใจได้

คำสำคัญ: การนวดแบบมวยไทย, การยืดเหยียดกล้ามเนื้อ, การฟื้นสภาพ, นักกีฬาเซปักตะกร้อ

Abstract

The purposes of this research are to study the effects of Muay Thai massage, stretching and sitting on recovery rest of resting heart rate, legs strength and flexibility between set in male's Sepak Takraw player Surindra Rajabhat university. The sample group was 12 male; Sepak Takraw Player in Surindra Rajabhat University and the player were divided into 3 equal groups by simple random sampling method, and then studied on recovery rest between set of 3 methods, including Muay Thai massage, stretching and sitting. The same sample group conducted all 3 methods in experiment and each experiment was spaced 1 week apart, tested the measured resting heart rate, legs strength and flexibility after each training section. The data were analyzed using mean, standard deviation, one-way analysis of variance with repeated measures, and compared the differences in pairs. When a significant difference was found, Tukey's post-hoc test was applied for pair-wise comparisons, the statistical significance was set at .05 level. The results showed that recovery through Muay Thai massage, stretching, and sitting can effectively reduce resting heart rate.

However, no statistically significant differences were found in leg strength and flexibility at the .05 level. Coaches may implement these recovery methods in Sepak Takraw to help lower athletes' heart rates.

Keywords: Muay Thai massage, Stretching, Recovery, Sepak Takraw Player

1. Introduction

Sports are a fundamental factor of paramount importance in human resource development, as evidenced by the fact that every country promotes and encourages its citizens to engage in sporting activities (Millour et al., 2025). Sepak Takraw has a long history of play. Matches are decided in a best of three sets format, where the team that wins two sets first is declared the winner. Consequently, the recovery process between sets is of paramount importance. If athletes can recover quickly, it provides a significant advantage in the subsequent set, shorter recovery durations resulted in a decrease in mean leg power and calorie expenditure, but led to a higher Rating of Perceived Exertion (RPE) compared to longer recovery periods (Rogers et al., 2024). Recovery is the application of specialized techniques, or a combination of multiple methods, aimed at accelerating the restoration process to reach full recovery as quickly as possible. It is the process of returning an athlete to a state equal to or better than their previous psychophysiological baseline or performance level (Vatne et al., 2025).

Currently, scholars have conducted various studies on recovery methods for different types of athletes. Massage therapy is one such method used for recovery; specifically, Deep Tissue Massage Therapy has become highly popular among athletes and professionals. It focuses on achieving results in enhancing physical performance and accelerating bodily recovery (Arsovski, 2025). In addition, Muay Thai Massage employs a dynamic technique of rhythmic squeezing, kneading, and pressing at a brisk pace, rather than applying heavy pressure throughout the body. This approach effectively releases muscle tension; it temporarily displaces blood from the vessels, and as pressure is released, a fresh surge of circulation returns to the area, promoting a profound sense of relaxation (Thongnum, 2025). Stretching has also been utilized as a recovery method, offering numerous physiological benefits. It helps reduce Delayed Onset Muscle Soreness (DOMS) after exercise. Furthermore, stretching is widely recognized for its role in fatigue recovery and is commonly used to increase the Range of Motion (ROM) of joints and reduce muscle tension (Daneshjoo et al., 2024). All of the aforementioned methods are highly beneficial to athletes. It is widely believed that active recovery promotes the restoration process by accelerating the body's return to homeostasis after competition. This process alleviates fatigue and muscle soreness, replenishes energy levels and physical performance, and enables athletes to tolerate higher training volumes ultimately leading to improved overall efficiency (Sedano & Izquierdo, 2025).

For these reasons, it was found that the majority of studies focus on post competition recovery, while the effects of recovery methods during active competition in Sepak Takraw athletes have not yet been studied. Consequently, the researcher is interested in studying the effects of Muay Thai massage, stretching, and sitting on recovery between Set in Male's Sepak Takraw Player Surindra Rajabhat University. The objective is to determine which method and format facilitate the fastest and most effective recovery for Sepak Takraw athletes during the two minute between set. The findings will serve as a practical guideline for athletes at all levels and effectively integrate sports science recovery principles to enhance the development of the Sepak Takraw community. Based on a review of the literature and relevant studies, the conceptual framework for this research is summarized as follows:

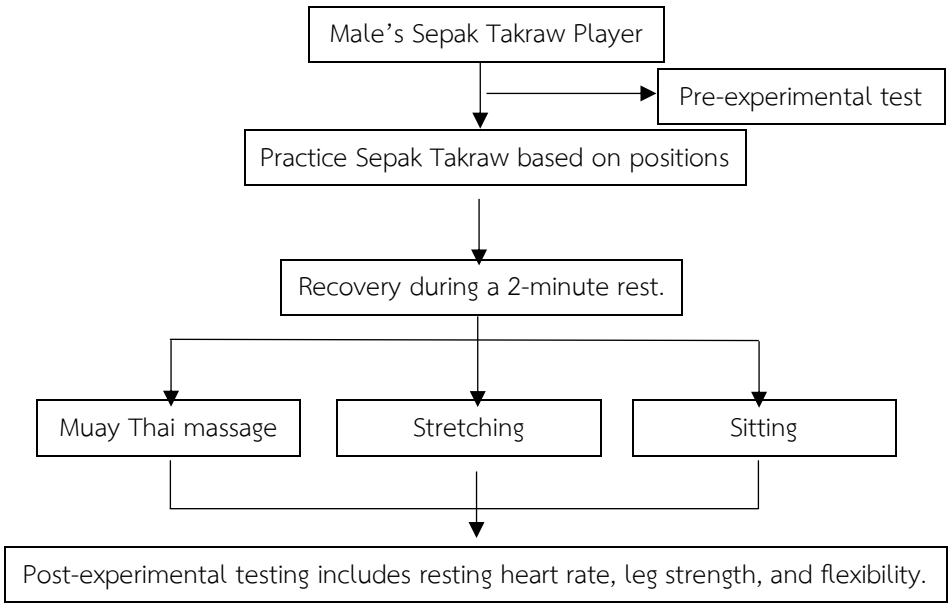


Figure 1. Conceptual Framework of the Study

2. Materials and methods

2.1 Participants

The sample size for this research was 12 male Sepak Takraw players from Surindra Rajabhat University who participated in the 48th Thailand University Games, selected using Purposive Sampling.

Inclusion criteria for this study were Sepak Takraw players of Surindra Rajabhat University who participated in the 48th Thailand University Games, no injuries in the past 6 months and provision of written consent.

Exclusion criteria for this study were history of recent surgeries or injuries (including injuries to the legs, ligaments, or joints) within the past 12 months and It is a serious contagious disease.

2.2 Research Instruments

2.2.1 The Muay Thai Massage Program (Thongnum & Eungpinichpong, 2016): The Muay Thai massage protocol lasted 2 minutes in total. Participants were seated on a chair while water was applied to the skin. The massage technique involved rhythmic squeezing, kneading, and pressing at a fast pace, without applying deep pressure, covering all body parts from the head, arms, and torso to the legs for 1.30 minutes. The remaining 30 seconds consisted of static stretching for the arms and legs, respectively.

2.2.2 The Stretching Program consists of the following:

1) Shoulder Stretch
2) Triceps and Lateral Trunk Stretch
3) Upper Back Stretch
4) Quadriceps Stretch
5) Calf Stretch
6) Knee-to-Chest Stretch
7) Toe-up stretch
8) Adductor Stretch
9) Hamstring Stretch
10) Thigh and Back Stretch

2.2.3 TKK Analog Leg Dynamometer (reliability = 0.89)

2.2.4 FBT Sit and Reach Box (reliability = 0.91)

2.2.5 Heart Rate measurement tool: Stethoscope (reliability = 0.89)

2.2.6 Weighing Scale

2.2.7 Stadiometer

2.2.8 Data Recording Form

2.3 Procedure

This study employed a quasi-experimental design with repeated measures. This research study has been approved by the Surindra Rajabhat University Institutional Review Board with approval number HE 642014.

2.3.1 The researcher submitted a formal letter requesting permission to conduct the research and use the facilities for data collection to the Dean of the Faculty of Education, Surindra Rajabhat University.

2.3.2 The researcher explained the research objectives, procedures, and duration, as well as the Muay Thai massage program and the 10-position muscle stretching program to the participants to ensure strict adherence to instructions. Furthermore, the researcher detailed the participants' rights and benefits, including the right to confidentiality and the right to accept or decline participation, ensuring that the decision to participate was made voluntarily.

2.3.3 The participants were divided into three groups to study three different types of inter-set recovery. Numbers 1–12 were written on slips for a random draw to assign participants to their respective experimental groups. Using a repeated measures design, the same set of participants was divided into three subgroups, and each group rotated through all three experimental conditions until they had completed all three trials, as shown in Table 1.

Table 1. Shows the three types of post-competition recovery for each group.

Sample Group	Trial 1	Trial 2	Trial 3
Group 1 (Nos. 1-4)	Muay Thai massage	stretching	Sitting
Group 2 (Nos. 5-8)	stretching	Sitting	Muay Thai massage
Group 3 (Nos. 9-12)	Sitting	Muay Thai massage	stretching

The same group of participants performed all three experimental protocols, with each trial separated by a one-week washout period.

2.3.4 Prior to the experiment, baseline measurements were recorded, including weight, height, resting heart rate, legs strength, and flexibility.

2.3.5 The participants performed Sepak Takraw practice by simulating an actual competition, regardless of whether the ball remained in play or was out of bounds. The procedures are as follows:

1) For the server position, the player performed 3 continuous serves (from a teammate's toss), alternating with receiving 3 balls hit by a coach using a tennis racket. This combined sequence was counted as 1 repetition. The players completed 4 repetitions per set, with a 2-minute rest interval between each of the 3 sets.

2) For the setter position, the coach used a tennis racket to hit 3 balls for the player to set continuously, alternating with receiving 3 balls also hit by the coach. This sequence was counted as 1 repetition. The players completed 4 repetitions per set, with a 2-minute rest interval between each of the 3 sets.

3) For the attacker position, the coach hit balls with a tennis racket to the setter or server, who then set the ball for the attacker to perform 3 continuous attacks at the net. This was alternated with receiving 3 balls hit by the coach. This combined sequence was counted as 1 repetition. The players completed 4 repetitions per set, with a 2-minute rest interval between each of the 3 sets.

2.3.6 During the rest interval of each set, the resting heart rate, legs strength, and flexibility were recorded immediately after completing the Sepak Takraw drills. Following this, participants underwent a 2-minute recovery period according to their randomly assigned method. A second measurement was then recorded. This process was repeated for the second and third sets, with data collection following the same procedure as the first set.

2.3.7 Each participant was required to complete the Sepak Takraw drills and all three recovery protocols over a total of three trials. Each trial was separated by a one-week interval, during which participants were instructed to avoid high-intensity exercise or strenuous sports.

2.3.8 The results were recorded for subsequent statistical analysis.

3. Result

This research aims to investigate the effects of Muay Thai massage, stretching and sitting on recovery rest of resting heart rate, legs strength and flexibility between set in male's Sepak Takraw player Surindra Rajabhat university. The results of the data analysis are as follows:

3.1 The participants in the group 1 had a mean weight of 64.00 ± 9.49 kg and a mean height of 172.50 ± 7.94 cm. Group 2 had a mean weight of 66.50 ± 3.32 kg and a mean height of 171.50 ± 2.65 cm, while Group 3 had a mean weight of 65.50 ± 3.70 kg and a mean height of 172.00 ± 4.69 cm in Table 2.

Table 2. The mean and standard deviation of the participants' baseline in the study.

Group	Weight		Height	
	Mean	S.D.	Mean	S.D.
Group 1	64.00	9.49	172.50	7.94
Group 2	66.50	3.32	171.50	2.65
Group 3	65.50	3.70	172.00	4.69

3.2 After the first experiment, it was shown that no statistically significant differences at the 0.05 level in recovery of resting heart rate, legs strength, and flexibility between sets among male's Sepak Takraw Player at Surindra Rajabhat University across Group 1, Group 2, and Group 3 after the first trial in Table 3.

Table 3. This table shows a comparison of the effects of Muay Thai massage, stretching, and sitting on the recovery of resting heart rate, legs strength, and flexibility in Male's Sepak Takraw Player at Surindra Rajabhat University after the first trial among groups 1, 2, and 3.

List	SS	df	MS	F	Sig.
Resting heart rate					
Between Groups	462.50	2	231.25	3.68	0.07
Within Groups	581.75	9	64.64		
Total	1044.25	11			

Table 3. This table shows a comparison of the effects of Muay Thai massage, stretching, and sitting on the recovery of resting heart rate, legs strength, and flexibility in Male's Sepak Takraw Player at Surindra Rajabhat University after the first trial among groups 1, 2, and 3. (Cont.)

List	SS	df	MS	F	Sig.
Legs Strength					
Between Groups	0.00	2	0.00	0.00	0.99
Within Groups	1.74	9	0.19		
Total	1.74	11			
Flexibility					
Between Groups	4.17	2	2.08	0.13	0.88
Within Groups	146.50	9	16.28		
Total	150.67	11			

3.3 Following after the second trial, it was found that the recovery between sets of resting heart rate among Group 1, Group 2, and Group 3 was statistically significantly different at the .05 level. Meanwhile, leg strength and flexibility showed no statistically significant difference at the .05 level (Table 4). Therefore, a pairwise comparison of heart rate after the second trial among Group 1, Group 2, and Group 3 was conducted using Tukey's method, as shown in Table 5.

Table 4. This table shows a comparison of the effects of Muay Thai massage, stretching, and sitting on the recovery of resting heart rate, legs strength, and flexibility in Male's Sepak Takraw Player at Surindra Rajabhat University after the second trial among groups 1, 2, and 3.

List	SS	df	MS	F	Sig.
Resting heart rate					
Between Groups	513.17	2	256.58	4.28*	0.04
Within Groups	539.50	9	59.94		
Total	1052.67	11			
Legs Strength					
Between Groups	.02	2	0.01	0.05	0.95
Within Groups	1.73	9	0.19		
Total	1.75	11			
Flexibility					
Between Groups	56.00	2	28.00	1.65	.25
Within Groups	153.00	9	17.00		
Total	209.00	11			

*$p<0.05$

Table 5. Presenting the results of the post-hoc pairwise comparison of heart rates after the second experiment between Group 1, Group 2, and Group 3 using Tukey's method.

Group	Mean Difference	Sig.
Group 1 vs Group 2	15.50*	0.04
Group 1 vs Group 3	4.25	0.73
Group 3 vs Group 2	11.25	0.16

*$p<0.05$

According to Table 5, the post-hoc pairwise comparison of resting heart rates after the second trial revealed a statistically significant difference between Group 1 and Group 2 at the 0.05 level.

3.4 After the third trial, the recovery between sets of resting heart rate among Group 1, Group 2, and Group 3 was statistically significantly different at the .05 level. Meanwhile, leg strength and flexibility showed no statistically significant difference at the .05 level (Table 6). Consequently, Tukey's post hoc test was performed to determine the pairwise differences in resting heart rate among Groups 1, 2, and 3 after the third trial, as shown in Table 7.

Table 6. This table shows a comparison of the effects of Muay Thai massage, stretching, and sitting on the recovery of resting heart rate, legs strength, and flexibility in Male's Sepak Takraw Player at Surindra Rajabhat University after the third trial among groups 1, 2, and 3.

List	SS	df	MS	F	Sig.
Resting Heart Rate					
Between Groups	592.67	2	296.33	7.15*	.01
Within Groups	373.00	9	41.44		
Total	965.67	11			
Legs Strength					
Between Groups	.02	2	.01	.07	.94
Within Groups	1.45	9	.16		
Total	1.47	11			
Flexibility					
Between Groups	52.17	2	26.08	1.50	.28
Within Groups	156.75	9	17.42		
Total	208.92	11			

*$p<0.05$

Table 7. Presenting the results of the post-hoc pairwise comparison of resting heart rates after the third experiment between Group 1, Group 2, and Group 3 using Tukey's method

Group	Mean Difference	Sig.
Group 1 vs Group 2	16.00*	.02
Group 1 vs Group 3	2.50	.85
Group 3 vs Group 2	13.50*	.04

*$p<0.05$

Table 7 indicates that after the third trial, there were statistically significant differences in resting heart rate ($p<0.05$) between group 1 and group 2, and between group 3 and group 2.

4. Discussion

The hypothesis stated that the Muay Thai massage, stretching and sitting have significantly different effects on recovery resting heart rate, legs strength and flexibility between set in male's Sepak Takraw player Surindra Rajabhat University.

4.1 Resting heart rate

This finding supports the proposed hypothesis, the research findings revealed that after the second experiment, there was a significant difference between Group 1 (stretching) and Group 2 (sitting). Furthermore, after the third experiment, significant differences were observed between Group 1 (sitting) and Group 2 (Muay Thai massage), as well as between Group 3 (stretching) and Group 2 (Muay Thai massage). Specifically: after Sepak Takraw athletes have completed the prescribed training program, the heart will work harder. With consistent training, heart rate will undergo physiological changes, as noted by Benavides-Roca et al. (2025) concluded that Resistance Training (RT) and High-Intensity Interval Training (HIIT) result in immediate significant changes in blood pressure and heart rate variability. Notably, HIIT demonstrates a more pronounced impact on autonomic nervous system adaptation, which is consistent with the findings of Guo & Wang (2025) stated that regular exercise, performed for 30–40 minutes per session with a frequency of 3–5 times per week, significantly improves blood pressure and resting heart rate. Furthermore, Yunus et al (2023) found that incorporating aerobic exercise into the treatment process can help reduce resting heart rate in patients with chronic stroke, as noted by Deng et al. (2024) found that exercise training has positive effects on heart rate variability, resting systolic blood pressure, and heart rate in patients with hypertension, which is consistent with Song et al. (2025) concluded that both High-Intensity Interval Training (HIIT) and Moderate-Intensity Interval Training (MIT) can similarly improve Heart Rate Recovery (HRR) in patients with coronary heart disease in the short term, which is also consistent with Edwards et al. (2023) stated that various forms of exercise training can help reduce resting blood pressure, particularly Isometric Exercise, which is consistent with the findings of Chauhan & Kumar (2023) discovered that regular exercise can lead to improved cardiovascular health, as measured by a decrease in heart rate, which may result in more efficient cardiac function. Furthermore, Yasuda & Kubo (2024) concluded that the significant reduction in heart rate observed during static stretching was not associated with changes in blood circulation within the tendons and muscles. Similarly, Ahirvar & Pathak (2024) concluded that active recovery is significantly more effective than passive recovery. Consequently, it is recommended that after exercise or physical activity, athletes should utilize active recovery techniques to facilitate a more efficient reduction in heart rate.

4.2 Legs Strength

The results did not support the stated hypothesis. This is because leg strength increases or decreases depending on a training program using an intensity of 80% of the maximum capacity for each exercise over a period of 6 – 8 weeks, as stated by Maliki et al. (2025) concluded that plyometric training yields better results than the control group, and bodyweight training can increase the peak power of leg muscles in youth volleyball players. Consequently, all three recovery methods could not increase or decrease leg strength, which is consistent with Mpampoulis et al. (2024) concluded that training only once a week (or once every two weeks) for a period of 3 months may help maintain muscle mass or strength adaptations and aerobic power gained from systematic concurrent training (a combination of endurance and strength training) at 90% to 95%, which is consistent with Zhang et al. (2025) found that post-exercise

stretching, when used as the sole recovery method, did not significantly improve muscle soreness, strength, physical performance, flexibility, or pain levels.

4.3 Flexibility

The results did not support the hypothesis. This may be attributed to the fact that the sample group underwent a warm-up session involving stretching prior to training. Generally, all types of exercise enhance flexibility, thereby increasing the range of motion and preventing injuries. Therefore, recovery using the aforementioned methods resulted in no significant difference in the flexibility of the sample group, as noted by Pranoto et al. (2025) stated that this study confirms that

regular exercise significantly improves flexibility, particularly in athletes, which is consistent with the findings of Alimoradi et al. (2023) concluded that incorporating calf muscle stretching into regular training routines can provide benefits to female soccer players in terms of performance variables, as noted by Hidayatullah et al. (2022) explained the study findings that both passive tactical stretching and PNF (Proprioceptive Neuromuscular Facilitation) can increase flexibility. However, empirical evidence indicates that PNF stretching is more effective in improving flexibility, which is also consistent with the findings of Favro et al. (2024) concluded from the experimental results that Resistance Training can be utilized as a strategy to improve joint flexibility. Specifically, high-intensity resistance training yields better results in increasing body flexibility. Furthermore, Hosseini et al. (2025) specified in the research that both NHE (Nordic Hamstring Exercise) and DHS (Dynamic Hamstring Stretching) have positive effects on muscle performance, range of motion, balance, and agility. However, NHE has been proven to be more effective in developing these various variables compared to DHS training.

5. Conclusion and suggestions

The study results indicate that all three recovery methods effectively reduce heart rate between set. Consequently, coaches and trainers can implement Muay Thai massage, stretching, and sitting as recovery protocols for Sepak Takraw athletes across all levels of competition. However, a limitation of this study is that the recovery methods were conducted within a timeframe of only two minutes. Consequently, applying these methods to other sports with longer or shorter rest intervals must be carefully considered and adjusted accordingly to ensure maximum benefit for the athletes.

6. References

Ahirvar, M. K., & Pathak, M. (2024). A comparative study between active recovery and passive recovery on heart rate. International Journal of Physiology, Nutrition and Physical Education, 9(1), 251–254. http://www.journalofsports.com

Alimoradi, M., Sahebozamani, M., Hosseini, E., Konrad, A., & Noorian, S. (2023). The effect on flexibility and a variety of performance tests of the addition of 4 weeks of soleus stretching to a regular dynamic stretching routine in amateur female soccer players. Sports, 11(7), 138. https://doi.org/10.3390/sports11070138

Arsovski, D. (2025). Deep Tissue Massage Therapy: Effects on Muscle Recovery and Performance in Athletes. International Journal of Therapeutic Massage & Bodywork, 18(2), 40–51. https://doi.org/10.3822/ijtmb.v18i2.1139

Benavides-Roca, L., Miranda, M., Hernández, S., Vega, A., Campos, L., Benavides, M., & Benavides, G. (2025). Effects of high intensity interval training and resistance training on blood pressure and heart rate variability in young subjects. Journal of Human Sport and Exercise, 20(2), 694-705. https://doi.org/10.55860/qepkyn98

Chauhan, B. S., & Kumar, S. (2023). Effect of Physical Training on Pulse Rate of Under-Graduate Students. European Chemical Bulletin, 12(Special Issue 10), 4381 – 4386. https://doi:10.48047/ecb/2023.12.si10.00503.

Daneshjoo, A., Hosseini, E., Heshmati, S., Sahebozamani, M., & Behm, D. G. (2024). Effects of slow dynamic, fast dynamic, and static stretching on recovery of performance, range of motion, balance, and joint position sense in healthy adults. BMC Sports Science, Medicine and Rehabilitation, 16(167), 1-11. https://doi.org/10.1186/s13102-024-00841-5

Deng, Y., Zeng, X., Tang, C., Hou, X., Zhang, Y., & Shi, L. (2024). The effect of exercise training on heart rate variability in patients with hypertension: A systematic review and meta-analysis. Journal of Sports Sciences, 42(13), 1272-1287. https://doi.org/10.1080/02640414.2024.2388984

Edwards, J. J., Deenmamode, A. H., Griffiths, M., Arnold, O., Cooper, N. J., Wiles, J. D., & O'Driscoll, J. M. (2023). Exercise training and resting blood pressure: a large-scale pairwise and network meta-analysis of randomised controlled trials. British journal of sports medicine, 57(20), 1317-1326. https://doi.org/10.1136/bjsports-2022-106503

Favro, F., Roma, E., Gobbo, S., Bullo, V., Di Blasio, A., Cugusi, L., & Bergamin, M. (2024). The influence of resistance training on joint flexibility in healthy adults: a systematic review, meta-analysis, and meta-regression. Journal of strength and conditioning research, 39(3), 386. https://doi.org/10.1519/JSC.0000000000005000

Guo, L., & Wang, C. (2025). The effect of exercise on cardiovascular disease risk factors in sedentary population: a systematic review and meta-analysis. Frontiers in Public Health, 13, 1470947. https://doi.org/10.3389/fpubh.2025.1470947

Hidayatullah, M. A., Doewes, M., Kunta, S., & Purnama. (2022). The effect of stretching exercises on flexibility for students. Journal Penelitian Pembelajaran, 8(1), 118-130. https://doi.org/10.29407/js_unpgri.v8i1.17742

Hosseini, E., Alimoradi, M., Iranmanesh, M., Saki, F., & Konrad, A. (2025). The effects of 8 weeks of dynamic hamstring stretching or nordic hamstring exercises on balance, range of motion, agility, and muscle performance among male soccer players with hamstring shortness: a randomized controlled trial. BMC Sports Science, Medicine and Rehabilitation, 17(187), 1-13. https://doi.org/10.1186/s13102-025-01216-0.

Maliki, O., Suherman, W. S., Prasetyo, Y., et al. (2025). Effect of Plyometric Training and Body Weight Training on Volleyball Player's Leg Muscle Power. International Journal of Human Movement and Sports Sciences 13(1), 98-104. https://doi.org/10.13189/saj.2025.130111

Millour, G., Lepers, R., Coste, A., & Hausswirth, C. (2025). Effects of combining cold exposure and compression on muscle recovery: a randomized crossover study. Frontiers in Physiology, 16,1-11. https://doi.org/10.3389/fphys.2025.1598075

Mpampoulis, T., Stasinaki, A. N., Methenitis, S., Zaras, N., Bogdanis, G. C., & Terzis, G. (2024). Effect of Different Reduced Training Frequencies after 12 Weeks of Concurrent Resistance and Aerobic Training on Muscle Strength and Morphology. Sports, 12(7), 198. https://doi.org/10.3390/sports12070198

Pranoto, N. W., Andika, H., Ockta, Y., Firdaus, K., Hendri, N., Zarya, F., ... & Fauziah, V. (2025). The effect of training on flexibility: a case study of athletes and non-athletes. Retos: nuevas tendencias en educación física, deporte y recreación, (62), 974-978. https://doi.org/10.47197/retos.v62.109740

Rogers, T., Gill, N., & Beaven, C. M. (2024). A comparison of three different work to rest periods during intermittent sprint training on maintaining sprint effort performance. Journal of Exercise Science & Fitness, 22(2), 97 – 102. https://doi.org/10.1016/j.jesf.2023.12.004

Sedano, S., & Izquierdo, S. M. (2025). Effectiveness of Different Neuromuscular Recovery Strategies in Elite Youth Female Football Players. Sports, 13(2), 36. https://doi.org/10.3390/sports13020036

Song, Q., Chang, J., Bai,. B., et al. (2025). Comparable Improvements in Heart Rate Recovery Following Short-Term High-Intensity and Moderate-Intensity Interval Training in Patients with Cardiovascular Disease. Dovepress journals, 2025(18), 8185—8196. https://doi.org/10.2147/JMDH.S560641

Thongnum, P. (2025). Effects of Muaythai Massage, Muscular Stretching and Sitting on Recovery Rest of Fatigue Level Between Sets in Male Sepak Takraw Players of Surindra Rajabhat University. Academic Journal of Thailand National Sports University, 17(3), 195–206. retrieved from https://he02.tci-thaijo.org/index.php/TNSUJournal/article/view/268436

Thongnum, P., & Eungpinichpong, W. (2016). Effects of Muaythai Massaging on Recovery of Perceive Fatigue in Thai Boxing. Koch Cha Sarn Journal of Science, 38(2), 51-59. (in Thai). https://science.srru.ac.th/kochasarn-files/files/5.

Vatne, E., Lozano, J. M. O., Saenz, C., Cost, R., & Hagen, J. (2025). Post-Exercise Recovery Modalities in Male and Female Soccer Players of All Ages and Competitive Levels: A Systematic Review. Sports (Basel), 13(10), 343. https://doi.org/10.3390/sports13100343

Yasuda, A., & Kubo, K. (2024). Effects of Static Stretching on the Blood Circulation of Human Tendon In Vivo. Translational Sports Medicine. 10, 4413113. https://doi.org/10.1155/2024/4413113

Yunus, F. T., Julianti, H. P., & Setiawati, E. (2023). The Effect of Additional of Aerobic Exercise to Functional Therapy on Resting Heart Rate in Patients with Chronic Phase Post Stroke Patients. Indonesian Journal of Physical Medicine and Rehabilitation, 12(1), 43 – 51. https://doi.org/10.36803/indojpmr.v12i01.336

Zhang, P., Chen, J., & Xing, T. (2025). Effects of post-exercise stretching versus no stretching on lower limb muscle recovery and performance: a meta-analysis. Frontiers in Physiology, 16:1674871, 1-17. https://doi.org/10.3389/fphys.2025.1674871

ปัจจัยที่มีความสัมพันธ์กับความสุขและการเตรียมความพร้อมเข้าสู่วัยสูงอายุของบุคคลที่มีความหลากหลายทางเพศในชุมชนชนบท

Factors Associated with Happiness and Aging Preparation among LGBTQ+ Individuals in Rural Communities

เตชภณ ทองเติม[1] และ จีรนันท์ แก้วมา[2*]

Tachapon Tongterm[1] and Jeeranan Kaewma [2*]

[1]คณะศิลปศาสตร์และวิทยาศาสตร์ มหาวิทยาลัยราชภัฏศรีสะเกษ จังหวัดศรีสะเกษ

[2]คณะพลศึกษา มหาวิทยาลัยศรีนครินทรวิโรฒ จังหวัดนครนายก

[1]Faculty of Liberal Arts and Science, Sisaket Rajabhat University, Sisaket Province

[2]Faculty of Physical Education, Sports and Heath, Srinakharinwirot University, Nakhon nayok Province

*Corresponding Author: jeerananka@g.swu.ac.th

Received: April 9, 2026 **Revised:** May 29, 2026 **Accepted:** June 11, 2026

บทคัดย่อ

การเข้าสู่สังคมสูงวัยของกลุ่มบุคคลที่มีความหลากหลายทางเพศ (LGBTQ+) ในชุมชนชนบทเป็นประเด็นที่ได้รับความสนใจเพิ่มขึ้น แต่หลักฐานเชิงประจักษ์เกี่ยวกับปัจจัยที่เกี่ยวข้องกับความสุขและการเตรียมความพร้อมเข้าสู่วัยสูงอายุยังมีอยู่อย่างจำกัด การวิจัยเชิงวิเคราะห์แบบภาคตัดขวางนี้มีวัตถุประสงค์เพื่อศึกษาปัจจัยที่มีความสัมพันธ์กับความสุขและการเตรียมความพร้อมเข้าสู่วัยสูงอายุของบุคคลที่มีความหลากหลายทางเพศในชุมชนชนบท กลุ่มตัวอย่างคือบุคคลที่มีความหลากหลายทางเพศอายุ 40 ปีขึ้นไปที่อาศัยอยู่ในพื้นที่ชนบทของจังหวัดศรีสะเกษ จำนวน 220 คน ซึ่งได้มาจากการเลือกกลุ่มตัวอย่างแบบลูกโซ่ผ่านเครือข่ายสังคมบนฐานของความไว้วางใจ เก็บรวบรวมข้อมูลด้วยแบบสอบถามชนิดตอบด้วยตนเองที่ผ่านการตรวจสอบคุณภาพด้านความตรงเชิงเนื้อหา (IOC = 0.88) และความเชื่อมั่น (Cronbach's alpha = 0.87) วิเคราะห์ข้อมูลด้วยสถิติเชิงพรรณนา สัมประสิทธิ์สหสัมพันธ์ของเพียร์สัน และการวิเคราะห์การถดถอยพหุคูณแบบขั้นตอนย้อนกลับ ผลการศึกษาพบว่า การสนับสนุนจากครอบครัวเป็นปัจจัยเดียวที่มีความสัมพันธ์กับความสุขอย่างมีนัยสำคัญทางสถิติ ($\beta = 0.376$, $p < 0.001$) โดยอธิบายความแปรปรวนได้ร้อยละ 14.2 ($R^2 = 0.142$) ขณะที่ความสัมพันธ์ทางสังคมเป็นปัจจัยเดียวที่สัมพันธ์กับการเตรียมความพร้อมเข้าสู่วัยสูงอายุอย่างมีนัยสำคัญทางสถิติ ($\beta = 0.168$, $p = 0.012$) โดยอธิบายความแปรปรวนได้ร้อยละ 2.8 ($R^2 = 0.028$) ข้อค้นพบสะท้อนให้เห็นว่า ภายใต้บริบทชนบทที่มีข้อจำกัดด้านระบบสวัสดิการและการสนับสนุนเชิงโครงสร้าง การยอมรับจากครอบครัวและความสัมพันธ์ทางสังคมอาจทำหน้าที่เป็นทรัพยากรทางจิตสังคมที่สำคัญต่อความมั่นคงทางอารมณ์และความพร้อมในชีวิตช่วงสูงวัยของกลุ่ม LGBTQ+ อีกทั้งผลการศึกษานี้สามารถใช้เป็นข้อมูลเชิงประจักษ์สำหรับการพัฒนากระบวนการสุขศึกษา การส่งเสริมสุขภาพชุมชน และการออกแบบสภาพแวดล้อมทางสังคมที่เอื้อต่อการสูงวัยอย่างมีคุณภาพในชุมชนชนบทของไทยในอนาคตได้

คำสำคัญ: ความสุข, การเตรียมความพร้อมเข้าสู่วัยสูงอายุ, ความหลากหลายทางเพศ, สุขภาวะทางจิตสังคม, การส่งเสริมสุขภาพชุมชน

Abstract

The transition toward an aging society among LGBTQ+ individuals in rural communities has received increasing attention; however, empirical evidence regarding psychosocial factors related to happiness and later-life readiness remains limited. This cross-sectional analytical study aimed to investigate factors associated with happiness and aging preparation among LGBTQ+ individuals in rural communities. The participants comprised 220 LGBTQ+ individuals aged 40 years and older residing in rural communities of Sisaket Province, Thailand. Participants were recruited via snowball sampling through trust-based social

networks. Data were collected using a self-administered questionnaire that demonstrated acceptable content validity (IOC = 0.88) and reliability (Cronbach's alpha = 0.87). Data were analyzed using descriptive statistics, Pearson's product-moment correlation coefficient, and backward stepwise multiple regression analysis. The findings revealed that family support was the only factor significantly associated with happiness (β = 0.376, $p < 0.001$), accounting for 14.2% of the variance (R^2 = 0.142). By contrast, social relationships were the only factor significantly associated with aging preparation (β = 0.168, p = 0.012), explaining 2.8% of the variance (R^2 = 0.028). The findings suggest that within rural contexts characterized by limited welfare systems and structural support, family acceptance and social relationships may function as important psychosocial resources supporting emotional security and later-life readiness among LGBTQ+ individuals. Furthermore, the findings may provide empirical evidence for the development of health education processes, community health promotion, and socially supportive environments that facilitate quality aging among LGBTQ+ populations in rural Thai communities.

Keywords: Happiness, Aging preparation, LGBTQ+, Psychosocial well-being, Community health promotion

1. Introduction

Over the past decade, gender diversity and the human rights of sexual and gender minority populations have become increasingly visible within legal, policy, and public discourse. However, the development and implementation of inclusive legal and social policies remain uneven across countries, reflecting both advances in rights recognition and continuing sociopolitical contestation (Langarita et al., 2025; Queiroz et al., 2026). Nevertheless, LGBTQ+ individuals, particularly those entering later life, continue to experience persistent health disparities and psychosocial vulnerabilities rooted in long-standing structural inequalities and cumulative minority stress across the life course (Fredriksen-Goldsen et al., 2017; Frost & Meyer, 2023). In the fields of health education and sport science, healthy aging is increasingly understood not merely as the absence of disease but as the capacity to sustain active living, psychosocial stability, meaningful social participation, and long-term engagement in movement and recreational activities. Emerging evidence suggests that prolonged exposure to discrimination, identity concealment, and chronic vigilance may progressively undermine psychological well-being, social participation, and movement engagement among LGBTQ+ older adults (Pistella et al., 2024). Such experiences may also contribute to broader biopsychosocial deterioration across the life course, including elevated psychological distress, social withdrawal, and accelerated health vulnerability (Christian et al., 2021; Christian et al., 2025). In many physical activity and recreational settings structured around rigid gender binaries, LGBTQ+ individuals may experience discomfort, exclusion, or psychological distress that further suppresses participation and long-term movement engagement (Pistella et al., 2024; Antoniucci et al., 2026). Furthermore, concerns regarding discrimination and inadequate understanding among healthcare providers may discourage LGBTQ+ older adults from accessing health services and health promotion resources, thereby increasing vulnerability to chronic illness, depression, and social isolation compared with the general older adult population (Fredriksen-Goldsen et al., 2013; Westwood, 2020).

In Thailand, despite progressive policy developments such as the enactment of the Marriage Equality Act in 2024, disparities in social acceptance and health support systems remain evident, particularly within rural communities where traditional gender norms and heteronormative expectations continue to shape everyday life. Recent Thai studies have reported ongoing experiences of interpersonal and environmental microaggressions, stigma, discrimination, and depressive symptoms among LGBTQ+

populations despite increasing public visibility and legal progress (Yodlorchai et al., 2024; Iamko & Boonnun, 2021). This situation reflects a form of policy lag in which legal advancement has progressed more rapidly than the adaptation of local health promotion systems, recreational environments, and community-based support structures. In many rural areas, LGBTQ+ individuals continue to experience pressure to conceal their identities to avoid stigmatization and social judgment, which may function as a chronic proximal stressor throughout the life course (Whitehead et al., 2016; Pachankis et al., 2020). Limited access to inclusive recreational spaces, social support networks, and health promotion resources may further reduce opportunities for psychosocial participation and active aging in later life. Moreover, many rural communities in Thailand continue to rely heavily on informal caregiving systems centered on family obligation and kinship relationships, potentially creating additional emotional strain for LGBTQ+ adults who experience fragile family relationships or social exclusion. These conditions are particularly significant within the context of Thailand's rapidly aging society, where successful aging increasingly depends not only on formal welfare systems but also on the quality of local social support and opportunities for meaningful community participation.

Consequently, Sisaket Province was purposively selected as the study setting because it reflects several structural characteristics commonly found in rural areas of Northeast Thailand. The province remains strongly connected to extended family traditions, local cultural expectations, and community-based social relationships that position children and family members as primary caregivers in old age. Such expectations may create additional challenges for LGBTQ+ individuals who do not have biological children or who experience strained family relationships, resulting in heightened concerns regarding long-term support and caregiving in later life. In parallel, the migration of working-age populations toward urban centers has contributed to increasing self-reliance among older adults remaining in rural communities. Sisaket Province also represents a predominantly agricultural society characterized by relatively limited access to specialized healthcare services, formal welfare infrastructure, and inclusive recreational resources compared with major urban areas. These contextual conditions may heighten vulnerability among LGBTQ+ adults transitioning into older age, particularly those with limited economic resources or restricted access to supportive social environments. From health education and sport science perspectives, such conditions are not merely social circumstances but ecological factors capable of influencing health behaviors, psychosocial adaptation, participation opportunities, and readiness for active aging in later life. Within these contexts, supportive social relationships, inclusive recreation, and community participation may function as important psychosocial support mechanisms that help preserve emotional stability, reinforce social belonging, and sustain meaningful engagement with community life among LGBTQ+ older adults (Fredriksen-Goldsen et al., 2019; Hurd & Li, 2023; Tongterm et al., 2026).

A review of previous literature reveals several important research gaps. Existing studies concerning LGBTQ+ aging have predominantly focused on urban populations and Western societies, particularly within North America and Europe, where healthcare systems, welfare structures, and LGBTQ+ support services differ considerably from those found in many Asian rural communities (Fredriksen-Goldsen et al., 2017; Westwood, 2020; Hurd & Li, 2023; Fredriksen-Goldsen et al., 2019). Although scholarly attention toward LGBTQ+ aging has expanded substantially in recent years, empirical evidence from rural Southeast Asian contexts remains limited, especially regarding the interaction between psychosocial conditions, health behaviors, recreational participation, and aging preparation within community-based environments (United Nations Development Programme: UNDP, 2014; Pistella et al., 2024). Furthermore, previous studies have often examined happiness, psychosocial well-being, and aging preparation as separate dimensions, despite growing evidence suggesting that these domains are closely interconnected within the broader context of

active aging and health behavior processes (Fredriksen-Goldsen et al., 2015; World Health Organization: WHO, 2002). According to Minority Stress Theory, chronic exposure to stigma, discrimination, and identity concealment may adversely affect psychological well-being and reduce motivation for long-term health maintenance and future planning (Meyer, 2003; Frost & Meyer, 2023). At the same time, health education perspectives emphasize that social support, environmental conditions, and opportunities for community participation serve as important enabling factors for sustaining health-promoting behaviors across the lifespan (Cohen & Wills, 1985). Therefore, this study had two primary objectives: 1) to examine factors associated with happiness among LGBTQ+ individuals in rural Thailand, and 2) to investigate factors associated with aging preparation among LGBTQ+ individuals in rural Thailand. The findings are expected to provide empirical evidence for the development of community-based health education processes, inclusive recreational environments, and health promotion strategies that support sustainable active aging and psychosocial well-being among LGBTQ+ populations in rural communities.

2. Materials and methods

This section presents the research design, participants, recruitment procedures, research instruments, data collection procedures, statistical analyses, and ethical considerations employed to examine factors associated with happiness and aging preparation among LGBTQ+ individuals, as detailed below.

2.1 Research design

This study employed a quantitative research design utilizing a cross-sectional analytical approach. The primary objective was to investigate factors associated with happiness and aging preparation among LGBTQ+ individuals residing in rural communities of Sisaket Province, Thailand.

2.2 Population and sample

The target population consisted of LGBTQ+ individuals aged 40 years and older residing in rural areas of Sisaket Province, Thailand. The required sample size was determined using the G*Power software, yielding a minimum sample of 220 participants (Faul et al., 2007). Due to the socially sensitive nature of the target population, particularly among individuals who may not openly disclose their sexual or gender identities within rural community settings, a snowball sampling technique was employed to facilitate participant recruitment through trust-based social networks.

The inclusion criteria were as follows: 1) residing in a rural area of Sisaket Province, 2) self-identifying and accepting their LGBTQ+ identity, 3) aged 40 years or older, and 4) capable of communicating in Thai and willing to participate in the study. The exclusion criteria included individuals unwilling to participate or those with severe psychiatric, neurological, or hearing impairments that could interfere with effective communication.

2.3 Research instruments

The data collection instrument was a self-administered questionnaire developed by researchers. The questionnaire was developed in accordance with the study's conceptual framework by integrating concepts related to subjective well-being (Diener, 2012), minority stress (Meyer, 2003), social support (House, 1981), successful aging (Fredriksen-Goldsen et al., 2015), and active aging (WHO, 2002). These concepts were applied to operationalize psychosocial and aging-related constructs relevant to LGBTQ+ individuals living in rural communities. The questionnaire consisted of four major sections covering demographic information, selected psychosocial factors, happiness, and multidimensional aging preparation.

To ensure instrument quality, content validity was evaluated by a panel of five experts, yielding an Index of Item-Objective Congruence (IOC) of 0.88. A pilot test subsequently demonstrated a reliability coefficient (Cronbach's alpha) of 0.87, indicating satisfactory internal consistency.

2.4 Data collection

Quantitative data collection was conducted through face-to-face and online surveys. This dual approach was implemented to facilitate participation and broaden access for participants dispersed across rural communities, thereby supporting adequate sample recruitment in accordance with the predetermined sample size.

2.5 Data analysis

The collected data were processed and analyzed using a statistical software package. Data analysis was divided into two parts:

2.5.1 Descriptive statistics

General demographic information and variable levels were analyzed using frequency, percentage, mean, and standard deviation. To interpret the levels of selected factors, happiness, and aging preparation, the researchers employed a 5-point rating scale. The interpretation criteria for mean scores were determined using class interval calculations (Best, 1981) and categorized into five levels as follows:

- Mean 4.21 to 5.00 = highest level
- Mean 3.41 to 4.20 = high level
- Mean 2.61 to 3.40 = moderate level
- Mean 1.81 to 2.60 = low level
- Mean 1.00 to 1.80 = lowest level

2.5.2 Inferential statistics

Hypothesis testing was conducted using Pearson's Product - Moment Correlation Coefficient to examine relationships among selected factors, happiness, and aging preparation. Multiple regression analysis was subsequently employed to investigate factors associated with happiness and aging preparation among LGBTQ+ individuals in rural communities. The level of statistical significance was set at 0.05. To identify the most parsimonious subset of predictors, Backward Stepwise Multiple Regression was employed. This approach enabled the systematic removal of non-significant variables while retaining predictors demonstrating meaningful statistical contribution within the final regression model (Field, 2024). Prior to regression analysis, assumptions regarding multicollinearity and normality of residuals were examined and deemed acceptable.

2.6 Ethical considerations

This research was conducted in accordance with established ethical principles for human research. Prior to data collection, all participants received clear and detailed information regarding the objectives and procedures of the study. Informed consent was obtained from all participants, emphasizing voluntary participation and the right to refuse or withdraw from the study at any stage without consequence. All personal information was kept strictly confidential, and participant anonymity was fully protected throughout the research process. The findings are presented only in aggregate form for academic purposes. This study was reviewed and approved by the Human Research Ethics Committee of Sisaket Rajabhat University, - Approval No. HE681010.

3. Result

3.1 General information of the sample

The results indicated that the majority of the sample identified their sexual identity as "Others" (Kathoey and Tom) (32.73%) and gay (32.72%). Most participants were aged between 40–49 years (66.36%) and were single (80.00%). Regarding educational attainment, the highest proportion had completed high school or an equivalent (26.82%), followed by primary education (25.91%). In terms of economic status, the majority reported an average monthly income between 5,001–10,000 THB (32.27%) and 10,001–20,000 THB (30.91%). Furthermore, concerning environment and health, most participants resided outside municipal areas (78.18%) and reported being in good health without underlying or chronic diseases (91.36%).

3.2 Analysis of Factor Levels

The analysis regarding the levels of selected factors affecting happiness and aging preparation (as presented in Table 1) revealed that, overall, the factors affecting the happiness of the sample were at a high level (M = 4.00, SD = 0.94). When examining each dimension, it was found that the respondents primarily emphasized social capital and psychological factors. Community acceptance exhibited the highest level (M = 4.20, SD = 0.88), followed by family support (M = 4.17, SD = 0.86) and mental health (M = 4.05, SD = 1.00), respectively. Conversely, income and economic status had the lowest mean score (M = 3.59, SD = 0.93). This overall interpretation clearly reflects that for LGBTQ+ individuals in rural areas, happiness and psychological well-being are anchored more profoundly in social acceptance and having a recognized place in society than in material or economic stability.

Regarding the factors affecting aging preparation, the overall score was also at a high level (M = 3.87, SD = 1.01). The sample demonstrated the highest level in social relationships (M = 4.02, SD = 0.92), followed by mental health (M = 3.97, SD = 0.96), and technology and innovation (M = 3.85, SD = 1.08). In contrast, housing and environment (M = 3.77, SD = 1.11) and physical health (M = 3.80, SD = 0.99) yielded the lowest mean scores. This overarching picture indicates that although the target population is proactive in establishing social support networks to prepare for retirement (which aligns with social health promotion mechanisms), the dimensions of physical infrastructure and physical health remain vulnerable points. These vulnerabilities reflect the inherent limitations of rural settings, underscoring the pressing need for additional policy support.

Table 1. Mean, standard deviation, and levels of selected factors affecting happiness and aging preparation

No.	Factors	M	SD	Level
Factors affecting happiness				
1	Income and economic status	3.59	0.93	high level
2	Physical health	3.99	0.88	high level
3	Mental health	4.05	1.00	high level
4	Family support	4.17	0.86	high level
5	Community acceptance	4.20	0.88	high level
	Mean	4.00	0.94	high level

Table 1. Mean, standard deviation, and levels of selected factors affecting happiness and aging preparation (Cont.)

No.	Factors	M	SD	Level
Factors affecting aging preparation				
1	Physical health	3.80	0.99	high level
2	Mental health	3.97	0.96	high level
3	Economic stability	3.84	0.97	high level
4	Social relationships	4.02	0.92	high level
5	Housing and environment	3.77	1.11	high level
6	Technology and innovation	3.85	1.08	high level
	Mean	3.87	1.01	high level

3.3 Correlation between selected factors, happiness, and aging preparation

Hypothesis testing to examine the relationship between selected factors and the happiness level of rural LGBTQ+ individuals revealed that all five selected factors were positively correlated with happiness at a statistical significance level of $p < 0.05$ and $p < 0.001$. Family support demonstrated a moderate positive correlation with happiness, yielding the highest correlation coefficient ($r = 0.376$, $p < 0.001$). This was followed by community acceptance ($r = 0.285$, $p < 0.001$) and mental health ($r = 0.283$, $p < 0.001$). Meanwhile, physical health and income and economic status showed a low level of positive correlation, as shown in Table 2.

Table 2. Pearson's correlation coefficients between selected factors and happiness

Factors		Income and economic status	Physical health	Mental health	Family support	Community acceptance	Happiness
1. Income and economic status	Pearson's r	—					
	p-value	—					
2. Physical health	Pearson's r	0.517***	—				
	p-value	< 0.001	—				
3. Mental health	Pearson's r	0.384***	0.639***	—			
	p-value	< 0.001	< 0.001	—			
4. Family support	Pearson's r	0.325***	0.465***	0.531***	—		
	p-value	< 0.001	< 0.001	< 0.001	—		
5. Community acceptance	Pearson's r	0.217**	0.419***	0.428***	0.543***	—	
	p-value	0.001	< 0.001	< 0.001	< 0.001	—	
6. Happiness	Pearson's r	0.172*	0.230***	0.283***	0.376***	0.285***	—
	p-value	0.011	< 0.001	< 0.001	< 0.001	< 0.001	—

*$p < 0.05$, **$p < 0.01$, ***$p < 0.001$

Regarding the relationship between selected factors and overall aging preparation, it is noteworthy that only three factors exhibited a statistically significant positive correlation at the 0.05 level. These were social relationships (r = 0.168, p = 0.012), followed by physical health (r = 0.165, p = 0.014), and housing and environment (r = 0.137, p = 0.043). In contrast, mental health, economic stability, and technology and innovation did not show a statistically significant correlation with overall aging preparation, as shown in Table 3.

Table 3. Pearson's correlation coefficients between selected factors and aging preparation

Factors		Physical health	Mental health	Economic stability	Social relationships	Housing and environment	Technology and innovation	Aging preparation
1. Physical health	Pearson's r	—						
	p-value	—						
2. Mental health	Pearson's r	0.707***	—					
	p-value	< 0.001	—					
3. Economic stability	Pearson's r	0.637***	0.640***	—				
	p-value	< 0.001	< 0.001	—				
4. Social relationships	Pearson's r	0.650***	0.658***	0.570***	—			
	p-value	< 0.001	< 0.001	< 0.001	—			
5. Housing and environment	Pearson's r	0.679***	0.662***	0.572***	0.556***	—		
	p-value	< 0.001	< 0.001	< 0.001	< 0.001	—		
6. Technology and innovation	Pearson's r	0.580***	0.585***	0.663***	0.500***	0.566***	—	
	p-value	< 0.001	< 0.001	< 0.001	< 0.001	< 0.001	—	
7. Aging preparation	Pearson's r	0.165*	0.060	0.101	0.168*	0.137*	0.047	—
	p-value	0.014	0.378	0.136	0.012	0.043	0.486	—

*p < 0.05, **p < 0.01, ***p < 0.001

3.4 Factors predicting happiness and aging preparation

To isolate the most impactful predictors from the five candidate factors, a multiple regression analysis using the backward stepwise method was conducted. The results revealed that family support was the sole significant predictor of happiness (β) = 0.376, t = 5.998, p < 0.001), accounting for 14.2% of the variance (R^2 = 0.142, F = 35.976, p < 0.001). Consequently, factors including income and economic status, physical health, mental health, and community acceptance were systematically excluded from the final model, as detailed in Table 4. The predictive equation in raw score form can be formulated as follows:

$$\hat{Y}_{Happiness} = 2.177 + 0.304\ (Family\ Support) \quad (1)$$

The equation demonstrates that for every one-unit increase in family support, the level of happiness increases by 0.304 units.

Table 4. Multiple regression analysis of factors predicting happiness

Predictors	B	SEB	β	t	*p*
Constant	2.177	0.216	-	10.087	< 0.001***
Family Support	0.304	0.051	0.376	5.998	< 0.001***
Variables Excluded: Income and economic status, physical health, mental health, community acceptance	-	-	-	-	-
Model Statistics: R = 0.376; R^2 = 0.142; Adjusted R^2 = 0.138 F (1, 218) = 35.976; *p*-value < 0.001					

****p* < 0.001

Regarding the prediction of overall aging preparation, the analysis revealed that social relationships were the sole factor capable of significantly predicting aging preparation at the 0.05 level (t = 2.521, *p* = 0.012), with a standardized regression coefficient (β) of 0.168. This factor explained 2.8% of the variance in aging preparation (R^2 = 0.028, F = 6.353, *p* = 0.012). Physical health, mental health, economic stability, housing and environment, and technology and innovation were excluded from the model, as shown in Table 5.

The predictive equation in raw score form can be formulated as follows:

$$\hat{Y}_{\text{Aging Preparation}} = 2.242 + 0.113\ (\text{Social Relationships}) \quad (2)$$

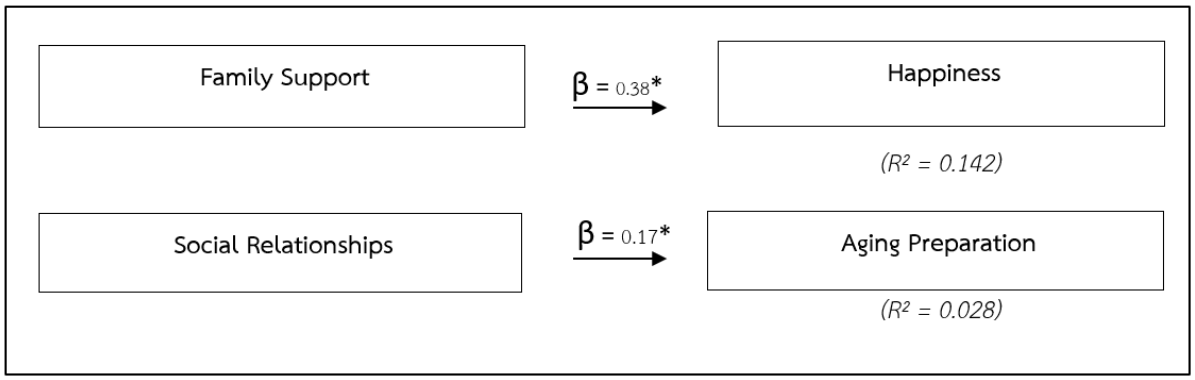
The equation illustrates that for every one-unit increase in social relationships, the level of aging preparation increases by 0.113 units.

Table 5. Multiple regression analysis of factors predicting aging preparation

Predictors	B	SEB	β	t	*p*
Constant	2.242	0.185	-	12.138	< 0.001***
Social Relationships	0.113	0.045	0.168	2.521	0.012*
Variables Excluded: Physical health, Mental health, Economic stability, Housing and environment, Technology and innovation	-	-	-	-	-
Model Statistics: R = 0.168; R^2 = 0.028; Adjusted R^2 = 0.024 F (1, 218) = 6.353; *p*-value = 0.012					

**p* < 0.05, ****p* < 0.001

Based on the aforementioned predictive analysis results, to provide a clearer visualization of the relationships and the influences of independent variables on the happiness and aging preparation of the target population, the researchers summarized the findings in a path diagram, as illustrated in Figure 1.



*$p < 0.05$

Figure 1 Path diagram of factors predicting happiness and aging preparation among rural LGBTQ+ individuals.

4. Discussion

Based on the hypothesis testing that examining factors associated with happiness and aging preparation among LGBTQ+ individuals in rural Thailand, the findings may be interpreted through contemporary perspectives on minority stress, social safety, active aging, and community-based health promotion within the context of rural Thai society.

4.1 Factors Associated with Happiness

The findings demonstrated that family support was the sole statistically significant predictor of happiness among rural LGBTQ+ individuals, accounting for 14.2 percent of the variance ($R^2 = 0.142$). This outcome is consistent with contemporary extensions of Minority Stress Theory, which suggest that long-term exposure to stigma, discrimination, and identity concealment may adversely affect psychological well-being across the life course (Frost & Meyer, 2023; Meyer, 2003). Recent studies further indicate that cumulative minority stress may contribute not only to emotional distress but also to social withdrawal and reduced perceptions of social safety among marginalized populations (Pistella et al., 2024). Within this context, supportive family relationships may function as an important psychosocial buffer that helps reduce emotional strain and supports emotional stability in later life.

This finding aligns with recent LGBTQ+ aging literature emphasizing the importance of social connectedness in later-life adaptation, although the present findings appear to place greater emphasis on interpersonal relational security within rural family structures than has commonly been reported in urban Western settings. In rural Northeast Thailand, specifically in agrarian contexts such as Sisaket Province, kinship structures and interpersonal interdependence remain strongly embedded in everyday community life. Older adults in these areas often rely heavily on close family relationships due to labor migration, limited formal welfare systems, and restricted access to specialized psychosocial services (Knodel et al., 2015; Teerawichitchainan et al., 2015). For LGBTQ+ individuals who may not have biological children or stable long-term caregiving structures, emotional support from family members may therefore contribute substantially to subjective well-being and psychological stability. Rather than functioning solely as interpersonal affection, family support may represent a broader form of relational safety that enables LGBTQ+ older adults to navigate aging-related uncertainty within socially conservative environments. These dynamics may be particularly visible in socially close rural communities where interpersonal familiarity and long-term social visibility simultaneously facilitate community connectedness and reinforce pressures toward identity conformity (Westwood, 2020; Whitehead et al., 2016).

Interestingly, community acceptance did not remain statistically significant in the final regression model despite demonstrating positive correlations at the bivariate level. This finding may suggest that generalized social coexistence alone may not provide the same degree of emotional reassurance as trusted family-based relationships. Recent literature has increasingly discussed the possible role of inclusive social environments, noting that LGBTQ+ older adults frequently continue to experience subtle forms of heteronormative expectation and invisible social boundary maintenance even within relatively tolerant communities (Antoniucci et al., 2026; Baiocco et al., 2024). Consequently, individual well-being may depend more strongly on trusted interpersonal relationships than on broader symbolic acceptance within the community. From health education and community health promotion perspectives, these findings suggest that interventions aimed at strengthening family understanding, emotional communication, and supportive relational contexts may help promote psychosocial well-being among LGBTQ+ older adults in rural settings.

4.2 Factors Associated with Aging Preparation

The findings revealed that social relationships were the sole statistically significant predictor of aging preparation, although the explanatory power of the model remained relatively modest ($R^2 = 0.028$). This finding aligns with contemporary LGBTQ+ aging literature emphasizing that social connectedness and meaningful interpersonal participation within everyday community life play important roles in promoting active aging and psychosocial adaptation among sexual minority older adults (Fredriksen-Goldsen et al., 2015; Hurd & Li, 2023). Recent perspectives further suggest that aging well among LGBTQ+ populations may involve maintaining meaningful social participation and sustaining social belonging within everyday community life rather than relying solely on biomedical indicators of successful aging (Fredriksen-Goldsen et al., 2019; Hurd & Li, 2023).

Within the rural Thai context, these findings may reflect the importance of socially embedded relationships in sustaining emotional continuity and later-life readiness. Rural communities are often characterized by close interpersonal familiarity, informal reciprocity, and community interdependence (Knodel et al., 2015; Teerawichitchainan et al., 2015). Supportive social relationships may therefore facilitate emotional reassurance, practical support, and opportunities for continued engagement in community life. Recent literature has discussed the possible role of meaningful social participation, suggesting that inclusive social environments and participation opportunities may contribute to social confidence and perceptions of future aging readiness among LGBTQ+ adults (Pistella et al., 2024; Tongterm et al., 2026). Although the present study did not directly assess physical activity participation, these findings may indirectly reflect the importance of maintaining socially connected and supportive environments that encourage continued participation in community life (Pistella et al., 2024; WHO, 2002).

The non-significant effects of economic stability, housing and environment, technology and innovation, and mental health may indicate that aging preparation among rural LGBTQ+ individuals is shaped by complex psychosocial conditions extending beyond material resources alone. Recent literature has increasingly emphasized that LGBTQ+ older adults often negotiate aging within environments influenced by accumulated minority stress, social exclusion, and uncertainty regarding future care systems (Westwood, 2020). Consequently, interpersonal support systems may carry greater perceived value than structural resources in contexts where formal institutional support remains limited. Rather than suggesting that environmental or economic conditions are unimportant, the findings may indicate that relational support functions as an essential enabling condition for psychological adaptation and future-oriented planning among marginalized populations in rural communities (Cohen & Wills, 1985).

Although the predictive power of the regression model for aging preparation was relatively low, small effect sizes are anticipated and considered typical within behavioral and health education sciences when examining complex, multidimensional psychosocial phenomena involving marginalized populations (WHO, 2002). The modest explanatory power observed in this study may indicate the presence of additional contextual variables not included in the current model, such as individual resilience, identity affirmation, or culturally embedded coping mechanisms. Recent LGBTQ+ aging literature increasingly suggests that experiences of aging, participation, and well-being emerge through dynamic interactions between minority stress, community participation, and supportive environments across the life course (Frost & Meyer, 2023; Fredriksen-Goldsen et al., 2019; Pistella et al., 2024). Therefore, the findings should be interpreted cautiously as reflecting associative patterns within a specific sociocultural context rather than definitive causal pathways (WHO, 2002).

4.3 Limitations of the Study

Several limitations should be acknowledged. First, although snowball sampling was appropriate for accessing potentially hidden and socially vulnerable populations, the use of non-probability sampling may limit representativeness and reduce generalizability to LGBTQ+ populations in other sociocultural settings (Whitehead et al., 2016). Second, the study relied exclusively on self-reported questionnaire data collected from a single source, which may increase susceptibility to common method bias and social desirability effects, particularly when assessing emotionally sensitive constructs such as happiness, family support, and aging preparation. Third, the cross-sectional design limits interpretation regarding temporal or causal relationships among variables. Additionally, the findings emerged from a specific rural sociocultural context in Northeast Thailand, where kinship systems, community familiarity, and local cultural expectations may shape LGBTQ+ aging experiences differently from urban or international settings. These contextual characteristics should be carefully considered when interpreting the transferability of the findings to other LGBTQ+ populations (Westwood, 2020).

5. Conclusion and suggestions

This study provides empirical evidence regarding factors associated with happiness and aging preparation among LGBTQ+ individuals in rural Thailand, indicating that family support was the strongest predictor of happiness, whereas social relationships emerged as the only statistically significant factor associated with aging preparation. The findings suggest that within rural environments characterized by limited formal welfare systems and strong kinship-oriented social structures, supportive interpersonal relationships function as important psychosocial resources contributing to emotional well-being and later-life readiness. Furthermore, the relatively modest explanatory power of the predictive models reflects the context-dependent nature of psychosocial adaptation and aging processes among sexual and gender minority populations living in rural communities. Within these socially close environments, emotional reassurance and family acceptance contribute substantially to emotional security, facilitating continued social participation and emotional connectedness within community life among LGBTQ+ older adults during later-life transitions.

From health education and community health promotion perspectives, these outcomes underscore the necessity of strengthening supportive social environments, enhancing mutual understanding within families, and promoting socially inclusive participation opportunities for LGBTQ+ individuals transitioning into later life. Local public health organizations, community networks, and rural healthcare systems may therefore consider utilizing family-centered educational processes, peer-support mechanisms,

and existing community social structures as channels for communicating health information, promoting psychosocial support, and strengthening health literacy within rural settings. Such approaches may facilitate healthier, more socially supported, and dignified aging processes among LGBTQ+ populations living within rapidly transforming rural communities. Future health education and sport science research may further expand these findings through mixed-methods approaches, participatory community-based inquiry, and longitudinal comparative studies capable of providing deeper contextual understanding of social support processes, interpersonal adaptation, and aging experiences across different sociocultural environments. Comparative investigations between rural and urban settings may also help clarify whether psychosocial, environmental, and economic conditions influence aging preparation differently across geographical and community contexts, though these characteristics should be carefully acknowledged when interpreting the transferability of the present findings to other LGBTQ+ populations and sociocultural settings.

6. Acknowledgements

This research was supported by Thailand Science Research and Innovation (TSRI) through the Science, Research and Innovation (SRI) Fund (Fiscal Year 2025), with grant administration and oversight provided by Sisaket Rajabhat University. The researchers extend their profound gratitude to the peer reviewers for their invaluable feedback and to the LGBTQ+ participants in rural Sisaket Province whose willingness to share their experiences made this study both possible and academically rigorous.

7. References

Antoniucci, C., Entilli, L., Pistella, J., Lucidi, F., & Baiocco, R. (2026). Older LGB Adults and Sport-Related Contexts: Discrimination, Evolving Context, Motivations, and Attitudes Toward LGBTQ+ Sports Associations. Journal of homosexuality, 1-24. https://doi.org/10.1080/00918369.2026.2642703

Baiocco, R., Antoniucci, C., Pistella, J., Alessandri, G., Alivernini, F., Borghi, A., Chirico, A., Filosa, L., Fini, C., Palombi, T., Rosati, F., Tavolucci, S., & Lucidi, F. (2024). Aging well in an aging society: physical health in older lesbian, gay, and bisexual adults. Frontiers in Psychology, 15, 1369021. https://doi.org/10.3389/fpsyg.2024.1369021

Best, J. W. (1981). Research in education (4th ed.). Englewood Cliffs, NJ: Prentice-Hall.

Christian, L. M., Cole, S. W., McDade, T., Pachankis, J. E., Morgan, E., Strahm, A. M., & Dush, C. M. K. (2021). A Biopsychosocial Framework for Understanding Sexual and Gender Minority Health: A Call for Action. Neuroscience & biobehavioral reviews, 129, 107-116. https://doi.org/10.1016/j.neubiorev.2021.06.004

Christian, L. M., Wilson, S., Madison, A. A., Dush, C. M. K., McDade, T. W., Peng, J., Andridge, R. R., Morgan, E., Manning, W., & Cole, S. W. (2025). Sexual minority stress and epigenetic aging. Brain, behavior, and immunity, 126, 24-29. https://doi.org/10.1016/j.bbi.2025.01.022

Cohen, S., & Wills, T. A. (1985). Stress, social support, and the buffering hypothesis. Psychological Bulletin, 98(2), 310–357. https://doi.org/10.1037/0033-2909.98.2.310

Diener, E. (2012). New findings and future directions for subjective well-being research. American Psychologist, 67(8), 590–597. https://doi.org/10.1037/a0029541

Faul, F., Erdfelder, E., Lang, A. G., & Buchner, A. (2007). G*Power 3: A flexible statistical power analysis program for the social, behavioral, and biomedical sciences. Behavior Research Methods, 39(2), 175–191. https://doi.org/10.3758/BF03193146

Field, A. (2024). Discovering statistics using IBM SPSS statistics (6th ed.). London: SAGE Publications.

Fredriksen-Goldsen, K. I., Kim, H. J., Bryan, A. E., Shiu, C., & Emlet, C. A. (2017). The cascading effects of marginalization and pathways of resilience in attaining good health among LGBT older adults. The Gerontologist, 57, suppl_1, S72–S83. https://doi.org/10.1093/geront/gnw170

Fredriksen-Goldsen, K. I., Kim, H. J., Shiu, C., Goldsen, J., & Emlet, C. A. (2015). Successful aging among LGBT older adults: Physical and mental health-related quality of life by age group. The Gerontologist, 55(1), 154–168. https://doi.org/10.1093/geront/gnu081

Fredriksen-Goldsen, K. I., Jen, S., & Muraco, A. (2019). Iridescent Life Course: LGBTQ Aging Research and Blueprint for the Future – A Systematic Review. Gerontology, 65(3), 253 - 274. https://doi.org/10.1159/000493559

Fredriksen-Goldsen, K. I., Kim, H. J., Barkan, S. E., Muraco, A., & Hoy-Ellis, C. P. (2013). Health Disparities Among Lesbian, Gay, and Bisexual Older Adults: Results from a Population-Based Study, American Journal of Public Health, 103(10), 1802-1809. https://doi.org/10.2105/AJPH.2012.301110

Frost, D. M., & Meyer, I. H. (2023). Minority stress theory: Application, critique, and continued relevance. Current opinion in psychology, 51, 101579. https://doi.org/10.1016/j.copsyc.2023.101579

House, J. S. (1981). Work stress and social support. Reading, MA: Addison-Wesley.

Hurd, L., & Li, L. Y. (2023). "I Want to Grow Older with Dignity": Older LGBTQ+ Canadian Adults' Perceptions and Experiences of Aging. Journal of Applied Gerontology, 43(5), 536 - 549. https://doi.org/10.1177/07334648231219414

Iamko, S., & Boonnun, V. (2021). Stigmatization and pressing LGBT STIGMATIZATION AND PRESSING LGBTQ IN THAI SOCIETY. Academic Journal Phranakhon Rajabhat University, 12(1), 384–398. retrieved from https://so01.tci-thaijo.org/index.php/AJPU/article/view/246770 (in Thai)

Knodel, J., Teerawichitchainan, B., Prachuabmoh, V., & Pothisiri, W. (2015). The situation of Thailand's older population: An update based on the 2014 survey of older persons in Thailand. Research Collection School of Social Sciences [Online]. Retrieved October 22, 2025, from: https://ink.library.smu.edu.sg/soss_research/1948

Langarita, J. A., Montserrat, C., Fustier-García, N., & Albertín, P. (2025). Exploring the Impact of LGBTIQ Policies on Childhood: A Comparative Analysis in Three EU Countries. Sexuality Research and Social Policy, 1 - 1 5 . https://doi.org/10.1007/s13178-025-01196-3

Meyer, I. H. (2003). Prejudice, social stress, and mental health in lesbian, gay, and bisexual populations: Conceptual issues and research evidence. Psychological Bulletin, 129(5), 674–697. https://doi.org/10.1037/0033-2909.129.5.674

Pachankis, J. E., Mahon, C. P., Jackson, S. D., Fetzner, B. K., & Bränström, R. (2020). Sexual orientation concealment and mental health: A conceptual and meta-analytic review. Psychological bulletin, 146(10), 831-837. https://doi.org/10.1037/bul0000271

Pistella, J., Baiocco, R., Antoniucci, C., Alessandri, G., Alivernini, F., Borghi, A., Filosa, L., Fini, C., Palombi, T., Tavolucci, S., & Lucidi, F. (2024). Older LGBT+ Adults and Physical Activity: A Systematic Review of Qualitative and Quantitative Data. Sexuality Research and Social Policy, 22(1), 226 - 251. https://doi.org/10.1007/s13178-023-00925-w

Queiroz, A. L. N., Meng, Z., Hall, C. D. X., Lane, B., Wang, L., Haughbrook, R., ... & Ibragimov, U. (2026). A multilevel analysis of LGBT-relevant laws and sexual and gender minority mental health: evidence for the protective role of inclusive policies. BMC Public Health, 26(733), 1-13. https://doi.org/10.1186/s12889-026-26309-4

Teerawichitchainan, B., Pothisiri, W., & Long, G. T. (2015). How do living arrangements and intergenerational support matter for psychological health of elderly parents? Evidence from Myanmar, Vietnam, and Thailand. Social Science & Medicine, 136, 106–116. https://doi.org/10.1016/j.socscimed.2015.05.019.

Tongterm, T., Nantasing, W., Setthamas, M., & Kaewma, J. (2026). From minority stress to active aging readiness: inclusive recreation as community-level social infrastructure for LGBTQ+ adults in rural Thailand. Retos, 78, 41-52. https://doi.org/10.47197/retos.v78.118481

United Nations Development Programme (UNDP). (2014). Being LGBT in Asia: Thailand country report [Online]. Retrieved October 22, 2025, from: https://www.undp.org/thailand/publications/being-lgbt-asia-thailand-country-report

Westwood, S. (2020). The myth of 'older LGBT+' people: Research shortcomings and policy/practice implications for health/care provision. Journal of Aging Studies, 55, 100880. https://doi.org/10.1016/j.jaging.2020.100880

Whitehead, J., Shaver, J., & Stephenson, R. (2016). Outness, stigma, and primary health care utilization among rural LGBT populations. PLoS One, 11(1), e0146139. https://doi.org/10.1371/journal.pone.0146139

World Health Organization (WHO). (2002). Active ageing: A policy framework [Online]. Retrieved October 22, 2025, from: https://iris.who.int/handle/10665/67215

Yodlorchai, R., Suttiwan, P., Walch, S. E., & Ngamake, S. (2024). Interpersonal and environmental microaggressions & depression: Thai LGBQ+ perspectives. Humanities, Arts and Social Sciences Studies, 24(2), 353–363. https://doi.org/10.69598/hasss.24.2.266035

การกำกับติดตามการบังคับใช้กฎหมายสิ่งแวดล้อมทางทะเล กรณีน้ำมันรั่วไหลจากเรือเดินสมุทรในท่าเรือหลักของไทย

Oil Spill Monitoring and Marine Environmental Law Enforcement for Ship-Source Pollution in Major Ports of Thailand

สิรภูมิ กระต่ายทอง[1*] นันท์นภัสร อินยิ้ม[1] เสรีย์ ตู้ประกาย[1] และ ปิยะรัตน์ ปรีย์มาโนช[1]

Siraphum Krataithong[1*], Nannapasorn Inyim[1], Seree Tuprakay[1] and Piyarat Premanoch[1]

[1]คณะวิศวกรรมศาสตร์ มหาวิทยาลัยรามคำแหง กรุงเทพมหานคร

[1]Faculty of Engineering, Ramkhamhaeng University, Bangkok

[*]Corresponding Author: 6419770004@rumail.ru.ac.th

Received: February 17, 2026 **Revised:** April 20, 2026 **Accepted:** May 19, 2026

บทคัดย่อ

การรั่วไหลของน้ำมันจากเรือยังคงเป็นปัญหาสิ่งแวดล้อมที่สำคัญในท่าเรือขนาดใหญ่ โดยเฉพาะในประเทศที่กำลังพัฒนาศักยภาพทางทะเล งานวิจัยนี้ศึกษาการติดตามกำกับดูแลการบังคับใช้กฎหมายกรณีน้ำมันรั่วไหลในท่าเรือหลักของไทย ท่าเรือมาบตาพุด ท่าเรือสัตหีบ และท่าเรือแหลมฉบัง เน้นความสัมพันธ์ระหว่างการบังคับใช้กฎหมายกับการนำเทคโนโลยีสมัยใหม่มาใช้ในกระบวนการปฏิบัติงานและประสิทธิผลของการปฏิบัติการ ใช้ระเบียบวิธีวิจัยแบบผสมผสาน ขั้นที่ 1 เก็บข้อมูลเชิงคุณภาพผ่านการสัมภาษณ์เชิงลึกแบบกึ่งโครงสร้างจากผู้เชี่ยวชาญและผู้บริหารหน่วยงานที่มีส่วนได้เสียแบบเฉพาะเจาะจง 11 ท่าน พบว่าการใช้เทคโนโลยีสมัยใหม่ เช่น ดาวเทียม ยานไร้คนขับ และปัญญาประดิษฐ์ รวมทั้งการจัดการข้อมูลดิจิทัลและการบูรณาการระบบเฝ้าระวังแบบเรียลไทม์ มีผลต่อการติดตามกำกับดูแลการบังคับใช้กฎหมาย ในขั้นที่ 2 ทำการประเมินเชิงปริมาณในการรับรู้ประสิทธิผลการกำกับดูแลกรณีน้ำมันรั่วไหลจากกลุ่มตัวอย่างในขั้นที่ 1 วิเคราะห์ข้อมูลโดยใช้สถิติเชิงพรรณา พบว่ากลไกการเฝ้าระวังและตอบสนองน้ำมันรั่วไหลต่ออุบัติเหตุการเดินเรือได้รับการประเมินว่ามีประสิทธิผลในระดับสูง แต่มีประสิทธิผลลดลงในกรณีข้อขัดข้องทางเทคนิคและความผิดพลาดจากผู้ปฏิบัติงาน และมีระดับต่ำในกรณีการสอบสวนและการดำเนินคดี การศึกษาชี้ให้เห็นว่าเทคโนโลยีตรวจจับและติดตามสมัยใหม่และการจัดการข้อมูลดิจิทัลเป็นปัจจัยสำคัญต่อการบรรลุเจตนารมย์ของกฎหมาย ดังนั้น จึงต้องพัฒนานโยบายพร้อมแนวทางบูรณาการกับการขับเคลื่อนด้วยเทคโนโลยีสมัยใหม่และการใช้ข้อมูลดิจิทัลทางกฎหมายตามมาตรฐานสากล ตลอดจนเสริมสร้างสมุทราภิบาลและการพัฒนาทางทะเลอย่างยั่งยืน

คำสำคัญ: น้ำมันรั่วไหลจากเรือเดินสมุทร, ประสิทธิภาพการบังคับใช้กฎหมาย, เทคโนโลยีการติดตาม, การจัดการท่าเรือ

Abstract

Ship-source oil spills remain a persistent environmental challenge in large ports, particularly in developing maritime states. This study investigates oil spill monitoring and law enforcement in Thailand's major ports, including Map Ta Phut, Laem Chabang, and Sattahip, with a focus on the interaction among technology, data, institutional coordination, and enforcement. It employs a mixed-methods research design (n = 11), combining qualitative interviews and quantitative expert elicitation. In Phase 1, qualitative data were collected through semi-structured in-depth interviews with eleven purposively selected key stakeholders and analyzed thematically to identify structural, technological, and legal constraints. The findings indicate that advanced monitoring technologies, including satellite-based surveillance, unmanned aerial vehicles (UAVs), real-time sensing systems, AI-based data analytics, digital data management systems, and integrated real-time monitoring platforms, are critical for effective detection and response. In Phase 2, quantitative assessments were conducted with the same group using a five-point Likert scale to evaluate

perceived government effectiveness. The findings reveal a clear disparity in enforcement effectiveness across different types of oil spill incidents. Monitoring and response mechanisms for navigation-related accidents were perceived as highly effective (mean = 4.00-4.27). In contrast, effectiveness declined to moderate levels for incidents caused by technical failures and human error (mean = 3.00-3.27). It was rated low for the investigation and prosecution of illegal oil discharges (mean = 2.73). The results highlight a significant enforcement gap between law enforcement practices and the adoption of advanced monitoring technologies, as well as their impact on operational effectiveness, primarily due to limitations in legal frameworks, evidentiary standards, and inter-agency coordination. The study underscores the need to develop integrated policies to enhance technological integration, recognize digital data as admissible legal evidence, and strengthen institutional coordination to meet international standards, thereby improving maritime good governance and sustainable marine development.

Keywords: Ship-source oil spills, Law enforcement effectiveness, Monitoring technology, Port governance

1. Introduction

Marine oil pollution from ships continues to pose significant environmental and governance concerns, particularly in large commercial and industrial ports where maritime traffic and oil-related activities are highly concentrated. Oil spill incidents in such areas can cause significant ecological damage, disrupt port operations, and undermine public confidence in environmental regulation (Ebisi et al., 2025). Effective management of ship-source oil pollution, therefore, requires not only a comprehensive legal framework but also robust institutional capacity and operational mechanisms that enable prevention, detection, and enforcement in practice (Siraphum & Nannapasorn, 2021).

At the international level, marine oil pollution is governed by well-established legal instruments, including the United Nations Convention on the Law of the Sea (UNCLOS), the International Convention for the Prevention of Pollution from Ships (MARPOL), and the International Convention on Civil Liability for Oil Pollution Damage (CLC) (Hadavand et al., 2022; Jumphot, 2017; Department of Legal Treaties, 2005; Subcommittee on Knowledge Management for National Maritime Interest, 2019). These instruments establish obligations related to pollution prevention, monitoring, reporting, and liability. However, existing literature suggests that the primary challenge lies not in the absence of legal frameworks, but in the effective implementation and enforcement of pollution control regimes at the operational level. Previous studies further indicate that ship-source oil spill incidents arise from multiple causes, including maritime accidents, technical and design failures, human error, and intentional illegal discharges. These causes are closely linked to broader systemic issues, including policy clarity, legal adaptation, inter-agency coordination, data integration, and gaps in operational and personnel standards (Purohit et al., 2024).

In light of these findings, in large port contexts, oil spill governance is shaped by the interaction of multiple authorities responsible for environmental protection, maritime safety, and maritime security. Fragmented mandates, limited inter-agency coordination, and uneven access to operational data have been widely identified as factors that weaken enforcement outcomes, particularly in cases involving operational failures or covert non-compliant practices. These challenges are further compounded when incidents involve foreign-flagged vessels, giving rise to jurisdictional and evidentiary constraints that complicate investigation and prosecution processes (Siraphum & Nannapasorn, 2022).

A recent study highlights the growing role of advanced monitoring and surveillance technologies in enhancing oil spill detection and enforcement capacity. Such technologies include sensing systems,

unmanned vehicles, mathematical and trajectory models, artificial intelligence and data analytics, communication networks, and environmental data integration platforms (Siraphum et al., 2025). Beyond their technical functions, these technologies increasingly serve as institutional enablers by linking regulatory intent to enforcement outcomes through improved situational awareness, coordinated responses, and evidentiary support for investigation and prosecution. Nevertheless, limitations persist in inter-agency data integration and in the absence of clear legal mechanisms to support the admissibility of technological evidence in judicial processes. Empirical research examining how these technologies are operationalized within legal enforcement practices at the port level remains limited, particularly in developing maritime states (Al-Qassim, 2023).

In Thailand, major ports such as Map Ta Phut, Laem Chabang, and Sattahip play a critical role in international trade and industrial development; however, increasing maritime traffic and energy-related activities (Marine Department, 2024), particularly within the Eastern Economic Corridor, pose a significant risk of ship-source oil pollution (Marine Department, 2021). Although Thailand has ratified relevant international instruments governing ship-source oil pollution, limitations persist in operational enforcement and preventive capacity at the port level. At the domestic level, an extensive legal framework has been enacted to support the implementation of these international obligations (Govindarajan et al., 2021). Key legislation includes the Enhancement and Conservation of National Environmental Quality Act, the Promotion of Marine and Coastal Resources Management Act, and the Thai Navigation in Thai Waters Act, as well as related maritime liability and compensation laws. However, the enforcement of these laws is distributed across multiple government agencies with overlapping mandates, resulting in challenges related to coordinated operations, data sharing, and consistent enforcement practices (De Kerf et al., 2024).

Although previous studies have identified constraints related to monitoring capacity, institutional coordination, and enforcement effectiveness in ship-source oil pollution governance, existing literature remains largely descriptive, with limited integration of technological, institutional, and legal dimensions, particularly in developing maritime states. Consequently, there is limited empirical understanding of how existing legal and institutional frameworks function in practice at the operational level within major port environments. In this study, effectiveness is operationally defined as the perceived performance of monitoring and enforcement systems across operational stages, including prevention, emergency response, investigation, and prosecution, based on expert Likert-scale assessments and qualitative insights. This study addresses these gaps by examining stakeholder perspectives on the effectiveness of oil spill monitoring systems, legal enforcement, and institutional coordination in Thailand's major ports, including Map Ta Phut, Laem Chabang, and Sattahip, using a mixed-methods approach that integrates qualitative interviews with quantitative assessments of enforcement effectiveness.

The study addresses the following research questions: 1) How effective are current monitoring and law enforcement mechanisms across operational stages? and 2) What technological and institutional factors influence enforcement effectiveness? It also identifies key technological, institutional, and legal factors shaping ship-source oil spill governance and provides policy-relevant insights for strengthening technology-enabled enforcement and sustainable port management.

2. Materials and methods

This study employed a mixed-methods research design comprising two successive stages: (1) a qualitative stage aimed at exploring key challenges in oil spill monitoring, law enforcement, and institutional coordination, and (2) a quantitative stage designed as an expert elicitation approach to assess the perceived

effectiveness of monitoring and law enforcement. The study framework is informed by a socio-technical perspective, conceptualizing oil spill governance as an interaction among monitoring technology, institutional capacity, and legal enforcement. These three dimensions are analytically framed as interdependent components, where technological capabilities enable detection and monitoring, institutional capacity determines coordination and implementation effectiveness, and legal enforcement provides the regulatory authority for compliance and accountability.

While previous studies have examined these dimensions in isolation, this study contributes by integrating them into a unified socio-technical framework. Furthermore, the expert elicitation approach provides empirical evidence from real-world experience on how the interactions among these factors affect the effectiveness of monitoring and law enforcement in the context of maritime governance. In-depth interviews were conducted with experts from a range of stakeholder groups involved in maritime operations and environmental law enforcement in Thailand. This design enabled the collection of detailed qualitative insights into key challenges, alongside structured quantitative data on stakeholders' assessments of the effectiveness of existing monitoring and enforcement systems. This study was approved by the Institutional Review Board (IRB) of Ramkhamhaeng University, RU-HRE 67/0086, 17 May 2024. Informed consent was obtained from all participants.

2.1 Data Collection

In Phase 1, qualitative data were collected through semi-structured in-depth interviews with 11 purposively selected key informants who had direct responsibilities for, or professional expertise in, the monitoring, regulation, and response to marine oil pollution incidents in Thailand. The informants represented a broad range of institutional perspectives and included academics and senior officials from relevant organizations, namely the Map Ta Phut Industrial Port Office, 1 person; Sattahip Commercial Port, 1 person; the Operations Office of the Marine Department, 1 person; the Thai Maritime Enforcement Command Center (TH-MECC), 2 persons; the Marine Police, 1 person; the Judge Advocate General's Office, 1 person; HTMS Similan, 1 person; the Investigation and Legal Office of TH-MECC, 1 person; the Meteorological Department, 1 person; and the Faculty of Logistics (Maritime Business), Burapha University, 1 person.

The interviews followed a semi-structured format, using predefined guiding questions aligned with the research objectives while allowing flexibility for open discussion and follow-up probing based on the informants' expertise and responses. This approach enabled the collection of detailed, context-specific insights into practical challenges related to oil spill monitoring, legal enforcement, and institutional coordination. The interviews focused on three primary issues: (1) challenges in law enforcement under domestic and international legal frameworks; (2) the role and adequacy of existing technologies for monitoring and enforcement; and (3) the effectiveness of current preventive measures addressing different causes of oil spill incidents. The research instrument consisted of two components: an introductory component collecting general background information from the informants, and a substantive component comprising questions organized into five thematic areas. These areas addressed: (1) limitations in the enforcement of marine environmental laws at national and international levels, particularly in cases involving foreign-flagged vessels; (2) the application of technological and engineering-based approaches for oil spill monitoring and control; (3) preventive measures related to technical failures, human error, and intentional violations; (4) regulatory performance in prevention, emergency response, investigation, and prosecution; and (5) the consistency of Thailand's monitoring systems and legal framework with international marine environmental law principles.

In Phase 2, following the qualitative interviews, each informant was asked to provide quantitative assessments of the perceived effectiveness of government monitoring and supervision across key operational stages, including prevention, emergency response, and legal action. These assessments were rated on a five-point Likert scale to enable comparative evaluation across different operational scenarios.

This approach was adopted to ensure that the quantitative results (mean and SD) reflected the consensus of high-level practitioners. In this context, oil spill monitoring and enforcement involve technically complex systems and require coordination. Accordingly, expert elicitation provides a more suitable analytical approach by capturing specialized expertise and strategic insights from senior practitioners and policymakers, rather than statistical generalization to a broader population. The structured questionnaire was developed based on insights from the qualitative phase, ensuring conceptual alignment between the two phases of the study.

The data collection instrument was designed to support a systematic assessment of the governance framework for ship-source oil spill management and to enable a gap analysis between international legal requirements and their practical implementation within the Thai context. Subject-matter experts reviewed the semi-structured interview questions and the five-point Likert scale to ensure content validity, including assessment using the IOC index to refine the clarity, relevance, and reliability of the research tools, as approved by the IRB of Ramkhamhaeng University.

2.2 Data Analysis and Integration of Findings

Qualitative and quantitative data were analyzed in parallel in accordance with the mixed-methods research design. Qualitative data obtained from the semi-structured interviews were subjected to thematic analysis. Interview transcripts and detailed field notes were systematically reviewed, coded, and organized to identify recurring patterns and key themes related to law enforcement, technological capacity, institutional coordination, and preventive measures in ship-source oil spill management. This analysis aimed to identify structural, legal, and operational constraints affecting the effectiveness of monitoring and enforcement within Thailand's port governance framework.

Quantitative data derived from the five-point Likert scale assessments were analyzed using descriptive statistical methods. Mean values and standard deviations were calculated to evaluate stakeholders' perceptions of government performance across three core operational stages: prevention, emergency response, and investigation and prosecution. These measures were used to compare perceived performance levels across different operational scenarios and causes of oil spill incidents, as well as to assess the consistency of regulatory implementation.

The integration of qualitative and quantitative findings was conducted through comparative and interpretive analysis. Qualitative insights were used to explain and contextualize patterns observed in the quantitative results, thereby supporting a systematic gap analysis between international marine environmental law standards and their practical implementation in Thailand. This integrated analysis provided a robust empirical basis for identifying governance weaknesses and formulating evidence-based recommendations to strengthen ship-source oil spill monitoring and legal enforcement in Thailand's major ports.

3. Results

This section presents the study findings from both qualitative and quantitative analyses. The qualitative results highlight key themes derived from stakeholder perspectives on ship-source oil spill

management, followed by quantitative findings on perceived government effectiveness in monitoring, response, and enforcement.

3.1 Qualitative findings: key challenges in ship-source oil spill management

The analysis identified five major themes reflecting underlying governance challenges in ship-source oil spill management. These themes are summarized in Table 1.

Table 1 summarizes the five major themes derived from the thematic analysis, together with their core analytical focus and key issues identified by stakeholders. The following subsections elaborate on each theme and provide a detailed qualitative account of the institutional, technological, and operational challenges shaping ship-source oil spill governance in Thailand.

Table 1. Summary of qualitative themes on ship-source oil spill management

Theme	Core Focus	Key Issues Identified
Theme 1: Limitations in Legal Enforcement and Regulatory Structure	Institutional and legal governance	Fragmented mandates; overlapping agency responsibilities; jurisdictional ambiguity; enforcement challenges involving foreign-flagged vessels
Theme 2: Insufficient Application of Monitoring and Surveillance Technologies	Technological capacity for enforcement	Limited real-time monitoring coverage; insufficient reliability of monitoring data for legal evidence; underutilization of technology in investigation and prosecution
Theme 3: Systematic Approaches to Oil Spill Prevention	Preventive governance mechanisms	Reactive management orientation; weaknesses in inspection regimes; inconsistent maintenance and preventive controls
Theme 4: Human Factors and Operational Risks	Operational and behavioral dimensions	Human error during oil transfer operations; inconsistent training and supervision; variability in operational standards
Theme 5: Interagency Integration and International Cooperation	Coordination and transboundary governance	Limited inter-agency information sharing; lack of integrated monitoring systems; need for international cooperation in cross-jurisdictional cases

Theme 1: Limitations in legal enforcement and regulatory structure

The interview findings indicate that, although Thailand has adopted relevant international maritime environmental conventions and enacted domestic legislation on oil pollution prevention, the effectiveness of enforcement remains limited in practice. Most respondents identified the regulatory framework as structurally fragmented, characterized by the involvement of multiple agencies with overlapping responsibilities. This fragmentation was consistently highlighted as a major barrier to effective enforcement, as it often leads to unclear institutional authority and delays in enforcement actions.

Furthermore, interviewees emphasized the particular challenges associated with enforcing environmental laws against foreign-flagged vessels. These challenges include ambiguities in jurisdiction, procedural delays, and difficulties in coordinating legal processes across responsible agencies. Such

constraints were perceived to significantly undermine the operational capacity to investigate and prosecute oil pollution cases, especially within large port areas. Overall, the interview data suggest that improving enforcement effectiveness requires clearer institutional coordination and more integrated implementation of existing regulatory frameworks, rather than the introduction of additional legal instruments alone.

Theme 2: Insufficient application of monitoring and surveillance technologies

A second major theme concerns the limited application of modern monitoring and surveillance technologies in oil spill detection and enforcement. Respondents consistently noted that existing technological systems are insufficient for continuous, real-time monitoring of oil discharges and spill movements, particularly during nighttime operations and across extensive maritime areas surrounding major ports.

In addition to these operational limitations, interviewees expressed concern regarding the legal utility of current monitoring data. Monitoring outputs were often perceived as lacking the technical reliability and evidentiary credibility required for use in judicial proceedings, thereby constraining their effectiveness in supporting investigation and prosecution. As a result, the potential of technology to function as an enforcement enabler remains underutilized.

From the stakeholders' perspective, enhanced and integrated monitoring systems capable of generating verifiable and legally defensible data were viewed as essential for strengthening enforcement capacity. Such systems were expected to improve situational awareness, facilitate inter-agency coordination, and enable more effective detection of covert illegal oil discharges.

Theme 3: Systematic approaches to oil spill prevention

The interviews reveal a shared view that oil spill management in Thailand remains predominantly reactive, with greater emphasis placed on emergency response than on preventive control. Respondents emphasized that effective prevention requires a systematic governance approach encompassing regular vessel and port inspections, strict enforcement of maintenance standards, and oversight of repair and modification procedures.

Stakeholders indicated that weaknesses in inspection regimes and preventive maintenance increase the likelihood of technical failures and operational accidents that may lead to oil spill incidents. Preventive governance was therefore viewed as a critical component of effective marine environmental protection, particularly in high-risk port environments. Interviewees suggested that strengthening preventive mechanisms through more consistent inspection practices and risk-based monitoring would reduce spill risks and enhance overall management outcomes.

Theme 4: Human factors and operational risks

Human error emerged as a significant contributor to oil spill incidents, particularly during oil transfer and handling operations. Interviewees noted that, despite the presence of technical systems and regulatory controls, operational mistakes by ship crews and port personnel remain a persistent risk.

Contributing factors identified by respondents included inconsistent training standards, limited supervision, and variations in operational procedures among vessels and operators. These findings suggest that technological and regulatory measures alone are insufficient to address operational risks without parallel efforts to strengthen human capacity. Improved training, competency development, and operational discipline were therefore identified as essential complements to technical and legal controls in reducing spill incidents and supporting effective enforcement in practice.

Theme 5: Interagency integration and international cooperation

The final theme highlights the importance of integrated interagency collaboration and international cooperation in managing ship-source oil pollution. Respondents widely agreed that oil

pollution from ships is a transboundary issue that cannot be effectively addressed by a single agency or within national jurisdiction alone.

Interviewees emphasized the need for enhanced information sharing, coordinated monitoring systems, and joint investigations among domestic agencies. In addition, cooperation with international organizations and neighboring states was viewed as essential, particularly in cases involving high-risk or foreign-flagged vessels operating across multiple jurisdictions. From the stakeholders' perspective, stronger interagency and international integration was regarded as a key factor in improving enforcement efficiency and addressing complex oil pollution incidents in major port areas.

3.2 Quantitative findings: perceived effectiveness of government oversight in ship-source oil spill management

Following the qualitative interviews, informants provided quantitative assessments of the perceived effectiveness of government monitoring and supervision across key stages of ship-source oil spill management: prevention, emergency response, and legal action. The quantitative results are presented below according to these operational stages.

3.2.1 Perceived effectiveness of government oversight in oil spill prevention

Stakeholders' assessments of the effectiveness of government oversight in preventing oil spill incidents arising from different causes are presented in Table 2. Overall, preventive monitoring related to navigational accidents received the highest effectiveness score among all categories, suggesting strong confidence in existing preventive measures for overt maritime operational risks.

In contrast, the preventive effectiveness of government oversight was rated at a moderate level for oil spill incidents caused by technical failures of vessels or equipment and human error during oil transfer operations. These comparatively lower ratings indicate that preventive monitoring and oversight mechanisms are perceived to be less effective in addressing risks associated with complex technical systems and operational practices. Variability in stakeholder responses, particularly with respect to technical failures, suggests differences in professional perspectives and institutional roles among the respondents.

Similarly, although the prevention of illegal oil discharges received slightly higher ratings than those related to technical failures and human error, the results indicate only a moderate level of perceived deterrence effectiveness. When considered in conjunction with the qualitative findings, this pattern points to potential limitations in existing preventive measures, particularly in their capacity to deter intentional violations under conditions of enforcement complexity, including cases involving foreign-flagged vessels.

Table 2. Effectiveness of government oversight in preventing major causes of oil spills

Cause of Oil Spill	Mean	Standard Deviation	Level of Efficiency
Accidents from Navigation	4.27	0.45	High
Technical failures of vessels or equipment	3.09	0.67	Moderate
Human error during oil transfer operations	3.09	0.51	Moderate
Illegal discharge of oil	3.45	0.50	Moderate

Note: The level of efficiency is interpreted based on the mean score as follows: 1.00–1.80 = Very Low; 1.81–2.60 = Low; 2.61–3.40 = Moderate; 3.41–4.20 = High; and 4.21–5.00 = Very High. This interpretation applies to Tables 2–5.

3.2.2 Perceived Effectiveness of Government Oversight in Emergency Response and Control

Stakeholders' perceptions of the effectiveness of government oversight in controlling and responding to oil spill incidents are presented in Table 3. Across incident categories, emergency response capacity received relatively high effectiveness ratings for incidents associated with navigational accidents and illegal oil discharges. However, effectiveness ratings remained at a moderate level for incidents caused by technical failures and human error. This pattern mirrors the prevention-stage findings and indicates that response effectiveness varies depending on the underlying cause of the incident. The persistence of moderate ratings for technical and human-related incidents reinforces qualitative insights regarding operational complexity and uneven enforcement capacity.

Taken together, these findings suggest that while emergency response mechanisms are generally effective, their performance is less consistent in scenarios involving less visible or more operationally complex causes of oil spills.

Table 3. Effectiveness of government oversight in emergency response and control

Cause of Oil Spill	Mean	Standard Deviation	Level of Efficiency
1. Accidents from Navigation	4.18	0.39	High
2. Technical failures of vessels or equipment	3.27	0.75	Moderate
3. Human error during oil transfer operations	3.36	0.48	Moderate
4. Illegal discharge of oil	3.73	0.45	High

3.2.3 Perceived Effectiveness of Government Oversight in Investigation and Prosecution

Table 4 shows stakeholders' assessments of government effectiveness in the post-incident phases of investigation and legal proceedings. The data indicate notable variation in perceived enforcement effectiveness across different types of oil spill incidents.

Investigation and prosecution associated with navigational accidents were rated as relatively effective, consistent with the clearer attribution of causation and responsibility in such cases. By comparison, effectiveness ratings declined to a moderate level for incidents involving technical failures and human error, indicating greater difficulty in establishing liability.

Most critically, the investigation and prosecution of illegal oil discharges received the lowest ratings among the incident categories and were rated as low. The consistency of responses indicates a shared stakeholder perception of limited enforcement effectiveness in this area. These results are consistent with qualitative evidence pointing to constraints related to detection capability, evidentiary adequacy, jurisdictional complexity, and the enforcement of regulations against foreign-flagged vessels.

Table 4. Perceived effectiveness of government oversight in investigating and prosecuting major causes of oil spills

Cause of Oil Spill	Mean	Standard Deviation	Level of Efficiency
Accidents from Navigation	4.00	0.60	High
Technical failures of vessels or equipment	3.18	0.39	Moderate
Human error during oil transfer operations	3.00	0.60	Moderate
Illegal discharge of oil	2.73	0.45	Low

3.2.4 Perceived Impact of Monitoring Systems on the Effectiveness of Oil Spill Management Processes

Stakeholders assessed the perceived impact of monitoring systems on the effectiveness of key stages in oil spill management, as summarized in Table 5. The results indicate that monitoring systems were perceived to have a high level of impact on the effectiveness of oil spill management across all stages. Among the assessed stages, emergency response management received the highest perceived impact rating, followed by incident prevention, investigation and legal action, pollution management planning, and environmental restoration, respectively.

Although the perceived impact of monitoring systems on pollution management planning and environmental restoration remained within the high category, these stages received comparatively lower ratings than other management stages. This pattern indicates that the role of monitoring systems is more clearly recognized in stages that rely on real-time information and operational decision-making, such as emergency response and incident prevention, whereas their perceived impact is less pronounced in longer-term or post-incident management processes, including planning and environmental restoration.

The results show that monitoring systems are perceived as highly effective, particularly in cases involving visible oil spills that can be directly detected and controlled. However, monitoring is less effective in detecting non-visible violations, such as illegal discharges at night or equipment-related failures. These limitations are more pronounced for foreign-flagged vessels due to constraints in data access, limited inspection time, and protections under international law.

Table 5. Perceived impact of monitoring systems on oil spill management processes

Process in Oil Spill Management	Mean	Standard Deviation	Level
Pollution Management Planning	4.00	0.60	High
Incident Prevention	4.27	0.45	High
Emergency Response Management	4.45	0.50	High
Investigation and Legal Action	4.18	0.39	High
Environmental Restoration	3.91	0.51	High

4. Discussion

This section integrates and interprets findings from both qualitative and quantitative data to develop a comprehensive understanding of the challenges and opportunities in strengthening Thailand's regulatory framework for ship-source marine oil pollution control. Evidence from both sets of data reveals that the current system is strong in dealing with visible spill incidents, while exhibiting significant weaknesses in proactive prevention and legal enforcement against covert and difficult-to-detect violations. These findings underscore an urgent need for strategic investment and structural reform (UNEP, 2019).

A key finding is the pronounced disparity in the perceived effectiveness of government oversight across different dimensions of ship-source oil spill management. While stakeholders generally regarded surveillance and response capacities for clearly observable incidents, such as navigation-related accidents, as highly effective, perceived effectiveness declined markedly when addressing less visible causes, including technical failures and human error. Most concerning is the finding that effectiveness was rated as low for the investigation and prosecution of illegal oil discharges. This pattern suggests that the existing system is predominantly reactive rather than preventive in nature: it is well equipped to manage overt crises, yet

struggles to deter, detect, and prosecute clandestine activities or incidents where the pollution source cannot be readily identified. Such incidents may nonetheless account for a substantial proportion of oil pollution entering the marine environment (De Kerf et al., 2024).

This enforcement gap related to covert violations directly aligns with the qualitative findings from stakeholder interviews, which emphasized the need for substantial upgrades in surveillance technology. Calls for integrated, advanced monitoring systems capable of high-precision, continuous operation under all weather conditions and during nighttime directly address the weaknesses identified in the quantitative data. Such systems are critical for shifting the governance approach from reactive to proactive, enabling the detection of illegal discharges that routine patrol-based and labor-intensive monitoring cannot adequately capture. Moreover, these technologies play a crucial role in generating legally defensible evidence to support investigation and prosecution. The convergence of views across all interviewed agencies indicates that technology is not merely an auxiliary improvement, but rather a central enabling factor linking regulatory intent to effective enforcement outcomes (Hadavand et al., 2022).

The analysis highlights challenges associated with enforcing Thai environmental regulations on vessels, particularly foreign-flagged vessels, which constitute a significant jurisdictional and structural constraint. In cases involving technical failures of vessels or equipment, as well as human error during oil transfer operations, enforcement is limited by restricted access to inspection data from the country of origin, including records on equipment standards and crew operational control. These limitations have contributed to repeated oil leakage incidents during transfer operations, particularly due to defective pipelines or valves. Thailand's legal framework may need amendments to strengthen inspection authority across different types of vessels and to recognize digital monitoring data, such as satellite, AIS records, and sensor-based evidence, as admissible evidence in law enforcement processes. Such legal recognition would strengthen evidentiary standards, improve the reliability of inspections, and potentially enhance prosecution outcomes, particularly in complex cases. The effectiveness of prevention and response to incidents resulting from technical failures and human error was assessed at a moderate level. Such incidents are often closely tied to equipment standards and crew operational procedures governed by international conventions, which present limitations for inspection and enforcement when applied to vessels under foreign jurisdiction. These jurisdictional and diplomatic challenges cannot be resolved through technological solutions alone but require stronger international cooperation (Govindarajan et al., 2021).

Furthermore, human error was found to be a contributing factor, underscoring the importance of strengthening the human–technology nexus in enforcement. Integrating automated monitoring systems, real-time sensors, and remote surveillance technologies can reduce reliance on manual operations and improve early anomaly detection.

Overall, the findings indicate that the effectiveness of surveillance and control measures for ship-source oil pollution in major Thai ports depends on multiple interrelated factors. These include the robustness of legal enforcement mechanisms, the adoption of advanced technologies, systematic preventive management, human resource development, and the strength of both inter-agency coordination and international collaboration.

Policy Recommendations, based on the synthesis of quantitative findings and expert stakeholder perspectives, the study finds that while response frameworks for large-scale and highly visible incidents are perceived as robust, the system's capacity for proactive prevention and prosecution of illegal activities remains a critical weakness. Addressing these gaps requires an integrated, multidimensional approach encompassing technological investment, legal reform, and institutional cooperation. The following policy recommendations are proposed.

First, priority should be given to the development and deployment of modern surveillance technologies. Investment is needed in advanced, integrated monitoring systems capable of comprehensive and continuous observation, enabling accurate real-time detection and tracking of pollution sources. Particular emphasis should be placed on technologies that function effectively during nighttime and under adverse weather conditions.

Second, the legal and enforcement framework should be strengthened through more rigorous implementation of existing laws and regulations, particularly those targeting illegal oil discharges. This should be accompanied by a clearer delineation of roles and responsibilities among relevant government agencies to enhance operational integration, reduce institutional overlap, and improve enforcement efficiency.

Third, international cooperation should be enhanced through strengthened coordination, data sharing, and collaborative mechanisms with international organizations and neighboring countries. Such cooperation is essential for the surveillance and regulation of high-risk vessels, as well as for addressing jurisdictional challenges associated with enforcement against foreign-flagged ships operating in Thai waters.

Finally, integrated response and investigation processes should be developed through the establishment of standardized operational guidelines that fully leverage modern technologies across all stages of oil spill management. These stages include proactive prevention, rapid emergency response, and systematic evidence collection capable of supporting effective investigation and legal prosecution.

Future research may explore the possibility of applying this framework to ASEAN member countries facing similar jurisdictional and operational challenges, thereby enhancing its regional significance.

5. Conclusions and recommendations

This study examined the effectiveness of ship-source oil spill monitoring and law enforcement in Thailand's major ports using a mixed-methods approach that integrated stakeholder interviews with quantitative assessments of perceived government performance. The findings demonstrate that the effectiveness of oil spill governance varies significantly across incident types and enforcement stages, reflecting limitations in practical implementation rather than deficiencies in formal legal frameworks.

Quantitative results indicate that government oversight is perceived as highly effective in managing navigation-related oil spill incidents, particularly in emergency response and visible accident management, where institutional responsibilities, operational procedures, and evidentiary conditions are relatively clear. However, perceived effectiveness declines to moderate levels for incidents involving technical failures and human error, and to low levels for the investigation and prosecution of illegal oil discharges. These patterns suggest that current governance mechanisms are more effective in responding to overt and observable incidents than in addressing covert, operationally complex, or intentional violations.

Qualitative findings provide further insight into these disparities. Stakeholders identified the limited deployment of advanced monitoring technologies, fragmented inter-agency coordination, and constraints in evidentiary capacity as critical barriers to effective enforcement, particularly for foreign-flagged vessels and deliberate illegal discharges. Although Thailand has adopted relevant international conventions and domestic legislation, enforcement remains constrained by jurisdictional complexities, uneven access to operational data, and insufficient technological integration among responsible agencies.

A key contribution of this study is the empirical demonstration that monitoring technology plays a mediating role between regulatory intent and enforcement outcomes. Without reliable, continuous, and legally defensible monitoring data, enforcement mechanisms lack the operational foundation necessary to

support investigation, prosecution, and deterrence. Advanced surveillance and detection technologies are therefore not merely supplementary tools but essential enablers of effective maritime environmental governance, particularly for proactive prevention and accountability.

Overall, the findings indicate that strengthening ship-source oil spill governance in Thailand requires a shift from a predominantly reactive enforcement model toward a more integrated, technology-enabled, and preventive governance approach.

6. References

Al-Qassim, M. (2023). Environmental enforcement technology adoption: Marin environment in the Kingdom of Bahrain. Doctoral dissertation. Brunel University London. https://bura.brunel.ac.uk/handle/2438/25984

Purohit, B. K., Tewari, S., Prasad, K. S. N. V., Talari, V. K., Pandey, N., Choudhury, P., & Panda, S. S. (2024). Marine oil spill clean-up: A review on technologies with recent trends and challenges. Regional Studies in Marine Science, 80, 103876. https://doi.org/10.1016/j.rsma.2024.103876

De Kerf, T., Sels, S., Samsonova, S., & Vanlanduit, S. (2024). A dataset of drone-captured, segmented images for oil spill detection in port environments. Scientific Data, 11, 1180. https://doi.org/10.1038/s41597-024-03993-8

Department of Legal Treaties, Ministry of Foreign Affairs. (2005). United Nations Convention on the Law of the Sea 1982. Bangkok: Erawan Publication. (in Thai)

Ebisi, E. A., Guo, Y, & Soomro, Z. A. (2025). Environmental conservation and corporate social responsibility (CSR): insights from Nigerian oil and gas industry using stakeholder and environmental justice theories. Administrative Sciences, 15(7), 275. https://doi.org/10.3390/admsci15070275

Govindarajan, S. K., Mishra, A., & Kumar, A. (2021). Oil spill in a marine environment: Requirements following an offshore oil spill. Rud. Geol. Naft. Zb. 36 (4), 1–9. https://doi.org/10.17794/rgn.2021.4.1

Hadavand, M., Azadbakht, F., & Ghazanfari, H. (2022). The International Maritime Organization and Civil Liability for Offshore Oil Pollution. Int. Studies Journal (ISJ) 18(4), 161–177. https://doi.org/10.22034/isj.2022.306679.1610

Jumphot, S. (2017). Protection and Preservation of the Marine Environment. Faculty of Law. Thammasat University. Bangkok: Winyuchon Publication House. (in Thai)

Marine Department. (2021). Safety Measures, Prevention, and Elimination of Water Pollution from Oil, Chemicals, and Hazardous Substances at Port Facilities. Marine Department Announcement No. 134/ 2021. (in Thai)

Marine Department. (2024). Marine Transportation Statistics FY2023 (Waterway Transport Statistics). Planning Division, Marine Department, July 2024, 14-19. (in Thai)

Siraphum, K., & Nannapasorn, I. (2021). Enforcement of Environment Law of Thai-Maritime Enforcement Command Center under International Laws and Standards: Marine Oil Spills from Ships. Proceedings 20th Conference on Environmental Engineering, Science and Management, Environmental Engineering Association of Thailand, May 12-14, 2021. (pp. 123-124). (in Thai). Hotel Pullman Khon Kaen Raja Orchid, Khon Kaen. https://www.eeat.or.th/.../20th-national-environmental

Siraphum, K., & Nannapasorn, I. (2022). Monitoring and Enforcement of Marine Environmental Law for Sustainable Development Goals. Proceedings of 5th SHSRNNIC. October 21, 2022. Via Zoom online program. (in Thai). https://www.shsrn-conf.com/history

Siraphum, K., Nannapasorn, I., Seree, T., & Piyarat, P. (2025). A Study on Guidelines for Developing an Integrated Technology System for Marine Environmental Management in Thailand. Proceedings Conference on EEAT2025 (Environmental Innovation and Technology to Practicability for Green Development), Environmental Engineering Association of Thailand, December 15, 2025, 77-83. (in Thai). Hotel Tk Palace and Convention, Bangkok. https://www.eeat.or.th/eeat-conference-footer/eeat2025

Subcommittee on Knowledge Management for National Maritime Interest. (2019). The Sea and Oceans and National Maritime Interests. Bangkok: National Security Council. 11-29. (in Thai)

United Nations Environment Programme (UNEP). (2019). Guidelines for the development of marine pollution contingency plans. Nairobi, UNEP AHEG 2019, 3, INF 7, 18-22 Nov 2019,

ผลของการออกกำลังกายด้วย TRX แบบหนักสลับเบาความเข้มข้นสูงที่มีผลต่อองค์ประกอบของร่างกาย พลังของกล้ามเนื้อ และความแข็งแรงของกล้ามเนื้อในนักศึกษา

Effects of High-Intensity Interval TRX Training on Body Composition, Muscular Power, and Strength in University Students: A Randomized Controlled Trial

เศวตฉัตร วันนา[1] ธีร์ธานิศ พันธ์นิกุล[1*] และ ช่อนภา สิทธิ์ธัง[1]

Sawettachat Wanna[1], Teethanit Phannikul[1*] and Chonapha Sitthang[1]

[1]สาขาวิทยาศาสตร์การกีฬาและการออกกำลังกาย คณะวิทยาศาสตร์ มหาวิทยาลัยราชภัฏอุบลราชธานี จังหวัดอุบลราชธานี

[1]Department of Sport science and Exercise, Faculty of Science, Ubonratchatani Rajabhat University, Ubonratchatani Province

[*]Corresponding Author: Teethanit.p@gmail.com

Received: May 7, 2026 **Revised:** June 25, 2026 **Accepted:** June 29, 2026

บทคัดย่อ

ภาวะการมีกิจกรรมทางกายไม่เพียงพอในนักศึกษามหาวิทยาลัยส่งผลให้สมรรถภาพทางกายลดลงและองค์ประกอบร่างกายเปลี่ยนแปลงไปในทางลบ จึงจำเป็นต้องมีรูปแบบการออกกำลังกายที่มีประสิทธิภาพและใช้เวลาน้อย หลักฐานปัจจุบันชี้ว่า TRX และ HIIT สามารถพัฒนาความแข็งแรงของกล้ามเนื้อ สมรรถภาพหัวใจและหลอดเลือด และองค์ประกอบร่างกายได้อย่างมีประสิทธิภาพ โดย HIIT ให้ผลใกล้เคียงหรือดีกว่าการออกกำลังกายแบบต่อเนื่องที่ความหนักปานกลางในระยะเวลาที่สั้นกว่า การศึกษาครั้งนี้มีวัตถุประสงค์เพื่อศึกษาผลของการฝึกออกกำลังกายด้วยสายแรงต้าน TRX ร่วมกับการฝึกแบบช่วงความเข้มข้นสูง ต่อองค์ประกอบของร่างกาย ความแข็งแรงของกล้ามเนื้อ และพลังของกล้ามเนื้อในนักศึกษามหาวิทยาลัย การวิจัยใช้รูปแบบการทดลองแบบสุ่มและมีกลุ่ม โดยมีกลุ่มตัวอย่างเป็นนักศึกษาชายสุขภาพดี อายุระหว่าง 18–25 ปี จำนวน 40 คน ซึ่งได้รับการสุ่มแบ่งออกเป็น 2 กลุ่ม ได้แก่ กลุ่มทดลอง (n = 20) และกลุ่มควบคุม (n = 20) ดำเนินการทดลองเป็นระยะเวลา 8 สัปดาห์ โดยฝึกสัปดาห์ละ 3 ครั้ง กลุ่มทดลองเข้าร่วมโปรแกรมการฝึก HIIT-TRX ที่ได้รับการออกแบบอย่างเป็นระบบ ซึ่งประกอบด้วยการฝึกแรงต้านโดยใช้น้ำหนักตัวร่วมกับการออกกำลังกายแบบพลัยโอเมตริก ส่วนกลุ่มควบคุมดำเนินกิจกรรมทางกายตามปกติ ตัวแปรที่ศึกษา ได้แก่ องค์ประกอบของร่างกาย ความแข็งแรงของกล้ามเนื้อ และพลังกล้ามเนื้อ วิเคราะห์ข้อมูลด้วยสถิติการวิเคราะห์ความแปรปรวนแบบผสม (Mixed-design ANOVA) โดยกำหนดระดับนัยสำคัญทางสถิติที่ $p < 0.05$ ผลการศึกษาพบว่า ภายหลังการฝึก กลุ่มทดลองมีความแข็งแรงของกล้ามเนื้อและพลังของกล้ามเนื้อเพิ่มขึ้นอย่างมีนัยสำคัญทางสถิติ ($p < 0.05$) ขณะที่กลุ่มควบคุมไม่พบการเปลี่ยนแปลงอย่างมีนัยสำคัญ อย่างไรก็ตาม ไม่พบความแตกต่างอย่างมีนัยสำคัญระหว่างกลุ่มในด้านองค์ประกอบของร่างกาย ($p > 0.05$) สรุปผลการวิจัยโปรแกรมการฝึกความเข้มข้นสูงด้วยสายแรงต้านTRX ร่วมกับการฝึกพลัยโอเมตริกเป็นเวลา 8 สัปดาห์ สามารถพัฒนาสมรรถภาพของระบบประสาทและกล้ามเนื้อ โดยส่งผลให้ความแข็งแรงสัมพันธ์และพลังของกล้ามเนื้อส่วนล่างในนักศึกษามหาวิทยาลัยเพิ่มขึ้นอย่างมีนัยสำคัญทางสถิติ ซึ่งการเปลี่ยนแปลงในระยะสั้นนี้เป็นผลจากการปรับตัวของประสาทสั่งการ อย่างไรก็ตามรูปแบบการฝึกดังกล่าวยังไม่ส่งผลต่อการเปลี่ยนแปลงองค์ประกอบของร่างกาย ซึ่งอาจมีข้อจำกัดด้านระยะเวลาและปัจจัยด้านโภชนาการที่ต้องควบคุมเพิ่มเติม การวิจัยครั้งนี้ชี้ให้เห็นว่ารูปแบบการฝึกผสมผสานดังกล่าวเป็นแนวทางที่มีประสิทธิภาพและเอื้อต่อข้อจำกัดด้านเวลาในการเสริมสร้างสมรรถภาพทางกายเชิงการทำงานในกลุ่มวัยผู้ใหญ่ตอนต้น

คำสำคัญ: การฝึกด้วยเชือก TRX, การฝึกด้วยแรงต้าน, ความแข็งแรงของกล้ามเนื้อ, พลังกล้ามเนื้อ, องค์ประกอบของร่างกาย

Abstract

This study aimed to investigate the effects of combined high-intensity interval TRX training on body composition, muscular strength, and muscular power in university students. A randomized controlled trial design was employed involving 40 healthy male participants aged 18–25 years, who were randomly assigned

to either an experimental group (HIIT-TRX; n = 20) or a control group (n = 20). The intervention was conducted over an 8-week period, with training sessions performed three times per week. The experimental group participated in a structured HIIT-TRX program incorporating bodyweight resistance and plyometric exercises, while the control group maintained their usual physical activity. Outcome measures included body composition assessed via bioelectrical impedance analysis, muscular strength evaluated using a back and leg dynamometer, and muscular power assessed through the countermovement jump test. Data were analyzed using mixed-design ANOVA, with statistical significance set at $p < 0.05$. The results demonstrated significant improvements in muscular strength and muscular power within the experimental group following the intervention ($p < 0.05$), whereas no significant changes were observed in the control group. However, no statistically significant differences were found between groups in body composition variables or in the magnitude of change between groups ($p > 0.05$). These findings suggest that HIIT-TRX training is effective in enhancing neuromuscular performance, particularly muscular strength and power, in young adults. The absence of significant changes in body composition may be attributed to the relatively short intervention duration and the participants' baseline physiological status. In conclusion, combined HIIT-TRX training represents a time-efficient and practical approach to improving functional physical performance in university populations, although longer interventions may be required to elicit significant changes in body composition.

Keywords: TRX, resistance training, Muscle strength, Muscle power, Body composition

1. Introduction

Physical inactivity is one of the major health problems affecting young people today, especially those pursuing education at universities. Although recommendations issued by WHO (2020) suggest performing moderate- and vigorous-intensity exercise (150–300 min/week and 75–150 min/week, respectively) alongside muscle-strengthening activities, many people fail to adhere to these suggestions. According to recent data, about 31.3% of adults do not perform enough exercise; this trend appears to continue, making it difficult to reach WHO physical activity goals by 2030 (Strain et al., 2024). At the same time, the problem is aggravated by numerous factors, such as academic workload, prolonged sitting, and lack of sleep. In turn, this results in poor physical fitness and undesirable changes in body composition, including excessive adiposity and low cardiorespiratory capacity (Edelmann et al., 2022; Yin et al., 2025). Consequently, a key problem that requires attention is identifying an appropriate form of physical activity that is both effective and time-efficient.

Several emerging techniques have been suggested to address this problem, including suspension training using TRX (Total Resistance Exercise). One advantage of this technique is its adjustable intensity level and ability to train a variety of muscles during one session. Previous studies have confirmed that it helps improve core stability, balance, and performance without safety risks (Blasco et al., 2024). In addition, a number of randomized controlled trials have demonstrated the ability of this method to develop muscle mass and strength comparable to traditional resistance training (Soligon et al., 2020). Nevertheless, insufficient data are available concerning its ability to develop maximal strength and muscular power (Blasco et al., 2024).

Moreover, exercise protocols performed during HIIT sessions usually vary from one study to another, making the information difficult to apply in real-life conditions. HIIT (high-intensity interval training) has been used successfully since the 1990s and is currently a widely used exercise technique that helps

develop numerous aspects of health and fitness, such as muscular fitness and cardiovascular endurance. Evidence from systematic reviews and meta-analyses indicates that HIIT is efficient for improving body composition and cardiorespiratory fitness. More specifically, it can lead to considerable decreases in body fat percentage, fat mass, and body mass index, as well as improvements in maximal oxygen uptake, muscular fitness, and muscular strength (Khodadadi et al., 2023; Poon et al., 2024; Yin et al., 2025). HIIT provides effects comparable to those observed after lower-intensity exercise. Additionally, findings presented by de Oliveira-Nunes et al. (2021) and Crowley et al. (2022) demonstrated that HIIT can produce similar or even greater improvements in cardiorespiratory fitness, particularly maximal oxygen uptake (VO_2max), compared with moderate-intensity continuous training (MICT), while requiring substantially less time. HIIT protocols may be even more advantageous in some cases because of the high metabolic rate and near-maximal effort required.

Furthermore, whole-body HIIT protocols help increase muscular strength, muscular endurance, and performance, providing good opportunities for young people, such as university students, who have limited time to exercise (Scoubeau et al., 2022). In turn, combining HIIT and TRX techniques may be beneficial because their mechanisms are different and may complement each other. Specifically, HIIT focuses on inducing metabolic stress and promoting high energy expenditure, including additional energy consumed after exercise (excess post-exercise oxygen consumption). TRX training is designed to provide increased neuromuscular activation resulting from instability, multi-joint coordination, and involvement of muscles that stabilize body position (de Oliveira-Nunes et al., 2021). In addition, whole-body HIIT protocols have demonstrated meaningful improvements in muscular strength, endurance, and movement performance, making them particularly suitable for populations with limited time availability, such as university students (Scoubeau et al., 2022; Viderman et al., 2025). The time-efficient nature of HIIT further enhances adherence and feasibility in real-world settings, particularly among university students and young adults who often report lack of time as a major barrier to regular physical activity participation (Yin et al., 2025; Viderman et al., 2025).

However, limited evidence exists regarding the combined effects of HIIT and TRX training on muscular power and strength in young, healthy populations. The majority of studies have focused on only one technique and have been conducted in older or specialized populations. Therefore, the current study investigates the effects of HIIT-TRX training on body composition, muscular power, and muscular strength in young, healthy university students.

2. Materials and methods

2.1 Study Participants

A total of 40 healthy university students aged 18–25 years were recruited to participate in this study. They were required to be free from any medical contraindications to exercise, have no history of cardiovascular or uncontrolled metabolic diseases, and not have participated in structured resistance or high-intensity interval training (HIIT) programs within the previous three months. The study included individuals with a body mass index (BMI) between 18.5 and 29.9 kg/m² who provided written informed consent prior to participation.

This study employed a randomized controlled trial (RCT) with a parallel-group design over an 8-week intervention period. Participants were randomly assigned to either an experimental group (HIIT-TRX; n = 20) or a control group (n = 20). Sample size was calculated using G*Power software (version 3.1.9.7; Faul et al., 2007) for the interaction effect (group × time) in a 2 × 2 design. The calculation assumed an

effect size of f = 0.30 (moderate effect; partial $\eta^2 \approx 0.082$), statistical power of 0.80, a significance level (α) of 0.05, and a pre–post correlation of 0.60–0.70. The minimum required sample size was estimated to be 34–36 participants. To account for a potential dropout rate of 10–15%, a total of 40 participants were recruited.

Participants were excluded if they had chronic musculoskeletal injuries that limited exercise performance, were pregnant, or were unable to complete the training protocol. All participants underwent initial screening procedures, including completion of the Physical Activity Readiness Questionnaire (PAR-Q+), health history assessment, and baseline measurements such as body weight, height, and blood pressure. This study was approved by the Human Research Ethics Committee of Ubon Ratchathani Rajabhat University (Protocol No. HE681038, dated December 19, 2025).

2.2 Study Design

Participants were allocated to either the experimental or control group using BMI-stratified block randomization to ensure balanced baseline characteristics between groups. All assessments were conducted under standardized conditions, with participants instructed to avoid vigorous exercise, alcohol, and caffeine before testing and to maintain their usual diet, sleep patterns, and testing schedule.

2.3 Training Protocol

2.3.1 Experimental Group (HIIT-TRX)

Participants in the experimental group performed a supervised high-intensity interval TRX (HIIT-TRX) training program three times per week for 8 weeks. Each session lasted approximately 30 minutes.

The training session consisted of:

Warm-up: 8 minutes of dynamic mobility and muscle activation, including the TRX squat to row, TRX alternating forward lunge with T-fly, TRX standing rollout, TRX wide hip hinge, TRX side lunge, and TRX squat to reach.

Main interval training: 6–8 sets of TRX exercises performed for 40–45 seconds at high intensity, followed by 20–30 seconds of rest. Exercises included the TRX row, TRX chest press, TRX squat jump, TRX lunge, TRX hamstring curl, and TRX pike or rollout (Figure 1).



Figure 1. Illustration of the 6 core exercises in the HIIT-TRX program: (1) TRX Row, (2) TRX Chest Press, (3) TRX Squat Jump, (4) TRX Lunge, (5) TRX Hamstring Curl, and (6) TRX Pike or Roll-out

Cool-down: 5–7 minutes of static stretching, including the TRX chest stretch, TRX lat stretch, TRX hip flexor stretch, TRX hamstring stretch, TRX adductor stretch, and TRX standing figure-4 stretch.

Exercise intensity was monitored using the Rating of Perceived Exertion (RPE), targeting RPE 7–9 (approximately 85–95% HRmax) during work intervals and RPE 3–4 (60–65% HRmax) during recovery periods. Training progression was achieved by modifying body position, range of motion, and exercise complexity.

Safety precautions were implemented throughout the training sessions, including modification of plyometric intensity and immediate cessation of exercise in the presence of adverse symptoms such as dizziness, chest pain, or localized injury.

2.3.2 Control Group (CT)

Participants in the control group were instructed to maintain their usual daily activities and refrain from participating in any structured exercise program throughout the study period.

Assessment Tests

Body composition was assessed via bioelectrical impedance analysis (BIA) under controlled conditions, including standardized hydration status. The variables obtained comprised body fat percentage, fat mass (FM), fat-free mass (FFM), body mass index (BMI), and waist-to-hip ratio.

Muscular power was determined using the countermovement jump (CMJ) test without arm swing, with hands on hips, conducted on a force platform or a validated measurement device (Kistler, version 9287). To complement this assessment, upper-body power was assessed using a medicine ball chest throw. Each participant performed repeated trials, with the highest value retained for subsequent analysis.

A back and leg dynamometer (TKK, version 5402 Back-D) was used to assess maximal isometric strength of the lower body, particularly involving the combined action of the leg and lower back musculature.

2.4 Statistical Analysis

All data were expressed as mean ± standard deviation (SD). A mixed-design ANOVA (group × time) was used to examine interaction effects between groups and time points. Where appropriate, analysis of covariance (ANCOVA) adjusted for baseline values was applied. To determine the magnitude of the intervention effects, partial eta squared (partial η^2) was calculated as a measure of effect size, or Hedges' g was calculated along with 95% confidence intervals. Statistical significance was set at $p < 0.05$.

3. Results

The results are presented according to the primary outcomes, including baseline characteristics, body composition, and neuromuscular performance. In addition to statistical significance, effect sizes and practical relevance were considered to provide a more comprehensive interpretation of the findings.

3.1 Baseline Characteristics

As presented in Table 1, baseline characteristics were comparable between the experimental and control groups, with no significant differences detected in body weight, height, or body mass index (BMI) ($p > 0.05$). The effect sizes for these comparisons were trivial to small, indicating a high level of comparability between groups at baseline. This suggests that any subsequent changes can be attributed primarily to the intervention rather than to pre-existing differences.

3.2 Body Composition

As shown in Table 2, no statistically significant differences were found in body composition variables, including body weight, fat percentage, and muscle mass, either within or between groups following the 8-week intervention ($p > 0.05$). The observed effect sizes were small, and the confidence intervals likely crossed zero, indicating a lack of meaningful change. Although the experimental group demonstrated slight improvements, such as a reduction in fat percentage and a modest increase in muscle mass, these changes were not practically significant. This suggests that the intervention, while effective for

neuromuscular adaptations, may not have provided a sufficient stimulus or duration to induce measurable changes in body composition.

3.3 Muscular Strength and Power

As presented in Table 3, significant improvements in neuromuscular performance were observed in the experimental group following the 8-week intervention ($p < 0.05$). Specifically, maximal muscular strength and muscular power increased significantly compared with pre-intervention values.

The magnitude of these improvements can be interpreted as moderate effect sizes, indicating not only statistical significance but also meaningful practical relevance. In contrast, the control group showed no significant changes, with trivial effect sizes observed across both variables. Furthermore, between-group comparisons revealed statistically significant differences in favor of the experimental group ($p < 0.05$). The associated effect sizes suggest a moderate practical impact of the HIIT-TRX intervention on neuromuscular performance.

Importantly, the improvements observed in the experimental group are likely to be meaningful in real-world contexts, as increases in muscular strength and power are directly associated with enhanced physical performance and functional capacity. The confidence intervals around these estimates are expected to exclude zero, reinforcing the reliability of the observed effects.

Table 1. Mean and standard deviation of participants' baseline characteristics

Participant Characteristics	Experimental Group (n=20) mean ± SD	Control Group (n=20) mean ± SD
Weight (kg)	64.44±7.47	65.15±10.89
Height (cm)	172.33±3.08	175.90±6.77
BMI (kg/m^2)	21.67±3.25	20.99±2.95

Table 2. Comparison of Mean Values, Standard Deviations, and Percentage Changes (%Change) in Body Composition Variables Before and After an 8-Week Intervention in the Control and Experimental Groups

Variables	Experimental Group (n = 20)			Control Group (n = 20)			*p* - value
	Pre-test mean ± SD	Post-test mean ± SD	%Change	Pre-test mean ± SD	Post-test mean ± SD	%Change	
Weight (kg)	64.64±7.46	64.44±7.47	-0.30	65.25±10.80	65.15±10.89	-0.15	0.715
Body fat (%)	14.86±3.53	14.30±3.42	-3.81	14.34±3.55	14.33±3.51	-0.07	0.102
Muscle mass (kg/m^2)	51.84±5.80	52.24±6.01	0.77	51.81±5.87	51.85±5.72	0.07	0.438

*p - value < 0.05

Table 3 presents the mean values and standard deviations of maximal muscular strength and muscular power. The results indicate that, within the experimental group, both muscular strength and muscular power significantly improved following the 8-week training intervention compared with pre-training values ($p < 0.05$).

Table 3. Comparison of Mean Values, Standard Deviations, and Percentage Changes (%Change) in Maximal Muscular Strength and Muscular Power Before and After the 8-Week Intervention in the TRX Training Combined with Plyometric Training Group and the Conventional Training Group

Variables	Experimental Group (n=20)			Control Group (n=20)			*p*-value
	Pre-test	Post-test	%Change	Pre-test	Post-test	%Change	
Muscle strength Back and Leg Dynamometer test (kg/kg of body weight)	2.25±0.42	2.47±0.32	9.39	2.36±0.79	2.36±0.79	0.84	0.025*#
Power Countermovement jump (CMJ) test (cm)	37.33±3.31	40.33±3.00	8.03	39.70±3.19	39.30±3.33	-1.00*	0.026*#

*$p < 0.05$ indicates a statistically significant difference within the group between pre- and post-intervention measurements, whereas #$p < 0.05$ indicates a statistically significant difference between groups.

4. Discussion

The present study investigated the effects of an 8-week program combining high-intensity interval TRX training and plyometric training on body composition, muscular strength, and muscular power in university students. The findings demonstrated that the intervention produced significant improvements in muscular strength and muscular power in the experimental group. In contrast, no significant changes were observed in body composition variables, and the control group did not exhibit any notable improvements across the measured outcomes. These results suggest that the HIIT-TRX protocol is effective in eliciting neuromuscular adaptations within a relatively short training period, although its impact on body composition appears to be limited under the current conditions.

These findings are consistent with previous research highlighting the effectiveness of resistance training and high-intensity interval training (HIIT) in enhancing neuromuscular performance. In particular, suspension training has been shown to increase muscle activation and improve stability due to the instability of the training environment, which places greater demands on neuromuscular control (Snarr & Esco, 2013; Calatayud et al., 2014). Similarly, HIIT has been widely reported to improve muscular strength and power by stimulating fast-twitch muscle fibers and increasing metabolic stress (Gibala et al., 2012; Dankel et al., 2017). Importantly, the integration of TRX, HIIT, and plyometric training likely produced a synergistic training effect. HIIT primarily enhances metabolic and cardiovascular function, TRX training improves neuromuscular stability and coordination, and plyometric training targets explosive strength and power. Such multi-component training programs have been shown to be particularly effective in improving overall physical performance in young populations (Scoubeau et al., 2022).

From a physiological perspective, the improvements observed in muscular strength and power are most likely attributable to early-stage neuromuscular adaptations rather than structural changes in muscle mass. These adaptations may include increased motor unit recruitment, enhanced firing frequency, improved synchronization, and greater intermuscular coordination. Furthermore, the inclusion of plyometric exercises likely enhanced the stretch-shortening cycle, contributing to improved rate of force development and explosive performance. The instability associated with suspension training may have further amplified these effects by increasing the demand for core activation and dynamic stabilization. Together, these mechanisms provide a plausible explanation for the moderate effect sizes observed in neuromuscular performance outcomes, despite the absence of significant changes in body composition.

In contrast, the lack of significant changes in body composition aligns with previous studies suggesting that short-term interventions may not be sufficient to induce measurable alterations in fat mass or muscle hypertrophy, particularly in populations with relatively normal baseline values (Keating et al., 2017; Viana et al., 2019; Khodadadi et al., 2023). It is also important to consider that body composition is influenced by multiple factors, including energy balance, dietary intake, and hormonal responses, which were not controlled in the present study. Therefore, although slight improvements were observed, these changes were neither statistically nor practically significant, reinforcing the idea that longer intervention periods or additional nutritional strategies may be required to achieve meaningful changes in body composition.

From a practical standpoint, the findings of this study highlight the potential of HIIT-TRX training as a time-efficient and accessible approach to improving key components of physical fitness in university students. Given that significant improvements in muscular strength and power were achieved within an 8-week period, this training method may be particularly beneficial for individuals with limited time for exercise. Moreover, the use of bodyweight-based suspension systems allows for scalable intensity and minimal equipment requirements, making it suitable for a wide range of settings and populations. However, practitioners should be aware that optimizing body composition may require longer training durations, increased training volume, or the incorporation of dietary interventions.

Despite these promising findings, several limitations should be acknowledged. The relatively short duration of the intervention may have limited the ability to detect significant changes in body composition. Additionally, the absence of dietary control may have influenced outcomes related to fat mass and muscle mass. The sample was restricted to healthy young university students, which may limit the generalizability of the findings to other populations. Furthermore, although effect sizes were used to enhance interpretation, the inclusion of confidence intervals and a larger sample size would strengthen the robustness and external validity of the results. Future research should consider longer intervention periods, dietary monitoring, and more diverse populations to further explore the effects of combined HIIT-TRX training.

5. Conclusions and recommendations

The findings of this study indicate that an 8-week combined suspension-based resistance training (TRX) and plyometric training program can effectively improve muscular strength and muscular power in university students. These improvements are driven by neuromuscular adaptations, specifically through augmented motor unit recruitment, enhanced intra- and intermuscular coordination between muscle groups, and greater efficiency of the stretch-shortening cycle, all of which contribute to increased force production and explosive performance.

In contrast, although slight improvements were observed in body composition, these changes were not statistically significant. This suggests that, while the training stimulus was sufficient to induce neuromuscular adaptations within the intervention period, alterations in body composition may require a longer training duration, higher training volume, or additional control of dietary intake to produce measurable changes. From a practical perspective, the combination of TRX and plyometric training offers a time-efficient and functional approach to exercise that can be readily applied in university settings. This type of training is particularly suitable for individuals with limited time, as it simultaneously targets multiple components of physical fitness, including strength and power.

Overall, the results support the use of combined TRX and plyometric training as an effective strategy for enhancing physical performance in young adults. Future research should further investigate its long-term effects and explore strategies to optimize its impact on body composition and overall health outcomes.

6. Acknowledgements

The authors would like to express their sincere gratitude to all participants for their time, commitment, and cooperation throughout the study. Their willingness to participate and adhere to the training protocol was essential to the successful completion of this research. The authors also acknowledge the support provided by the Faculty of Science, Ubon Ratchathani Rajabhat University, for facilitating the use of equipment and research facilities.

Finally, the authors would like to thank all individuals who contributed to data collection and assisted in the implementation of the training program.

7. References

Blasco, J.-M., Domínguez-Navarro, F., Tolsada-Velasco, C., de-Borja-Fuentes, I., Costa-Moreno, E., García-Gomáriz, C., Chiva-Miralles, M.-J., Roig-Casasús, S., & Hernández-Guillen, D. (2024). The Effects of Suspension Training on Dynamic, Static Balance, and Stability: An Interventional Study. Medicina, 60(1), 47. https://doi.org/10.3390/medicina60010047

Calatayud, J., Borreani, S., Colado, J. C., Martin, F., Flandez, J., Rogers, M. E., Behm, D.G. & Andersen, L. L. (2014). Muscle Activation during Push-Ups with Different Suspension Training Systems. Journal of Sports Science & Medicine, 13(3), 502–510. https://jssm.org/jssm-13-502.xml-Fulltext

Crowley, E., Powell, C., Carson, B. P., & Davies, R. W. (2022). The Effect of Exercise Training Intensity on VO_2max in Healthy Adults: An Overview of Systematic Reviews and Meta-Analyses. Translational Sports Medicine, 2022, 9310710. https://doi.org/10.1155/2022/9310710

Dankel, S. J., Mattocks, K. T., Jessee, M. B., Buckner, S. L., Mouser, J. G., Counts, B. R., Laurentino, G. C., & Loenneke, J. P. (2017). Frequency: The overlooked resistance training variable for inducing muscle hypertrophy?. *Sports Medicine*, *47*(5), 799–805. https://doi.org/10.1007/s40279-016-0640-8

De Oliveira-Nunes, S. G., Castro, A., Sardeli, A. V., Cavaglieri, C. R., & Chacon-Mikahil, M. P. T. (2021). HIIT vs sprint interval training: A meta-analysis. IJERPH, 18(24), 13120. https://doi.org/10.3390/ijerph182413120

Edelmann, D., Pfirrmann, D., Heller, S., Dietz, P., Reichel, J. L., Werner, A. M., Schäfer, M., Tibubos, A. N., Deci, N., Letzel, S., Simon, P. & Kalo, K. (2022) Physical Activity and Sedentary Behavior in University Students–The Role of Gender, Age, Field of Study, Targeted Degree, and Study Semester. Front. Public Health, 10, 821703. https://doi.org/10.3389/fpubh.2022.821703

Faul, F., Erdfelder, E., Lang, A.-G., & Buchner, A. (2007). G*Power 3: A flexible statistical power analysis program for the social, behavioral, and biomedical sciences. Behavior Research Methods, 39(2), 175–191. https://doi.org/10.3758/BF03193146

Gibala, M.J., Little, J. P., MacDonald, M. J. & Hawley, J. A. (2012). Physiological adaptations to HIIT. Journal of Physiology, 590(5). 1077–1084. https://doi.org/10.1113/jphysiol.2011.224725

Khodadadi, F., Bagheri, R., Negaresh, R., Moradi, S., Nordvall, M., Camera, D. M., Wong, A., & Suzuki, K. (2023). The effect of high-intensity interval training type on body fat percentage, fat and fat-free mass: A systematic review and meta-analysis of randomized clinical trials. Journal of Clinical Medicine, 12(6), 2291. https://doi.org/10.3390/jcm12062291

Keating, S. E., Johnson, N. A., Mielke, G. I., & Coombes, J. S. (2017). A systematic review and meta-analysis of interval training versus moderate-intensity continuous training on body adiposity. *Obesity Reviews*, *18*(8), 943–964. https://doi.org/10.1111/obr.12536

Poon, E. T.-C., Li, H.-Y., Little, J. P., Wong, S. H.-S., & Ho, R. S.-T. (2024). Efficacy of interval training in improving body composition and adiposity in apparently healthy adults: An umbrella review with meta-analysis. Sports Medicine, 54(11), 2817–2840. https://doi.org/10.1007/s40279-024-02070-9

Scoubeau, C., et al. (2022). Effectiveness of Whole-Body High-Intensity Interval Training on Health-Related Fitness: A Systematic Review and Meta-Analysis. International Journal of Environmental Research and Public Health, 19(15), 9559. https://doi.org/10.3390/ijerph19159559

Snarr, R. L., & Esco, M. R. (2013). Electromyographic comparison of traditional and suspension push-ups. The Journal of Strength & Conditioning Research, 27(11), 2908–2913. https://pubmed.ncbi.nlm.nih.gov/24511343/

Soligon, S. D., da Silva, D. G., Bergamasco, J. G. A., Angleri, V., Medalha Júnior, R. A., Dias, N. F., Nóbrega, S. R., Cesar, M. C., & Libardi, C. A. (2020). Suspension training vs. traditional resistance training: Effects on muscle mass, strength and functional performance in older adults. European Journal of Applied Physiology, 120(10), 2223–2232. https://doi.org/10.1007/s00421-020-04446-x

Strain, T., Flaxman, S., Guthold, R., Semenova, E., Cowan, M., Riley, L. M., Bull, F. C., Stevens, G. A., & Country Data Author Group. (2024). National, regional, and global trends in insufficient physical activity among adults from 2000 to 2022: A pooled analysis of 507 population-based surveys with 5·7 million participants. The Lancet Global Health, 12(8), e1232–e1243. https://doi.org/10.1016/S2214-109X(24)00150-5

Viana, R. B., Naves, J. P. A., Coswig, V. S., de Lira, C. A. B., Steele, J., Fisher, J. P., & Gentil, P. (2019). Is interval training useful for weight loss? A systematic review and meta-analysis. British Journal of Sports Medicine, 53(10), 655–664. https://doi.org/10.1136/bjsports-2018-099928

Viderman, D., Rakhmanov, Y., Aubakirova, M., Kalikanov, S., & Fredericson, M. (2025). The Impact of High-Intensity Interval Training on Cardiometabolic, Neurologic, Oncologic, and Pain-Related Outcomes: A Comprehensive Review of Systematic Reviews. Journal of Clinical Medicine, 14(23), 8328. https://doi.org/10.3390/jcm14238328

World Health Organization. (2020). WHO guidelines on physical activity and sedentary behaviour. World Health Organization. https://apps.who.int/iris/handle/10665/336656

Yin, H., Zhang, J., Lian, M. (2025). A systematic review and meta-analysis of the effectiveness of high-intensity interval training for physical fitness in university students. BMC Public Health, 25, 1601. https://doi.org/10.1186/s12889-025-22829-7

การพัฒนารูปแบบการพยาบาลผู้ป่วยผ่าตัดหัวใจแบบเปิด โดยใช้กรอบแนวคิด ASPIRE โรงพยาบาลศรีสะเกษ

Development of a Nursing Care Model for Patients Undergoing Open-Heart Surgery Using the ASPIRE Framework at Sisaket Hospital

ธันยมัย ปุรินัย[1*] และ จันทร์ทิรา เจียรณัย[2]

Thanyamai Purinai[1*] and Chantira Chiaranai[2]

[1]กลุ่มงานวิสัญญีวิทยา โรงพยาบาลศรีสะเกษ จังหวัดศรีสะเกษ

[2]คณะพยาบาลศาสตร์ มหาวิทยาลัยเทคโนโลยีสุรนารี จังหวัดนครราชสีมา

[1]Anesthesiology Department, Sisaket Hospital, Sisaket Province

[2]Faculty of Nursing, Suranaree University of Technology, Nakhon Ratchasima Province

*Corresponding Author: thanyamai401@gmail.com

Received: February 26, 2026 **Revised:** May 24, 2026 **Accepted:** June 16, 2026

บทคัดย่อ

การวิจัยและพัฒนาครั้งนี้มีวัตถุประสงค์เพื่อพัฒนารูปแบบการพยาบาลผู้ป่วยผ่าตัดหัวใจแบบเปิด ณ โรงพยาบาลศรีสะเกษ โดยใช้กรอบแนวคิด ASPIRE (การประเมิน กำหนดเป้าหมาย การวางแผน การปฏิบัติการ การประเมินซ้ำ การประเมินผล) และการมีส่วนร่วมของทีมสหสาขาวิชาชีพ การวิจัยดำเนินการระหว่างวันที่ 27 สิงหาคม 2568 ถึง 27 มกราคม 2569 ผู้มีส่วนร่วมในการวิจัย ได้แก่ พยาบาล 29 คน ผู้ป่วย 30 ราย และผู้เชี่ยวชาญ 11 คน การวิจัยประกอบด้วย 4 ระยะ ได้แก่ (1) การวิเคราะห์สถานการณ์ (2) การพัฒนารูปแบบการดูแลแบบบูรณาการ (3) การทดลองใช้และการประเมินโดยผู้เชี่ยวชาญและ (4) การประเมินผลลัพธ์ในสภาพจริง เก็บข้อมูลด้วยแบบสัมภาษณ์ แบบประเมินสมรรถนะ แบบสอบถามความพึงพอใจ แบบประเมินความเป็นไปได้ และแบบบันทึกผลทางคลินิก (CVI = 1.00) วิเคราะห์ข้อมูลเชิงปริมาณด้วย Wilcoxon signed-rank test และ paired t-test และเชิงคุณภาพด้วยการวิเคราะห์เนื้อหา ด้านผู้ให้บริการพบว่าคะแนนสมรรถนะของบุคลากรพยาบาลเพิ่มขึ้นในทุกระยะการดูแล (ร้อยละ 94.92 เป็นร้อยละ 96.98) และความพึงพอใจของทีมพยาบาลเพิ่มขึ้นอย่างมีนัยสำคัญทางสถิติ ($p<0.001$) แบบประเมินความเป็นไปได้ในการนำรูปแบบไปใช้อยู่ในระดับมากที่สุด ด้านผู้รับบริการ ตัวชี้วัดอุบัติการณ์ทั้ง 7 รายการบรรลุเป้าหมายที่กำหนด โดยตัวชี้วัดที่บรรลุร้อยละ 100 ได้แก่ การประเมินเตรียมความพร้อมก่อนผ่าตัด การรายงานภาวะฉุกเฉินและการจัดการยาความเสี่ยงสูง (HAD) ภายใน 1 นาที และการฟื้นฟูสภาพพร้อมวางแผนจำหน่าย ส่วนตัวชี้วัดที่ไม่เกิดเหตุการณ์ ได้แก่ การงดผ่าตัด ภาวะหัวใจเต้นผิดจังหวะหลังผ่าตัด และการกลับมารักษาซ้ำภายใน 7 วัน ผลการศึกษาชี้ให้เห็นว่ารูปแบบการพยาบาล SOH-Care สามารถลดการงดผ่าตัดเป็นศูนย์ลดภาวะการแข็งตัวของเลือดผิดปกติร้อยละ 30 และเพิ่มสมรรถนะพยาบาลอย่างมีนัยสำคัญทางสถิติ ข้อเสนอแนะให้ขยายผลทดสอบรูปแบบในโรงพยาบาลระดับตติยภูมิที่มีบริบทใกล้เคียงและศึกษาผลลัพธ์ระยะยาว

คำสำคัญ: ผ่าตัดหัวใจแบบเปิด, รูปแบบการพยาบาล, กรอบแนวคิด ASPIRE, ทีมสหสาขาวิชาชีพ, การวิจัยและพัฒนา

Abstract

This research and development (R&D) study aimed to develop a nursing care model for patients undergoing open-heart surgery at Sisaket Hospital using the ASPIRE framework (Assess–Set goals–Plan–Implement–Reassess–Evaluate) with multidisciplinary team participation. The study was conducted from August 27, 2025, to January 27, 2026. Participants included 29 nurses, 30 patients, and 11 experts. The research consisted of four phases: (1) situation analysis; (2) development of an integrated care model; (3) tryout and expert evaluation; and (4) outcome evaluation in real-world practice. Data were collected using interview guides, competency assessment forms, satisfaction questionnaires, feasibility assessment

forms, and clinical outcome recording forms (CVI = 1.00). Quantitative data were analyzed using the Wilcoxon signed-rank test and paired t-test, whereas qualitative data were analyzed using content analysis. Among providers, nursing staff competency scores increased across all care phases (from 94.92% to 96.98%), and team satisfaction improved with statistical significance ($p < 0.001$). The feasibility of model implementation was rated at the highest level. Among patients, all seven incidence indicators achieved their specified targets. Indicators achieving 100% included preoperative assessment, intraoperative emergency reporting, and high-alert drug (HAD) management within 1 minute, and rehabilitation/discharge planning. Indicators with zero incidence included surgery cancellation, postoperative arrhythmia, and 7-day readmission. The findings suggest that the SOH-Care nursing care model can reduce surgery cancellations to zero, decrease coagulopathy by 30%, and significantly improve nursing competency. It is recommended that the model be tested in tertiary hospitals with similar contexts and that long-term outcomes be further studied.

Keywords: Open-heart surgery, Nursing care model, ASPIRE framework, Multidisciplinary team, Research and development

1. Introduction

Cardiovascular disease is the leading cause of death worldwide. The World Health Organization (WHO) reported nearly 20 million deaths from cardiovascular diseases annually in 2023, with the majority attributable to acute myocardial infarction and stroke (World Health Organization, 2023). The increasing prevalence is driven by metabolic risk factors such as obesity, diabetes, and hypertension, compounded by air pollution and climate change (Global Burden of Disease Collaborators, 2023). Internationally, the management of cardiac conditions has continued to advance, emphasizing revascularization, antiplatelet therapy, and the expanding role of specialized cardiology nursing care. Sanders et al. (2022) identified inadequate preoperative risk assessment and fragmented interdisciplinary communication as the primary structural drivers of cardiac surgical morbidity and mortality. Similarly, Noor et al. (2024) reported that cardiac complications following noncardiac surgery remain a major cause of perioperative morbidity and mortality, with urgent surgeries demonstrating a significantly higher incidence of complications than elective procedures.

In Thailand, the number of patients undergoing open-heart surgery has continued to increase. The Thai Thoracic Surgery Association reported that the number of open-heart surgeries increased from 9,577 in 2017 to 11,465 in 2020 (Thai Thoracic Surgery Association, 2020). Despite advances in surgical technology, significant postoperative complications, including acute renal failure, hemorrhage, arrhythmias, and stroke, continue to affect patient outcomes and healthcare costs. Previous studies have demonstrated that integrated care pathways and standardized nursing protocols can significantly reduce postoperative complications and improve patient outcomes in cardiac surgery, including clinical pathway approaches and care bundle strategies. However, limited research has specifically addressed the development of comprehensive, multidisciplinary nursing care models for open-heart surgery in regional tertiary hospitals in Thailand.

Sisaket Hospital was designated as a Level II Cardiac Surgery Center serving Health Region 10 and began providing open-heart surgery services in 2022. Although the hospital follows established protocols for preoperative, intraoperative, and postoperative care according to the Royal College of Surgeons of Thailand guidelines, an analysis in 2024 identified three surgery cancellations (5.88%), exceeding the zero-

cancellation target. The existing care delivery system was organized by individual units: the outpatient department managed initial assessments, the anesthesiology team conducted pre-anesthetic evaluations independently, and the ICU handled postoperative care without a shared interdisciplinary care plan or standardized handoff protocols. Root cause analysis of 60 medical records, patient interviews, and multidisciplinary team (MDT) consultations revealed fragmented care, inadequate inter-unit communication during patient preparation, and the absence of unified standard clinical guidelines across multidisciplinary teams.

Therefore, this research and development (R&D) study aimed to develop an open-heart surgery (OHS) nursing care model at Sisaket Hospital using the ASPIRE conceptual framework (Assess–Set goals–Plan–Implement–Reassess–Evaluate), integrated with principles of continuity of cardiac surgical care for seamless perioperative transitions, a case management approach for individualized patient coordination, and the nursing process for systematic clinical decision-making. The conceptual framework linking the inputs, processes, and expected outcomes of this study is illustrated in Table 1.

2. Materials and methods

2.1 Study Design and Setting

This study employed a research and development (R&D) design comprising four sequential phases aligned with the ASPIRE conceptual framework (Assess–Set goals–Plan–Implement–Reassess–Evaluate): Phase 1, Situation Analysis (corresponding to Assessment); Phase 2, Model Development (corresponding to systematic review and Planning); Phase 3, Tryout and Expert Evaluation (corresponding to Implementation and Review); and Phase 4, Outcome Evaluation (corresponding to Evaluation). The study was conducted at the Anesthesiology Department and Cardiovascular ICU (ICU CVT) of Sisaket Hospital, a 900-bed provincial tertiary hospital in northeastern Thailand serving as the cardiac surgery center for Health Region 10.

Table 1. Conceptual Framework for Open-Heart Surgery Care Development at Sisaket Hospital

INPUT	PROCESS	OUTCOME
Patient Care Concepts for Open-Heart Surgery (Case-Based) • Access and admission to OHS services • MDT pre-anesthetic readiness assessment • OHS care planning • Holistic patient care • Patient and family empowerment • Continuity of care through community	**SOH - Care Compond ASPIRE** **Phase 1: Situation Analysis** Staff/patient interviews, medical record review **Phase 2: Model Development** Literature review, MDT collaborative design **Phase 3: Tryout & Expert Evaluation** Pilot testing, expert review, refinement **Phase 4: Outcome Evaluation** Full implementation, outcome measurement	**Provider Outcomes:** • Competency scores (5 phases) • Staff satisfaction (t-test) **Patient Outcomes:** • Pre-op assessment 100% • Surgery cancellations 0% • Emergency assessment ≤1 min 100% • HAD management ≤1 min 100% • Post-op arrhythmia 0% • 7-day readmission 0% • Rehab & discharge planning 100%

2.2 Participants

Provider sample: 29 nursing staff members (25 nurse anesthetists and four ICU nurses) involved in open-heart surgery care. Patient sample: 30 patients who underwent open-heart surgery during the implementation period (Phase 4). Medical record review: 30 records for Phase 1 retrospective analysis, comprising records from the one year preceding model implementation. Expert panel: 11 experts for Phase 3 evaluation and five content validity experts for instrument development. Inclusion criteria for nursing staff were registered nurses with at least one year of experience in open-heart surgery care at Sisaket Hospital who provided informed consent. Exclusion criteria were staff on extended leave during the study period or those who withdrew consent. Inclusion criteria for patients were adults aged ≥18 years scheduled for elective open-heart surgery during the implementation period. Exclusion criteria were emergency surgical cases, patients with cognitive impairment precluding informed consent, or patients who declined participation.

2.3 Research Instruments

Phase 1 instruments included: (1) a structured interview guide for multidisciplinary team members, (2) a patient experience interview guide, and (3) a clinical outcome recording form based on medical records; all were reviewed by five experts and achieved a Content Validity Index (CVI) of 1.00. The multidisciplinary team interview guide used open-ended questions organized into three domains: perceptions of the care process, communication barriers, and patient preparation practices. The patient experience guide covered five domains: fear, anxiety, and risk perception; communication and shared decision-making; continuity of care and systematic management; holistic physical and psychological care; and confidence, concerns, and post-discharge self-care support. The clinical outcome recording form captured perioperative complications, ICU length of stay, use of cardiac assist devices and vasoactive medications, functional recovery at one month, readmission, and mortality. Interview responses were analyzed using content analysis.

Phase 2 instruments included a competency assessment tool covering five care phases (29 items) using a 5-point rating scale (1 = needs improvement to 5 = excellent), with a pass criterion of ≥80% of the total score, Cronbach's alpha = 0.78, and an expanded clinical outcome recording form.

Phase 3 instruments included a Care Model Implementation Assessment Form and Problem Documentation Form.

Phase 4 instruments included a nursing team competency assessment form (29 items across five phases), a team satisfaction questionnaire (7 items, 5-point Likert scale, Cronbach's alpha = 0.78), a feasibility assessment form, and a patient clinical outcome recording form.

2.4 Data Collection Procedure

Phase 1 (Situation Analysis): Staff interviews (5–10 minutes each), patient interviews, and retrospective medical record reviews were conducted following institutional ethics approval (SSKH 030/2025) and informed consent.

Phase 2 (Model Development): Data synthesis, a systematic literature review using the PICO framework (Google Scholar, Thai Journal Online, CINAHL, PubMed, and EMBASE), and MDT workshops were conducted to co-design the care model.

Phase 3 (Tryout): Pilot testing was conducted with 11 staff members (eight nurse anesthetists, two ICU nurses, and one operating room circulator nurse) for one month, with continuous feasibility monitoring and refinement.

Phase 4 (Outcome Evaluation): Full model implementation was conducted with 29 nursing staff members and 30 OHS patients for four months, with collection of competency, satisfaction, and clinical outcome data.

2.5 Data Analysis

Quantitative data were analyzed using descriptive statistics, including frequency, percentage, mean, and standard deviation. For pre- and post-model comparisons of nursing competency scores (Table 2), the Wilcoxon signed-rank test was applied due to the ordinal nature of the competency percentage data. For team satisfaction scores (Table 3), the paired samples t-test was used because satisfaction domain scores met the assumptions of normality (Shapiro–Wilk, $p > 0.05$). Statistical significance was set at $p < 0.05$ for all tests. Qualitative data were analyzed using content analysis to identify themes and patterns from interviews and feedback. The research activities and the corresponding tools and instruments used in each of the four phases are summarized in Table 2.

Table 2. Research Phase Workflow

Phase / Activity	Tools / Instruments
Phase 1: Situation Analysis 1. Document/data review 2. MDT staff interviews 3. Retrospective medical record review (n = 30)	• MDT situation interview form • Patient experience interview form • Medical record outcome form (CVI = 1.00)
Phase 2: Model Development 1. MDT planning meetings 2. Literature review & evidence synthesis 3. Draft model development	• Expert appropriateness assessment form (n = 5) Outcome: Draft OHS Care Model
Phase 3: Tryout & Evaluation 1. Pilot testing: n = 11 staff, 1 month 2. Full tryout: n = 29 staff, 4 months 3. Expert panel evaluation (n = 11)	• CVT pre-anesthetic visit form • Patient education leaflet • Care model assessment form • ICU CVT rehabilitation & discharge plan
Phase 4: Outcome Evaluation 1. Nursing compliance with care model 2. Team satisfaction assessment 3. Clinical patient outcomes (n = 30 patients; n = 29 nursing staff)	• Competency assessment (29 items, 5 phases) • Team satisfaction questionnaire • Feasibility assessment form • Patient clinical outcome recording form

3. Results

3.1 Phase 1: Situation Analysis

An analysis of open-heart surgery patient care at Sisaket Hospital revealed that the existing system aligned with international anesthesia safety standards (SIMPLE framework), covering three anesthesia phases. However, a systematic analysis identified variations in documentation and inter-unit communication practices that affected patient readiness.

The 2024 operating room safety report identified four key problem categories: (1) preoperative patient preparation gaps, (2) discontinuous monitoring and evaluation systems, (3) limited clinical support resources, and (4) postoperative safety and complication outcomes (WHO, 2023). The overarching theme was “Fragmented Holistic Care System,” reflecting inadequate system-wide integration across all care phases.

Retrospective clinical data (n = 30 records spanning the one year preceding model implementation; a subset of n = 30 records was randomly selected for in-depth complication profiling) revealed that 93.34% of patients had cardiopulmonary bypass (CPB) times of 50–150 minutes. All patients (100%) developed anemia and hypocalcemia postoperatively, 96.67% experienced hypokalemia, and 70% had coagulopathy. Despite these expected complications, 86.67% of patients showed improved ejection

fraction (EF) at discharge, and no patients died or were readmitted within 30 days (Sisaket Hospital medical records, 2025).

Patient interviews (n = 10) generated five major themes: (1) fear, anxiety, and preoperative risk perception; (2) communication support and shared decision-making; (3) care continuity and systematic management; (4) holistic physical and psychological care; and (5) confidence, concerns, and post-discharge self-care support.

3.2 Phase 2: Model Development — The SOH-Care Model

Based on Phase 1 findings and a systematic literature review, the research team developed the Sisaket Open-Heart Surgery Nursing Care Model (SOH-Care Model), which comprised four integrated components:

Phase 1 findings were combined with a systematic literature review conducted using the PICO framework across Google Scholar, Thai Journal Online, CINAHL, PubMed, and EMBASE. Search terms included open-heart surgery, nursing care model, ASPIRE, ERAS cardiac, pre-anesthetic assessment, and multidisciplinary perioperative care, with an inclusion period of 2018–2024. After screening 184 records, 27 articles were appraised for evidence quality and operational relevance. Key elements extracted and incorporated into the SOH-Care Model included: (a) structured pre-anesthetic assessment items and risk stratification (Arjomandi Rad et al., 2025) into the CVT form; (b) empowerment-based patient education content (Arjomandi Rad et al., 2025) into the patient leaflet; (c) phase-aligned nursing competency domains for cardiac surgery (Arjomandi Rad et al., 2025) into the competency tool; and (d) ERAS-cardiac early mobilization principles and structured day-by-day rehabilitation milestones (Engelman et al., 2019) into the ICU rehabilitation and discharge plan. These elements were then refined through three MDT co-design workshops to ensure contextual fit at Sisaket Hospital. The resulting SOH-Care Model comprised four integrated components.

Component 1, CVT Pre-Anesthetic Evaluation Form: A structured multidisciplinary pre-anesthetic assessment form covering patient demographics, cardiac diagnosis, surgical history, current medications, laboratory values, echocardiographic findings, anesthetic risk stratification, and nursing care planning across the preoperative period. The form was designed to facilitate standardized, team-shared documentation and replace the previously fragmented unit-based records.

Component 2, Patient Education Leaflet: An easy-language bilingual leaflet covering basic cardiac anatomy, preoperative preparation, in-hospital conduct, and post-discharge self-care, developed through MDT consensus.

Component 3, Competency Assessment Tool: A 29-item tool covering five care phases—pre-preparation (three items), preoperative (seven items), intraoperative (seven items), postoperative (eight items), and discharge (four items)—assessing technical skills, clinical decision-making, and interprofessional collaboration.

Component 4, ICU CVT Rehabilitation and Discharge Plan (Day 0–7): A structured daily rehabilitation protocol from the immediate postoperative period through day 7, emphasizing early mobilization, progressive activity, patient education, and discharge preparation.

3.3 Phase 3: Expert Evaluation and Tryout

Based on the evaluation by 11 experts, all four components of the SOH-Care Model were rated at the highest level of appropriateness, as shown in Table 3.

Table 3. Expert Evaluation Results for SOH-Care Model Components (n = 11 experts)

Component	Mean	SD	Rating
Overall Care Model (care process flowchart)	4.55	0.32	Highest
Pre-Anesthetic Evaluation Form (CVT)	4.92	0.21	Highest
Patient Education Leaflet	4.86	0.28	Highest
Competency Assessment Tool (overall)	4.60	0.50	Highest
Pre-preparation phase	4.61	0.48	Highest
Pre-operative phase	4.58	0.51	Highest
Intraoperative phase	4.64	0.49	Highest
Post-operative phase	4.59	0.52	Highest
Discharge phase	4.62	0.49	Highest
ICU CVT Rehabilitation & Discharge Plan (overall)	4.68	0.28	Highest
Day 0 (immediate post-op)	4.73	0.31	Highest
Day 4	4.77	0.29	Highest
Day 6 (pre-discharge)	4.82	0.26	Highest

All four model components achieved mean appropriateness scores between 4.55 and 4.92, with consistently low standard deviations indicating strong consensus among evaluators. The Pre-Anesthetic Evaluation Form (CVT) received the highest rating (mean = 4.92, SD = 0.21), reflecting expert confidence in its clinical comprehensiveness. Across the five phases of the Competency Assessment Tool, mean scores ranged narrowly from 4.58 to 4.64, suggesting that the instrument achieved uniform quality across all care phases rather than concentrating strength in any single domain. The ICU CVT Rehabilitation and Discharge Plan showed a progressively increasing rating from Day 0 to Day 6 (4.73 to 4.82), indicating that experts particularly valued the structured pre-discharge preparation component.

3.4 Phase 4: Outcome Evaluation

3.4.1 Provider Outcomes

The assessment of nursing staff competency before and after implementing the SOH-Care Model (n = 29) revealed that competency scores improved in all five care phases, as shown in Table 4.

Table 4. Nursing Competency Scores Pre- and Post-Model Implementation (n = 29)

Care Phase	Before (%)	After (%)	Change (%)	*p*-value*
Pre-preparation	93.85	96.21	+2.36	< 0.05
Pre-operative	94.10	96.65	+2.55	< 0.05
Intraoperative	95.37	97.32	+1.95	< 0.05
Post-operative	94.88	97.05	+2.17	< 0.05
Discharge planning	96.38	97.66	+1.28	< 0.05
Overall	94.92	96.98	+2.06	< 0.05

*Wilcoxon signed-rank test; significance set at $p < 0.05$.

Competency scores improved across all five care phases following model implementation, with overall compliance advancing from 94.92% to 96.98% (Δ +2.06%, $p < 0.05$). The largest gain was observed in the preoperative phase (Δ +2.55%), while the smallest was in the discharge planning phase (Δ +1.28%), a phase that had the highest baseline score (96.38%), suggesting a ceiling effect in that domain. The statistically significant improvement across all phases indicates a consistent, model-attributable effect rather than random variation. The qualitative findings from Phase 4 (Outcome Evaluation) complement the quantitative results by providing deeper insights into the experiences and perceptions of nursing staff and patients regarding the implementation of the SOH-Care Model. Content analysis of interviews and focus group discussions revealed several key themes.

1) Enhanced Continuity and Systematic Care. Nursing staff reported that the SOH-Care Model facilitated more continuous and systematic care across all phases from pre-preparation to discharge. They highlighted improved adherence to standardized protocols and clearer role definitions, which reduced ambiguity and enhanced confidence in clinical decision-making. Nurses emphasized that the model helped minimize fragmented care and promoted a more integrated multidisciplinary approach.

2) Improved Communication and Team Collaboration. Participants noted that communication within the multidisciplinary team became more structured and effective, particularly through the use of standardized tools such as the pre-anesthetic evaluation form (CVT) and the competency assessment tool. This enhanced information exchange contributed to safer patient transitions between care phases and reduced errors related to miscommunication.

3) Patient Empowerment and Education. Patients and their families expressed appreciation for the clear, accessible information provided through the patient education leaflet and ongoing education during hospitalization. Themes emerged around increased understanding of the surgical process, reduced preoperative anxiety, and greater confidence in self-care after discharge. Patients valued the opportunities to ask questions and felt supported by the healthcare team.

4) Challenges and Areas for Further Improvement. While overall satisfaction was high, nursing staff identified workload and resource constraints as ongoing challenges that could impact the consistent application of the model. Some patients mentioned a need for more tailored education materials to accommodate varying literacy levels and requested enhanced follow-up support after discharge to address lingering concerns.

5) Professional Development and Competency Growth. Nurses reported that the competency assessment tool supported their professional development by clearly outlining expected skills and behaviors across care phases. This structured evaluation encouraged reflective practice and highlighted areas for targeted training, contributing to improved clinical competency and patient safety. A comparison of nursing team satisfaction before and after model implementation using a paired-samples t-test (n = 29) revealed significant improvement in all domains, as shown in Table 5.

Table 5. Nursing Team Satisfaction Before and After Model Implementation (n = 29)

Domain	Before ($\bar{x}$±SD)	After ($\bar{x}$±SD)	Δ	t	*p*-value
Clarity of model and guidelines	4.10 ± 0.45	4.80 ± 0.32	+0.70	6.25	< .001**
Appropriateness of the model	4.05 ± 0.50	4.70 ± 0.36	+0.65	5.89	< .001**
Feasibility of implementation	4.00 ± 0.47	4.65 ± 0.48	+0.65	5.12	0.001**
Overall satisfaction	4.04 ± 0.46	4.68 ± 0.39	+0.64	6.11	< .001***

**$p < 0.01$; ***$p < 0.001$. Paired-samples t-test.

Overall team satisfaction improved significantly from a mean of 4.04 (SD = 0.46) to 4.68 (SD = 0.39), representing a mean gain of 0.64 points ($t(28) = 6.11$, $p < 0.001$). All three domains showed statistically significant improvement at $p < 0.01$. The greatest gain occurred in clarity of model and guidelines (Δ +0.70, $t = 6.25$, $p < 0.001$), which directly corresponds to the structural ambiguity identified as a key problem in Phase 1, suggesting that the model effectively resolved the communication and role-definition deficiencies that staff had previously experienced. The reduction in standard deviation across all domains after implementation (e.g., overall SD: 0.46 ⟶ 0.39) indicates not only higher satisfaction but also greater consistency of experience among nursing staff.

3.4.2 Patient Outcomes — Operational Indicators

Evaluation of patient operational outcomes before and after model implementation (n = 30) showed that all seven operational indicators met their specified targets, as shown in Table 6.

All seven operational indicators reached their specified targets following model implementation. Four indicators that were below target before implementation—preoperative assessment completion, surgery cancellations, emergency assessment timeliness, and HAD management timeliness—all achieved 100% or 0% as required. Notably, postoperative arrhythmia incidence was eliminated, decreasing from 3.33% to 0%, and no 7-day readmissions occurred in either period. The sole indicator that had already achieved its target before implementation—rehabilitation and discharge planning coverage—was maintained at 100%, confirming that the model did not disrupt existing best practices while improving areas of deficiency.

Table 6. Operational Outcome Indicators Before and After Model Implementation (n = 30)

Indicator	Target	Before n (%)	After n (%)
Patients received pre-op assessment by nursing team	100%	29 (96.67%)	30 (100%)
Surgery cancellations due to patient unreadiness	0%	1 (3.33%)	0 (0%)
Emergency assessment reported within 1 min (anesthesia)	100%	29 (96.67%)	30 (100%)
High-alert drug (HAD) management within 1 min	100%	29 (96.67%)	30 (100%)
Post-operative arrhythmia incidents	0%	1 (3.33%)	0 (0%)
7-day readmission incidents	0%	0 (0%)	0 (0%)
Patients received rehabilitation & discharge planning	100%	30 (100%)	30 (100%)

3.4.3 Clinical Outcomes

The incidence of coagulopathy decreased from 100% to 70%. The ICU length of stay in the optimal 8–14-day range increased from 33.33% to 56.67%. No patients required cardiac assist devices after model implementation, compared with 6.7% before implementation. The vasodilator requirement decreased from 80% to 60%. At the one-month follow-up, 100% of patients could walk independently and climb stairs, increasing from 73.33% and 83.34%, respectively, before implementation. No deaths occurred within 30 days of the operation.

Patient satisfaction was high, with an overall mean of 4.70 (SD = 0.47). The highest-rated domains were information received (4.77), equipment care (4.73), and staff attentiveness (4.77). No patient was readmitted or died within 30 days post-discharge. A review of clinical outcome records found that several postoperative complications decreased after model implementation, most notably a 30% reduction in coagulopathy, as shown in Table 7.

Beyond complication reduction, functional recovery outcomes at one-month follow-up were notable: all 30 patients achieved full independence in daily activities, including walking and stair climbing, representing a meaningful improvement over the pre-implementation baseline. Patient satisfaction was high overall (mean = 4.70, SD = 0.47), with information received and staff attentiveness emerging as the most highly rated domains. No patient died or was readmitted within 30 days of discharge.

Table 7. Clinical Outcomes — Complications During Hospitalization (n = 30)

Complication	Before n (%)	After n (%)	Change
Anemia	30 (100%)	30 (100%)	No change
Hypokalemia	30 (100%)	29 (96.67%)	Decreased
Hypocalcemia	30 (100%)	30 (100%)	No change
Coagulopathy	30 (100%)	21 (70%)	↓ 30%
Hypothermia	9 (30%)	13 (43.33%)	Increased
Bradycardia	4 (13.33%)	1 (3.33%)	↓ 10%
Hypomagnesemia	2 (6.67%)	3 (10%)	Slight increase

4. Discussion

4.1 Situation Analysis

The identification of a "Fragmented Holistic Care System" as the overarching structural problem in Phase 1 carries important clinical meaning. It indicates that poor patient outcomes were not attributable to individual professional incompetence, but rather to the absence of system-level coordination mechanisms, specifically unified clinical guidelines, structured handoff protocols, and shared documentation tools across the multidisciplinary team. The resulting 5.88% surgery cancellation rate, while numerically modest, represents a concrete patient safety failure with measurable downstream consequences, including delayed treatment, extended hospital stays, and avoidable psychological distress for patients and families.

This finding is consistent with Sanders et al. (2022), who identified inadequate preoperative risk assessment and fragmented interdisciplinary communication as primary structural drivers of cardiac surgical morbidity and mortality. Similarly, Noor et al. (2024) reported that cardiac complications following non-cardiac surgery remain a major cause of perioperative morbidity and mortality, with urgent surgeries demonstrating a significantly higher incidence of complications compared with elective procedures. A recent meta-analysis reported cardiac complication rates of 5.4% in urgent surgeries and 2.8% in elective surgeries, with urgent procedures associated with a markedly increased risk of adverse cardiac events.

The observed pattern at Sisaket Hospital therefore reflects a systemic challenge well recognized in the international cardiac surgery literature, rather than an isolated institutional failing. The additional finding that nurse burnout and high workload constrained double-check adherence aligns with Moss et al. (2016), who demonstrated that staffing intensity directly limits safety-critical process compliance in specialized nursing environments.

These findings were broadly anticipated given the hospital's relatively recent designation as a Level II Cardiac Surgery Center in 2022, a context in which clinical protocols are typically established before the supporting coordination infrastructure is fully developed. That said, the scale of fragmentation spanning all four identified problem categories simultaneously was more pronounced than initially expected, which underscored the need for a comprehensive model rather than targeted protocol adjustments alone.

4.2 Model Development — The SOH-Care Model

The consistently high expert appropriateness ratings across all four SOH-Care Model components (overall mean range: 4.55–4.92) indicate that the model achieved strong content validity and practical relevance, as judged by specialist clinicians. The particularly high rating for the CVT Pre-Anesthetic Evaluation Form (mean = 4.92, SD = 0.21) is notable, as it suggests that the instrument captured the clinical complexity of pre-anesthetic assessment in a format that experts regarded as both comprehensive and operationally feasible. The slightly lower, though still high, rating for the Competency Assessment Tool (mean = 4.60, SD = 0.50) likely reflects the inherent difficulty of operationalizing multidimensional clinical competencies, particularly interprofessional collaboration, into discrete, assessable items.

These outcomes align with Grant et al. (2023), who demonstrated that structured MDT preoperative assessment frameworks developed through collaborative clinical design significantly reduce unnecessary resource utilization and improve patient outcomes, precisely because they are grounded in the contextual realities of the implementing institution. The Day 0–7 ICU rehabilitation protocol represents a deliberate shift from reactive to proactive nursing care, consistent with ERAS principles as documented by Zhang et al. (2021), whose meta-analysis confirmed that structured early rehabilitation protocols reduce ICU length of stay and postoperative complications in cardiac surgery patients. The empowerment-oriented

patient education leaflet reflects the broader principle that bilingual, accessible cardiac surgery education materials can improve patient self-care adherence and reduce preoperative anxiety.

The high expert ratings were expected given the participatory design methodology; models co-constructed with frontline clinicians and reviewed by domain specialists typically achieve stronger face and content validity than those developed through top-down policy processes alone. This expectation was confirmed.

4.3 Outcome Evaluation

4.3.1 Provider Outcomes

The increase in nursing competency scores across all five care phases, from an overall mean of 94.92% to 96.98%, is clinically meaningful, even though the absolute magnitude of change appears modest. In high-acuity surgical nursing, performance in safety-critical behaviors is already constrained near ceiling levels by professional regulation and existing protocols; consequently, even small percentage gains reflect substantive improvements in systematic compliance rather than basic skill acquisition. Phase-level Wilcoxon signed-rank testing confirmed that these improvements were statistically significant across all phases ($p < 0.05$), indicating a consistent rather than incidental effect of model implementation.

The significant improvement in team satisfaction ($t(28) = 6.11$, $p < 0.001$, Δ +0.64) is particularly important because satisfaction among specialist nursing staff is a recognized leading indicator of sustained protocol adherence and staff retention in high-demand clinical environments. The domain showing the largest gain, clarity of model and guidelines (Δ +0.70), directly reflects the resolution of the structural ambiguity identified in Phase 1, confirming that the model addressed the root cause of the problem rather than its symptoms. This pattern is consistent with prior evidence that implementation of structured interdisciplinary care planning in cardiac surgery settings produced significant and durable improvements in both outcomes and staff satisfaction, particularly where clear role definition had previously been absent.

4.3.2 Patient Outcomes — Operational and Clinical Indicators

The achievement of all seven operational indicator targets represents the most direct evidence of the model's practical effectiveness. The transition from 96.67% to 100% in preoperative assessment completion, and the elimination of surgery cancellations due to patient unreadiness, confirms that the structural integration achieved through the SOH-Care Model translated into measurable patient safety gains. These findings align with Kaneko et al. (2023), who demonstrated that structured MDT preoperative pathways for high-risk cardiac surgery patients are the single most effective intervention for reducing avoidable cancellations and operative complications.

The 30% reduction in coagulopathy incidence, from 100% to 70%, is a clinically significant finding. While some degree of coagulopathy is an expected consequence of cardiopulmonary bypass due to hemodilution, platelet activation, and clotting factor consumption, the reduction observed here is consistent with Mutsuga M. (2023), who demonstrated that optimized operative duration management and perioperative monitoring protocols, both of which are central elements of the SOH-Care Model's intraoperative and postoperative phases, substantially mitigate coagulopathy severity.

Despite the overall improvement in other outcomes, hypothermia increased from 9/30 (30%) to 13/30 (43.33%), whereas hypomagnesemia increased from 2/30 (6.67%) to 3/30 (10%). These findings represent increases of four and one cases, respectively, and should be interpreted cautiously because each comparison group comprised only 30 patients and the study was not designed or powered to determine the causes of individual complications. Possible explanations include differences in operative

complexity or cardiopulmonary bypass duration, changes in the sensitivity of monitoring and documentation, and variation in perioperative warming or magnesium replacement practices; however, these factors were not measured systematically. Accordingly, the increases cannot be attributed to the SOH-Care Model. Future prospective studies with larger samples should use standardized definitions and collect risk-adjustment variables, including procedure type and complexity, bypass and cross-clamp times, serial core-temperature measurements, magnesium concentrations, and replacement therapy.

The finding that 100% of patients recovered full functional independence within one month of discharge, including independent walking and stair climbing, exceeds the preoperative baseline of 73.33% and 83.34%, respectively, and is consistent with Alvarez et al. (2020), who demonstrated that structured nurse-led rehabilitation beginning in the immediate postoperative period significantly accelerates cardiovascular recovery and reduces pulmonary complications. The zero 30-day mortality and readmission rates, while favorable, should be interpreted cautiously given the small sample size and the relatively short follow-up window.

It should be noted that the improvements observed across all outcome domains cannot be attributed exclusively to the SOH-Care Model. The absence of a concurrent control group means that concurrent changes in staffing experience, surgical caseload maturation, or broader institutional quality improvement activities may have contributed to the results. These findings are therefore best interpreted as indicative of the model's potential value within this specific institutional context, pending validation in controlled or multi-site studies.

5. Conclusion and suggestions

5.1 Conclusion

Open-heart surgery nursing in provincial tertiary hospitals demands a level of system-wide coordination that informal, role-based practice alone cannot sustain. This study addressed that gap by developing and evaluating the SOH-Care Model—a four-component, evidence-based nursing care model grounded in the ASPIRE framework and constructed through genuine multidisciplinary collaboration at Sisaket Hospital.

The model successfully fulfilled each of its three research objectives. First, situation analysis confirmed that fragmented care integration, rather than individual professional competence, was the primary structural barrier to consistent patient safety outcomes. Second, the development process produced a coherent set of clinical tools—the CVT pre-anesthetic evaluation form, patient education leaflet, competency assessment tool, and ICU rehabilitation and discharge plan—each achieving expert appropriateness ratings at the highest level (overall mean = 4.60, SD = 0.50). Third, outcome evaluation demonstrated that model implementation yielded measurable improvements across all dimensions: nursing competency scores advanced across all five care phases, team satisfaction improved significantly ($t(28) = 6.11$, $p < 0.001$), all seven operational indicators reached their targets, and coagulopathy incidence decreased by 30%, with 100% of patients recovering full functional independence within one month of discharge.

Taken together, these findings indicate that the SOH-Care Model addressed the identified research problem and met the study's anticipated outcomes within the scope of a single-site, pre–post design. The significance of these results extends beyond operational performance metrics: they demonstrate that standardized, multidisciplinary nursing care—when co-designed with frontline staff and validated by clinical experts—can meaningfully reduce system-level fragmentation and strengthen patient

safety in a resource-constrained provincial setting. For nursing practice, the model offers a replicable framework for cardiac surgery care development; for the broader field, it contributes an empirically evaluated prototype for constructing competency-aligned, phase-specific nursing care models in complex surgical contexts. Multi-site validation across comparable provincial hospitals is recommended as the logical next step toward national-level implementation.

5.2 Suggestions for Future Research

1) Health economic evaluation: Compare the cost-effectiveness of the developed model versus standard care for hospital resource allocation decisions.

2) Long-term patient-reported outcomes: Extend the assessment to 6–12 months post-discharge to evaluate quality of life, physical function, and psychological outcomes, including anxiety and depression.

3) National standardized competency development: Develop a nationally standardized competency framework for Thai nurse anesthetists in open-heart surgery, using this model as a prototype.

6. References

Alvarez, C., Vera, M., Castillo, C., & Rojas, M. (2020). Effects of structured nurse-led rehabilitation on functional recovery after cardiac surgery: A systematic review and meta-analysis. Heart & Lung: The Journal of Cardiopulmonary and Acute Care, 49(5), 543–552. https://doi.org/10.1016/j.hrtlng.2020.04.007

Arjomandi Rad, A., Streukens, S., Vainer, J., Athanasiou, T., Maessen, J., & Sardari Nia, P. (2025). The current state of the multidisciplinary heart team approach: a systematic review. European Journal of Cardio-Thoracic Surgery, 67(1), ezae461. https://doi.org/10.1093/ejcts/ezae461

Engelman, D. T., Ben Ali, W., Williams, J. B., Perrault, L. P., Reddy, V. S., Arora, R. C., Roselli, E. E., Khoynezhad, A., Gerdisch, M., Levy, J. H., Lobdell, K., Fletcher, N., Kirsch, M., Nelson, G., Engelman, R. M., Gregory, A. J., & Boyle, E. M. (2019). Guidelines for perioperative care in cardiac surgery: Enhanced Recovery After Surgery Society recommendations. JAMA Surgery, 154(8), 755–766. https://doi.org/10.1001/jamasurg.2019.1153

Global Burden of Disease Collaborators. (2023). Global burden of cardiovascular diseases and risks, 1990–2022. Journal of the American College of Cardiology, 82(25), 2350–2473. https://doi.org/10.1016/j.jacc.2023.11.007

Grant, S. W., Jenkins, D. P., Dalrymple-Hay, M. J., Trivedi, U., & Uppal, R. (2023). Collaborative preoperative assessment in cardiac surgery: A multicentre analysis. Interactive CardioVascular and Thoracic Surgery, 36(4), ivad009. https://doi.org/10.1093/icvts/ivad009

Moss, M., Good, V. S., Gozal, D., Kleinpell, R., & Sessler, C. N. (2016). An official Critical Care Societies Collaborative statement: Burnout syndrome in critical care healthcare professionals: A call for action. American Journal of Respiratory and Critical Care Medicine, 194(1), 106–113. https://doi.org/10.1164/rccm.201604-0708ST

Mutsuga, M. (2023). Perioperative Management of Coagulation After the Weaning of Cardiopulmonary Bypass in Cardiac Surgery. Kyobu geka. The Japanese Journal of Thoracic Surgery, 76(10), 824-828.

Noor, S., Rascón-Martínez, D. M., Khoso, A., et al. (2024). Incidence and predictors of cardiac complications following elective versus urgent non-cardiac surgeries. Cureus, 16(12), e75946. https://doi.org/10.7759/cureus.75946

Sanders, J., Makariou, N., Tocock, A., Magboo, R., Thomas, A., & Aitken, L. M. (2022). Preoperative risk assessment tools for morbidity after cardiac surgery: A systematic review. European Journal of Cardiovascular Nursing, 21(7), 655–664. https://doi.org/10.1093/eurjcn/zvac003

Sisaket Hospital. (2025). Medical record data: Open-heart surgery patients 2024–2025. Sisaket: Anesthesiology Department, Sisaket Hospital. (in Thai)

Thai Thoracic Surgery Association. (2020). Statistics on heart surgery in Thailand, 2020. Bangkok: ThaiSTS. (in Thai)

World Health Organization. (2023). Cardiovascular diseases (CVDs) — Fact sheet [Online]. Retrieved January 10, 2026, from. https://www.who.int

Wyler von Ballmoos, M. C., Kaneko, T., Iribarne, A., Kim, K. M., Arghami, A., Fiedler, A., Habib, R., Parsons, N., Elhalabi, Z., Krohn, C., & Bowdish, M. E. (2024). The Society of Thoracic Surgeons Adult Cardiac Surgery Database: 2023 update on procedure data and research. The Annals of Thoracic Surgery, 117(2), 260–270. https://doi.org/10.1016/j.athoracsur.2023.11.016

การพัฒนาระบบตรวจวัดคุณภาพอากาศและแจ้งเตือนฝุ่น PM2.5 แบบเรียลไทม์ โดยประยุกต์ใช้เทคโนโลยีอินเทอร์เน็ตของสรรพสิ่ง

The Development of a Real-Time Air Quality Monitoring and PM2.5 Alert System Using Internet of Things Technology

สุกัญชลิกา บุญมาธรรม[1] พีรศุษย์ บุญมาธรรม[1*] ปราโมทย์ ตงฉิน[1] และ ศิริพร อ่วมศิริ[1]

Sukanchalika Boonmatham[1], Pheerasut Boonmatham[1*], Pramote Tongchin[1] and Siriporn Uamsiri[1]

[1]คณะเทคโนโลยีสารสนเทศ มหาวิทยาลัยราชภัฏเพชรบุรี จังหวัดเพชรบุรี

[1]Faculty of Information Technology, Phetchaburi Rajabhat University, Phetchaburi Province

[*]Corresponding Author: pheerasut.boo@mail.pbru.ac.th

Received: April 30, 2026 **Revised:** July 19, 2026 **Accepted:** September 17, 2026

บทคัดย่อ

งานวิจัยนี้มีวัตถุประสงค์เพื่อพัฒนาระบบตรวจวัดคุณภาพอากาศและแจ้งเตือนฝุ่น PM2.5 แบบเรียลไทม์โดยใช้เทคโนโลยีอินเทอร์เน็ตของสรรพสิ่ง ประเมินประสิทธิภาพของระบบ และประเมินการยอมรับของผู้ใช้งาน การวิจัยดำเนินการตามรูปแบบการวิจัยและพัฒนา ระบบที่พัฒนาขึ้นประกอบด้วย 3 ส่วน ได้แก่ สถานีตรวจวัดคุณภาพอากาศภายนอกอาคาร ระบบประมวลผลและจัดเก็บข้อมูลบนคลาวด์ และส่วนแสดงผลพร้อมระบบแจ้งเตือนผู้ใช้งาน สถานีตรวจวัดใช้พลังงานแสงอาทิตย์ร่วมกับแบตเตอรี่สำรอง สามารถทำงานกลางแจ้งได้อย่างต่อเนื่อง โดยตรวจวัดข้อมูล PM2.5 และอุณหภูมิ แล้วส่งข้อมูลผ่านเกตเวย์ IoT ด้วยเครือข่าย 4G ไปยังระบบคลาวด์โดยใช้โพรโทคอล MQTT ข้อมูลถูกแสดงผลผ่านเว็บแดชบอร์ด ป้าย LED ณ จุดติดตั้ง และแจ้งเตือนผ่านแอปพลิเคชันเทเลแกรม เมื่อค่าฝุ่น PM2.5 เกินเกณฑ์ที่กำหนด การประเมินประสิทธิภาพใช้การทดสอบแบบแบล็กบ็อกซ์และการประเมินค่าความคลาดเคลื่อน ผลการทดสอบพบว่ารายการทดสอบทั้ง 10 รายการผ่านเกณฑ์ทั้งหมด ครอบคลุมการตรวจวัด การส่งข้อมูล การประมวลผล การแสดงผล การแจ้งเตือน การจำแนกระดับความเสี่ยง และการทำงานโดยรวมของระบบ การเปรียบเทียบค่าการตรวจวัดของระบบ AQMS กับอุปกรณ์ IQAir AirVisual ซึ่งเป็นอุปกรณ์ตรวจวัดเชิงพาณิชย์ โดยใช้ข้อมูลรายชั่วโมงที่จับคู่ตามเวลาได้จำนวน 720 คู่ จากระยะเวลา 30 วัน พบว่ามีค่าความคลาดเคลื่อนร้อยละสัมบูรณ์เฉลี่ยร้อยละ 7.72 ค่าความคลาดเคลื่อนสัมบูรณ์เฉลี่ย 1.65 ไมโครกรัมต่อลูกบาศก์เมตร และค่ารากของความคลาดเคลื่อนกำลังสองเฉลี่ย 1.96 ไมโครกรัมต่อลูกบาศก์เมตร ผลดังกล่าวสะท้อนว่าค่าการตรวจวัดจากอุปกรณ์ทั้งสองมีความสอดคล้องกันภายใต้พื้นที่ ช่วงเวลา และสภาพแวดล้อมที่ศึกษา ทั้งนี้ ผลการเปรียบเทียบไม่ถือเป็นการยืนยันความแม่นยำเชิงมาตรวิทยาของระบบ เนื่องจากไม่ได้สอบเทียบกับ เครื่องมือมาตรฐาน FRM/FEM การประเมินการยอมรับจากกลุ่มตัวอย่าง 30 คน พบว่าผู้ใช้งานมีการยอมรับระบบโดยรวมอยู่ในระดับมากที่สุด มีค่าเฉลี่ยโดยรวม 4.51 และส่วนเบี่ยงเบนมาตรฐาน 0.51 ผลการศึกษาสะท้อนว่าระบบสามารถทำงานตามฟังก์ชันที่กำหนด และให้ค่าการตรวจวัดที่มีความสอดคล้องกับอุปกรณ์เปรียบเทียบภายใต้เงื่อนไขของการศึกษานี้ อย่างไรก็ตาม ควรมีการสอบเทียบกับเครื่องมือมาตรฐาน การทดสอบระยะยาว และการประเมินกับผู้ใช้จำนวนมากขึ้นก่อนนำไปใช้งานในวงกว้าง

คำสำคัญ: ฝุ่นละอองในอากาศ PM2.5, ระบบแบบเรียลไทม์, การตรวจวัดคุณภาพอากาศ, อินเทอร์เน็ตของสรรพสิ่ง, ระบบแจ้งเตือน

Abstract

This research aimed to develop a real-time air quality monitoring and PM2.5 alert system using Internet of Things technology, evaluate the system's performance, and assess user acceptance. The study followed a research-and-development approach. The developed system consisted of three main components: an outdoor air quality monitoring station, a cloud-based data processing and storage system, and a display and user notification module. The monitoring station was powered by solar energy with

backup batteries and was capable of continuous outdoor operation. It measured PM2.5 and temperature and transmitted the data through an IoT gateway over a 4G network to the cloud system using the MQTT protocol. The data were displayed through a web dashboard and an on-site LED display, while notifications were sent via Telegram when PM2.5 levels exceeded the specified thresholds. System performance was evaluated using black-box testing and error assessment. All ten test items passed, covering measurement, data transmission, processing, display, notification, risk-level classification, and overall system operation. Measurement agreement was evaluated using 720 time-aligned paired hourly observations collected over 30 days from the AQMS and an IQAir AirVisual commercial monitor. The comparison yielded a Mean Absolute Percentage Error of 7.72%, a Mean Absolute Error of 1.65 μg/m³, and a Root Mean Squared Error of 1.96 μg/m³. These results indicated agreement between the measurements from the two devices under the study location, period, and environmental conditions. However, the comparison did not confirm the system's metrological accuracy because it was not calibrated against an FRM/FEM standard instrument. The user acceptance evaluation was conducted with 30 participants, and overall acceptance was at the highest level, with a mean of 4.51 and a standard deviation of 0.51. The findings indicate that the system performed the predefined functions and produced measurements consistent with those of the comparison device under the conditions of this study. However, calibration against a standard instrument, long-term testing, and evaluation with a larger user sample should be conducted before wider deployment.

Keywords: PM2.5, Real-time system, Air quality monitoring, Internet of things (IoT), Alert system

1. Introduction

Air pollution is the contamination of air by substances or objects that are harmful to health and the environment. It has many sources, such as fuel combustion, industrial emissions, and the burning of agricultural residues. Air pollution is an environmental problem that severely and continuously affects public health and quality of life (Chang et al., 2023; Jindawet, 2023). PM2.5, or fine particulate matter, is defined as particles with a diameter of no more than 2.5 microns (U.S. Environmental Protection Agency, 2026; World Health Organization, 2021). These suspended particles disperse in the atmosphere and may exist in liquid or solid form. They can penetrate the respiratory system and bloodstream, which may result in respiratory and cardiovascular diseases and increase morbidity and premature mortality. The impacts of air pollution are not limited to health; they also significantly affect the economy and society (Li et al., 2022; Manisalidis et al., 2020). Consequences include increased healthcare costs, reduced labor productivity, and negative effects on tourism and agriculture. In the long term, this problem may contribute to social inequality and reduce the overall quality of life of the population.

In Thailand, PM2.5 levels are high across many areas, especially during the winter season. During this period, temperature inversions often occur, leading to the accumulation of particulate matter near the ground. In particular, PM2.5 levels in Phetchaburi Province have generally increased (Pollution Control Department, 2023). Additionally, agricultural burning is frequently observed and contributes to higher pollution levels. Statistics on PM2.5 from November 2024 to March 2025 indicated concentrations exceeding 75 micrograms per cubic meter (μg/m³) (Division of Health Impact Assessment, Department of Health, 2026). As a result, public health may be adversely affected. Notably, children, pregnant women, older adults, and people with underlying diseases are more sensitive to air pollution exposure than the general population. Currently, information and communication technology, especially the Internet of Things (IoT), plays an important role in monitoring and alerting by speeding up response times and improving monitoring efficiency. Specifically, a mobile application alert system can deliver timely warnings when important events

occur, ensuring that stakeholders are immediately informed. In addition, a web dashboard can consolidate warning information on a single screen, streamlining situation monitoring and facilitating quicker decision-making. Given these benefits, improved data accessibility, faster response, and greater monitoring efficiency, these approaches have strong potential to help address this problem.

Previous studies have demonstrated the feasibility of integrating particulate-matter sensors, Internet of Things technology, and mobile notification services for PM2.5 monitoring. However, several limitations remain for site-specific outdoor deployment, including dependence on local Wi-Fi infrastructure; limited integration of outdoor monitoring, cloud-based processing, public display, and automated notification functions; and insufficient reporting of measurement agreement based on extended paired outdoor observations. In addition, province- or region-level air quality services may not adequately represent PM2.5 conditions at a specific installation site. To address these gaps, this study developed a solar-powered outdoor PM2.5 monitoring system that uses RS485 communication, a 4G cellular gateway, MQTT-based cloud transmission, a web dashboard, an on-site LED display, and automated Telegram notifications. The system was functionally verified, its measurements were compared with simultaneous measurements from a commercial comparison monitor, and descriptive user feedback was collected through a pilot user acceptance evaluation.

Therefore, this research aimed to develop a real-time air quality monitoring and PM2.5 alert system using Internet of Things technology; verify the predefined system functions; evaluate measurement agreement between the developed AQMS and a commercial IQAir AirVisual monitor under the study conditions; and obtain descriptive feedback through a pilot user acceptance evaluation. The developed system was intended to support site-specific PM2.5 surveillance, environmental risk communication, and local decision-making.

2. Materials and Methods

This study was conducted as a research and development project. The objectives were to develop a real-time air quality monitoring and PM2.5 alert system, evaluate its performance, and assess user acceptance of the system when particulate matter levels were high enough to have immediate health effects. The research procedure was divided into four stages, as follows.

2.1 Study of problems, theories, and related research

In this study, the researchers systematically examined the problem and reviewed concepts, theories, documents, and related research to establish a knowledge base for the analysis, design, and development of a real-time air quality monitoring and PM2.5 alert system. The details are as follows.

2.1.1 Study of the PM2.5 problem

The researchers studied air pollution, focusing on particulate matter with a diameter of no more than 2.5 microns (PM2.5). PM2.5 is an air pollutant that affects public health and environmental quality. The researchers considered major sources of air pollution, such as vehicle emissions, industrial facilities, open agricultural burning, wildfires, transportation, dust, and black smoke. Climatic factors and the area's geographical characteristics were also examined because these factors can contribute to the accumulation of particulate matter in the atmosphere, especially in winter. During this season, the ground is often cooler than the upper atmosphere, and this temperature difference can cause a temperature inversion. The inversion acts as a dome, trapping particulate matter and keeping unusually high levels of particulate matter near the ground (Bilal et al., 2022; Serttikul et al., 2023). The researchers reviewed PM2.5 data in Phetchaburi Province and found that concentrations tended to increase (Pollution Control Department, 2023). From November 2024 to March 2025, PM2.5 concentrations exceeded 75 micrograms

per cubic meter (µg/m³) (Division of Health Impact Assessment, Department of Health, 2026). This period often coincides with agricultural burning and weather conditions that favor pollution accumulation. At times, air quality reached levels that can affect public health. Children, pregnant women, older adults, and individuals with chronic illnesses are particularly vulnerable to air pollution because they are more sensitive than the general population.

2.1.2 Study of standards and alert criteria

In this study, the researchers reviewed air quality standards and PM2.5 assessment criteria from academic documents and relevant agencies. Based on this review, Thailand's air quality index, developed by the Pollution Control Department (Pollution Control Department, 2023) was used as a guideline for surveillance levels, risk assessment, and user notification. The index is divided into five levels, with color-coded warnings that are easy to interpret and effective for communicating with users, as shown in Table 1.

This study also covered practical approaches to classifying air quality levels for warning purposes, using an index that defines categories such as good air quality, levels beginning to affect health, and hazardous levels. The index provided clear criteria for setting conditions in the data processing system, generating alert messages, and designing communication formats that matched the severity of the situation. In the developed system, the researchers applied this index to guide alert generation within the application.

Table 1. Concentration values of air pollutants for the air quality index

PM2.5 (µg/m^3)	Air Quality Level	Color
0 – 15.0	Very Good	Blue
15.1 -25.0	Good	Green
25.1 – 37.5	Moderate	Yellow
37.6 – 75.0	Beginning to have health effects	Orange
≥ 75.1	Has health effects	Red

2.1.3 Study of IoT technology and related systems

The researchers examined principles, concepts, and technologies related to the Internet of Things (IoT), focusing on their application to real-time air quality monitoring. They outlined how each key system component contributes to this purpose (Bacquet et al., 2022). Monitoring devices and air quality sensors detect pollutant levels; preliminary processing systems prepare sensor data; data communication devices and transmission networks relay information; cloud systems provide data storage and processing; and user interfaces display results and trigger notifications.

The researchers evaluated the feasibility of a continuously operating, solar-powered outdoor air quality monitoring station. The station consisted of solar panels, which convert sunlight into electricity; a charge controller, which regulates battery charging; backup batteries, which store energy for periods without sunlight; and a voltage converter, which adjusts the voltage for device compatibility. PM2.5 sensors, which measure fine particulate matter in the air; signal conversion devices, which transform sensor outputs into digital signals; and a gateway, which transmits data to the online system, enabled data collection and transmission. Studying these components supported the design of an outdoor monitoring system with solar power, backup energy storage, and field data transmission capabilities.

In addition, the researchers studied the cloud-based data storage system and the web dashboard system to define the data flow from the monitoring point to the display point. On this basis, the

research emphasized the need for permanent data storage, rapid data processing, and data presentation in easily interpretable forms (Sahin & Ifenthaler, 2021), including graphical representations, statistics, and maps showing the locations of monitoring stations. The comparison processes for sensors and monitoring devices were also described to ensure the accuracy and reliability of real-time PM2.5 monitoring data. In addition, previous studies have used a range of approaches for communication, data sources, and notifications for PM2.5 monitoring. Phonrit et al. (2020) developed a particulate matter monitoring system using smartphones with sensors connected to a network. Pongphab & Santakij (2021) combined PM2.5 monitoring with notifications via the LINE application, while Tantatsanawong (2026) created an air-pollution alert system based on air-quality data from an external API rather than measurements collected directly at the installation site. AlAwadhi and Dashti (2021) discussed Telegram as a platform for information sharing. These studies demonstrated the feasibility of sensor-based monitoring and mobile notifications, but they differed in communication infrastructure, data sources, and display functions. For the present study, a 4G cellular gateway was chosen as a context-specific solution for an outdoor installation site where fixed Wi-Fi infrastructure was not reliably available. The developed system combined outdoor measurements, cloud-based storage, a web dashboard, an on-site LED display, and automated Telegram notifications.

2.1.4 Synthesis of the conceptual framework for system development

After studying the problem, air quality standards, and related technologies, the researchers synthesized findings from the literature and related research to develop a conceptual framework for a real-time air quality monitoring and PM2.5 alert system. Based on this framework, the system was defined as consisting of three main components: an air quality data monitoring component that collects and transmits air quality information; a cloud-based data processing and storage component that analyzes and stores the collected data; and a user display and alert component that presents air quality data and sends alerts to users.

In this conceptual framework, PM2.5 sensors collect data along with weather-related variables and transmit them via a 4G network to a cloud server. The server stores, analyzes, and processes the data. The system displays the processed results in real time on a web dashboard. If air quality exceeds the specified criteria, the system immediately generates and transmits alert messages to users via the application, notifying them of the associated risk, as shown in Figure 1. This process aligns with the system framework presented in the article and integrates air quality monitoring technology, data communication, and information systems to support environmental risk communication.

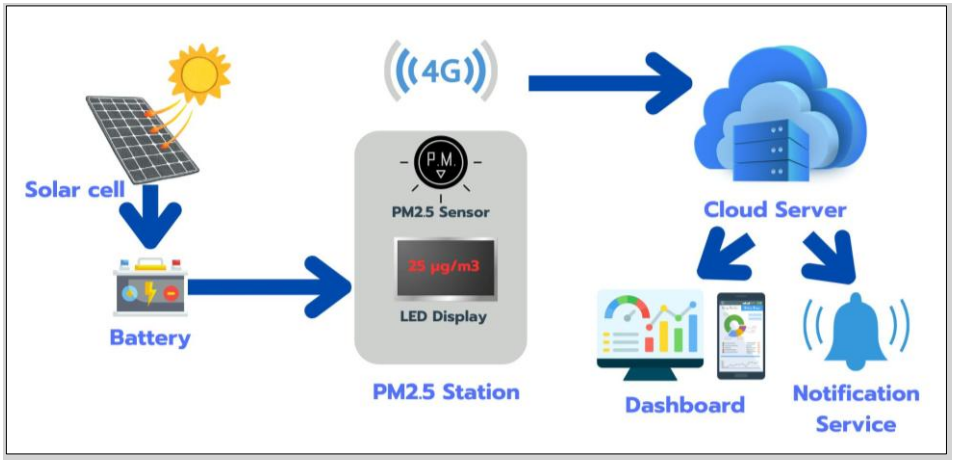


Figure 1. System concept framework

2.2 System analysis, design, and development

After conducting a comprehensive problem analysis and reviewing the relevant literature, the researchers systematically defined the system requirements, designed the operational architecture, and implemented a real-time air quality monitoring and PM2.5 alert system. The system continuously provides reliable measurements, processing, visualization, and alerts for practical outdoor applications. It integrates monitoring station modules, data communication interfaces, cloud-based processing and storage units, and user display and notification modules into a cohesive framework.

2.2.1 System Requirements Analysis

The researchers analyzed system requirements based on the nature of the problem and the actual context of use. The system was required to continuously monitor PM2.5 concentrations and related weather variables in an outdoor environment, use a power source suitable for the installation area, transmit data from the monitoring point to the central system in real time, present information in a form that users could easily understand, and automatically send alert messages when air quality values exceeded predefined thresholds. This analysis led to the definition of the main system components: the air quality monitoring station, the data storage and processing system, the web dashboard, and the application-based alert system.

2.2.2 System architecture design

In designing the system, the researchers defined its architecture as consisting of three main components: 1) the air quality monitoring station, 2) cloud-based data processing and storage, and 3) a user web dashboard with alert notifications. The workflow progressed as follows: solar energy powered the monitoring station, which collected PM2.5 measurements. A 4G network was used to send sensor data to the cloud server for processing, storage, and analysis. The processed data were then presented on the web dashboard. If monitored values exceeded the thresholds, alert notifications were sent to users via Telegram. This sequence efficiently connected data from monitoring points to end users, exemplifying an integrated hardware–software system design based on the conceptual framework in Section 2.1.4.

2.2.3 Design and development of the air quality monitoring station

The Renke RS-BYH-M-EX monitoring unit was selected because it is designed for outdoor installation, has the necessary PM2.5 measurement range, and supports RS485 Modbus RTU communication. The Protoss-PG41 gateway was selected because it can receive RS485 data directly and transmit them over a 4G cellular network, eliminating the need for a separate microcontroller. The researchers chose RS485 Modbus RTU because it is compatible with the monitoring unit and the industrial gateway and is suitable for wired communication in outdoor installations. A 4G cellular connection was selected because the fixed Wi-Fi infrastructure at the installation site was unreliable. MQTT was selected because it supports lightweight publish–subscribe messaging, which is well suited to the transmission of IoT data. Telegram notifications were selected because they enabled automated group notifications within the existing server environment without requiring the researchers to develop and maintain a dedicated mobile application. A 100 W solar panel and two 12 V, 20 Ah batteries were selected to support outdoor operation during periods of limited grid-power availability and reduced sunlight, as shown in Table 2.

Table 2. Hardware and communication specifications of the developed system

Component	Model/Specification	Main Function
Air quality monitoring unit	Renke RS-BYH-M-EX	Measures PM2.5 and temperature
PM2.5 measurement principle	Laser light scattering	Detects particulate-matter concentration
Measurement range	0–1,000 μg/m³	Defines the manufacturer-specified operating range
Communication gateway	Protoss-PG41 RS485-to-4G gateway	Receives sensor data and transmits it to the cloud
Sensor–gateway interface	RS485 Modbus RTU	Transfers measurements from the monitoring unit to the gateway
Outdoor network	4G cellular network	Transfers data from the outdoor station to the cloud server
Application protocol	MQTT	Publishes monitoring data to the cloud system
Solar panel	100 W monocrystalline panel	Supplies electrical power to the station
Backup batteries	Two 12 V, 20 Ah batteries	Support operation during limited sunlight
Comparison monitor	IQAir AirVisual	Provides simultaneous measurements for comparison

The AQMS was not compared with a Federal Reference Method (FRM) or Federal Equivalent Method (FEM) certified instrument, and no correction equation was developed. Instead, its measurements were compared with those from an IQAir AirVisual commercial monitor.

The AQMS and IQAir AirVisual were installed in the same general area, with their air inlets approximately 4 meters apart and at a height of about 2.5 meters above ground level. Both devices recorded measurements during the same 30-day period. AQMS data recorded at 60-second intervals were processed and converted into hourly averages. After alignment, 720 paired hourly observations were obtained.

Measurement agreement was evaluated using MAPE, MAE, and RMSE. These metrics represent the differences between the two devices under the study conditions and do not confirm the absolute accuracy of the AQMS because IQAir AirVisual is not an FRM/FEM comparison monitor.

2.2.4 Design of the data display system

After the data were transmitted to the central system, display interfaces were designed for local and online monitoring. The LED display at the station showed current PM2.5 levels, color-coded according to the air quality index and accompanied by warning messages, enabling immediate recognition. The web dashboard provided an overview of all stations by showing their locations on a map and graphing and summarizing real-time PM2.5 values to support clear trend analysis.

2.2.5 Design of the alert system via application

The researchers developed an automated Telegram notification system to promptly communicate air quality risks based on readings from selected monitoring stations. To simplify automated notifications, the five AQI categories were consolidated into three alert groups: good (Very Good, Good, and Moderate: ≤37.5 μg/m³), poor (Beginning to Affect Health: 37.6–75.0 μg/m³), and very poor (Affects Health:

≥75.1 μg/m³). This helped users easily assess severity and take protective action, such as limiting outdoor activities or using protective equipment. Automated alerts were sent to members of the Telegram group when the predefined PM2.5 threshold conditions were met.

2.2.6 Prototype development

After designing the system components, the researchers developed a prototype that functioned as an integrated whole, encompassing air quality data measurement, network data transmission, server storage and processing, web dashboard display, and application-based alerts. Development focused on three main areas: the air quality monitoring station, the web dashboard display, and Telegram notifications. The diagram illustrates the devices within the air quality station and the display, as shown in Figure 2. The results demonstrated that all components were correctly connected and operated continuously.

In summary, the system analysis, design, and development stage was an important process that enabled the researchers to transform knowledge from the literature review into a usable prototype system. It covered hardware, software, data communication, display, and notification dimensions, resulting in a system with the potential for concrete use in local air quality surveillance and environmental risk communication.

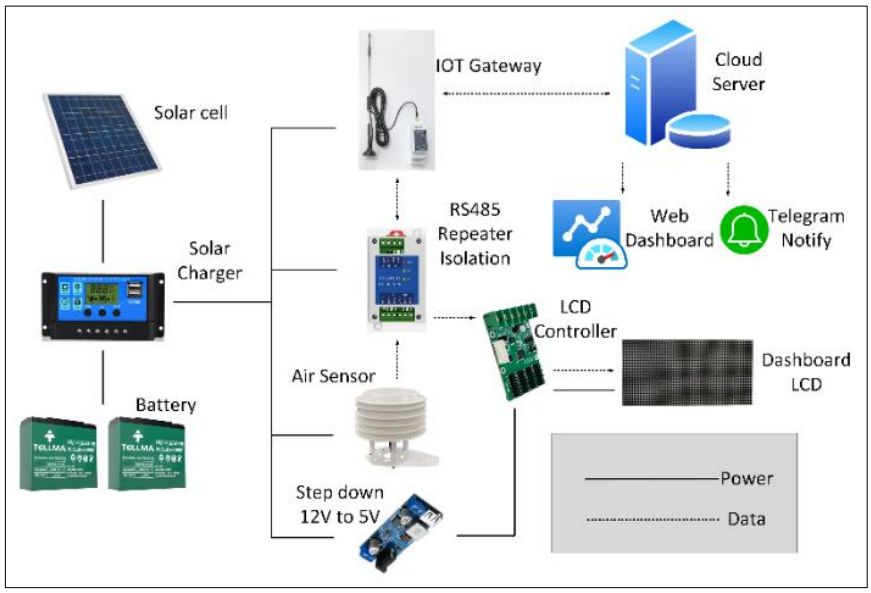


Figure 2. Diagram of devices inside the air quality monitoring station and display

2.3 System functional and measurement agreement evaluation

The evaluation consisted of two components: functional verification of the predefined system operations and evaluation of measurement agreement between the AQMS and the IQAir AirVisual commercial monitor. Functional verification examined whether the system produced the expected observable outputs for monitoring, data transmission, processing, display, classification, and notification. The evaluation did not include a comprehensive quantitative assessment of network or system performance, such as latency, packet loss, system uptime, response time, or notification delay.

2.3.1 Functional verification using Black-Box testing

Black-box testing (Sommerville, 2021) was used to verify that predefined system functions produced the desired visible outputs without examining the internal program structure. The

verification covered PM2.5 and temperature data acquisition, RS485 communication between the monitoring unit and the gateway, 4G data transmission to the cloud server, server-side data processing and storage, web dashboard display, LED display, air-quality classification, and Telegram notifications.

The verification was performed in two stages. The alpha test was conducted in a controlled environment to assess the performance of the respective system functions, including data acquisition, communication, processing, display, classification, and notification. During the study period, the integrated workflow of the system under development was validated outdoors. The black-box testing was limited to functional verification and did not include any quantitative evaluation of latency, packet loss, system uptime, response time, notification delay, or long-term operational reliability.

2.3.2 Evaluation of Measurement Agreement Using Error Metrics

The AQMS recorded PM2.5 measurements at 60-second intervals. Measurements recorded within each clock hour were grouped, and the arithmetic mean of the available observations was calculated to produce one hourly mean value. An hourly mean was retained only when at least 45 of the expected 60 minute-level measurements were available. This hourly averaging reduced short-term fluctuations and random variability in the minute-level measurements; however, no separate moving-average filter or outlier-removal procedure was applied. The hourly AQMS measurements were then time-aligned with the corresponding hourly measurements obtained from a nearby IQAir AirVisual commercial monitor. Only hours with valid measurements from both devices were included in the paired analysis, resulting in 720 paired hourly observations collected over 30 consecutive days. The AirVisual device is certified by IQAir (IQAir, 2026). Measurement agreement between the AQMS and the IQAir AirVisual commercial monitor was quantified using the Mean Absolute Percentage Error (MAPE), Mean Absolute Error (MAE), and Root Mean Squared Error (RMSE), as shown in Equations (1), (2), and (3).

$$MAPE = \frac{100}{n}\sum_{i=1}^{n}\left|\frac{y_i-\hat{y}_i}{y_i}\right| \quad (1)$$

$$MAE = \frac{1}{n}\sum_{i=1}^{n}|y_i-\hat{y}_i| \quad (2)$$

$$RMSE = \sqrt{\frac{1}{n}\sum_{i=1}^{n}(y_i-\hat{y}_i)^2} \quad (3)$$

where y_i = value measured by IQAir AirVisual at the i^{th} data point
$\hat{y}_i$ = value measured by the AQMS at the i^{th} data point
n = total number of data points

The performance evaluation in this study verified the system's functionality and quantified differences between the two devices in the measured data. These results demonstrate the system's potential for practical application in local air quality surveillance.

2.4 Pilot User Acceptance Evaluation

The researchers conducted a pilot user acceptance evaluation to assess perceptions and adoption of the real-time air quality monitoring and PM2.5 alert system. This evaluation was used to examine the system's suitability for practical use, including responsiveness to user needs, system design, performance, and usability. Lecturers, staff, students, and members of the public participated in the evaluation.

2.4.1 Evaluation Sample Group

The pilot acceptance evaluation included four types of users, namely, lecturers, staff, students, and the public, to reflect the diversity of users within the framework of the study. The population was divided into four user types, and purposive sampling (Oguguo et al., 2026) was applied to each group to ensure representation of all user types in the evaluation, yielding a final sample of 30 participants.

2.4.2 The acceptance evaluation tools

The acceptance evaluation tool was a 20-item questionnaire covering four dimensions: functional requirements, design, functionality, and usability. The questionnaire used a Likert scale (Likert, 1961). The content validity of the questionnaire was assessed by three experts using the Index of Item–Objective Congruence (IOC). The IOC values ranged from 0.67 to 1.00, exceeding the acceptability criterion of 0.50. The items were subsequently revised for clarity before data collection. However, internal consistency reliability was not examined in this pilot study. Therefore, the questionnaire results should be interpreted as descriptive feedback.

2.4.3 Data Analysis

The researchers used descriptive statistics to analyze the questionnaire results and assess user acceptance of the developed system. The analysis included the mean and standard deviation. Mean scores were interpreted using a five-level Likert scale: scores of 4.50 to 5.00 indicated the highest acceptance; scores of 3.50 to 4.49 indicated high acceptance; scores of 2.50 to 3.49 indicated moderate acceptance; scores of 1.50 to 2.49 indicated low acceptance; and scores of 1.00 to 1.49 indicated the lowest acceptance. This framework provided a systematic basis for explaining user acceptance.

3. Results

The development of a real-time air quality monitoring and PM2.5 alert system using Internet of Things technology showed that the system met its specified objectives. These objectives included air quality data monitoring, data transmission from monitoring stations to the central system, data processing and display on the web dashboard, and real-time notifications to users via the application. To present the findings clearly, the results were divided into three parts: 1) system development results, 2) performance evaluation results, and 3) pilot user acceptance evaluation results.

3.1 System Development Results

The results showed that the real-time air quality monitoring and PM2.5 alert system based on Internet of Things (IoT) technology achieved the research objective. The system architecture consisted of PM2.5 monitoring stations that collected outdoor data and transmitted them via a 4G network using the MQTT protocol to a cloud server for processing, storage, and forwarding to a web dashboard and user alert service, as illustrated in Figure 3. The system continuously monitored, tracked, transmitted, and processed air quality data. It was divided into three main parts: (1) air quality monitoring stations, as shown in Figure 4; (2) a web dashboard display system, as shown in Figure 5; and (3) an alert system using Telegram notifications, as shown in Figure 6. These three parts were integrated into one system.

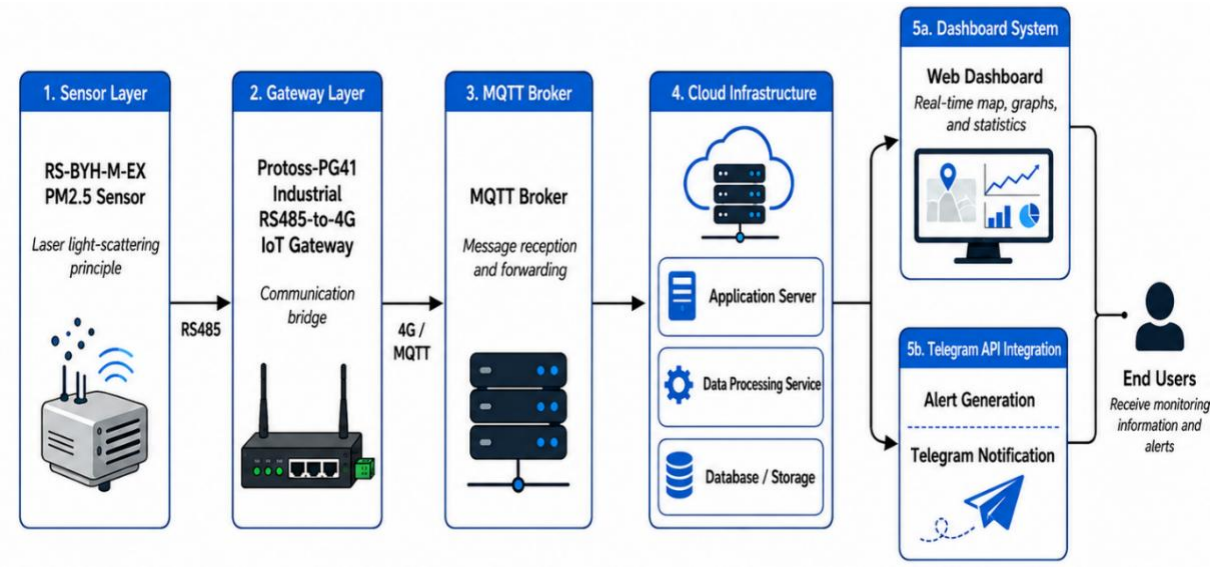


Figure 3. System Architecture



Figure 4. Air Quality Monitoring Station

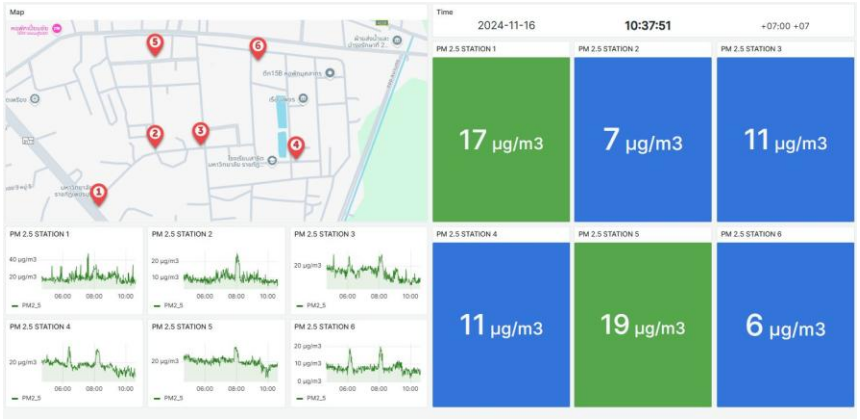


Figure 5. Web dashboard display screen

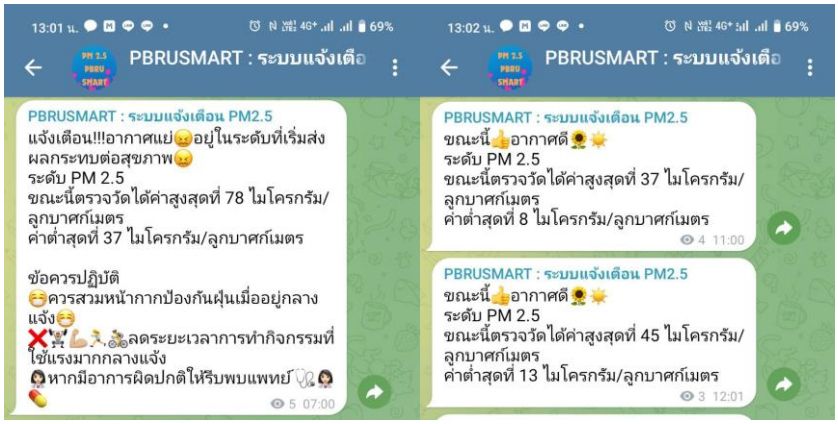


Figure 6. PM2.5 notification via Telegram notifications

In summary, the developed system included monitoring, processing, display, and notification functions, demonstrating the potential of Internet of Things technology to support local air pollution surveillance, as shown in Table 3.

Table 3. Summary of System Development Results

System Component	Development Details	Result
Air quality monitoring station	Developed an outdoor monitoring station with PM2.5 and temperature sensors, powered by a solar energy system and backup batteries	Able to continuously monitor and transmit data in a real-world environment
Data transmission system	Used an IoT gateway to transmit data over a 4G network to the central server	Enabled rapid, continuous data transmission to the central system
Web dashboard	Displayed real-time PM2.5 data as maps, graphs, and statistics	Users could easily monitor the air quality
LED display screen	Displayed PM2.5 values and warning messages at the station installation site	Helped directly communicate information within the installation area
Telegram notifications alert system	Automatically alerted at three levels based on air quality criteria	Users could recognize risks and protect themselves in time

3.2 System Functional and Measurement Agreement Evaluation Results

3.2.1 Functional Verification Results Using Black-Box Testing

Black-box testing was conducted to verify whether the developed system completed the predefined functional operations. The verification covered data acquisition, RS485 communication, 4G data transmission, server-side processing and storage, web dashboard display, LED display, air-quality classification, Telegram notification, and integrated system operation. The observed outputs were compared with the predefined expected results for each test item. All ten functional test items produced the expected observable outputs and were therefore classified as Pass. These findings represent functional verification only and should not be interpreted as a comprehensive assessment of network performance, long-term stability, or operational reliability. Details are shown in Table 4.

3.2.2 Evaluation of Measurement Agreement Using Error Metrics

The comparison of 720 paired hourly PM2.5 measurements collected over 30 days yielded an MAPE of 7.72%, an MAE of 1.65 μg/m³, and an RMSE of 1.96 μg/m³. These results indicate that the AQMS measurements differed from the IQAir AirVisual measurements by approximately 1.96 μg/m³ under the specific location, period, and environmental conditions of the study, suggesting close agreement between the two devices within the evaluated dataset.

However, the findings should not be interpreted as evidence of absolute measurement accuracy because IQAir AirVisual is a commercial optical monitor rather than an FRM/FEM comparison monitor, as shown in Figure 7.

Table 4. Functional Verification Results Using Black-Box Testing

Functional Test	Predefined Expected Behavior	Observed Result	Status
PM2.5 data acquisition	The system receives a PM2.5 value from the monitoring unit	PM2.5 values were received and stored	Pass
Temperature data acquisition	The system receives a temperature value	Temperature values were received and stored	Pass
Sensor-to-gateway communication	The gateway receives data through RS485 Modbus RTU	Sensor data were received by the gateway	Pass
4G data transmission	The gateway delivers monitoring data to the cloud server	Data were delivered to the server during the test	Pass
Server processing and storage	The server processes and stores received data	Received data were processed and stored	Pass
Web dashboard display	The dashboard displays the received values	PM2.5 values were displayed on the dashboard	Pass
LED display	The LED unit displays the current PM2.5 level	The received PM2.5 value and warning level were displayed	Pass
Threshold notification	An alert is generated when the predefined threshold is met	Telegram notifications were generated under the tested threshold conditions	Pass
Air-quality classification	The system classifies values according to predefined rules	Test values were assigned to the expected categories	Pass
Integrated operation	Monitoring, transmission, storage, display, and notification operate sequentially	The predefined workflow was completed during the test	Pass

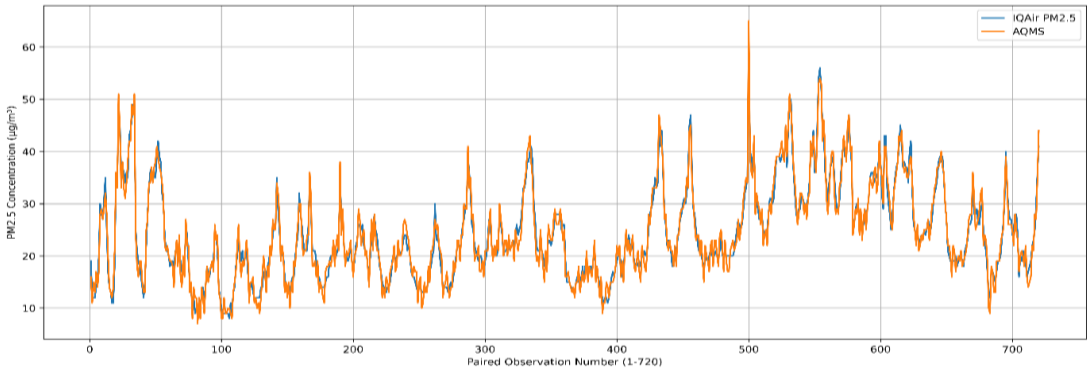


Figure 7. Comparison of 720 time-aligned paired hourly PM2.5 observations obtained from the AQMS and IQAir AirVisual over 30 days.

3.3 Pilot User Acceptance Evaluation Results

The pilot user acceptance evaluation of the real-time air quality monitoring and PM2.5 alert system was conducted using a questionnaire distributed to a sample group comprising lecturers, staff, students, and members of the public. The mean and standard deviation were used to analyze the data and evaluate user acceptance of different system features.

The results showed that users accepted the system at the highest level, with a mean of 4.51 and a standard deviation of 0.51. When each aspect was considered, functionality had the highest mean of 4.60, corresponding to the highest level, followed by usability, with a mean of 4.50 at the highest level; functional requirements, with a mean of 4.48 at a high level; and design, with a mean of 4.47 at a high level, as shown in Table 5.

Table 5. Pilot User Acceptance Evaluation Results (n = 30)

Evaluation Item	$\overline{x}$	$S.D.$	Acceptance Level
1. Functional Requirements	4.48	0.50	High
2. Design	4.47	0.50	High
3. Functionality	4.60	0.52	Highest
4. Usability	4.50	0.50	Highest
Overall Average	4.51	0.51	Highest

4. Discussion

This research developed a real-time air quality monitoring and alert system that builds on previous work by improving system architecture, data communication stability, measurement agreement, and alert channels. The results demonstrate the system's suitability for real-world applications.

Regarding infrastructure and connectivity, Phonrit et al. (2020) and Pongphab and Santakij (2021) used Wi-Fi networks for data transmission. In the present study, a 4G cellular network was selected because fixed Wi-Fi infrastructure was not consistently available at the outdoor installation site. The 4G connection was combined with the MQTT protocol to transmit monitoring data from the outdoor station to the cloud server. This design should be interpreted as a context-specific solution for the study site rather than evidence that 4G is generally superior to Wi-Fi, as no direct comparison between the two network technologies was conducted.

The present study extended previous work by quantitatively evaluating measurement agreement using 720 paired hourly observations. This study reported PM2.5 measurement results with an RMSE of 1.96 μg/m³, based on a comparison dataset of 720 hourly averages. This indicates a low level of measurement difference and provides quantitative evidence of agreement when compared with the research of Pongphab and Santakij (2021), which used 100 test datasets, and the research of Tantatsanawong (2026), which did not report quantitative error from direct sensor measurements because it used air quality data from the OpenWeather API, an external data source not derived from measurements taken in the actual experimental area.

This research integrated several communication channels, including Telegram notifications, a web dashboard, and an LED display, to provide public access to information. The system supports both individual users and people in public spaces. This differs from the study by Pongphab and Santakij (2021), which focused on LINE notifications, and the study by Tantatsanawong (2026), which developed a specific

smartphone application. Both approaches may have limitations related to application installation and users' internet connectivity.

Regarding user acceptance, this research achieved an overall average acceptance score of 4.51, corresponding to the highest level. This score exceeds the average score of 4.10 reported by Pongphab and Santakij (2021) and is close to the evaluation results of Tantatsanawong (2026), who reported average scores ranging from 4.30 to 4.70. Furthermore, the standard deviation in this research was low (S.D. = 0.51), indicating that user opinions of the system were consistent within the study sample.

Although the developed real-time PM2.5 monitoring and alert system demonstrated strong measurement agreement, functional reliability, and user acceptance, several limitations remain. Outdoor measurements may be affected by dust accumulation, weather changes, physical obstructions, airflow variation, and the 4-meter spacing between devices. Moreover, the RMSE reflects agreement with IQAir AirVisual under the study conditions rather than absolute accuracy because no FRM/FEM comparison or environmental correction model was applied.

Network instability may occasionally delay or interrupt data transmission. Cybersecurity was also not formally assessed through penetration testing, vulnerability scanning, or attack simulation; therefore, the security of the MQTT broker, gateway, cloud system, web dashboard, and API credentials, as well as resistance to unauthorized access or denial-of-service attacks, requires further evaluation.

The black-box testing verified the observable functions of the developed system under the tested conditions. However, because latency, packet loss, system uptime, response time, and notification delay were not quantitatively recorded, the results should not be interpreted as a comprehensive evaluation of system or network performance.

The user acceptance assessment was limited by the small pilot sample and the absence of a formal technology acceptance framework. Future studies should conduct co-location comparisons with standard instruments, develop independent comparison and validation datasets, test the system across different seasons and pollution conditions, implement automated logging, evaluate cybersecurity, and apply a validated Technology Acceptance Model (TAM)-based instrument to a larger and more diverse sample. In addition, the questionnaire's internal consistency reliability was not examined. Therefore, the user evaluation findings should be interpreted as descriptive and specific to the participants in this study and should not be generalized to the broader user population.

Furthermore, this research provides avenues for future development. It is recommended that the scope of measurements be expanded to include additional air quality parameters, such as PM10, humidity, and carbon dioxide, and that machine learning techniques be applied to forecast air quality trends. This aligns with the recommendations of the related research mentioned above and would upgrade the system from real-time monitoring and alerts to a more efficient air quality monitoring and decision-support system.

5. Conclusions and Recommendations

The developed system integrated an outdoor PM2.5 monitoring station, RS485 communication, a 4G cellular gateway, MQTT-based cloud transmission, a web dashboard, an on-site LED display, and automated Telegram notifications. During the study period, all ten black-box testing items produced the expected observable outputs for monitoring, transmission, processing, display, classification, and notification. These results represent functional verification under the tested conditions and do not constitute a comprehensive assessment of network performance, long-term stability, or operational reliability.

The comparison of 720 paired hourly observations collected over 30 days yielded an MAPE of 7.72%, an MAE of 1.65 μg/m³, and an RMSE of 1.96 μg/m³, indicating close measurement agreement between the AQMS and the IQAir AirVisual commercial monitor under the study conditions. However, the findings do not establish absolute measurement accuracy because the AQMS was not calibrated against a regulatory-grade FRM/FEM instrument, and no environmental correction model was developed.

The pilot user acceptance evaluation of 30 participants yielded an overall mean score of 4.51 and a standard deviation of 0.51. These results reflect descriptive feedback from the participants and should not be generalized to the broader population because the sample was limited and the questionnaire's internal consistency was not examined.

Before wider deployment, future studies should include calibration and validation with a regulatory-grade instrument; long-term testing across multiple locations and seasons; quantitative evaluation of latency, packet loss, uptime, response time, and notification delay; and a formal cybersecurity assessment. Larger user samples and validated usability or technology acceptance instruments should also be used. Additional air quality parameters and machine-learning methods may be incorporated to support forecasting and decision-making.

6. Acknowledgements

Phetchaburi Rajabhat University funded this research. The researchers thank the Research and Arts and Culture Promotion Institute and the Faculty of Information Technology for their support and guidance. This study may help develop and apply methods for air quality management and digital innovation.

7. References

AlAwadhi, S., & Dashti, M. (2021). The Use of the Telegram Application as an Information-Sharing Tool. Journal of Information & Knowledge Management, 20(02), 2150024. https://doi.org/10.1142/S0219649221500246

Bacquet, J., Riemenschneider, R., & Wintlev-Jensen, P. (2022). Future Trends in IoT. In Next Generation Internet of Things–Distributed Intelligence at the Edge and Human-Machine Interactions (pp. 9-17). River Publishers.

Bilal, M., Hassan, M., Tahir, D. B. T., Iqbal, M. S., & Shahid, I. (2022). Understanding the role of atmospheric circulations and dispersion of air pollution associated with extreme smog events over South Asian megacity. Environmental Monitoring and Assessment, 194(2), 82. https://doi.org/10.1007/s10661-021-09674-y

Chang, J. H., Lee, Y. L., Chang, L. T., Chang, T. Y., Hsiao, T. C., Chung, K. F., Ho, K. F., Kuo, H. P., Lee, K. Y., Chuang, K. J. & Chuang, H. C. (2023). Climate change, air quality, and respiratory health: a focus on particle deposition in the lungs. Annals of Medicine, 55(2), 2264881. https://doi.org/10.1080/07853890.2023.2264881

Division of Health Impact Assessment, Department of Health. (2026). Indicators for assessing the health impacts related to PM2.5 [Online]. Retrieved January 15, 2026, from https://hia.anamai.moph.go.th/th/kpi68-3-44 (in Thai)

IQAir. (2026). Faculty of Information Technology air quality index (AQI) and Phetchaburi air pollution [Online]. Retrieved January 15, 2026, from https://www.iqair.com/th/thailand/phetchaburi/phetchaburi/faculty-of-information-technology

Jindawet, M. (2023). Exploring the causes of air pollution and the impacts that must be addressed! Health & Envitech [Online]. Retrieved January 15, 2026, from https://healthenvi.com/causes-and-effects-of-air-pollution/ (in Thai)

Li, C., Yan, Y., Lu, Y., Zeng, G., Zhou, L., Jin, H., Xu, Y., & Chen, Y. (2022). Air pollution, investor sentiment and stock liquidity. Frontiers in Public Health, 10, 989457. https://doi.org/10.3389/fpubh.2022.989457

Likert, R. (1961). New patterns of management. New York, NY: McGraw-Hill.

Manisalidis, I., Stavropoulou, E., Stavropoulos, A., & Bezirtzoglou, E. (2020). Environmental and Health Impacts of Air Pollution: A Review. Frontiers in Public Health, 8(14). https://doi.org/10.3389/fpubh.2020.00014

Oguguo, B. C. E., Ocheni, C. A., Okebanama, C. I., Ezugwu, I. J., & Oguguo, E. C. (2026). Stakeholders' awareness of digital security as a test security measures for preventing large-scale educational assessment breaches in the cyberspace. Computers and Security, 170, 105053. https://doi.org/10.1016/j.cose.2026.105053

Phonrit, O., Arnansanti, N., Laotrakulngam, N., & Wattana, N. (2020). Measuring Dust System in the Air on Smartphone Devices. Journal of Information Science and Technology, 10(1), 1–9. https://doi.org/10.14456/jist.2020.1

Pollution Control Department. (2023). Announcement of Thailand's air quality index, B.E. 2566, with stricter pollutant concentration standards, published in the Royal Gazette [Online]. Retrieved January 15, 2026, from https://www.pcd.go.th/pcd_news/30028/ (in Thai)

Pongphab, D., & Santakij, P. (2021). Dust PM2.5 Monitoring and Alert System via LINE Application. UTK Research Journal, 15(2), 45–57. https://ph02.tci-thaijo.org/index.php/rmutk/article/view/244792

Sahin, M., & Ifenthaler, D. (2021). Visualizations and dashboards for learning analytics: A systematic literature review. In M. Sahin & D. Ifenthaler (Eds.), Visualizations and dashboards for learning analytics (pp. 3–22). Springer. https://doi.org/10.1007/978-3-030-81222-5_1

Serttikul, C., Rattanadecho, P., & Prapasawat, T. (2023). The Effect of Building Arrangement Pattern on the Behavior of Air Flow Under Inverse Temperature Condition. Science & Technology Asia, 152–163. https://doi.org/10.14456/scitechasia.2023.34

Sommerville, I. (2021). Software engineering (10th ed.). Harlow, England: Pearson.

Tantatsanawong, P. (2026). Development of Air Pollution Alert System: A Case Study of Particulate Matter 2.5 micron (PM2.5). Academic Journal of Science and Applied Science, 10(19), e3967. https://ph03.tci-thaijo.org/index.php/ajsas/article/view/3967

U.S. Environmental Protection Agency. (2026). Particulate matter (PM) basics [Online]. Retrieved January 15, 2026, from https://www.epa.gov/pm-pollution/particulate-matter-pm-basics

World Health Organization. (2021). WHO global air quality guidelines: Particulate matter ($PM_{2.5}$ and PM_{10}), ozone, nitrogen dioxide, sulfur dioxide and carbon monoxide: Executive summary [Online]. Retrieved January 15, 2026, from https://www.who.int/publications/i/item/9789240034433

ผลของการฝึกความเร็วอดทนโดยใช้แรงต้านแบบยางยืดเปรียบเทียบกับการฝึกแบบการวิ่งต่อสมรรถภาพแอโรบิกและแอนแอโรบิกในนักกีฬาฟุตซอลเยาวชน

The Effects of Elastic Resistance–Based Versus Running-Based Speed Endurance Training on Aerobic and Anaerobic Performance in Youth Futsal Players

ธนัมพร ทองลอง[1] สุทธิรักษ์ นาโสม[1] สุภาวดี กสิกรรม[1] อิศวรา จันทร์สมคอย[1] และ วารุณี กิจรักษา[1*]

Thanumporn Thonglong[1], Suttirak Nasome[1], Suphawadee Kasikam[1], Itsavara Jansomkoy[1] and Warunee Kitraksa[1*]

[1]คณะวิทยาศาสตร์ มหาวิทยาลัยราชภัฏอุดรธานี จังหวัดอุดรธานี

[1]Faculty of Sciences, Udonthani Rajabhat University, Udonthani Province

[*]Corresponding Author: warunee.kit@udru.ac.th

Received: May 7, 2026 **Revised:** June 19, 2026 **Accepted:** June 20, 2026

บทคัดย่อ

การวิจัยครั้งนี้มีวัตถุประสงค์เพื่อศึกษาและเปรียบเทียบผลของการฝึกความเร็วอดทนโดยใช้แรงต้านจากยางยืดและการฝึกความเร็วอดทนด้วยการวิ่งที่มีต่อสมรรถภาพด้านแอโรบิกและแอนแอโรบิกในนักกีฬาฟุตซอลเยาวชน กลุ่มตัวอย่างเป็นนักกีฬาฟุตซอลเยาวชน อายุ 16–18 ปี จำนวน 32 คน แบ่งเป็น 2 กลุ่ม กลุ่มละ 16 คน ด้วยวิธีการสุ่มแบบจับคู่ กลุ่มที่ 1 ฝึกความเร็วอดทนโดยใช้แรงต้านจากยางยืด และกลุ่มที่ 2 ฝึกความเร็วอดทนด้วยการวิ่ง ทั้งสองกลุ่มฝึกเป็นเวลา 4 สัปดาห์ สัปดาห์ละ 3 ครั้ง ที่ความเข้มข้นประมาณ 85% ของความเร็วสูงสุดในการวิ่งสปรินต์ การทดสอบสมรรถภาพแอโรบิกใช้แบบทดสอบ Multistage Fitness Test (Beep Test) และสมรรถภาพแอนแอโรบิกใช้แบบทดสอบ Running-Based Anaerobic Sprint Test (RAST) ประกอบด้วยตัวแปรความสามารถแอนแอโรบิก กำลังสูงสุด และดัชนีความล้า วิเคราะห์ข้อมูลด้วยสถิติ Paired t-test และ Independent t-test กำหนดระดับนัยสำคัญทางสถิติที่ 0.05 ผลการวิจัยพบว่า กลุ่มที่ฝึกความเร็วอดทนโดยใช้แรงต้านจากยางยืดมีการพัฒนาความสามารถแอนแอโรบิก (p = 0.005) และดัชนีความล้า (p = 0.021) อย่างมีนัยสำคัญทางสถิติ ขณะที่กลุ่มฝึกความเร็วอดทนด้วยการวิ่งไม่พบการเปลี่ยนแปลงอย่างมีนัยสำคัญในตัวแปรดังกล่าว เมื่อเปรียบเทียบระหว่างกลุ่มหลังการฝึก ไม่พบความแตกต่างอย่างมีนัยสำคัญทางสถิติในทุกตัวแปร ($p > 0.05$) สรุปได้ว่าการฝึกความเร็วอดทนโดยใช้แรงต้านจากยางยืดสามารถพัฒนาความสามารถแอนแอโรบิกและลดดัชนีความล้าได้ภายในกลุ่ม อย่างไรก็ตาม ยังไม่สามารถยืนยันได้ว่ามีประสิทธิผลเหนือกว่าการฝึกความเร็วอดทนด้วยการวิ่ง เนื่องจากไม่พบความแตกต่างอย่างมีนัยสำคัญทางสถิติระหว่างกลุ่ม จึงควรมีการศึกษาเพิ่มเติมโดยใช้ระยะเวลาการฝึกที่ยาวขึ้นและกลุ่มตัวอย่างที่มากขึ้น

คำสำคัญ: ความเร็วอดทน, การฝึกด้วยยางยืด, ความสามารถแอโรบิก, ความสามารถแอนแอโรบิก, ฟุตซอล

Abstract

This study aimed to compare the effects of elastic resistance–based speed-endurance training and running-based speed-endurance training on aerobic and anaerobic performance in youth futsal players. Methods: Thirty-two youth futsal players aged 16–18 years were assigned to two groups (n = 16 per group) using matched-pair randomization. The Elastic Resistance Group (ERG) performed speed-endurance training with elastic resistance, whereas the Running-Based Group (RBG) performed running-based speed-endurance training. Both groups trained for 4 weeks, 3 sessions per week, at approximately 85% of maximal sprint velocity. Aerobic performance was assessed using the Multistage Fitness Test (Beep Test), while anaerobic performance was evaluated using the Running-Based Anaerobic Sprint Test (RAST), including anaerobic capacity, peak anaerobic power, and fatigue index. Data were analyzed using paired and independent t-tests with statistical significance set at $p < 0.05$. Results: The ERG demonstrated significant improvements

in anaerobic capacity (p = 0.005) and fatigue index (p = 0.021). No significant changes were observed in the RBG for these variables. However, no statistically significant differences were found between groups in any outcome measure following the intervention (p > 0.05). Conclusion: Elastic resistance–based speed-endurance training produced significant within-group improvements in anaerobic capacity and fatigue resistance. However, superiority over running-based speed-endurance training was not statistically confirmed because no significant between-group differences were observed. These findings suggest that elastic resistance training may be a promising conditioning strategy for youth futsal players, although further research is required.

Keywords: Speed-endurance, Elastic resistance training, Aerobic capacity, Anaerobic capacity, Youth futsal players

1. Introduction

Futsal is a high-intensity intermittent team sport characterized by frequent transitions between offensive and defensive phases, repeated accelerations and decelerations, changes of direction, and explosive actions performed under considerable time pressure. These match demands require players to repeatedly execute high-intensity movements while maintaining technical and tactical performance throughout the competition. Recent evidence indicates that elite futsal players are exposed to substantial physiological, neuromuscular, and metabolic stress during both training and match play, highlighting the importance of well-developed physical fitness capacities (Spyrou et al., 2022).

Due to the intermittent nature of futsal, both aerobic and anaerobic energy systems contribute significantly to performance. Players must possess adequate aerobic fitness to facilitate recovery between high-intensity efforts, while anaerobic capacity is essential for repeated sprinting, rapid accelerations, and explosive movements. Furthermore, physical qualities such as muscular strength, power, speed, agility, and neuromuscular coordination have been identified as key determinants of successful futsal performance (Albalad-Aiguabella et al., 2025; González-Fernández et al., 2024).

Among these physical qualities, speed endurance is particularly important because it enables athletes to sustain repeated high-intensity efforts while delaying the onset of fatigue. Enhanced speed endurance contributes to improved sprint performance, repeated acceleration ability, and movement efficiency during the later stages of competition, where fatigue often impairs performance. Consequently, training methods that simultaneously develop strength and speed-related capacities have become increasingly relevant in modern futsal conditioning programs (Albalad-Aiguabella et al., 2025).

One practical training approach is elastic resistance training (ERT), which provides variable resistance throughout the range of motion and allows athletes to perform sport-specific movements under externally imposed loading conditions. Unlike traditional resistance methods, elastic bands progressively increase resistance as they elongate, creating a unique loading profile that may better accommodate natural strength curves during movement. Recent evidence suggests that elastic band training can effectively improve sprint performance, change-of-direction ability, explosive power, and sport-specific physical performance in team-sport athletes (Stanković et al., 2025).

From a physiological perspective, elastic resistance training may induce favorable neuromuscular adaptations, including enhanced motor-unit recruitment, increased neural drive, improved intermuscular coordination, and greater force production capacity. These adaptations are considered fundamental mechanisms underlying improvements in athletic performance, particularly during explosive and repeated

high-intensity activities. Recent reviews have highlighted the importance of resistance training-induced neuromuscular adaptations for enhancing strength, power, and movement efficiency in athletic populations (Aslam et al., 2025; Rong et al., 2025).

Furthermore, resistance-based training interventions have been shown to improve movement economy and physical performance by increasing the neuromuscular demands imposed during exercise. Variable and elastic resistance methods may also enhance sprint performance and repeated high-intensity exercise capacity through improvements in force production and neuromuscular efficiency (Shi et al., 2022; Van Hooren et al., 2024). Given the high-intensity and repeated-sprint nature of futsal, elastic resistance training may represent an effective strategy for enhancing speed endurance and related performance capacities.

Despite the growing popularity of elastic resistance training, evidence regarding its effectiveness for improving speed endurance in youth futsal players remains limited. Most previous studies have focused on football players or have investigated resistance training and running-based conditioning separately. Moreover, few studies have directly compared elastic-resistance-based speed-endurance training with conventional running-based speed-endurance training in futsal-specific populations. This gap in the literature is important because the physiological and movement demands of futsal differ from those of other team sports and may require sport-specific conditioning strategies to maximize performance outcomes (Ribeiro et al., 2025).

Therefore, the purpose of this study was to compare the effects of elastic-resistance-based speed-endurance training and running-based speed-endurance training on aerobic capacity and anaerobic performance in youth futsal players. The findings may provide practical evidence for coaches, strength and conditioning specialists, and sport scientists seeking effective and sport-specific conditioning methods for improving futsal performance.

2. Materials and methods

The study protocol was approved by the Human Research Ethics Committee of Udon Thani Rajabhat University (Approval No. 132/2024). Written informed consent was obtained from all participants and their parents or legal guardians before participation because all participants were minors. The following sections describe the study participants, training program, outcome assessments, and statistical procedures.

2.1 Subjects

This study employed a matched-pairs randomized experimental design with two parallel groups. The participants were 32 youth futsal players (aged 16–18 years) from Phibunrak Pittaya School, Udon Thani, Thailand. Sample size was determined using GPower version 3.1 (Faul et al., 2009) with an effect size of 0.50, statistical power of 0.80, and alpha level of 0.05, resulting in a minimum required sample of 32 participants.

Aerobic capacity was assessed using the Multistage Fitness Test, and participants were ranked according to their estimated VO_2max values. Participants were then matched in pairs according to VO_2max and randomly allocated by lottery into either the elastic-resistance group or the running-based group (16 participants per group). This procedure ensured baseline equivalence between groups. Each group consisted of 16 participants, resulting in a total sample of 16 males and 16 females.

2.2 Training Program

The speed-endurance training program (Tables 1 and 2) was conducted for 4 weeks, 3 sessions per week. Training intensity was prescribed at approximately 85% of maximal sprinting effort, determined from the participants' individual maximal sprint performance during familiarization testing.

Training intensity was monitored throughout the intervention using sprint completion time and Rating of Perceived Exertion (RPE; Borg CR-10 scale). Participants were required to maintain sprint times within ±5% of their baseline maximal sprint performance. If performance dropped below the target range, additional recovery was provided.

The duration of each session was standardized to 60 minutes and consisted of 10 minutes of warm-up, 40 minutes of speed-endurance training, and 10 minutes of cool-down.

Before each training session, participants completed a standardized warm-up consisting of 5 minutes of light jogging followed by dynamic stretching exercises involving the lower extremities and trunk musculature.

Table 1. Training Program for the Elastic Resistance Speed Endurance Group

Day	Type of Activities	Type of Movement	Duration
Monday	Warm Up	Static or Dynamic Stretching in Major Muscle Groups	10 minutes
Wednesday Friday	Work Out	For the elastic resistance training, the program was structured into three progressive rounds: • **Round 1:** Two elastic bands on each side • **Round 2:** One elastic band on each side • **Round 3:** No elastic resistance Each round was performed for 10 seconds. **Weeks 1–2**, participants performed 3 rounds per set, for a total of 4 sets, with a rest interval of 3 minutes between sets. **Weeks 3–4**, participants performed 3 rounds per set, for a total of 5 sets, with a rest interval of 2.5 minutes between sets.	40 minutes
	Cool Down	Static Stretching in Major Muscle Groups	10 minutes

Table 2. Training Program for the Running-Based Speed Endurance Group

Day	Type of Activities	Type of Movement	Duration
Monday Wednesday Friday	Warm Up	Static or Dynamic Stretching in Major Muscle Groups	10 minutes
	Work Out	The running program consisted of 20-meter shuttle runs. **Weeks 1–2**, Continuous running for 30 seconds per set, completing 4 sets with 3 minutes of rest between sets. **Weeks 3–4**, Continuous running for 30 seconds per set, completing 5 sets with 2.5 minutes of rest between sets.	40 minutes
	Cool Down	Static Stretching in Major Muscle Groups	10 minutes

2.3 Procedures

2.3.1 Body composition: subjects' mass (weight) and height were used to calculate Body Mass Index (BMI). The BMI was expressed in kilograms per square meter ($kg \cdot m^{-2}$) with mass in kilograms and height in meters. It was calculated by dividing body mass by the square of the body height.

2.3.2 Multistage Fitness Test (Beep Test): Aerobic fitness was assessed using the 20-m Multistage Fitness Test, commonly known as the Beep Test. This test is widely used to estimate maximal oxygen uptake (VO_{2max}) in athletes and youth populations (Léger et al., 1988). Participants ran back and forth between two lines set 20 meters apart, following audio signals from the standardized Beep Test recording. The initial running speed was 8.5 km/h and increased by 0.5 km/h at each stage. Participants were required to reach the 20-m line before or at the sound signal. The test was terminated when a participant failed to reach the line on two consecutive signals or voluntarily stopped due to fatigue. The final stage and shuttle completed were recorded. The maximal running speed corresponding to the final attained stage was subsequently used to estimate VO_2max. The test was conducted on a flat indoor futsal court under similar environmental conditions for all participants. Estimated VO_{2max} was calculated using the equation proposed by Léger et al. (1988):

$$VO_{2max} = 31.025 + 3.238V - 3.248A + 0.1536\,(V \times A) \quad (1)$$

where

VO_2max = estimated maximal oxygen uptake ($mL \cdot kg^{-1} \cdot min^{-1}$)

V = maximal running speed ($km \cdot h^{-1}$)

A = age (years)

2.3.3 Running-Based Anaerobic Sprint Test (RAST): Anaerobic performance was assessed using the Running-Based Anaerobic Sprint Test (RAST), which is a valid and practical field test for evaluating anaerobic power and fatigue in running-based sports (Zagatto et al., 2009). Before the test, participants performed a standardized warm-up consisting of light jogging, dynamic stretching, and short acceleration runs. The RAST consisted of six maximal 35-m sprints, with 10 seconds of passive recovery between each

sprint. Sprint time for each repetition was recorded using a stopwatch or timing gates. Participants were instructed to perform each sprint with maximal effort. Power output for each sprint was calculated using the following equation: Power (W) = Body mass × Distance² ÷ Time³. where body mass is expressed in kilograms, distance is 35 meters, and time is recorded in seconds. The following variables were calculated: Peak power: the highest power value across the six sprints, Minimum power: the lowest power value across the six sprints, Mean power: the average power value across all six sprints, Fatigue index: the decline in power across repeated sprints.

2.3.4 The fatigue index**:** was calculated as: Fatigue index = (Peak power – Minimum power) ÷ Total sprint time. A lower fatigue index indicates a better ability to maintain anaerobic performance during repeated high-intensity efforts.

2.4 Statistical Analyses

Data normality was assessed using the Shapiro–Wilk test. Baseline characteristics between groups were compared using independent-samples t-tests. Intervention effects were analyzed using a two-way repeated-measures ANOVA (Group × Time). Significant interactions were followed by Bonferroni-adjusted post hoc comparisons. Effect sizes were calculated using partial eta squared (η^2p) and Cohen's d. Ninety-five percent confidence intervals (95% CI) were reported for all primary outcome variables. Statistical significance was set at $p < 0.05$.

3. Results

Table 3 presents the baseline characteristics of the participants in the Elastic Resistance Group (ERG) and the Running-Based Group (RBG). No significant differences were observed between groups for body weight, height, body fat percentage, body mass index (BMI), or aerobic capacity (VO_2max) ($p > 0.05$). These findings indicate that both groups were comparable at baseline.

Table 3. The Characteristics of the Participants

Variables	ERG	RBG	*p*-value
Body weight (kg)	64.18 ± 15.40	62.51 ± 13.46	0.162
Height (cm)	171.18 ± 5.13	172.63 ± 6.39	0.252
Body fat (kg)	11.82 ± 9.28	10.40 ± 9.57	0.391
BMI (kg/m²)	21.88 ± 5.00	21.10 ± 5.07	0.445
VO_{2max} ($ml \cdot kg^{-1} \cdot min^{-1}$)	33.54 ± 7.23	33.60 ± 7.80	0.268

Note: Values are presented as Mean ± SD.ERG = Elastic Resistance Group.RBG = Running-Based Group

Table 4 presents within-group changes following the four-week intervention. Significant improvements were observed in anaerobic capacity ($p = 0.005$) and fatigue index ($p = 0.021$) in the ERG. No significant changes were observed in VO_2max or peak anaerobic power. In contrast, the RBG did not demonstrate significant improvements in any of the measured variables.

The improvement in anaerobic capacity observed in the ERG may enhance repeated sprint performance, acceleration, and high-intensity actions during the futsal competition. Likewise, the reduction in fatigue index indicates an improved ability to maintain performance during repeated maximal efforts, which may be beneficial during the latter stages of match play.

Table 5. presents the between-group comparisons at pre-test and post-test. No significant differences were observed between groups at either assessment point ($p > 0.05$).

Table 4. Aerobic and Anaerobic Performance Within Groups

Variables	Group	Pre-test (Mean ± SD)	Post-test (Mean ± SD)	t	*p*–value
VO_2max (ml·kg^{-1}·min^{-1})	ERG	33.54 ± 7.23	34.89 ± 9.30	-1.705	0.119
	RBG	33.60 ± 7.80	34.26 ± 9.66	-.472	0.647
Anaerobic capacity (W/kg)	ERG	7.03 ± 0.72	7.82 ± 1.20	-3.624	0.005*
	RBG	7.19 ± 1.13	7.86 ± 0.95	-2.139	0.058
Peak anaerobic power (W/kg)	ERG	9.52 ± 2.55	11.00 ± 2.19	-2.134	0.059
	RBG	10.23 ± 1.42	10.83 ± 1.46	-1.098	0.298
Fatigue index (%)	ERG	70.74 ± 12.20	59.23 ± 11.04	2.745	0.021*
	RBG	65.42 ± 14.54	62.46 ± 17.67	0.352	0.732

Note: Significantly different from pre-test to post-test within the same group ($p < .05$). ERG = Elastic Resistance Group.RBG = Running-Based Group.

Table 5. Comparison of Aerobic and Anaerobic Performance Between Groups

Variables	Time	ERG Mean ± SD	RBG Mean ± SD	t	*p*–value
VO_2max (ml·kg^{-1}·min^{-1})	Pre	33.54 ± 7.23	33.60 ± 7.80	-.017	0.987
	Post	34.89 ± 9.30	34.26 ± 9.66	.155	0.878
Anaerobic capacity (W/kg)	Pre	7.03 ± 0.72	7.19 ± 1.13	-.408	0.688
	Post	7.82 ± 1.20	7.86 ± 0.95	-.092	0.928
Peak anaerobic power (W/kg)	Pre	10.05 ± 1.37	10.23 ± 1.42	-.303	0.765
	Post	11.00 ± 2.19	10.83 ± 1.46	.213	0.843
Fatigue index (%)	Pre	70.74 ± 12.20	65.42 ± 14.54	.928	0.365
	Post	59.23 ± 11.04	62.46 ± 17.67	-.514	0.614

Note: ERG = Elastic Resistance Group.RBG = Running-Based Group.

Table 6 To provide a more comprehensive evaluation of training effects, mean changes (**Δ**), effect sizes (Cohen's d), and 95% confidence intervals were calculated.

The ERG demonstrated a large improvement in anaerobic capacity (d = 1.80) and a moderate reduction in fatigue index (d = -0.72), whereas the RBG demonstrated only small-to-moderate changes. Although the ERG generally showed larger improvements across several performance variables, differences in change scores did not reach statistical significance ($p > 0.05$).

Therefore, both training methods may be considered effective for improving selected aspects of performance; however, elastic-resistance speed-endurance training tended to produce greater practical improvements in anaerobic performance and fatigue resistance in youth futsal players.

Table 6. Mean Change (Δ), Effect Size, and Confidence Interval

Variable	ERG Δ Mean ± SD	Cohen's d	95% CI	RBG Δ Mean ± SD	Cohen's d	95% CI	*p*-value
VO_2max ($ml \cdot kg^{-1} \cdot min^{-1}$)	+1.78 ± 2.85	0.62	-0.61 to 4.16	+1.01 ± 5.48	0.18	-3.57 to 5.59	0.732
Anaerobic Capacity	+1.06 ± 0.59	1.80	0.57 to 1.55	+0.58 ± 1.19	0.49	-0.41 to 1.57	0.323
Anaerobic capacity (W/kg)	+0.81 ± 2.04	0.40	-0.89 to 2.51	+0.87 ± 2.32	0.37	-1.07 to 2.81	0.959
Fatigue Index	-9.76 ± 13.59	-0.72	-21.12 to 1.60	-0.14 ± 27.60	-0.01	-23.22 to 22.93	0.391

4. Discussion

The present study investigated the effects of elastic resistance–based speed-endurance training and running-based speed-endurance training on aerobic and anaerobic performance in youth futsal players. The main findings indicated that the Elastic Resistance Group (ERG) demonstrated significant improvements in anaerobic capacity and fatigue index following the intervention, whereas the Running-Based Group (RBG) did not show significant changes in these variables. However, no statistically significant differences were observed between groups at post-test.

The improvement in anaerobic capacity observed in the ERG may be practically relevant for futsal performance because anaerobic fitness is closely associated with repeated sprint ability, acceleration, rapid changes of direction, and the ability to perform high-intensity actions throughout a match. Likewise, the reduction in fatigue index may indicate an enhanced capacity to sustain performance during repeated maximal efforts, which is particularly important during the latter stages of competitions when fatigue accumulates.

These findings are generally consistent with previous studies reporting positive effects of elastic resistance training on sprint performance, muscular power, and repeated high-intensity exercise capacity (Loturco et al., 2016; Lopes et al., 2019). Elastic resistance provides variable external loading throughout movement, which may increase neuromuscular demands while preserving sport-specific movement patterns. Nevertheless, some previous studies have reported larger improvements in sprint-related performance than those observed in the present study. Such differences may be attributed to variations in training duration, resistance magnitude, participant characteristics, and sport-specific training demands.

Importantly, the present findings do not support the conclusion that elastic resistance–based speed-endurance training is superior to running-based speed-endurance training. Although the ERG demonstrated significant within-group improvements and generally larger effect sizes, the absence of statistically significant between-group differences indicates that both training approaches may provide comparable benefits for youth futsal players.

Several physiological mechanisms may help explain the observed adaptations. Recent evidence suggests that resistance training can enhance motor-unit recruitment, increase neural drive, improve intermuscular coordination, and optimize neuromuscular efficiency, thereby contributing to improvements in force production and athletic performance (Škarabot et al., 2021; Aslam et al., 2025; Rong et al., 2025). These neuromuscular adaptations may improve athletes' ability to perform repeated high-intensity efforts and delay fatigue during intermittent sports such as futsal match play. However, because physiological variables related to these mechanisms were not directly measured in the present study, such explanations

should be interpreted as potential mechanisms rather than confirmed adaptations resulting from the intervention.

The lack of statistically significant between-group differences may be explained by several factors. First, the intervention period was relatively short (4 weeks), which may not have been sufficient to induce substantial training adaptations that could distinguish one method from the other. Second, the relatively small sample size may have limited the statistical power to detect small-to-moderate between-group effects. Third, both groups performed active speed-endurance training protocols, which may have elicited similar physiological adaptations. Finally, individual differences in biological maturation and training responsiveness among adolescent athletes may have contributed to variability in the results.

Several limitations of the present study should be acknowledged. The intervention period was relatively short, the sample size was limited, and male and female athletes were analyzed together. In addition, biological maturation status was not controlled, training-load monitoring was limited, and the use of field-based performance tests may have introduced measurement error. Furthermore, the absence of a non-training control group restricts the ability to distinguish intervention effects from normal developmental changes. Future studies should include larger sample sizes, longer intervention periods, more comprehensive load-monitoring procedures, and direct physiological measurements to better understand the mechanisms underlying performance adaptations.

Practical Applications: For coaches and practitioners, elastic resistance–based speed-endurance training may be incorporated into futsal conditioning programs as an alternative training strategy to enhance anaerobic performance and fatigue resistance. This method is relatively inexpensive, portable, and easy to implement within sport-specific training environments. Coaches may also consider combining elastic resistance sprint drills with conventional running-based speed-endurance training to simultaneously develop neuromuscular, anaerobic, and aerobic fitness components required for futsal performance. Nevertheless, current evidence remains insufficient to conclude that elastic resistance–based training is more effective than traditional running-based speed-endurance training.

5. Conclusion

This study demonstrated that elastic resistance–based speed endurance training significantly improved anaerobic capacity and fatigue index in youth futsal players, whereas running-based speed endurance training did not produce significant changes in these variables. Although the Elastic Resistance Group generally demonstrated larger improvements in anaerobic performance variables, no statistically significant differences were observed between groups. Therefore, the findings do not support the conclusion that elastic resistance training is superior to running-based speed endurance training. Nevertheless, elastic resistance training appears to be a promising training modality for improving anaerobic performance and fatigue resistance in youth futsal players. Coaches may consider incorporating elastic resistance exercises into speed-endurance programs as part of a comprehensive conditioning strategy. Further research with larger sample sizes, longer intervention periods, and more rigorous physiological assessments is required before stronger conclusions regarding the comparative effectiveness of elastic resistance training can be made.

6. Reference

Albalad-Aiguabella, R., Navarrete-Villanueva, D., Mainer-Pardos, E., Villanueva-Guerrero, O., Muniz-Pardos, B., & Vicente-Rodríguez, G. (2025). Physical Training Considerations for Futsal Players According to Strength and Conditioning Coaches: A Qualitative Study. Sports, 13, 126. https://doi.org/10.3390/sports13040126

Aslam, S., Habyarimana, J. D. D., & Bin, S. Y. (2025). Neuromuscular adaptations to resistance training in elite versus recreational athletes. Frontiers in physiology, 16,1598149. https://doi.org/10.3389/fphys.2025.1598149

Faul, F., Erdfelder, E., Buchner, A., & Lang, A. G. (2009). Statistical power analyses using G* Power 3.1: Tests for correlation and regression analyses. Behavior research methods, 41(4), 1149-1160. https://doi.org/10.3758/BRM.41.4.1149

González-Fernández, F. T., Ceylan, H. I., Silva, R., Clemente, F. M., Bezerra, P., & Chen, Y. (2024). Relationships between physical fitness and match running demands during a futsal congested-weeks training camp. Biology of Sport, 41(4), 11-30. https://doi.org/10.5114/biolsport.2024.134760

Léger, L. A., Mercier, D., Gadoury, C., & Lambert, J. (2007). The multistage 20 metre shuttle run test for aerobic fitness. Journal of sports sciences, 6(2), 93-101. https://doi.org/10.1080/02640418808729800

Lopes, J. S. S., Machado, A. F., Micheletti, J. K., de Almeida, A. C., Cavina, A. P., & Pastre, C. M. (2019). Effects of training with elastic resistance versus conventional resistance on muscular strength: A systematic review and meta-analysis. SAGE open medicine, 7, 1-7 https://doi.org/10.1177/2050312119831116

Loturco, I., Pereira, L. A., Kobal, R., Maldonado, T., Piazzi, A. F., Bottino, A., Kitamura, K., Abad, C. C. C., Arruda, M., & Nakamura, F. Y. (2016). Improving sprint performance in soccer: effectiveness of jump squat and Olympic push press exercises. PloS one, 11(4), e0153958. https://doi.org/10.1371/journal.pone.0153958

Ribeiro, J. N., Ferraz, A., Gonçalves, B., Serrano, C., Coutinho, D., Ballester, R., & Travassos, B. (2025). Training exercises, match demands, and variability in elite futsal. Frontiers in Sports and Active Living, 7, 1553046. https://doi.org/10.3389/fspor.2025.1553046

Rong, W., Geok, S. K., Samsudin, S., Zhao, Y., Ma, H., & Zhang, X. (2025). Effects of strength training on neuromuscular adaptations in the development of maximal strength: a systematic review and meta-analysis. Scientific reports, 15(1), 19315. https://doi.org/10.1038/s41598-025-03070-z

Shi, L., Cai, Z., Chen, S., & Han, D. (2022). Acute effects of variable resistance training on force, velocity, and power measures: a systematic review and meta-analysis. PeerJ, 10, e13870. https://doi.org/10.7717/peerj.13870

Škarabot, J., Brownstein, C. G., Casolo, A., Del Vecchio, A., & Ansdell, P. (2020). The knowns and unknowns of neural adaptations to resistance training. European journal of applied physiology, 121(3), 675-685. https://doi.org/10.1007/s00421-020-04567-3

Spyrou K, Freitas TT, Marín-Cascales E, Herrero-Carrasco R, Alcaraz PE. (2022). External match load and the influence of contextual factors in elite futsal. Biology of Sport, 39(2), 349-354. https://doi.org/10.5114/biolsport.2022.105332

Stanković, D., Lazić, A., Trajković, N., Okičić, M., Bubanj, A., Vencúrik, T., Gašić, T., & Bubanj, S. (2025). Effects of Elastic Band Training on Physical Performance in Team Sports: A Systematic Review and Meta-Analysis. Journal of Functional Morphology and Kinesiology, 10(4), 402. https://doi.org/ 10.3390/jfmk10040402

Van Hooren, B., Aagaard, P., & Blazevich, A. J. (2024). Optimizing resistance training for sprint and endurance athletes: balancing positive and negative adaptations. Sports Medicine, 54(12), 3019-3050. https://doi.org/10.1007/s40279-024-02110-4

Zagatto, A. M., Beck, W. R., & Gobatto, C. A. (2009). Validity of the running anaerobic sprint test for assessing anaerobic power and predicting short-distance performances. Journal of Strength and Conditioning Research, 23(6), 1820-1827. https://doi.org/10.1519/JSC.0b013e3181b3df32

การพัฒนาและประเมินประสิทธิภาพระบบเฝ้าระวังดัชนีความร้อนและแจ้งเตือนแบบเรียลไทม์ด้วยเทคโนโลยีอินเทอร์เน็ตของสรรพสิ่งสำหรับการฝึกทหาร: กรณีศึกษา กองพันทหารสื่อสาร กรมการสื่อสารทหาร กองบัญชาการกองทัพไทย

Development and Performance Evaluation of an IoT-Based Real-Time Heat Index Monitoring and Alert System for Military Training: A Case Study of the Signal Battalion, Directorate of Communications and Information Technology, Royal Thai Armed Forces Headquarters

อติกานต์ ม่วงเงิน[1*] นัฐพงศ์ ส่งเนียม[1] และ อชิตะ พ่วงตรง[1]

Atikan Muangngeon[1*], Nattapong Songneam[1] and Achita Phuangtrong[1]

[1]สาขาวิชาวิทยาการคอมพิวเตอร์ คณะวิทยาศาสตร์และเทคโนโลยี มหาวิทยาลัยราชภัฏพระนคร กรุงเทพมหานคร

[1]Department of Computer Science, Faculty of Science and Technology, Phranakhon Rajabhat University, Bangkok

[*]Corresponding Author: atikan.m@365.pnru.ac.th

Received: June 30, 2026 **Revised:** August 5, 2026 **Accepted:** August 17, 2026

บทคัดย่อ

การเจ็บป่วยจากความร้อนเป็นความเสี่ยงสำคัญที่ส่งผลกระทบต่อความปลอดภัยและประสิทธิภาพการฝึกทหาร ขณะที่ระบบเฝ้าระวังที่ใช้อยู่ยังขาดการประเมินความเสี่ยงและการแจ้งเตือนแบบเรียลไทม์ การวิจัยนี้มีวัตถุประสงค์เพื่อ 1) พัฒนาระบบเฝ้าระวังดัชนีความร้อนและแจ้งเตือนแบบเรียลไทม์ด้วยเทคโนโลยีอินเทอร์เน็ตของสรรพสิ่ง (IoT) สำหรับการฝึกทหาร 2) ประเมินประสิทธิภาพของระบบด้านความถูกต้องของการจำแนกระดับความเสี่ยง ความน่าเชื่อถือในการรับส่งข้อมูล และระยะเวลาในการแจ้งเตือน และ 3) ประเมินความพึงพอใจของผู้ใช้งาน การวิจัยเป็นการวิจัยและพัฒนา (Research and Development: R&D) ตามวงจรการพัฒนาระบบ (System Development Life Cycle: SDLC) โดยพัฒนาระบบที่ประกอบด้วยเซนเซอร์ SHT31 ไมโครคอนโทรลเลอร์ ESP32 ฐานข้อมูล Firebase Realtime Database เว็บแดชบอร์ด และ LINE Official Account ศึกษาจากบุคลากรที่เข้ารับการฝึกวินัยกำลังพล กรมการสื่อสารทหาร กองบัญชาการกองทัพไทย จำนวน 40 นาย โดยใช้การเก็บข้อมูลจากประชากรทั้งหมด และประเมินประสิทธิภาพด้วยการทดสอบการจำแนกระดับความเสี่ยง 50 กรณี การรับส่งข้อมูล 100 ครั้ง และการวัดระยะเวลาแจ้งเตือน 10 ครั้ง ผลการวิจัยพบว่า ระบบสามารถจำแนกระดับความเสี่ยงจากความร้อนได้ถูกต้องร้อยละ 100.00 อัตราความสำเร็จในการรับส่งข้อมูลร้อยละ 100.00 มีระยะเวลาเฉลี่ยในการแจ้งเตือน 2.49 วินาที และผู้ใช้งานมีความพึงพอใจอยู่ในระดับมากที่สุด ($\bar{x}$ = 4.71, S.D. = 0.38) ระบบสามารถบูรณาการการคำนวณดัชนีความร้อนแบบเรียลไทม์ การจำแนกระดับความเสี่ยงตามเกณฑ์ Heat Flag การเชื่อมโยงข้อมูลผ่านคลาวด์ และการแจ้งเตือนผ่าน LINE ภายในแพลตฟอร์มเดียว จึงช่วยสนับสนุนการบริหารจัดการความเสี่ยงจากความร้อนและการตัดสินใจด้านความปลอดภัยในการฝึกทหารได้อย่างมีประสิทธิภาพ นอกจากนี้ ผลการวิจัยยังแสดงให้เห็นถึงศักยภาพของการประยุกต์ใช้เทคโนโลยี IoT เพื่อพัฒนาระบบเฝ้าระวังและแจ้งเตือนแบบเรียลไทม์สำหรับงานภาคสนามและการปฏิบัติงานกลางแจ้ง รวมทั้งเป็นแนวทางเชิงวิชาการสำหรับพัฒนาระบบด้านความปลอดภัยในบริบทที่มีความเสี่ยงจากสภาพแวดล้อมในอนาคต

คำสำคัญ: อินเทอร์เน็ตของสรรพสิ่ง, ดัชนีความร้อน, การเฝ้าระวังแบบเรียลไทม์, การฝึกทหาร, การจัดการความเสี่ยงจากความร้อน

Abstract

Heat-related illness poses a significant risk to personnel safety and training effectiveness in military environments, while existing monitoring practices often lack real-time heat-risk assessment and alert capabilities. This study aimed to 1) develop an Internet of Things (IoT)-based real-time heat index monitoring and alert system for military training, 2) evaluate the technical performance of the developed system in terms of sensor validation, heat-risk rule-based classification verification, data transmission reliability, and alert latency, and 3) assess user satisfaction. This study employed a research and development (R&D) approach based on the System Development Life Cycle (SDLC). The developed system integrated an SHT31 temperature and humidity sensor, an ESP32 microcontroller, Firebase Realtime Database, a web-based dashboard, and a LINE Official Account. The study included all 40 personnel participating in the 2026 military discipline training program at the Directorate of Communications and Information Technology, Royal Thai Armed Forces Headquarters, using a census approach. Technical performance was evaluated through 50 predefined heat-risk classification test cases, 100 data transmission trials, and 10 alert latency measurements. The results demonstrated that the developed system achieved 100.00% correctness in heat-risk rule-based classification verification under controlled testing conditions and a 100.00% data transmission success rate, with an average alert latency of 2.49 seconds. Overall user satisfaction was rated at the highest level ($\bar{x}$ = 4.71, S.D. = 0.38). The system effectively integrates real-time heat index computation, military Heat Flag classification, cloud-based data synchronization, and instant LINE notifications within a single platform, thereby enhancing heat-risk monitoring and supporting timely safety decision-making during military training. These findings demonstrate the practical applicability of IoT-based real-time monitoring technologies for improving occupational safety in military training and other outdoor operational environments and provide a valuable framework for the future research and development of intelligent safety monitoring systems in high-risk settings.

Keywords: Internet of things, Heat index, Real-time monitoring, Military training, Heat-risk management

1. Introduction

Climate change and rising global temperatures have become major challenges affecting public health, occupational safety, and military readiness worldwide. The increasing frequency and intensity of extreme heat events have significantly elevated the risk of heat-related illnesses among individuals performing strenuous outdoor activities, particularly military personnel, emergency responders, and outdoor workers (Patton & Hoyt, 2023; Gibb et al., 2024). Heat-related illnesses range from mild conditions, such as heat cramps and heat exhaustion, to life-threatening heat stroke, which may result in multiple organ failure or death if not recognized and treated promptly (Epstein et al., 2025). Consequently, environmental heat has become an important non-combat hazard that directly affects personnel safety, operational performance, and training effectiveness in military organizations (Patton & Hoyt, 2023).

Thailand is located in a tropical region characterized by high temperatures and humidity throughout most of the year. Such environmental conditions substantially increase the risk of heat-related illnesses during outdoor military training. According to the Royal Thai Army Medical Department (2023), heat index values should be continuously monitored and classified according to the Heat Flag criteria to support decisions regarding hydration, work-rest cycles, and training intensity. However, many military units continue to rely on manual measurements or weather information obtained from centralized meteorological stations. These approaches may not accurately represent local microclimate conditions at the actual training site

and often delay risk assessment and operational decision-making, thereby increasing the likelihood of heat-related injuries.

Previous epidemiological research conducted among Royal Thai Army conscripts reported that 53 of 809 newly inducted conscripts (6.6%) developed heat-related illnesses during basic military training, highlighting that heat-related illness remains an important occupational health concern in military settings (Nutong et al., 2018). These findings underscore the need for effective real-time environmental monitoring and early warning systems capable of supporting timely operational decision-making and reducing heat-related risks during military training.

Recent studies have highlighted the growing importance of heat-risk surveillance and environmental monitoring in military and occupational settings. Narindrarangkura et al. (2024) demonstrated that predictive analytics could improve the surveillance of heat-related illnesses among Thai military recruits by enabling early identification of heat-risk factors. Similarly, Patton and Doyle (2024) reported increasing environmental heat exposure at U.S. Army basic combat training installations, emphasizing the need for more effective environmental monitoring to protect military personnel. Furthermore, the Defense Health Agency (2023) reported that continuous environmental surveillance and proactive heat-risk management are essential strategies for reducing severe heat-related illnesses during military operations and training. Although these studies provide valuable evidence for heat-risk prevention, they primarily focus on surveillance, prediction, or epidemiological analysis rather than the development of an integrated real-time monitoring and alert system for operational use.

Advances in the Internet of Things (IoT) have enabled intelligent environmental monitoring systems capable of collecting, processing, and transmitting environmental data in real time. IoT-based systems integrate sensing devices, wireless communication, cloud computing, and mobile applications to improve situational awareness and support rapid decision-making in safety-critical environments. Recent studies have demonstrated the effectiveness of IoT technologies for environmental monitoring and heat-alert prediction (Considine et al., 2023; Popescu et al., 2024). Nevertheless, most existing systems emphasize environmental data acquisition, visualization, or predictive analytics, while providing limited support for operational decision-making in military environments. To provide a clearer overview of existing studies, Table 1 compares representative heat monitoring and alert systems with respect to sensing technology, cloud integration, notification mechanisms, military-specific heat-risk classification, application domains, and existing limitations.

As shown in Table 1, previous studies have primarily focused on environmental monitoring, predictive analytics, or general heat-alert systems. However, none of these systems integrates real-time heat index computation, military Heat Flag classification, cloud-based synchronization, and instant LINE Official Account notification within a unified platform specifically designed for military training. Moreover, empirical validation of such systems under actual military training conditions remains limited.

Table 1 presents a comparative synthesis of the distinctive features and limitations of representative IoT-based heat-monitoring studies, including their sensing technologies, cloud platforms, notification mechanisms, military Heat Flag support, and application domains.

Table 1. Comparison of related IoT-based heat monitoring studies

Study	Sensor	Cloud Platform	Real-time Notification	Military Heat Flag	Application Domain	Limitation
Buller et al. (2021)	Wearable physiological sensors	Mobile cloud platform	✓ (Mobile application)	✗	Military heat injury prevention	No heat index or military heat-flag support
Narindrarangkura et al. (2024)	SHT31	Cloud Database	✓	✗	Occupational Health	No military application
Considine et al. (2023)	Meteorological Data	Cloud Analytics	✗	✗	Heat Alert Prediction	No IoT sensing platform
This Study	SHT31	Firebase Realtime Database	✓ (LINE OA)	✓	Military training	Integrated platform

Despite recent advances in IoT-based heat monitoring technologies, several research gaps remain: (1) existing studies have primarily focused on environmental monitoring or predictive analytics; (2) few studies have integrated real-time heat index computation, military Heat Flag classification, cloud synchronization, and instant LINE Official Account notifications within a single platform; and (3) empirical validation of integrated systems under actual military training conditions remains limited. Consequently, an integrated IoT-based solution is needed to provide real-time heat-risk assessment and decision support specifically for military training environments.

To address these research gaps, this study develops and evaluates an IoT-based real-time heat index monitoring and alert system specifically designed for military training. Unlike previous IoT-based environmental monitoring systems, the proposed platform integrates four key components within a single operational framework: (1) real-time heat index computation, (2) military Heat Flag classification based on Royal Thai Army guidelines, (3) cloud-based synchronization using Firebase Realtime Database, and (4) instant notification through the LINE Official Account. This integrated architecture supports real-time environmental monitoring and rapid operational decision-making during military training.

The main contributions of this study are fourfold. First, it develops an integrated IoT-based heat-risk monitoring platform tailored for military training environments. Second, it incorporates the Royal Thai Army Heat Flag criteria to automate heat-risk classification and support operational decision-making. Third, it combines cloud-based synchronization with instant LINE Official Account notifications to improve the timeliness of heat-risk communication. Finally, it evaluates the developed system through technical performance assessment, including heat-risk rule-based classification verification, data transmission success rate, and alert latency, together with user satisfaction under actual military training conditions.

Therefore, the objectives of this study were (1) to develop an IoT-based real-time heat index monitoring and alert system for military training; (2) to evaluate the technical performance of the developed system in terms of sensor validation, heat-risk rule-based classification verification, data transmission reliability, and alert latency; and (3) to assess user satisfaction regarding the effectiveness and usability of the system for supporting heat-risk management and safety decision-making during military training.

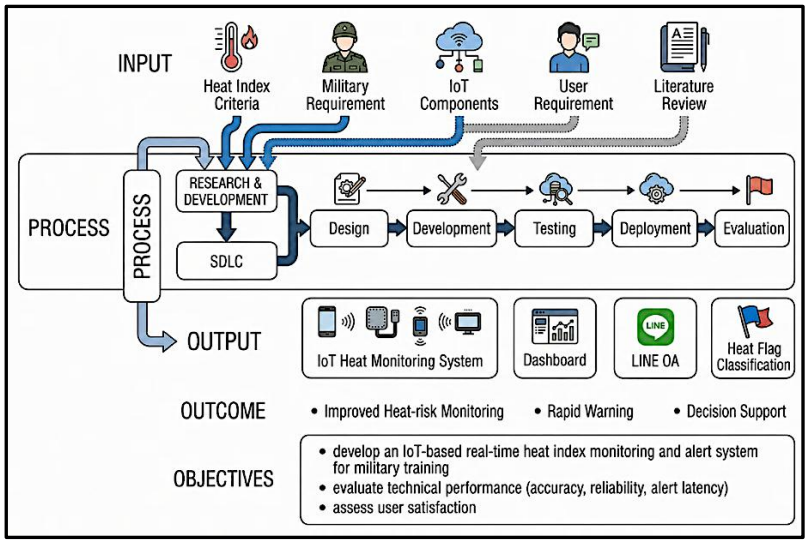


Figure 1. Conceptual framework for the proposed IoT-based real-time heat index monitoring and alert system

The conceptual framework illustrates the overall research process based on the Input–Process–Output (IPO) model. The framework begins with problem identification, military heat-risk criteria, IoT technologies, user requirements, and a literature review as research inputs. These inputs are integrated through a research and development (R&D) methodology using the System Development Life Cycle (SDLC), resulting in the development of the proposed IoT-based monitoring system. The developed system is subsequently evaluated through technical performance assessment and user satisfaction evaluation to achieve the three research objectives.

2. Materials and methods

2.1 Research Design

This study employed a research and development (R&D) methodology to design, implement, and evaluate an Internet of Things (IoT)-based real-time heat index monitoring and alert system for military training. The development process followed the System Development Life Cycle (SDLC), consisting of five phases: requirements analysis, system design, implementation, testing, and evaluation. The SDLC provides a systematic framework for developing reliable software systems and has been widely adopted for IoT applications because it facilitates the integration of sensing devices, cloud services, and user applications while improving system quality and maintainability (Pressman & Maxim, 2020; Fahmideh et al., 2022).

2.2 System Development

The overall architecture of the developed system is illustrated in Figure 2. The proposed platform consists of three functional layers: (1) an environmental sensing layer, (2) a cloud communication layer, and (3) an application layer. The sensing layer employed an SHT31 temperature and relative humidity sensor connected to an ESP32 microcontroller to continuously acquire environmental data. The measured data were transmitted through a wireless network to Firebase Realtime Database, which served as the cloud platform for real-time data synchronization and storage. Heat index values were automatically calculated using the National Weather Service heat index equation. The calculated values were subsequently classified according to the Royal Thai Army Heat Flag criteria to determine the corresponding heat-risk level.

The processed information was presented through a web-based dashboard, while heat-risk alerts were automatically delivered to users through the LINE Official Account using Flex Message.

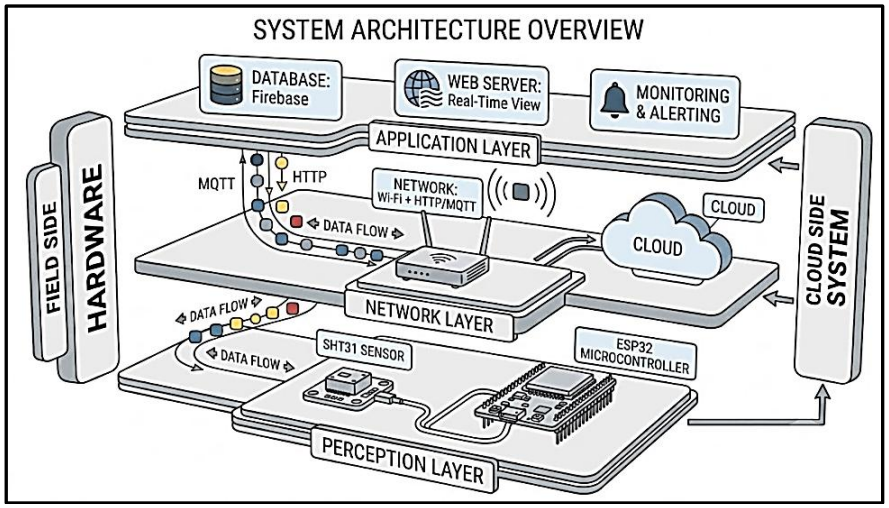


Figure 2. Architecture of the proposed IoT-based heat index monitoring and alert system

The developed system integrates hardware for environmental data acquisition with software services for data storage, visualization, and real-time notification. The specifications and functions of the principal components are summarized in Table 2.

To support automated operational decision-making, the calculated heat index was mapped to five Heat Flag levels and corresponding recommendations for military training activities, as shown in Table 3.

Table 2. Hardware and software components used in the developed system

Component	Specification	Function
ESP32	Wi-Fi-enabled microcontroller	Data processing and communication
SHT31	Temperature and humidity sensor	Environmental monitoring
OLED Display	0.96-inch I2C display	On-site data visualization
Firebase Real-time Database	Cloud database platform	Data storage and synchronization
LINE Messaging API	Messaging platform	Real-time notification delivery
Web Dashboard	HTML/CSS/JavaScript	Monitoring and data visualization

Table 3. Heat-risk classification based on heat index criteria

Heat flag	Heat index (°C)	Recommended training activity
White	< 27	Normal training
Green	27–32	Increased hydration monitoring
Yellow	33–39	Reduced training intensity
Red	40–51	Increased rest periods
Black	> 51	Training suspension recommended

2.3 Study Site and Participants

The study population consisted of military personnel who participated in the 2026 personnel discipline training program at the Directorate of Communications and Information Technology, Royal Thai Armed Forces Headquarters. These personnel were directly involved in outdoor military training and heat-risk management, including training supervisors, drill instructors, assistant instructors, medical officers, and military personnel representatives.

A census approach was employed, whereby all 40 eligible personnel were included in the study. The participants comprised five training supervisors, five medical officers, fifteen drill instructors, ten assistant instructors, and five military personnel representatives. Since the entire target population participated in the evaluation, no sampling procedure was required. The participants were responsible for training management, operational supervision, or medical support during field exercises, enabling them to evaluate both the technical performance and practical usability of the developed system under actual operational conditions (Creswell & Creswell, 2023).

This study involved the evaluation of a prototype IoT-based monitoring system and an anonymous user satisfaction survey. Participation was voluntary, and participants were informed of the study objectives prior to participation. No personally identifiable information was collected, and all responses were anonymized and kept confidential. Participants were free to decline or withdraw from the study without any consequences. Formal ethical approval was not obtained prior to data collection. This information has been transparently disclosed to the Editorial Board for consideration in accordance with the journal's ethical requirements.

Technical performance evaluation was conducted independently of participant assessment. The evaluation design was based on system and software quality measurement principles, particularly functional correctness, reliability, and time behavior. The heat-risk rule-based classification verification was evaluated using 50 predefined test cases, consisting of 10 cases for each Heat Flag level: WHITE, GREEN, YELLOW, RED, and BLACK. This design ensured balanced coverage of all predefined risk categories and allowed verification of the system's classification correctness under different environmental conditions. Data transmission reliability was assessed through 100 consecutive communication trials to verify the stability of data transfer from the ESP32 microcontroller to Firebase Realtime Database. Alert latency was measured across 10 repeated notification trials to evaluate the consistency of real-time notification delivery through the LINE application. These testing procedures were designed according to the quality measurement concepts of ISO/IEC 25023 and software testing principles recommended for validating functional correctness and system reliability (ISO/IEC 25023, 2016; Pressman & Maxim, 2020).

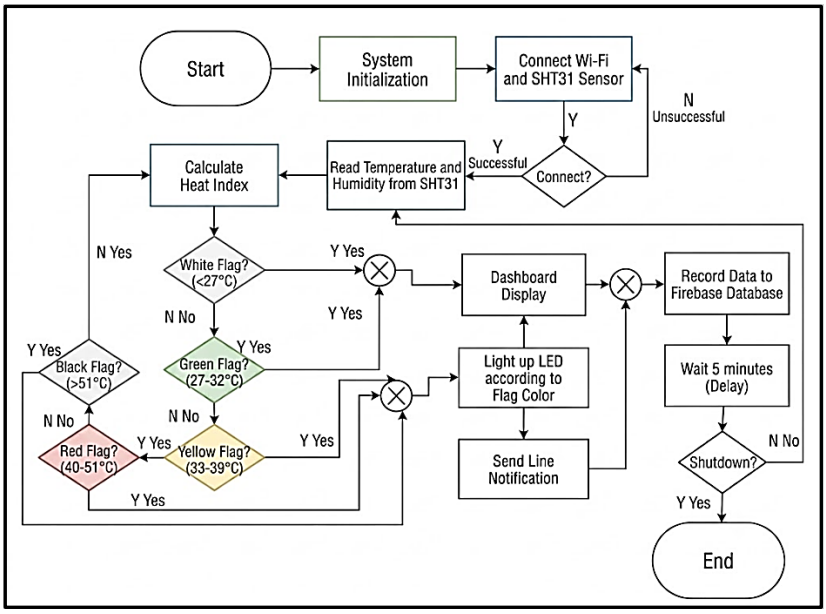


Figure 3. Workflow of data acquisition, heat index calculation, and real-time alert generation

2.4 Field Deployment and Data Collection

The developed system was deployed under actual military training conditions over a 10-day field deployment conducted from 3 to 12 May 2026. Environmental monitoring was performed daily from 08:00 to 16:00, corresponding to the period of highest heat exposure during routine military training. Ambient temperature (°C) and relative humidity (%RH) were automatically recorded at 1-minute intervals, resulting in approximately 4,800 environmental observations. Heat index values were computed in real time and synchronized with Firebase Realtime Database for continuous visualization through the web dashboard. Whenever the calculated heat index exceeded the predefined Heat Flag thresholds, the system automatically issued heat-risk notifications via the LINE Official Account. Participants were able to monitor real-time environmental conditions, Heat Flag statuses, and alert notifications through both the web dashboard and mobile devices.

2.5 Performance Evaluation

The developed system was evaluated using both technical performance assessment and user satisfaction assessment. Technical performance was assessed using four evaluation criteria: (1) sensor validation, performed by comparing SHT31 measurements with those of a calibrated digital thermo-hygrometer before field deployment; (2) heat-risk rule-based classification verification, evaluated using 50 predefined heat index test cases covering all Heat Flag categories defined by the Royal Thai Army Medical Department. To further verify the correctness of the classification algorithm around decision thresholds, boundary-value test cases were additionally included. The test cases were selected at values immediately below, equal to, and immediately above each Heat Flag threshold (e.g., 27°C, 33°C, 40°C, and 51°C) to ensure that the developed system correctly classified heat-risk levels at boundary conditions; (3) data transmission success rate, evaluated through 100 consecutive transmission trials between the ESP32 microcontroller and Firebase Realtime Database; and (4) alert latency, evaluated using 10 repeated notification tests, for which latency was defined as the elapsed time between environmental data acquisition and successful delivery of the notification through the LINE Official Account.

The field deployment was designed to evaluate the system under actual military training conditions. The study period, operating hours, sampling interval, number of records, observed environmental ranges, and deployment site are summarized in Table 4.

Table 4. Field deployment conditions

Parameter	Value
Study period	3–12 May 2026
Experimental duration	10 consecutive days
Operating hours	08:00–16:00
Sampling interval	Every 1 minute
Records collected per day	Approximately 480
Total environmental records	Approximately 4,800
Temperature range	30.8–37.4°C
Relative humidity range	58–86%RH
Study site	Signal Battalion, Directorate of Communications and Information Technology, Royal Thai Armed Forces Headquarters

The number of test cases and repeated trials was selected based on recommendations for software functional testing and IoT system performance evaluation, ensuring adequate repeatability and reliability of the experimental results (ISO/IEC 25023, 2016; Pressman & Maxim, 2020).

Following the field deployment, participants evaluated the developed system using a structured questionnaire covering four dimensions: (1) technical performance and hardware, (2) user interface and notification, (3) usefulness and practical applicability, and (4) system reliability and acceptance. Responses were recorded using a five-point Likert scale.

Questionnaire Validation and Reliability. The user satisfaction questionnaire was evaluated for content validity by three experts in information systems and software development. The Item–Objective Congruence (IOC) values ranged from 0.67 to 1.00, with an average IOC of 0.83, indicating acceptable content validity. A pilot study was subsequently conducted to assess the reliability of the questionnaire. The instrument demonstrated good internal consistency, with a Cronbach's alpha coefficient of 0.89.

System Quality Evaluation. Prior to user evaluation, the developed system was assessed by three experts. The overall system quality was rated at a high level ($\bar{x}$ = 4.18, S.D. = 0.55), confirming that the system was appropriate for field deployment and subsequent user satisfaction evaluation.

2.6 Performance Metrics

The performance of the developed IoT-based real-time heat index monitoring and alert system was evaluated in four areas: sensor validation, heat-risk rule-based classification verification, data transmission reliability, and alert latency. The evaluation was conducted to verify whether the system could reliably acquire environmental data, correctly implement the predefined Heat Flag classification rules, successfully transmit data to the cloud database, and deliver alert messages within an appropriate response time for real-time military training safety management.

For heat-risk rule-based classification verification, 50 predefined test cases were used, with 10 cases assigned to each of the five Heat Flag categories to ensure balanced verification across all predefined risk levels. For data transmission reliability, 100 consecutive transmission attempts were conducted to provide sufficient repeated observations for identifying possible communication failures or data loss during cloud synchronization. For alert latency, 10 repeated notification trials were considered appropriate because latency measurement focused on short response-time behavior under the same operational workflow. Repeated measurements helped verify whether the notification delay remained stable during real-time operation. This evaluation design aligns with ISO/IEC 25023, which emphasizes measurable indicators for software product quality, including functional correctness, reliability, and time behavior.

2.6.1 Sensor Validation

Before performance testing, the SHT31 sensor was validated against a standard digital thermo-hygrometer placed at the same location. Temperature and relative humidity were recorded simultaneously from both devices to examine measurement differences, consistency, and output stability before using the data for heat index calculation. The results showed that the SHT31 readings remained within an acceptable range, indicating that the sensor was suitable for environmental monitoring in the developed system.

2.6.2 Heat Index Calculation

Heat index values were calculated from the air temperature and relative humidity measured by the SHT31 sensor using the Rothfusz regression adopted by the U.S. National Weather Service (Rothfusz, 1990), as shown in Equation (1). The calculated values were subsequently used to classify heat-risk levels according to the predefined Heat Flag criteria.

$$HI = c_1 + c_2T + c_3RH + c_4TRH + c_5TT^2 + c_6RH^2 + c_7T^2RH + c_8TRH^2 + c_9T^2RH^2 \quad (1)$$

where HI = heat index (°F)

T = air temperature (°F)

RH = relative humidity (%)

$c_1, c_{2,\ldots}, c_9$ = The empirical constants in the NOAA Rothfusz regression are $c_1 = -42.379$, $c_2 = 2.04901523$, $c_3 = 10.14333127$, $c_4 = -0.22475541$, $c_5 = -0.00683783$, $c_6 = -0.05481717$, $c_7 = 0.00122874$, $c_8 = 0.00085282$, and $c_9 = -0.00000199$.

The temperature measured by the SHT31 sensor was initially obtained in degrees Celsius and converted to degrees Fahrenheit before being entered into the NOAA Rothfusz regression. The calculated heat index was subsequently converted from degrees Fahrenheit back to degrees Celsius for classification according to the Royal Thai Army Heat Flag criteria.

$$T_F = (T_C \, x \, \frac{9}{5}) + 32 \quad (2)$$

$$HI_C = (HI_F - 32) \times \frac{5}{9} \quad (3)$$

2.6.3 Heat-risk rule-based classification verification

Heat-risk rule-based classification verification was performed by comparing the Heat Flag level generated by the system with the expected Heat Flag level determined from the predefined criteria. The percentage of correctly classified test cases was calculated using Equation (4).

$$RCV\ (\%) = \frac{N_c}{N_t} \tag{4}$$

where $RCV(\%)$ = rule-based classification verification result of the developed system expressed as a percentage (%)

N_c = number of correctly classified test cases

N_t = total number of test cases evaluated

The heat-risk rule-based classification verification was evaluated using 50 test cases covering all predefined heat-risk categories, including WHITE, GREEN, YELLOW, RED, and BLACK levels. The test cases were generated from different combinations of temperature and relative humidity values representing a wide range of environmental conditions that may occur during military training activities. Using multiple test cases across all classification levels helps ensure that the developed system can consistently classify heat-risk conditions under various environmental scenarios and improves the reliability of the performance evaluation (ISO/IEC 25023, 2016; Pressman & Maxim, 2020).

2.6.4 Alert latency

Alert latency was defined as the time interval between data acquisition by the sensor and successful delivery of the alert message to the user through the LINE application. Alert latency was calculated using Equation (5).

$$Latency = T_a - T_s \tag{5}$$

where $Latency$ = alert latency (s)

T_a = alert reception timestamp

T_s = sensor acquisition timestamp

The average alert latency was calculated using Equation (6).

$$\bar{L} = \frac{1}{n}\sum_{i=1}^{n} L_i \tag{6}$$

where $\bar{L}$ = average alert latency (s)

L_i = latency measured in the i^{th} test trial (s)

n = total number of test trials

2.6.5 User Satisfaction Evaluation

User satisfaction was evaluated using a five-point Likert scale questionnaire. The questionnaire covered four evaluation dimensions: (1) technical performance and hardware, (2) user interface and notification, (3) usefulness and practical applicability, and (4) system reliability and acceptance. The mean and standard deviation were used to summarize user satisfaction scores.

The mean score was calculated using Equation (7).

$$\bar{x} = \frac{\sum_{i=1}^{n} x_i}{n} \quad (7)$$

where $\bar{x}$ = mean score
x_i = score obtained by each participant
n = total number of participants

The standard deviation was calculated using Equation (8).

$$S.D. = \sqrt{\frac{\sum_{i=1}^{n}(x_i - \bar{x})^2}{N-1}} \quad (8)$$

where $S.D.$ = standard deviation
x_i = score obtained by each participant
$\bar{x}$ = mean score
N = total number of participants

To evaluate the reliability of data transmission, the success rate was calculated using Equation (9):

$$\textbf{Success Rate (\%)} = \frac{N_s}{N_t} \, x \, 100 \quad (9)$$

where **Success Rate** (%) = percentage of successful data transmissions
N_s = number of successful data transmissions
N_t = total number of data transmission attempts

2.6.6 System Operation for Performance Evaluation

The system operation began when the ESP32 microcontroller initialized the hardware and established a connection with the Wi-Fi network and SHT31 sensor. After a successful connection, the sensor measured air temperature and relative humidity. The measured values were then transmitted to the ESP32 for heat index calculation. The calculated heat index was classified into heat-risk levels according to the Heat Flag criteria, including white, green, yellow, red, and black levels.

After classification, the system displayed the results on the web dashboard and activated the LED indicator according to the detected risk level. If the heat-risk level reached a warning condition, the system automatically sent an alert message through the LINE Official Account. All environmental data and heat-risk results were stored in Firebase Realtime Database for real-time monitoring and historical data review. The system repeated the monitoring cycle every minute unless the device was turned off.

2.7 Statistical Analysis

Descriptive statistics were employed to analyze the collected data. The mean ($\bar{x}$) and standard deviation (S.D.) were used to summarize user satisfaction scores, while appropriate descriptive measures were used for the technical performance metrics. The results were interpreted according to commonly accepted criteria for Likert-scale evaluation in information systems research (Creswell & Creswell, 2023).

3. Results

During the field deployment, the proposed system continuously monitored environmental conditions over a 10-day evaluation period. A total of approximately 4,800 environmental records were successfully collected and synchronized with Firebase Realtime Database without data loss. The recorded temperature ranged from 30.8°C to 37.4°C, while the relative humidity varied between 58% and 86%. These environmental conditions covered multiple heat-risk levels, enabling comprehensive evaluation of the developed monitoring and alert system.

3.1 Development of the IoT-Based Real-Time Heat Index Monitoring and Alert System

The first objective of this study was to develop an IoT-based real-time heat index monitoring and alert system for military training. The developed system integrated an SHT31 temperature and humidity sensor, an ESP32 microcontroller, Firebase Realtime Database, a web-based dashboard, and a LINE Official Account notification service.

Environmental data were continuously collected and transmitted to the cloud for real-time processing. The system calculated the heat index (HI) using the National Weather Service (NWS) algorithm based on the Rothfusz regression (Rothfusz, 1990) and classified heat-risk levels according to the Royal Thai Army Heat Flag criteria. The calculated results were displayed on both the OLED display and the web dashboard, while hazardous conditions automatically triggered warning notifications via the LINE Messaging API.

The developed prototype and its operational interfaces are shown in Figures 4 and 5.



Figure 4. Photograph of the developed IoT-based real-time heat index monitoring and alert system prototype for military training environments

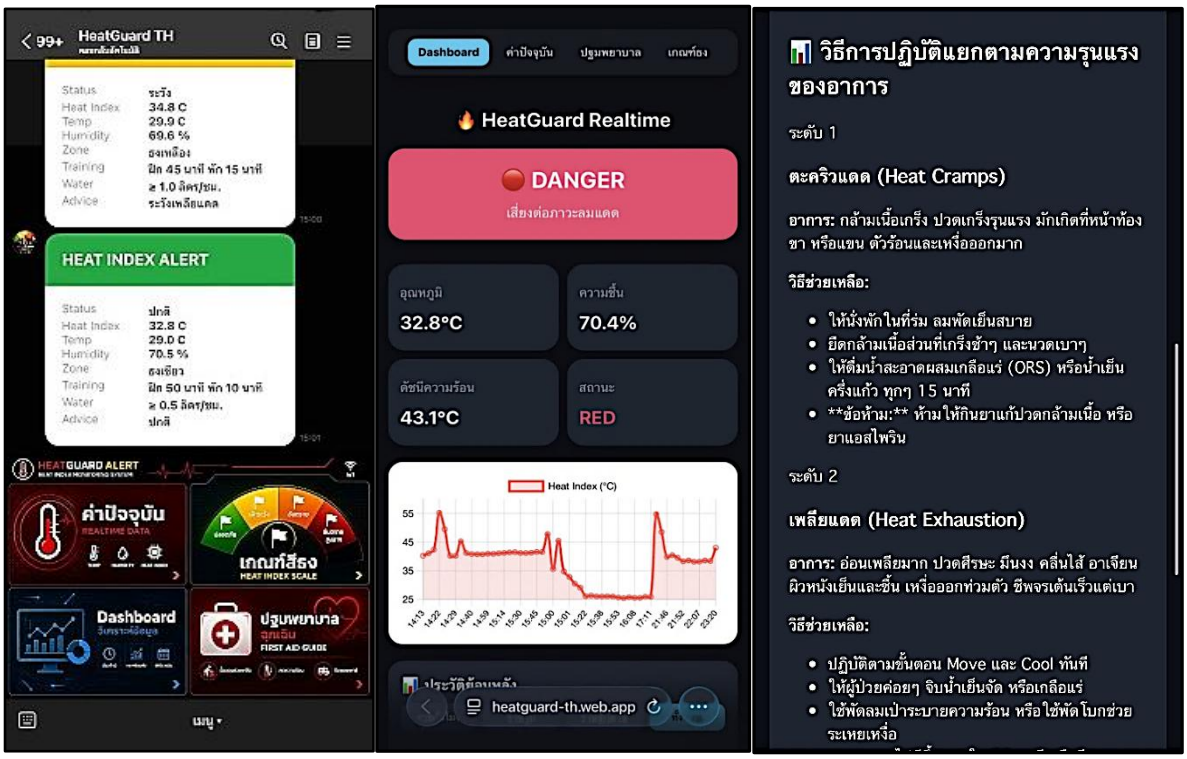


Figure 5. Screenshot of the developed real-time monitoring dashboard displaying environmental conditions and heat-risk levels

During field deployment, the platform operated continuously under actual military training conditions at the Signal Battalion, Directorate of Communications and Information Technology, Royal Thai Armed Forces Headquarters. The system demonstrated stable operation throughout the testing period and supported real-time heat-risk monitoring during military training activities.

3.2 Field Deployment and Real-Time System Operation

The developed IoT-based heat index monitoring system was deployed and evaluated under actual military training conditions over a 10-day field deployment conducted from 3 to 12 May 2026. Environmental monitoring was performed daily from 08:00 to 16:00, corresponding to the period of highest heat exposure during routine military training. Ambient temperature (°C) and relative humidity (%RH) were automatically recorded at 1-minute intervals, resulting in approximately 4,800 environmental observations. The collected data were processed in real time to calculate the heat index and synchronized with Firebase Realtime Database for continuous visualization through the web dashboard.

Whenever the calculated heat index reached or exceeded the predefined Heat Flag thresholds, the system automatically generated heat-risk notifications through the LINE Official Account. These notifications enabled instructors, medical personnel, and commanders to receive timely alerts and monitor current environmental conditions, Heat Flag statuses, and associated risk levels using both the web dashboard and mobile devices. The automated notification mechanism supported prompt decision-making for implementing appropriate heat-risk mitigation measures during military training. Overall, the field deployment results demonstrated that the proposed system operated continuously and reliably under real-world conditions. The integration of real-time environmental monitoring, automated heat index computation, cloud-based data synchronization, and instant LINE notifications provided effective operational support for heat-risk surveillance and safety management throughout the training period.

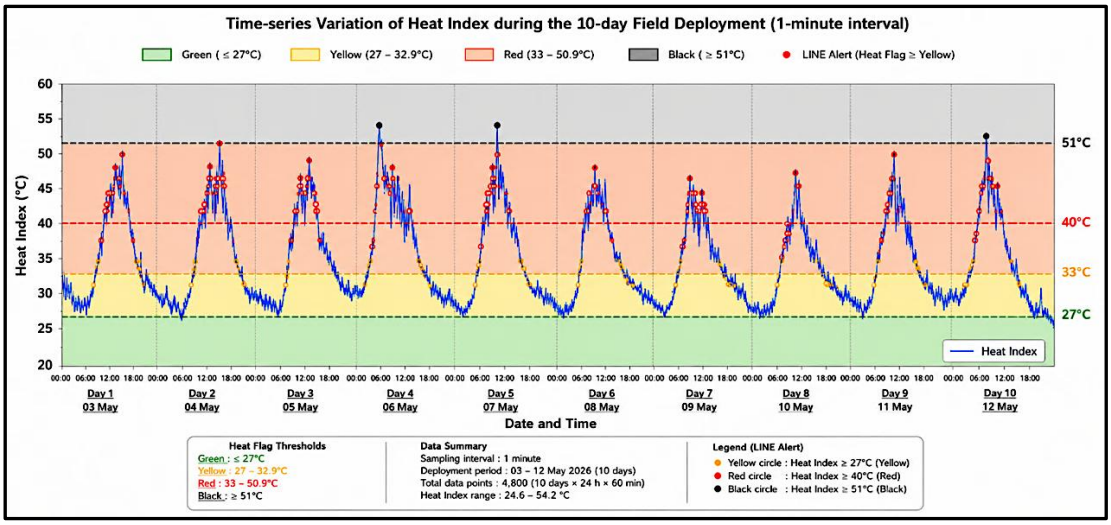


Figure 6. Time-series variation in the heat index during the 10-day field deployment. The system continuously monitored environmental conditions and synchronized data in real time, demonstrating stable operation under actual military training conditions

3.3 Technical Performance Evaluation of the Developed System

The second objective of this study was to evaluate the technical performance of the developed IoT-based heat index monitoring system in terms of sensor measurement agreement, heat-risk rule-based classification verification, alert latency, and data transmission reliability. The accuracy of the environmental sensing module was first evaluated by comparing measurements obtained from the SHT31 sensor with those from a calibrated digital thermo-hygrometer.

Sensor validation was performed by comparing simultaneous temperature and relative humidity readings from the SHT31 sensor with those from a calibrated digital thermo-hygrometer. The comparison results and measurement differences are presented in Table 5.

Table 5. Sensor validation results

Parameter	Reference Device	SHT31 Sensor	Difference	Interpretation
Temperature (°C)	32.7	32.8	0.1	Acceptable
Relative Humidity (%)	70.2	70.4	0.2	Acceptable

The SHT31 sensor produced measurements that closely matched those of the reference instrument, with differences of 0.1°C for temperature and 0.2% for relative humidity. These deviations were within acceptable limits for heat index computation and environmental monitoring.

Following sensor validation, representative temperature and relative-humidity values were used to demonstrate the heat index calculation and the resulting Heat Flag classification across the five risk levels, as shown in Table 6.

Table 6. Examples of heat index calculations and heat-risk classification results

Log ID	Temperature (°C)	Relative Humidity (%)	Heat Index (°C)	Heat Flag Level
L001	19.8	45.00	25.3	WHITE
L002	26.5	54.70	27.2	GREEN
L003	31.0	72.40	38.5	YELLOW
L004	32.8	70.40	43.1	RED
L005	34.9	78.30	54.8	BLACK

The calculated heat index increased as temperature and relative humidity rose, resulting in corresponding heat-risk classifications ranging from WHITE (safe conditions) to BLACK (extreme heat-risk conditions). These examples demonstrate the capability of the developed system to automatically compute the heat index and classify heat-risk levels according to the Royal Thai Army Heat Flag criteria. To evaluate the rule-based classification performance, 50 predefined test cases representing all Heat Flag categories were examined. In addition, boundary-value test cases were conducted to verify the correctness of the classification algorithm at decision thresholds.

To verify classification performance at critical decision points, boundary-value tests were conducted using heat index values immediately below, equal to, and immediately above the predefined thresholds. The expected classifications, system outputs, and verification results are presented in Table 7.

The boundary-value verification demonstrated that the developed system correctly classified all heat-risk levels at values immediately below, equal to, and immediately above each predefined Heat Flag threshold. These results indicate that the classification algorithm consistently handled decision boundaries without misclassification.

After boundary-value verification, the rule-based classification algorithm was evaluated using 50 predefined test cases distributed equally across the five Heat Flag levels. The number of correct classifications and the verification percentage for each level are summarized in Table 8.

Table 7. Boundary-value verification results for Heat Flag classification

Case	Heat Index (°C)	Expected Heat Flag	System Output	Result
B01	26.9	White	White	√
B02	27.0	Green	Green	√
B03	27.1	Green	Green	√
B04	32.9	Green	Green	√
B05	33.0	Yellow	Yellow	√
B06	33.1	Yellow	Yellow	√
B07	39.9	Yellow	Yellow	√
B08	40.0	Red	Red	√
B09	40.1	Red	Red	√
B10	51.0	Red	Red	√
B11	51.1	Black	Black	√

Table 8. Heat-risk rule-based classification verification results

Heat flag level	Number of test cases	Correctly classified test cases	Verification result (%)
WHITE	10	10	100
GREEN	10	10	100
YELLOW	10	10	100
RED	10	10	100
BLACK	10	10	100
Total	50	50	100

All 50 predefined test cases under controlled testing conditions were classified correctly, resulting in a rule-based classification correctness rate of 100.00%. This result verifies that the developed system correctly implemented the predefined Heat Flag classification rules for the tested cases.

The responsiveness of the notification module was assessed by measuring the elapsed time between environmental data acquisition and successful notification delivery through the LINE Official Account. The latency results are presented in Table 9. The measured alert latency ranged from 2.41 to 2.58 s, with an average response time of 2.49 s.

The reliability of wireless data transmission was assessed using 100 consecutive communication trials. The results are presented in Table 10.

All transmitted data were successfully synchronized with Firebase Realtime Database during the evaluation period, resulting in a data transmission success rate of 100.00%.

The responsiveness of the notification module was assessed across 10 repeated trials by measuring the elapsed time from environmental data acquisition to successful delivery through the LINE Official Account. The latency recorded in each trial and the average latency are presented in Table 9.

Data transmission reliability was evaluated through 100 consecutive attempts from the ESP32 microcontroller to Firebase Realtime Database. The numbers of successful and failed transmissions, along with the resulting success rate, are summarized in Table 10.

Table 9. Alert latency measurements.

Test trial	Alert latency (s)
1	2.41
2	2.53
3	2.46
4	2.58
5	2.47
6	2.50
7	2.51
8	2.48
9	2.52
10	2.44
Average Latency	**2.49**

Table 10. Data transmission success rate

Performance indicator	Value
Total transmission attempts (N_t)	100
Successful transmissions (N_s)	100
Failed transmissions	0
Success Rate (%)	100.00

3.4 User Satisfaction Evaluation

The third objective of this study was to evaluate user satisfaction with the developed IoT-based real-time heat index monitoring and alert system for supporting heat-risk management during military training.

A total of 40 participants, including training supervisors, drill instructors, assistant instructors, medical personnel, and military personnel representatives, participated in the user satisfaction evaluation. The assessment was conducted using a five-point Likert scale questionnaire covering four evaluation dimensions: (1) technical performance and hardware, (2) user interface and notification, (3) usefulness and practical applicability, and (4) system reliability and acceptance.

Overall user satisfaction was rated at the highest level, with a mean score of 4.71 and a standard deviation of 0.38, indicating a high level of acceptance of the developed system. The detailed evaluation results are presented in Table 11.

Among the four evaluation dimensions, User Interface and Notification received the highest satisfaction score ($\bar{x}$ = 4.90, S.D. = 0.24). Participants expressed high satisfaction with the LINE Flex Message notifications, the accessibility provided by the LINE Rich Menu, and the dashboard interface, which enabled rapid access to real-time environmental information and heat-risk status.

The Usefulness and Practical Applicability dimension achieved the second-highest score ($\bar{x}$ = 4.69, S.D. = 0.42). Respondents indicated that the developed system effectively supported real-time monitoring of environmental conditions, facilitated adherence to the military Heat Flag criteria, and was suitable for practical deployment during military training activities.

The Technical Performance and Hardware dimension received a satisfaction score of $\bar{x}$ = 4.65 (S.D. = 0.39), demonstrating high user satisfaction with the performance of the SHT31 sensor, wireless data transmission, and the hardware components used in the system.

The System Reliability and Acceptance dimension received a satisfaction score of $\bar{x}$ = 4.61 (S.D. = 0.46). Participants reported confidence in the accuracy of the displayed information, trusted the system to support operational decision-making, and expressed willingness to continue using the system in future military training operations.

Participants reported high levels of satisfaction across all evaluation dimensions. The developed IoT-based heat index monitoring and alert system was well accepted by end users and demonstrated high usability, practical applicability, and reliability for supporting heat-risk management during military training.

User satisfaction was evaluated among 40 participants across four dimensions covering technical performance, interface and notification, practical usefulness, and system reliability and acceptance. The mean, standard deviation, and interpretation for each dimension are presented in Table 11.

Table 11. User satisfaction by evaluation dimension (n = 40)

Evaluation Dimension	Mean ($\bar{X}$)	S.D.	Interpretation
Technical Performance and Hardware	4.65	0.39	Highest
User Interface and Notification	4.90	0.24	Highest
Usefulness and Practical Applicability	4.69	0.42	Highest
System Reliability and Acceptance	4.61	0.46	Highest
Overall Satisfaction	4.71	0.38	Highest

3.5 Summary of System Performance Evaluation

To provide an overall view of the system evaluation, the key performance indicators obtained from the technical performance assessment and user satisfaction evaluation are summarized in Table 12. The table consolidates the principal findings reported in the preceding sections without further interpretation.

The principal technical and user-satisfaction indicators and their interpretations are summarized in Table 12.

Table 12. Summary of the overall system performance evaluation results

Performance Metric	Result	Interpretation
Heat-risk rule-based classification verification	100.00%	All test cases correctly classified
Data Transmission Success Rate	100.00%	No communication failure observed
Average Alert Latency	2.49 s	Average notification response time
User Satisfaction	$\bar{x}$ = 4.71, S.D. = 0.38	Highest satisfaction level

4. Discussion

The findings demonstrate that the proposed IoT-based real-time heat index monitoring and alert system successfully achieved the research objectives by correctly implementing the predefined Heat Flag classification rules, maintaining reliable cloud communication, providing rapid alert delivery, and achieving high user acceptance. Unlike previous IoT-based environmental monitoring systems, the proposed platform integrates real-time heat index computation, Royal Thai Army Heat Flag classification, cloud synchronization, dashboard visualization, and instant LINE Official Account notifications into a unified framework for military training. This integration extends earlier studies that primarily focused on environmental monitoring or heat prediction without directly supporting operational decision-making (Buller et al., 2021; Popescu et al., 2024).

Rule-based classification verification demonstrated 100.00% correctness across 50 predefined test cases under controlled conditions. This result confirms that the classification algorithm correctly implemented the standardized Royal Thai Army Heat Flag criteria for the tested cases. Because the classification mechanism applies explicit threshold-based decision rules, the result should be interpreted as verification of rule implementation rather than as predictive classification accuracy. This finding is consistent with previous studies showing that rule-based environmental monitoring systems based on standardized operational criteria provide reliable and reproducible decision support for safety-critical applications (Royal Thai Army Medical Department, 2023; Buller et al., 2021).

Although the proposed system achieved 100% correctness in the predefined rule-based classification tests, this result should be interpreted as verification of rule implementation rather than evidence of predictive accuracy or universal performance across all operational environments. The generalizability of the findings may be limited because the evaluation was conducted using predefined Heat Flag criteria and controlled testing conditions. Further validation under diverse environmental conditions and multiple deployment sites is recommended.

The average alert latency of 2.49 seconds indicates that the developed system provided near real-time heat-risk notifications under the conditions of this study. This performance can be attributed to the integration of the ESP32 microcontroller, Firebase Realtime Database, and the LINE Messaging API, which enabled rapid data transmission, cloud synchronization, and notification delivery. Furthermore, the 100.00% data transmission success rate demonstrates the reliability of the proposed communication architecture during the evaluation period. These findings are consistent with previous studies reporting the effectiveness of cloud-based IoT monitoring systems for real-time environmental monitoring (Fahmideh et al., 2022).

The high user-satisfaction rating ($\bar{x}$ = 4.71, S.D. = 0.38) indicates strong user acceptance of the developed system. This positive outcome can be attributed to the system's real-time monitoring capability, intuitive web-based dashboard, and instant heat-risk notifications delivered through the LINE Official Account, which enabled users to access timely environmental information and make rapid decisions during military training. In addition, the use of the LINE Official Account, a widely adopted communication platform in Thailand, reduced the learning curve and facilitated user adoption. These findings are consistent with Narindrarangkura et al. (2024), who reported that familiar communication platforms and user-centered interface design contribute significantly to technology acceptance and user satisfaction.

Compared with previous IoT-based heat monitoring systems, the proposed platform integrates environmental sensing, automated heat index computation, military-specific heat-risk classification, cloud synchronization, dashboard visualization, and instant notification within a single operational platform. This integrated architecture supports timely decision-making during military training and can also be adapted to other outdoor occupations, such as construction, agriculture, disaster response, and industrial maintenance, where localized heat-risk monitoring is essential (Defense Health Agency, 2023; Patton & Hoyt, 2023).

This study has several limitations. The evaluation was conducted at a single military training unit, limiting the generalizability of the findings. Although the SHT31 sensor was validated against a reference digital thermo-hygrometer, future studies should use certified calibration equipment. Further research should also validate the system across multiple sites, incorporate multisensor environmental mapping and artificial intelligence-based prediction, and evaluate its long-term effectiveness in reducing heat-related illness.

Overall, the findings indicate that combining standardized military heat-risk criteria with IoT sensing, cloud communication, and real-time notification provides an effective decision-support platform for heat-risk management in military training and other outdoor occupational environments.

To position the contribution of the proposed system in relation to prior work, representative heat-monitoring and alert systems were compared in terms of heat index calculation, cloud support, real-time notification, military Heat Flag integration, field validation, and application context, as shown in Table 13.

Table 13. Comparison of representative IoT-based heat monitoring and alert systems

Study	Heat Index Calculation	Cloud Platform	Real-time Notification	Military Heat Flag	Field Validation	Application
Buller et al. (2021)	✗	✓	✓ (Mobile App)	✗	✗	Military heat injury prevention
Narindrarangkura et al. (2024)	✓	✓	✗	✗	✓	Military Health Surveillance
Considine et al. (2023)	✗	✓	✗	✗	✗	Heat alert prediction
This study	✓	✓	LINE Official Account	✓	✓	Military training

5. Conclusions and Recommendations

5.1 Conclusions

This study presented an IoT-based platform for real-time heat index monitoring and automated heat-risk alerts to support military training. Field evaluation showed that the platform consistently classified heat-risk levels, maintained reliable communication with the cloud database, delivered notifications with minimal delay, and received positive evaluations from users.

The findings suggest that integrating environmental sensing, cloud-based data synchronization, and rule-based heat-risk classification provides practical support for heat-risk management during outdoor military activities. Continuous monitoring enables commanders and training personnel to respond more promptly to changing environmental conditions and implement preventive measures before heat-related illnesses occur.

The successful deployment under operational conditions further indicates that the proposed platform can be applied beyond controlled laboratory settings. Its modular architecture also provides a foundation for adapting the system to other outdoor occupations where heat exposure is a significant safety concern, including construction, agriculture, emergency response, and industrial field operations.

5.2 Limitations and Future Research

This study was conducted at a single military training unit, and system performance was evaluated under the environmental conditions encountered at that site. Consequently, the findings should be interpreted within the context of the study setting, and additional validation in different operational environments would strengthen their generalizability.

The reported 100.00% classification result represents rule-based classification correctness for predefined Heat Flag test cases under controlled conditions, rather than predictive accuracy across all operational environments. Further validation under diverse climatic conditions, multiple deployment sites, and long-term field use is therefore required to improve the generalizability of the findings.

Future studies should examine system performance across multiple military training locations, seasons, and climatic conditions. Incorporating wearable physiological sensors, such as heart rate and body temperature monitoring, together with artificial intelligence for personalized heat-risk prediction, may further enhance early warning capabilities and support more informed decision-making during outdoor training. Long-term deployment studies could also provide valuable evidence regarding system reliability, user adoption, and operational sustainability.

6. References

Buller, M. J., Delves, S. K., Fogarty, A. L., & Veenstra, B. J. (2021). On the real-time prevention and monitoring of exertional heat illness in military personnel. Journal of Science and Medicine in Sport, 24(10), 975–981. https://doi.org/10.1016/j.jsams.2021.04.008

Buller, M. J., Delves, S. K., Fogarty, A. L., & Veenstra, B. J. (2021). On the real-time prevention and monitoring of exertional heat illness in military personnel. Journal of Science and Medicine in Sport, 24(10), 975–981. https://doi.org/10.1016/j.jsams.2021.04.008

Considine, E. M., Nethery, R. C., Wellenius, G. A., Dominici, F., & Tec, M. (2023). Optimizing heat alert issuance with reinforcement learning. arXiv. https://doi.org/10.48550/arXiv.2312.14196

Creswell, J. W., & Creswell, J. D. (2023). Research design: Qualitative, quantitative, and mixed methods approaches (6th ed.). SAGE Publications.

Defense Health Agency. (2023). Heat illness report. U.S. Department of Defense. https://health.mil/Reference-Center/Reports/2023/11/28/Heat-Illness-Report

Epstein, Y., Charkoudian, N., DeGroot, D. W., House, C., Ketko, I., Law, L. Y. L., Malgoyre, A., O'Connor, F., Tayari, O., & Lee, J. K. W. (2025). Exertional heat illness: International military-oriented lessons learned and best practices for prevention and management. Frontiers in Physiology, 16, 1456984. https://doi.org/10.3389/fphys. 2025.1456984

Fahmideh, M., Ahmad, A., Behnaz, A., Grundy, J., & Susilo, W. (2022). Software engineering for Internet of Things: The practitioners' perspective. IEEE Transactions on Software Engineering, 48(8), 2857–2878. https://doi.org/10.1109/TSE.2021.3070692

Gibb, K., Beckman, S., Vergara, X. P., Heinzerling, A., & Harrison, R. (2024). Extreme heat and occupational health risks. Annual Review of Public Health, 45, 315–335. https://doi.org/10.1146/annurev-publhealth-060222-034715

ISO/IEC. (2016). ISO/IEC 25023:2016 Systems and software engineering—Systems and software Quality Requirements and Evaluation (SQuaRE)—Measurement of system and software product quality. International Organization for Standardization.

Narindrarangkura, P., Hatthachote, P., Jongcherdchootrakul, K., Khiewchaum, R., & Rangsin, R. (2024). Using predictive analytics to improve surveillance of heat-related illness during military training. Journal of Southeast Asian Medical Research, 8, e189. https://doi.org/10.55374/jseamed.v8.189

Nutong, R., Mungthin, M., Hatthachote, P., Ukritchon, S., Imjaijit, W., Tengtrakulcharoen, P., Panichkul, S., Putwatana, P., Prapaipanich, W., & Rangsin, R. (2018). Personal risk factors associated with heat-related illness among new conscripts undergoing basic training in Thailand. PLoS ONE, 13(9), e0203428. https://doi.org/10.1371/journal.pone.0203428

Patton, E. M., & Doyle, M. W. (2024). Observed warming trends at U.S. Army basic combat training installations and implications for future recruit training. Military Medicine, 189, e1145–e1153. https://doi.org/10.1093/milmed/usad425

Patton, E. M., & Hoyt, C. L. (2023). Beating the heat: Military training and operations in the era of global climate change. Temperature, 10(4), 365–379. https://doi.org/10.1080/23328940.2023.2211795

Popescu, S. M., Mansoor, S., Wani, O. A., Kumar, S. S., Sharma, V., Sharma, A., Arya, V. M., Kirkham, M. B., Hou, D., Bolan, N., & Chung, Y. S. (2024). Artificial intelligence and IoT driven technologies for environmental pollution monitoring and management. Frontiers in Environmental Science, 12, 1336088. https://doi.org/10.3389/fenvs.2024.1336088

Pressman, R. S., & Maxim, B. R. (2020). Software engineering: A practitioner's approach (9th ed.). McGraw-Hill Education.

Rothfusz, L. P. (1990). The heat index "equation" (or, more than you ever wanted to know about heat index) (Technical Attachment SR 90-23). National Weather Service, Southern Region Headquarters.

Royal Thai Army Medical Department. (2023). Recommendations for prevention, surveillance, and first aid management of heat-related illnesses in military training. Royal Thai Army Medical Department.

การพัฒนากระบวนการวางแผนการขายและการดำเนินการเพื่อเพิ่มความแม่นยำการพยากรณ์และลดระดับสินค้าคงคลัง: กรณีศึกษาโรงงานแปรรูปสินค้าเกษตร

Development of a Sales and Operations Planning Process to Improve Forecast Accuracy and Reduce Inventory Level: A Case Study of an Agricultural Processing Plant

คลอเคลีย วจนะวิชากร[1] และ ธารชุดา พันธ์นิกุล[2]*

Klorklear Wajanawichakon[1] and Thanchuda Phannikul[2]*

[1]สาขาวิชาการจัดการโลจิสติกส์และซัพพลายเชน คณะเทคโนโลยีอุตสาหกรรม มหาวิทยาลัยราชภัฏอุบลราชธานี จังหวัดอุบลราชธานี

[2]ภาควิชาวิศวกรรมอุตสาหการ คณะวิศวกรรมศาสตร์ มหาวิทยาลัยอุบลราชธานี จังหวัดอุบลราชธานี

[1]Department of Logistics and Supply Chain Management, Faculty of Industrial Technology, Ubon Ratchathani Rajabhat University, Ubon Ratchathani Province

[2]Department of Industrial Engineering, Faculty of Engineering, Ubon Ratchathani University, Ubon Ratchathani Province

*Corresponding Author: thanchuda.p@ubu.ac.th

Received: April 16, 2026 **Revised:** July 7, 2026 **Accepted:** August 17, 2026

บทคัดย่อ

การวางแผนการขายและการดำเนินการ หรือ Sales and Operations Planning (S&OP) เป็นกลไกสำคัญที่เชื่อมโยงการตลาด การขาย การผลิต การจัดซื้อ และคลังสินค้า เพื่อให้สามารถตัดสินใจบนฐานข้อมูลชุดเดียวกัน ซึ่งงานวิจัยที่อธิบายขั้นตอนการพัฒนากระบวนการและผลลัพธ์เชิงปริมาณอย่างเป็นระบบยังมีอยู่อย่างจำกัด งานวิจัยนี้จึงมีวัตถุประสงค์เพื่อ (1) ศึกษาปัญหาของการขายและการดำเนินการในโรงงานแปรรูปสินค้าเกษตรขนาดกลางแห่งหนึ่งในภาคตะวันออกเฉียงเหนือของประเทศไทย ซึ่งมีผลิตภัณฑ์หลัก 5 รายการและมีรอบการผลิตแบบรายสัปดาห์ (2) พัฒนากระบวนการ S&OP ที่สอดคล้องกับบริบทขององค์กร และ (3) ประเมินผลของการนำกระบวนการดังกล่าวไปใช้ การวิจัยใช้เวลาเก็บข้อมูลเชิงปริมาณย้อนหลัง 6 เดือนก่อนการปรับปรุง (มกราคม-มิถุนายน) เปรียบเทียบกับ 6 เดือนหลังการปรับปรุง (กรกฎาคม-ธันวาคม) ของปีเดียวกัน ร่วมกับข้อมูลเชิงคุณภาพจากการสัมภาษณ์ผู้เกี่ยวข้องจำนวน 12 คน จากฝ่ายขาย ฝ่ายวางแผน ฝ่ายผลิต และฝ่ายคลังสินค้า จากนั้นออกแบบกระบวนการ S&OP รายเดือน 5 ขั้นตอน ประกอบด้วย การรวบรวมข้อมูล การทบทวนอุปสงค์ การทบทวนอุปทาน การประชุมก่อน S&OP และการประชุมผู้บริหารเพื่ออนุมัติแผนกลางขององค์กร ผลการวิเคราะห์เชิงคุณภาพชี้ว่าการขาดฐานข้อมูลร่วมและเวทีประสานงานข้ามสายงานเป็นสาเหตุหลักของความคลาดเคลื่อนในการวางแผน ผลการวิจัยเชิงปริมาณพบว่า หลังการนำกระบวนการ S&OP ไปใช้ ค่า MAPE ลดลงจากร้อยละ 28.40 เหลือร้อยละ 16.90 ระดับสินค้าคงคลังเฉลี่ยลดลงจาก 240 ตัน เหลือ 195 ตัน อัตราการส่งมอบตรงเวลาเพิ่มขึ้นจากร้อยละ 82.30 เป็น 93.10 จำนวนคำสั่งผลิตเร่งด่วนลดลงจาก 11 เหลือ 5 ครั้งต่อเดือน และค่า Forecast Bias ลดลงจากร้อยละ 12.60 เหลือ 4.20 โดยผลการทดสอบทางสถิติแบบ Paired t-test แบบ One-tailed (n = 6 คู่ข้อมูลรายเดือน) และการทดสอบยืนยันแบบ Wilcoxon signed-rank test ยืนยันว่าการเปลี่ยนแปลงของตัวชี้วัดทั้ง 5 ตัวมีนัยสำคัญทางสถิติที่ระดับ 0.05 ผลการวิจัยในกรณีศึกษานี้ชี้ให้เห็นว่า S&OP ช่วยสร้างความสอดคล้องระหว่างอุปสงค์และอุปทาน เพิ่มความแม่นยำของการพยากรณ์ ลดการถือครองสินค้าคงคลังเกินจำเป็น และสนับสนุนการตัดสินใจเชิงบูรณาการในองค์กร อย่างไรก็ตาม เนื่องจากเป็นการศึกษากรณีเดียวในระยะเวลา 6 เดือน ผลการวิจัยนี้จึงควรได้รับการตีความในขอบเขตของบริบทเฉพาะนี้ และควรมีการศึกษาเพิ่มเติมในหลายกรณีก่อนสรุปอ้างอิงในวงกว้าง

คำสำคัญ: การวางแผนการขายและการดำเนินการ, การพยากรณ์อุปสงค์, สินค้าคงคลัง, การวางแผนการผลิต, โลจิสติกส์

Abstract

Sales and Operations Planning (S&OP) is a critical managerial mechanism that integrates marketing, sales, production, procurement, and inventory functions through a shared information base. Despite its proven value, empirical studies on S&OP implementation in agricultural processing industries remain limited, particularly in Thailand and other emerging economies where raw material uncertainty and demand seasonality are pronounced. This study aimed to (1) investigate the problems and limitations of sales and operations planning in a medium-sized agricultural processing plant in northeastern Thailand, which produces five main product lines on a weekly production cycle, (2) develop an S&OP process appropriate to the organizational context, and (3) evaluate the effects of its implementation. A mixed-methods, applied case study approach was employed. Quantitative data were collected for six months before (January-June) and six months after (July-December) implementation, while qualitative data were obtained from semi-structured interviews with 12 personnel from sales, planning, production, and warehouse departments. The qualitative findings indicated that the absence of a shared database and a cross-functional coordination forum was the primary driver of planning inconsistency. A five-step monthly S&OP process was then developed, consisting of data gathering, demand review, supply review, pre-S&OP meeting, and executive S&OP meeting. The quantitative results showed that, after implementation, MAPE decreased from 28.40% to 16.90%, average inventory decreased from 240 tons to 195 tons, on-time delivery increased from 82.30% to 93.10%, the number of urgent production orders declined from 11 to 5 times per month, and forecast bias decreased from 12.60% to 4.20%. One-tailed paired t-test results (n = 6 paired months), corroborated by the Wilcoxon signed-rank test, confirmed that all five indicators changed significantly at the 0.05 level. Within the scope of this single case study, the findings suggest that S&OP can enhance demand-supply alignment, improve forecasting accuracy, reduce excess inventory, and strengthen integrated decision-making, particularly in agricultural processing plants facing uncertainty in raw material supply and market demand; broader generalization awaits multi-case confirmation.

Keywords: Sales and Operations Planning, Demand Forecasting, Inventory Management, Production Planning, Logistics

1. Introduction

In highly volatile and competitive business environments, manufacturing organizations must continuously align demand and supply in order to respond effectively to customer requirements while controlling operational costs. One of the major challenges faced by manufacturing firms is the inconsistency among sales plans, production plans, procurement activities, and inventory management due to fragmented decision-making across departments. In many organizations, each department uses different forecasting assumptions, data sources, and performance targets, resulting in inefficient coordination and operational instability (Thomé et al., 2012). In logistics and supply chain management, integrated planning mechanisms are considered essential for improving coordination among procurement, production, inventory management, and distribution activities (Rabop, 2013).

Sales and Operations Planning (S&OP) has emerged as an important managerial process that integrates sales, marketing, production, procurement, and logistics functions through a shared planning platform and cross-functional decision-making mechanism. The S&OP process enables organizations to balance demand and supply systematically by integrating forecasting, capacity planning, inventory management, and operational decision-making into a unified organizational plan. Wallace and Stahl (2008),

in one of the foundational practitioner-oriented accounts of S&OP, argued that the process functions effectively only when it combines a disciplined monthly cadence with a designated process owner and sustained executive participation; Ptak and Smith (2011) similarly emphasized that S&OP's value depends on tight integration between demand forecasting, material requirements planning, and production scheduling, rather than on any single component in isolation. Wagner et al. (2014) further argued that the organizational alignment created by structured planning processes, including clearly defined roles and shared performance metrics, is itself a critical driver of operational performance improvement, independent of the specific forecasting technique used. Accurate demand forecasting is particularly important because forecasting errors directly influence inventory levels, production planning, and customer service performance (Chase, 2013), and supports strategic alignment across organizational functions (Tuomikangas & Kaipia, 2014).

In the context of agricultural processing industries, planning and coordination challenges become even more critical due to the uncertainty of raw material availability, seasonality of agricultural products, fluctuating customer demand, and product shelf-life limitations. Agricultural processing plants frequently experience problems related to inaccurate forecasting, excessive inventory holding, urgent production scheduling, and delayed deliveries. These issues negatively affect operational efficiency, inventory costs, and customer satisfaction. Therefore, organizations operating in agro-industrial environments require an integrated planning mechanism capable of improving coordination between demand and supply under uncertain conditions. These characteristics distinguish agricultural processing from general discrete manufacturing in three important ways. First, raw material supply in agro-industries is governed by harvest cycles and weather conditions rather than purchase lead times, making the supply side of the S&OP balance inherently less controllable. Second, many agricultural products carry strict shelf-life constraints, which limit the feasibility of building safety stock as a buffer against forecast error, a strategy that is more readily available in general manufacturing. Third, demand for processed agricultural products is frequently linked to seasonal consumption patterns and agricultural commodity cycles, introducing a layer of demand variability that compounds, rather than substitutes for, ordinary market uncertainty. These distinctive characteristics mean that S&OP mechanisms validated in general manufacturing settings cannot be assumed to transfer directly to agricultural processing without contextual adaptation, which is a central motivation for the present study as shown in Table 1.

Table 1. Summarizes how the present study addresses three gaps identified in the existing S&OP literature, situating its contribution relative to prior research

Previous Studies	Research Gap	This Study
Concentrated in large-scale, general manufacturing in developed economies (Thomé et al., 2012; Tuomikangas & Kaipia, 2014)	Limited empirical evidence from agro-industrial contexts in emerging economies	Agricultural processing plant in northeastern Thailand

Table 1. (Continued)

Previous Studies	Research Gap	This Study
Report a single or narrow KPI, mainly forecast accuracy (Goh & Eldridge, 2019)	Limited evidence on how S&OP components jointly affect a fuller set of operational outcomes	Five linked KPIs: MAPE, inventory level, OTD, expedited orders, forecast bias
Predominantly quantitative or predominantly qualitative, rarely combined (Kreuter et al., 2022)	Few studies explain the mechanisms behind quantitative improvement using organizational evidence	Mixed-methods design: KPI tracking integrated with 12 informant interviews

Previous studies have extensively examined the role of S&OP in improving organizational performance. Thomé et al. (2012) synthesized that S&OP serves as a strategic coordination mechanism linking demand and supply functions across the organization. Tuomikangas and Kaipia (2014) further emphasized that S&OP contributes significantly to organizational integration, forecasting improvement, and operational responsiveness. More recent studies have highlighted the importance of information processing capability, cross-functional collaboration, and adaptability in S&OP implementation. Goh and Eldridge (2019) argued that organizational performance improvement depends not only on formal planning structures but also on effective coordination mechanisms and information alignment. Similarly, Kreuter et al. (2022) identified S&OP as a context-dependent capability requiring adaptation to specific industrial environments and organizational conditions.

Recent literature also emphasizes the increasing role of digital technologies, predictive analytics, and data integration in supporting S&OP effectiveness. AI-supported forecasting and data-driven planning systems have been reported to improve responsiveness and operational efficiency in complex supply chains (Kreuter et al., 2022). A recent systematic review by Walter et al. (2025) similarly found that artificial intelligence applications in demand planning are still concentrated in large, data-rich manufacturing environments, with limited evidence from smaller agro-industrial operations where digital infrastructure and historical data systems are less mature. In addition, Wu and Møller (2024) proposed that S&OP effectiveness depends on maintaining alignment between internal planning processes and external environmental uncertainty. These studies collectively indicate that S&OP is evolving from a traditional planning routine into an integrated and adaptive organizational capability. It is important to note that the digital and AI-supported S&OP literature cited above represents the broader trajectory of the field rather than the specific intervention evaluated in this study: the case-study factory's planning capability and data infrastructure corresponded to a foundational, meeting-based S&OP process built on shared spreadsheets and structured forms, not an AI-supported or fully digitalized system. This study therefore evaluates the foundational organizational mechanism that typically precedes digital S&OP adoption, a stage that remains under-documented in the literature despite being the practical starting point for most small and medium-sized agricultural processors in emerging economies (Kreuter et al., 2022; Walter et al., 2025).

Within the Thai context specifically, related work on demand forecasting and inventory management in food and agricultural product businesses remains scarce relative to general manufacturing. Tabporn et al. (2018), in a study of sales forecasting and inventory management for a frozen seafood product line, demonstrated that systematic time-series forecasting combined with economic order quantity techniques could materially reduce inventory holding in a Thai food-processing setting, illustrating the

practical relevance of structured forecasting discipline in this sector. Similarly, Chuchotthaworn (2020) showed that combining demand forecasting with optimal order-quantity determination reduced packaging inventory costs in a Thai agricultural product processing company. However, both studies, like most local work in this area, addressed forecasting and inventory control as isolated functions rather than as components of an integrated, cross-functional S&OP process. This further supports the research gap motivating the present study: namely, the need for an integrated, mixed-methods account of how a complete S&OP cycle, rather than forecasting alone, affects operational performance in a Thai agricultural processing context.

Despite these developments, several important research gaps remain. First, empirical studies focusing on S&OP implementation in agricultural processing industries remain limited, particularly in emerging economies and agro-industrial contexts where uncertainty in raw materials and demand variability are highly significant. Existing studies are largely concentrated in large-scale manufacturing sectors and developed-country environments. Second, although previous studies have reported positive relationships between S&OP implementation and organizational performance, limited empirical evidence explains how specific S&OP process components contribute to operational performance indicators such as forecast accuracy, inventory reduction, on-time delivery, and production stability. Third, few studies integrate both quantitative performance measurement and qualitative organizational analysis within a unified case-study framework to explain the mechanisms underlying operational improvements.

To address these gaps, this study aims to develop and evaluate an Sales and Operations Planning (S&OP) process for an agricultural processing plant. Specifically, the objectives of this research are: (1) to investigate the problems and limitations of the existing planning system in an agricultural processing factory, (2) to develop an S&OP process appropriate for the organizational context, and (3) to evaluate the operational outcomes of the implemented process using key performance indicators including forecast accuracy, inventory levels, on-time delivery rate, expedited production orders, and forecast bias.

Based on these objectives, five research hypotheses (H1-H5) were formulated, predicting a statistically significant improvement after S&OP implementation in the forecast accuracy (MAPE), the average inventory level, the On-Time Delivery rate, the number of expedited production orders, and forecast bias, respectively. Specifically, H1 predicts lower MAPE, H2 lower average inventory, H3 higher on-time delivery, H4 fewer expedited production orders, and H5 lower forecast bias after implementation. The inclusion of H4 and H5 reflects an established line of literature linking poor forecast quality to costly downstream symptoms: Chase (2013) demonstrated that forecast error is a direct driver of expediting and emergency production, while Wallace and Stahl (2008) identified persistent forecast bias as a recurring symptom of unresolved demand-supply misalignment that a properly functioning S&OP cycle is designed to correct. H4 and H5 were therefore included as operational consequences of improved forecasting discipline, rather than as independent constructs requiring separate theoretical grounding.

This study contributes to the literature by providing empirical evidence of S&OP implementation in an agricultural processing and by integrating quantitative and qualitative analyses to explain how cross-functional planning mechanisms improve operational performance under conditions of uncertainty.

2. Materials and Methods

2.1 Research Framework

The research framework defines "S&OP process development" as the independent variable, which consists of four main components: (1) Single Data Source, (2) Systematic Demand Forecasting, (3) Supply Constraint Review, and (4) Cross-Functional Decision Meeting. The dependent variables consist of the five operational indicators corresponding to the five research hypotheses: (1) forecast accuracy, measured by MAPE, (2) average inventory level, (3) On-Time Delivery rate, (4) the number of expedited production orders per month, and (5) Forecast Bias. It is expected that the developed S&OP process will lead to tangible improvement in all five indicators, as illustrated in Figure 1.



Figure 1. Conceptual Framework

2.2 Research Design

This research is an applied case study design, focusing on the development and evaluation of the Sales and Operations Planning (S&OP) process in the context of an agricultural processing factory in northeastern Thailand. The choice of a case study approach is appropriate for understanding the dimensions of decision-making processes, cross-functional coordination, and operational outcomes in the real organizational context.

The research employs a mixed-methods approach, combining quantitative and qualitative data. Specifically, quantitative data are used to evaluate the implementation of the S&OP process through key performance indicators such as forecast accuracy, inventory levels, and on-time delivery rates. Qualitative data are used to analyze existing system issues, diagnose the causes of demand-supply discrepancies, and explain the mechanisms by which the developed process impacts the organization's operations.

2.3 Case study unit and organizational context

The case study was an agricultural processing factory with a production plan scheduled on a weekly and monthly basis. The factory had five main products and faces operational issues related to inaccurate sales forecasts, high inventory holding, and continuous delays in product delivery during certain periods. The criteria used for selecting case studies are:

To provide sufficient context for assessing the transferability of the findings, the case organization is a medium-sized agricultural processing plant employing approximately 110 production and administrative staff, with a normal monthly production capacity of approximately 260-280 tons across its five product lines. Prior to the study, demand for each product was forecast using simple moving averages or, in several months, the sales department's unaided judgment, with no formal cross-functional review of the resulting plan. As part of the S&OP process developed in this study, the demand review step introduced a structured forecasting approach combining a three-month weighted moving average of historical sales

with a qualitative adjustment discussed and agreed upon during the monthly Demand Review meeting, replacing the prior practice of unadjusted judgmental forecasting by the sales department alone. The pre-implementation period spanned January-June and the post-implementation period spanned July-December of the same calendar year. Because these two windows fall in different halves of the annual agricultural cycle, the comparison is not free of seasonal influence (see Section 5 for this limitation).

1) It is an organization that has sales, production, and inventory planning interconnected at the operational level.

2) There is historical data that can be used for analysis before and after the improvement.

3) Executives and operators are ready to provide information and participate in the improvement process.

4) The organization has clear issues suitable for the application of S&OP, such as urgent production, fragmented planning, and the lack of shared metrics.

2.4 Population, informants, and analytical units

This research uses both qualitative informants and quantitative units of analysis.

2.4.1 Qualitative informant

A total of 12 key informants were selected through purposive sampling, choosing individuals who have direct roles in planning, decision-making, and plan implementation. There are two of each: sales manager, production planners, warehouse staff, middle management and four Production supervisors.

The informants in this group were selected based on three criteria: they have at least one year of planning-related experience, they are responsible for using or preparing data for decision-making, and they can clearly reflect the problems and limitations of the existing system.

The number of informants was considered appropriate for qualitative case study research because data saturation was achieved during the interview process. Recurrent themes and operational issues began to converge after the tenth interview, and no substantial new information emerged from the final interviews. The selected participants also represented all major functions involved in the S&OP process, including sales, production planning, operations, warehousing, and middle management, thereby ensuring cross-functional perspectives and analytical completeness.

2.4.2 Quantitative Analysis Unit

The main unit of analysis for quantitative data is "monthly data on planning processes and performance outcomes," considering two time periods, namely

1) The period before implementing the S&OP process

2) The period after implementing the S&OP process for 6 months

2.5 Data Sources

The sources of information used in the research were divided into two categories: primary data and secondary data. Primary data came from 12 key informants, stakeholders, observation the planning process and cross-functional meetings and the indicators used in S&OP. Secondary data consisted of actual sales data for the past 12 months, historical and post-improvement demand forecast data, production plan data and actual production results, customer delivery information, record urgent production orders and emergency plan adjustments and internal documents, such as meeting schedules, monthly reports, and related action plans.

2.6 Research tools

The tools used in the research consist of three main sets as follows.

2.6.1 Semi-structured interview

Used to collect information about the current state of planning, issues in inter-departmental coordination, causes of discrepancies, and suggestions for improving the S&OP process.

2.6.2 S&OP meeting form

Used as a tool to support the collection and presentation of information in each monthly meeting round, including performance results of the previous month, estimation of next month's demand, production capacity, raw materials and labor constraints and Issues to decide and management options.

2.6.3 Performance Indicator Record Form

Used for recording monthly data of key performance indicators, including MAPE, Forecast Bias, average inventory level, on-time delivery rate, and number of expedited production orders, for comparison before and after implementation.

2.7 Quality inspection of research instruments

The quality of research instruments was evaluated through content validity assessment, pilot testing, and data triangulation.

First, the interview protocol and S&OP meeting forms were reviewed by three experts in logistics, operations management, and supply chain planning to assess content relevance, clarity, and consistency with the research objectives. The Index of Item-Objective Congruence (IOC) values ranged between 0.80 and 1.00, indicating acceptable content validity.

Second, pilot interviews were conducted with two representatives from the case organization to evaluate question clarity, sequence, and practical applicability. Minor revisions were subsequently made to improve wording and reduce ambiguity.

Third, methodological triangulation was employed to enhance reliability and credibility. Information obtained from interviews was cross validated with organizational documents, historical operational records, production reports, and meeting observations. This triangulation process helped reduce potential bias and improve the trustworthiness of the findings.

2.8 Data collection methods

Data collection proceeded in three phases: (1) current situation study — collecting 12 months of historical data and conducting interviews to diagnose planning system issues; (2) S&OP process design — synthesizing Phase 1 findings into a five-step monthly process and validating with stakeholders; and (3) pilot implementation and monitoring — running the S&OP process for six months with continuous KPI tracking and event recording.

2.9 Quantitative data analysis

Quantitative data analysis uses descriptive statistics and comparisons before and after the improvement as follows.

2.9.1 Descriptive statistics

Use the average, percentage, standard deviation, and rate of change to describe the characteristics of the indicators.

2.9.2 Calculation of key performance indicators

The main indicators consist of Mean Absolute Percentage Error (MAPE), Forecast Bias, Percentage decrease in inventory and On-Time Delivery (OTD), calculated using the standard formulas below:

$$\text{MAPE} = \frac{1}{n}\sum_{t=1}^{n}\left|\frac{A_t - F_t}{A_t}\right| \times 100\% \quad (1)$$

$$\text{Forecast Bias} = \frac{\sum_{t=1}^{n}(A_t - F_t)}{\sum_{t=1}^{n} A_t} \times 100\% \quad (2)$$

$$\text{OTD Rate} = \frac{\text{Number of On-Time Deliveries}}{\text{Total Number of Deliveries}} \times 100\% \quad (3)$$

where A_t and F_t denote the actual and forecast demand in month t, respectively, and n is the number of months in the evaluation period. A positive Forecast Bias indicates a tendency toward over-forecasting and a negative value indicates under-forecasting.

Before selecting the statistical test method, the normality of paired differences was examined using the Shapiro-Wilk test for each indicator (n = 6 pairs). The results are presented in Table 6. Since all variables yielded W-statistics greater than the critical value and p-values exceeding 0.05, the normality assumption was not rejected. Therefore, the paired t-test was selected as the primary hypothesis testing method, with the Wilcoxon signed-rank test applied as a non-parametric verification. It should be noted that, with only six paired observations, the Shapiro-Wilk test has limited statistical power to detect departures from normality; the non-rejection of normality at this sample size should therefore be interpreted as inconclusive rather than as strong confirmatory evidence, which is precisely why the Wilcoxon signed-rank test was retained as a non-parametric cross-check rather than treated as a redundant formality. In addition to significance testing, Cohen's d was calculated for each paired comparison to quantify the magnitude of improvement independently of sample size, since statistical significance alone does not indicate the practical size of an effect.

2.9.3 Comparison before and after implementing S&OP

Compare the monthly indicators before and after the improvement during the corresponding periods. If the data was normally distributed, use the paired t-test statistics. However, if the data did not meet the normal distribution assumption, use the Wilcoxon signed-rank test statistic to test the difference between the values before and after the improvement. Because the research hypotheses were directional and explicitly predicted performance improvement after S&OP implementation, one-tailed statistical tests were considered appropriate for hypothesis testing. Nevertheless, non-parametric verification using the Wilcoxon signed-rank test was additionally conducted to ensure the robustness of the findings under the small-sample condition.

2.9.4 Statistical significance level

Set the statistical significance level at 0.05. Although the number of paired observations was relatively limited (n = 6 months before and after implementation), the paired analysis approach was considered appropriate because the study focused on repeated operational measurements within the same organizational system under comparable planning conditions. In addition, assumption testing was performed

prior to hypothesis testing, and both parametric and non-parametric methods were applied to improve statistical robustness and analytical reliability.

2.10 Qualitative data analysis

Interview and observation data were analyzed using content analysis: transcription, holistic review, thematic coding (forecasting issues, interdepartmental coordination, decision-making gaps), category grouping, and synthesis to explain the mechanisms underlying the quantitative results.

2.11 Research ethics and data confidentiality

This research prioritized the confidentiality of the case study organization's data. The researcher did not present the organization's name, individual names, or commercial information that could impact business competition. The presentation of research results used aggregated data solely for academic purposes and system development. All informants were informed of the research objectives and gave their consent before the interview.

3. Results

3.1 Current condition and issues before the improvement

The analysis of the current situation identified four main issues: (1) Sales forecasting relies primarily on the sales department's discretion without verifying historical data, (2) There are no systematic joint meetings between the sales and production departments, (3) There is a rush to produce when sudden orders are received, averaging 11 times per month, and (4) There are no shared performance indicators used by all parties to track results, leading to conflicts in decision-making between sales targets and cost control. Details are shown in Table 2.

Table 2. Summary of current problems and their impacts on operations

No.	Identified Problems	Key Causes	Impacts
1	Inaccurate sales forecasting	Reliance on personal experience without validation	Production does not align with demand
2	Lack of a cross-functional coordination platform	Sales, production, and warehouse work separately	Over production occurs and communication is misaligned
3	Inventory levels exceeding targets	Excessive planning buffers due to uncertainty	Inventory holding costs increase
4	Delayed deliveries during certain periods	Production capacity does not align with actual order demand	Customer satisfaction decreases

To substantiate the four issues summarized in Table 2 with first-hand organizational evidence, Table 3 presents the coded themes derived from content analysis of the 12 informant interviews, together with illustrative quotations for each theme.

Informants attributed to the absence of shared metrics in the fourth theme is consistent with the quantitative pattern reported in Section 3.3: because sales, production, and warehouse staff were each evaluated against different, unreconciled targets prior to the intervention, none of them had an incentive to flag a forecast or inventory problem before it escalated into an expedited order. This qualitative account helps explain, rather than merely describe, why the introduction of shared KPIs and a joint monthly review subsequently produced consistent month-on-month improvement across all five indicators.

Table 3. Coded qualitative themes from informant Interviews (n = 12)

Theme	Informants Citing	Illustrative Quotation
Forecasting by unaided judgment	9 of 12	*"We mostly go by feel and by what the customer tells us on the phone. We rarely pull up last year's numbers before sending the forecast to the factory." (Production Planner, Informant 4)*
Absence of cross-functional forum	11 of 12	*"Sales and the production floor barely talk except when something has already gone wrong. By then it's too late to plan properly." (Production Supervisor, Informant 7)*
Reactive expediting culture	8 of 12	*"Almost every week there's a rush order that throws off the whole production schedule. We just accept it as normal now." (Warehouse Staff, Informant 10)*
Conflicting goals, no shared metrics	10 of 12	*"Sales are measured in revenue, we are measured in cost. Nobody is measured on whether the two plans actually match." (Middle Management, Informant 12)*

3.2 The developed S&OP process

The developed S&OP process consists of 5 monthly steps: (1) Data Gathering - collecting actual sales, outstanding orders, inventory status, and production capacity; (2) Demand Review - reviewing market trends and preparing demand forecasts; (3) Supply Review - assessing constraints in production capacity, raw materials, and labor; (4) Pre-S&OP Meeting - comparing plan alternatives and identifying decision points; and (5) Executive S&OP Meeting-approving the mid-month plan. The process structure is shown in Table 4.

Table 4. Developed Structure of the Monthly S&OP Meeting

Process	Person in Charge	Inputs	Expected Outcomes
1. Data Gathering	Planner	Actual sales, orders, and inventory	Single source of data
2. Demand Review	Sales team	Market data, promotions, and seasonality	Monthly demand plan
3. Supply Review	Production/ Purchasing	Production Capacity, raw materials, and labor	Supply plan alternatives
4. Pre-S&OP	Department manager	Demand–supply gaps	Consensus plan proposal
5. Executive S&OP	Executives	Alternative plans and cost implications	Approved master plan

3.3 Results of the KPI assessment after using S&OP

The evaluation results of the key performance indicators after using S&OP for 6 months show that forecasting accuracy has continuously improved, inventory levels have decreased, and on-time delivery rates have increased. This is because all parties have shared information and can make better advance planning decisions. The overall results are shown in Table 5, and the monthly trends are shown in Fig 2.

Table 5. Comparison of Performance Indicators Before and After S&OP Implementation

Indicators	Before	After	Differences	Direction
MAPE (%)	28.40	16.90	-11.50 points	↓ (improved)
Average Inventory (tons)	240	195	-18.75%	↓ (improved)
On-Time Delivery Rate (%)	82.30	93.10	+10.80 points	↑ (improved)
Expedited Production Orders (times/month)	11	5	-54.55%	↓ (improved)
Forecast Bias (%)	12.60	4.20	-8.40 points	↓ (improved)

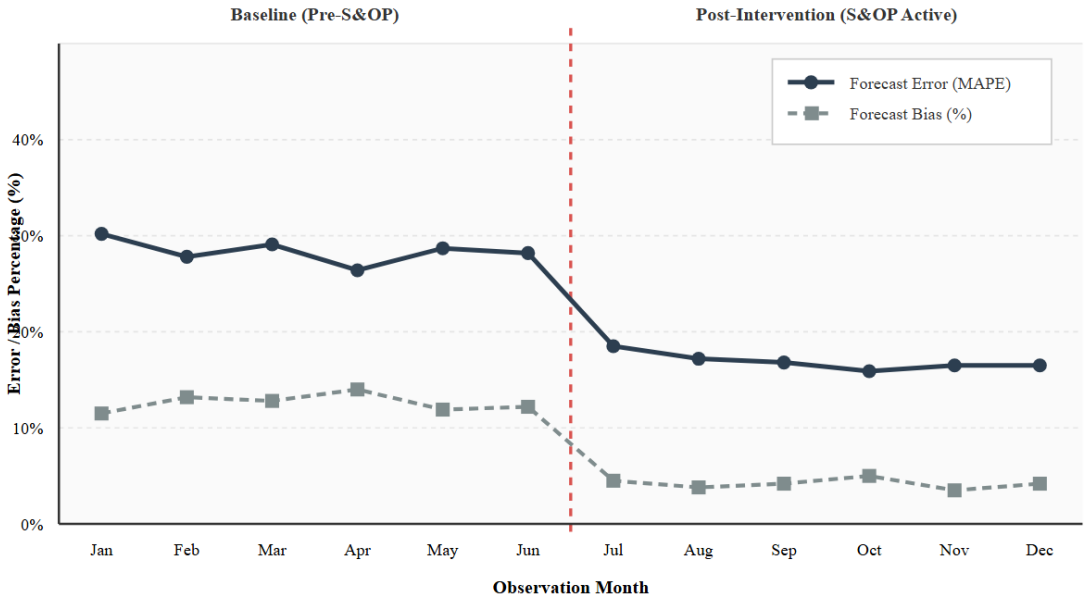


Figure 2. Monthly trend comparison of Mean Absolute Percentage Error (MAPE) before and after S&OP

From Table 5 and Figure 2, it can be seen that the trend in the results has improved in every indicator, especially the MAPE value, which has decreased by more than 10 points each month. The MAPE values after S&OP implementation were consistently lower across all six months compared with the pre-implementation period.

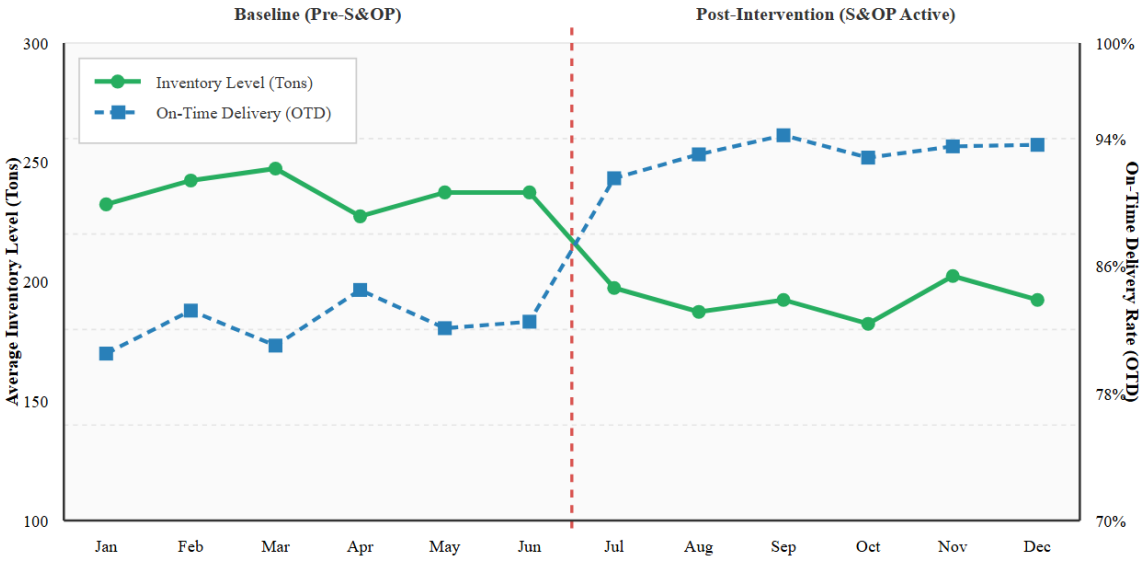


Figure 3. Monthly operational trajectories of Inventory Level, On-Time Delivery (OTD), Expedited Orders, and Forecast Bias.

From Figures 2 and 3, the paired monthly performance data over the six months before and after the implementation of the S&OP process shows that during the months when inventory decreased, the organization was still able to maintain a consistently high on-time delivery (OTD) rate. Additionally, the reduction in the number of monthly expedited production orders aligns with the steadily decreasing forecast bias. The monthly paired data showed consistent directional changes across all operational indicators following S&OP implementation, with no individual month showing a reversal in any of the five indicators. This uniform pattern should be read as a feature of this particular six-month trial rather than a guarantee of similar results elsewhere; possible seasonal confounding is discussed in Section 5.

Examining the monthly trend in Figure 2 more closely, the rate of MAPE improvement was not uniform: the largest month-on-month gain occurred between the first and third months after implementation (a drop of approximately 13.4 percentage points), coinciding with the period in which the Demand Review step was still being adjusted following the first two Pre-S&OP meetings, whereas the gain stabilized in the later months once the weighted moving-average forecast described in Section 2.3 had been consistently applied. This trajectory suggests that the early reduction in forecast error was driven primarily by the introduction of a structured forecasting method and the Demand Review step, while the more modest, stable gains in the later months reflect the Supply Review and Pre-S&OP Meeting steps absorbing the residual mismatch between demand estimates and production capacity. The parallel decline in expedited production orders (Figures 2 and 3) over the same months is therefore best interpreted not as an independent improvement but as a downstream consequence of the upstream gain in forecast accuracy: as the demand estimate used to trigger production runs became more reliable, the number of occasions on which production had to deviate from the plan to accommodate an unanticipated order fell correspondingly. This sequencing is consistent with the mechanism proposed in the conceptual framework (Figure 1), in which Systematic Demand Forecasting and Supply Constraint Review jointly, rather than independently, determine the downstream operational indicators.

3.4 Results of the statistical hypothesis test

To confirm that the changes in the indicators after implementing the Sales and Operations Planning (S&OP) process were not coincidental, the researchers conducted a paired comparison of the pre- and post-improvement data on key indicators according to the research hypothesis, including MAPE, average inventory level, On-Time Delivery (OTD) rate, average number of expedited production orders per month, and Forecast Bias, with a statistical significance level set at 0.05.

Prior to hypothesis testing, the normality of paired differences was assessed using the Shapiro-Wilk test. As reported in Table 6, all five variables yielded W-statistics above the critical value ($W_{critical} \approx 0.788$ for n = 6, $\alpha = 0.05$), with p-values ranging from 0.113 to 0.854, indicating that the normality assumption was not violated for any variable. The paired t-test was therefore applied as the primary statistical method. Detailed descriptive statistics of paired differences ($\overline{D}$, SD, and SE) and test results are reported in Table 7.

As a supplementary verification, the Wilcoxon signed-rank test was applied to all five variables. The results are presented in Table 7. All five variables produced a rank-sum statistic of T = 0 (W+ = 21, W– = 0) with a two-tailed p-value of 0.031. The uniform outcome is attributable to the consistent directionality of all six-monthly paired differences across every variable. That is no month showed a reversal in any indicator after S&OP implementation. Under this condition, with n = 6, the Wilcoxon statistic reaches its minimum possible value of T = 0, corresponding to the minimum attainable p-value of 0.031 (= $2/2^6$). These results are directionally consistent with the paired t-test findings. It is important to clarify that this agreement means only that no month reversed direction for any indicator; it does not, by itself, establish the statistical robustness of the underlying effect, since the Wilcoxon test is mechanically constrained to its minimum attainable p-value whenever a small sample shows no reversals. The two tests should be read as agreeing on the direction and statistical significance of the change.

Table 6. Results of the normality test of paired performance indicators using the Shapiro-Wilk method

Hyp.	Variable	Differences (D)	W-statistic	p-value	Result
H1	MAPE (%)	11.7, 10.6, 12.3, 10.5, 12.2, 11.7	0.8546	0.1713	Normal ($p > 0.05$)
H2	Inventory (tons)	35, 55, 55, 45, 35, 45	0.8532	0.1670	Normal ($p > 0.05$)
H3	OTD Rate (%)	11.0, 9.8, 13.2, 8.3, 11.4, 11.1	0.9646	0.8540	Normal ($p > 0.05$)
H4	Expedited Orders	4, 8, 8, 4, 7, 5	0.8326	0.1130	Normal ($p > 0.05$)
H5	Forecast Bias (%)	7.0, 9.4, 8.6, 9.0, 8.4, 8.0	0.9634	0.8454	Normal ($p > 0.05$)

Note: Shapiro-Wilk critical value for n = 6 at $\alpha = 0.05$ is approximately W = 0.788. All variables exceed this threshold

In addition to statistical significance, effect sizes (Cohen's d, calculated as the mean paired difference divided by the standard deviation of the differences) were computed to indicate the practical magnitude of each improvement, since p-values alone do not convey the size of an effect, particularly at a small sample size. The results, presented in Table 7, indicate very large effect sizes (d > 3.0) for all five indicators, consistent with the descriptive pattern that every monthly pair moved in the improving direction with no reversals.

4. Discussion

The research findings indicate that the implementation of the Sales and Operations Planning (S&OP) process in the case study factory coincided with enhanced coordination between the sales, planning, production, and warehouse departments. Previously, decisions relied on fragmented data and departmental discretion, but the interview evidence summarized in Table 3 suggests that this fragmentation persisted specifically because no informant, regardless of department, was evaluated against a metric that rewarded cross-functional accuracy; as one middle manager observed, "nobody is measured on whether the two plans actually match." After implementation, informants reported using shared data within a structured review cycle and meetings. These results are consistent with the concept proposed by Wallace and Stahl (2008), who argued that S&OP is effective when an organization has a clear joint decision-making process, a systematic agenda, and continuous executive support, and with Ptak and Smith (2011), who emphasized that effective coordination between forecasting, material planning, and production scheduling is essential for reducing operational instability. Because this study employed a single-case design without a control group, these findings should be read as evidence consistent with the mechanisms proposed in the literature rather than as definitive proof that S&OP, in isolation, caused the observed improvements.

In terms of forecasting accuracy, the research findings revealed that the MAPE value decreased from 28.40% to 16.90%, and statistical tests confirmed that this difference is statistically significant. This pattern is consistent with the introduction of the demand review process, the use of historical sales data, and inter-departmental information exchange, which together are the most plausible drivers of the improvement, although other contributing factors, such as a general learning effect among planning staff over the six-month trial, cannot be fully ruled out given the single-case design.

For the indicators of average inventory levels, on-time delivery rates, the number of expedited production orders, and Forecast Bias, this research found that all variables changed in a positive direction. When tested with paired monthly data, these differences were all statistically significant. This pattern is consistent with the qualitative account in Table 3, in which informants linked the prior reactive expediting culture directly to the absence of validated forecasts; once a shared, validated demand estimate was in place, the stated rationale for ad hoc rush orders was correspondingly reduced. This is consistent with the findings of Chuchotthaworn (2020) and Tabporn et al. (2018), who similarly found that structured forecasting and inventory control reduced holding costs and improved order fulfillment in Thai food-processing settings, although neither of those studies examined a full cross-functional S&OP cycle as the present study does.

Table 7. Consolidated statistical hypothesis tests with 95% confidence intervals and effect sizes (n = 6 paired months)

Hypothesis & Variable	Mean Values		Mean Diff. (*D*)	95% CI of Difference [Lower, Upper]	Std. Error (*SE*)	*t*-value (*df* = 5)	*p*-value (One-tailed)	Wilcoxon *T* (*p* - value)[a]	Cohen's *d* (Effect Size)[b]
	Before	After							
H1: Forecast Error (MAPE, %)	28.40	16.90	11.50	[10.68, 12.32]	0.317	36.25	< 0.001*	0 (0.031*)	14.80 (Very Large)
H2: Average Inventory (Tons)	240.00	195.00	45.00	[35.61, 54.39]	3.652	12.32	< 0.001*	0 (0.031*)	5.03 (Very Large)
H3: On-Time Delivery (OTD, %)	82.30	93.10	-10.80	[-12.53, -9.07]	0.671	-16.10	< 0.001*	0 (0.031*)	6.57 (Very Large)
H4: Expedited Orders (Times/Month)	11.00	5.00	6.00	[4.01, 7.99]	0.775	7.75	< 0.001*	0 (0.031*)	3.16 (Very Large)
H5: Forecast Bias (%)	12.60	4.20	8.40	[7.52, 9.28]	0.343	24.52	< 0.001*	0 (0.031*)	10.01 (Very Large)

Note: * Indicates statistical significance at the 0.05 level.

[a] Wilcoxon T-statistic represents the minimum sum of ranks (T). Under $n = 6$, the minimum achievable two-tailed p-value is 0.031.

[b] Cohen's d is calculated as the mean difference divided by the standard deviation of paired differences. Standard benchmarks: 0.2 (small), 0.5 (medium), 0.8 (large).

"Mean Diff. (D) = mean of paired differences (Before–After for H1, H2, H4, H5; After–Before for H3); SE = standard error; df = 5."

These findings are broadly consistent with the synthesis of Tuomikangas and Kaipia (2014) and Thomé et al. (2012), who identified S&OP as a key mechanism linking demand and supply to improve cost and customer-service outcomes. A more specific comparison is also possible: Thomé et al. (2012) reported that organizations with mature S&OP implementations achieved inventory carrying-cost reductions in the range of 10 to 30 percent, within which the 18.75 percent inventory reduction observed in this case study falls, suggesting that the magnitude of improvement, though derived from a single case, is broadly within the range previously documented in the literature rather than an outlier. With respect to forecast accuracy specifically, comparable published MAPE improvements following S&OP-type interventions in manufacturing settings are less consistently reported in percentage-point terms, which limits the precision of cross-study comparison; the 11.5-percentage-point MAPE reduction found here should accordingly be read as a case-specific result rather than benchmarked against a well-established norm. In this case study, the decrease in average inventory and the number of urgent production orders are consistent with the organization being able to plan more proactively, while the increase in OTD suggests that the reduction in inventory did not come at the expense of customer service. The improvement in cross-functional coordination observed in this study is also consistent with Wagner et al. (2014), who argued that organizational alignment and integrated planning processes are associated with operational performance improvement.

In the context of agricultural processing factories, this study is particularly significant because this type of industry faces specific constraints such as seasonal fluctuations in raw materials, product shelf life, and order uncertainties. Having a platform for regular data review and joint decision-making appears to help bridge the gap between planning and actual implementation and may enhance the organization's ability to respond more flexibly to changes. At the same time, these same agro-specific constraints also represent the principal challenges to sustaining S&OP success beyond the six-month window observed here: the agro-specific constraints noted in the Introduction (harvest-dependent supply and shelf-life limits) restrict how far even a well-functioning S&OP cycle can eliminate supply-side forecast error. The research thus suggests that S&OP can serve as a useful management mechanism for agricultural processing businesses in the Thai context, while acknowledging that its success is conditional on factors, particularly raw-material seasonality, that are largely outside the direct control of the planning process itself. Consistent with Tuomikangas and Kaipia (2014), such initiatives may stall when executive sponsorship or cross-functional metrics are not sustained; this risk is discussed in Section 5.

5. Conclusions and Recommendations

This study set out to investigate the problems and limitations of S&OP in an agricultural processing plant, develop an S&OP process suited to its organizational context, and evaluate the resulting effects on five operational indicators. Within the scope of this single case, all five indicators improved to a statistically significant degree over a six-month trial, and the accompanying qualitative evidence indicated that the absence of a shared database and a cross-functional review forum had been the primary driver of the pre-existing planning inconsistency. In practical terms, organizations looking to implement S&OP should focus on four key areas: creating a shared database, setting a fixed meeting schedule, clearly appointing process owners, and establishing joint metrics that reflect the goals of the entire organization. Sustaining these gains beyond the trial period, however, is likely to depend on continued executive sponsorship and the durability of the joint metrics introduced during this study, since the broader S&OP literature indicates that initiatives of this kind frequently stall once initial momentum fades. Meanwhile, in academic terms,

future research should expand the study to multiple case studies, extend the follow-up period, and collect data at the product or weekly level to enhance the detail and robustness of the research conclusions.

This research has several limitations. First, the study employed a single-case design, which may limit the generalizability of the findings to other industrial contexts; the very large effect sizes and uniform monthly pattern reported in Section 3.4 are characteristic of this specific case and should not be read as typical of S&OP implementations generally. Second, the evaluation period covered only six months before and six months after the implementation of the S&OP process, and the two windows fell in different halves of the annual agricultural cycle (January-June before, July-December after); this means that part of the observed improvement may be confounded with seasonal differences between the two periods rather than being attributable to the S&OP process alone, and the study cannot disentangle the intervention effect from this seasonal contrast. Although the paired monthly analysis enabled direct operational comparison under similar planning conditions, the relatively small number of observations limits statistical power, and the Shapiro-Wilk normality tests reported in Table 6, given the same small sample, should be regarded as inconclusive rather than confirmatory. Third, external factors such as raw material variability and market fluctuations may also have influenced operational performance during the study period, and because no control group was available, the improvements reported here cannot be attributed to the S&OP process with the same confidence that a controlled or multi-case design would permit. Fourth, the demand forecasting method introduced as part of the S&OP process, a weighted moving average combined with qualitative adjustment, was not benchmarked against alternative forecasting techniques, so the relative contribution of the forecasting method itself, as opposed to the cross-functional review process around it, cannot be isolated. Finally, while the qualitative component of this study identified four key organizational themes from 12 informant interviews, the depth of that analysis was constrained by the case-study scope; a larger or longitudinal qualitative inquiry could further illuminate how these themes evolve as an S&OP process matures. Future research should therefore extend the implementation horizon to cover a full annual cycle, increase the number of analytical periods, benchmark alternative forecasting techniques, and conduct multi-case comparative studies to strengthen external validity and empirical generalizability.

6. Acknowledgements

The researcher would like to thank the case study factory for providing information and facilitating field data collection, as well as the esteemed experts and all involved parties for their valuable suggestions in the development of this research. Special thanks to the Faculty of Industrial Technology, Ubon Ratchathani Rajabhat University, for their support in this research endeavor.

7. References

Chase, C. W. (2013). Demand-driven forecasting: A structured approach to forecasting. John Wiley & Sons.

Chuchotthaworn, C. (2020). The Forecasting and optimal order quantity determination as a guideline for packaging inventory management in production: A case study of an agricultural product processing company in Phatthalung Province. Humanities and Social Sciences Research Promotion Network Journal, 3(3), 92–108. (in Thai). https://so06.tci-thaijo.org/index.php/hsrnj/article/view/252187

Goh, S. H., & Eldridge, S. (2019). Sales and operations planning: The effect of coordination mechanisms on supply chain performance. International Journal of Production Economics, 214, 80–94. https://doi.org/10.1016/j.ijpe.2019.03.027

Kreuter, T., Scavarda, L. F., Thomé, A. M. T., Hellingrath, B., & Seeling, M. X. (2022). Empirical and theoretical perspectives in sales and operations planning. Review of Managerial Science, 16, 319–354. https://doi.org/10.1007/s11846-021-00455-y

Ptak, C. A., & Smith, C. (2011). Orlicky's material requirements planning (3rd ed.). McGraw-Hill.

Rabop, C. (2013). Logistics and Supply Chain Management. Bangkok: Huachiew Chalermprakiet University Press.

Tabporn, T., Katmuang, Y., Tabporn, A., & Pangjit, P. (2018). Sales forecasting and inventory management of frozen giant squid jaw products: A case study of Siam Makro Public Company Limited. Thonburi University Journal (Science and Technology), 2(2), 28-41. (in Thai). https://www.thonburi-u.ac.th/Journal_SIT/Vol2_No2-3.pdf

Thomé, A. M. T., Scavarda, L. F., Fernandez, N. S., & Scavarda, A. J. (2012). Sales and operations planning: A research synthesis. International Journal of Production Economics, 138(1), 1-13. https://doi.org/10.1016/j.ijpe.2011.11.027

Tuomikangas, N., & Kaipia, R. (2014). A coordination framework for sales and operations planning (S&OP): Synthesis from the literature. International Journal of Production Economics, 154, 243-262. https://doi.org/10.1016/j.ijpe.2014.04.026

Wagner, S. M., Ullrich, K. K. R., & Transchel, S. (2014). The game plan for aligning the organization. Business Horizons, 57(2), 189-201. https://doi.org/10.1016/j.bushor.2013.11.002

Wallace, T. F., & Stahl, R. A. (2008). Sales & operations planning: The how-to handbook (3rd ed.). T. F. Wallace & Company.

Walter, A., Ahsan, K., & Rahman, S. (2025). Application of artificial intelligence in demand planning for supply chains: A systematic literature review. The International Journal of Logistics Management, 36(3), 672-719. https://doi.org/10.1108/IJLM-02-2024-0120

Wu, Z., & Møller, C. (2024). Global sales and operations planning: Exploring transitional pathway from a fit perspective. Procedia CIRP, 130, 1200-1209. https://doi.org/10.1016/j.procir.2024.10.228

ผลของสารผสมล่วงหน้าประเภทวิตามินและแร่ธาตุผสมโพรไบโอติก (Pro Max Plus) ต่อสมรรถภาพการเจริญเติบโตและตอบสนองทางระบบภูมิคุ้มกันปลานิล

Effects of a Vitamin-Mineral Premix Containing Probiotic (Pro Max Plus) on Growth Performances and Innate Immune Responses of Nile Tilapia (*Oreochromis niloticus*)

ฐปนขจร ปันแจ่ม[1] สุดาพร ตงศิริ[1] จงกล พรมยะ[1] Ricardo A. De Guzman[2] และ ชนกันต์ จิตมนัส[1*]

Thapanakhajorn Punjam[1], Sudaporn Tongsiri[1], Jongkon Promya[1], Ricardo A. De Guzman[2] and Chanagun Chitmanat[1*]

[1]คณะเทคโนโลยีการประมงและทรัพยากรทางน้ำ มหาวิทยาลัยแม่โจ้ จังหวัดเชียงใหม่

[2]คณะวิทยาศาสตร์ มหาวิทยาลัยแห่งรัฐเซนทรัลลูซอน จังหวัดนูเอบาเอซิฮา ประเทศฟิลิปปินส์

[1]Faculty of Fisheries Technology and Aquatic Resources, Maejo University, Chiang Mai Province

[2]Central Luzon State University, Science City of Muñoz, Nueva Ecija 3120, Philippines

[*]Corresponding Author: chanagun9@gmail.com

Received: June 8, 2026 **Revised:** July 16, 2026 **Accepted:** August 18, 2026

บทคัดย่อ

การพัฒนาสารเสริมอาหารที่สามารถส่งเสริมการเจริญเติบโต สุขภาพและผลตอบแทนทางเศรษฐกิจของสัตว์น้ำเป็นประเด็นสำคัญของการเพาะเลี้ยงสัตว์น้ำเชิงพาณิชย์ งานวิจัยนี้มีวัตถุประสงค์เพื่อประเมินผลของสารผสมล่วงหน้าประเภทวิตามินและแร่ธาตุเสริมโพรไบโอติก (Pro Max Plus) ต่อสมรรถภาพการเจริญเติบโต การใช้ประโยชน์จากอาหาร การตอบสนองทางภูมิคุ้มกันแต่กำเนิดและผลตอบแทนทางเศรษฐกิจของปลานิล (*Oreochromis niloticus*) วัยรุ่น (ขนาดน้ำหนักเริ่มต้นเฉลี่ย 42.36 ± 3.95 กรัม) ภายใต้แผนการทดลองแบบสุ่มตลอด (CRD) ประกอบด้วย 3 ชุดการทดลอง ได้แก่ กลุ่ม Control ซึ่งได้รับอาหารพื้นฐานโดยไม่เสริมสาร กลุ่ม Pro Max ซึ่งได้รับอาหารพื้นฐานเสริมสารผสมล่วงหน้าประเภทวิตามินและแร่ธาตุ 5 กรัมต่อกิโลกรัมอาหาร และกลุ่ม Pro Max Plus ซึ่งได้รับอาหารพื้นฐานเสริมสารผสมล่วงหน้าประเภทวิตามินและแร่ธาตุที่มีโพรไบโอติก 5 กรัมต่อกิโลกรัมอาหาร โดยทดลอง 60 วัน ผลการศึกษาพบว่าปลานิลที่ได้รับอาหารในกลุ่ม Pro Max Plus มีสมรรถภาพการเจริญเติบโตดีกว่ากลุ่มอื่นอย่างมีนัยสำคัญทางสถิติ ($p < 0.05$) โดยมีน้ำหนักเพิ่มสูงสุด (68.80 กรัม) อัตราการเจริญเติบโตต่อวัน (1.15 กรัมต่อวัน) และอัตราการเจริญเติบโตจำเพาะ (1.85% ต่อวัน) สูงที่สุด ขณะเดียวกันมีประสิทธิภาพการใช้อาหารดีที่สุด โดยมีค่าอัตราแลกเนื้อ (FCR) ต่ำสุดที่ 0.80 และมีอัตราการรอดตายสูงสุดที่ร้อยละ 95.55 การเสริมโพรไบโอติกช่วยเพิ่มกิจกรรมของเอนไซม์ไลโซไซม์ กิจกรรมการใช้ออกซิเจนอย่างรวดเร็วเพื่อสร้างสารอนุมูลอิสระ (Respiratory burst) และระดับปฏิกิริยาการจับกลุ่มของแอนติบอดี (Agglutinating antibody titers) นอกจากนี้ยังส่งเสริมการแสดงออกของยีน IL-1β และปรับการแสดงออกของยีน TNF-α ซึ่งสะท้อนถึงการเสริมสร้างระบบภูมิคุ้มกันที่มีประสิทธิภาพมากขึ้น แม้อาหารสูตรเสริมโพรไบโอติกจะมีต้นทุนสูงกว่าเล็กน้อย แต่ให้ผลตอบแทนทางเศรษฐกิจดีที่สุด โดยมีค่าอัตราส่วนผลประโยชน์ต่อต้นทุน (BCR) สูงสุดเท่ากับ 1.91 และมีกำไร 2.19 ± 0.10 บาท/ตัว ผลการศึกษาชี้ให้เห็นว่าการเสริมสารผสมล่วงหน้าประเภทวิตามินและแร่ธาตุร่วมกับโพรไบโอติกเป็นแนวทางด้านโภชนาการที่มีศักยภาพในการเพิ่มประสิทธิภาพการผลิต เสริมสร้างภูมิคุ้มกันและเพิ่มความคุ้มค่าทางเศรษฐกิจในการเพาะเลี้ยงปลานิลเชิงพาณิชย์

คำสำคัญ: ปลานิล, โพรไบโอติก, สารผสมล่วงหน้าประเภทวิตามินและแร่ธาตุ, ภูมิคุ้มกัน, ผลตอบแทนทางเศรษฐกิจ

Abstract

Developing feed additives capable of enhancing growth performance, fish health, and economic profitability remains a major challenge in intensive aquaculture. This study evaluated the effects of a probiotic-enriched vitamin–mineral premix (Pro Max Plus) on growth performance, feed utilization, innate immune responses, and economic returns in juvenile Nile tilapia (initial mean weight of 42.36 ± 3.95 g). A

60-day feeding trial was conducted using a completely randomized design (CRD) with three dietary treatments: control, a basal diet without supplementation; Pro Max, a basal diet supplemented with a vitamin–mineral premix at 5 g/kg feed; and Pro Max Plus, a basal diet supplemented with a probiotic-containing vitamin–mineral premix at 5 g/kg feed. Fish fed the Pro Max Plus supplementary diet exhibited significantly superior growth performance compared with the other treatments ($p < 0.05$), achieving the highest weight gain (68.80 g), daily weight gain (1.15 g/day), and specific growth rate (1.85%/day). Feed utilization was also improved, as indicated by the lowest feed conversion ratio (FCR = 0.80) and the highest survival rate (95.55%). Immunological assessments revealed enhanced innate immune responses in fish receiving the probiotic-enriched diet, including increased lysozyme activity, respiratory burst activity, and agglutinating antibody titers. Furthermore, dietary supplementation upregulated the expression of the pro-inflammatory cytokine gene IL-1β while modulating TNF-α expression, suggesting improved immune regulation. Although the probiotic-supplemented diet incurred a slightly higher feed cost, it generated the greatest economic benefit, with the highest benefit–cost ratio (BCR = 1.91) and a profit of 2.19 ± 0.10 THB/fish. These findings demonstrate that supplementation of a vitamin–mineral premix combined with probiotics represents an effective nutritional strategy for improving growth performance, strengthening immune competence, and enhancing economic profitability in commercial Nile tilapia production.

Keywords: Nile tilapia, Probiotic, Vitamin–mineral premix, Immune response, Economic return

1. Introduction

Aquaculture has become one of the fastest-growing food production sectors worldwide and plays a major role in ensuring nutritional security for a growing global population. Among farmed finfish, Nile tilapia (*Oreochromis niloticus*) is one of the most economically important fish because of its rapid growth, high feed conversion efficiency, tolerance to uncertain environmental conditions, and strong market acceptance (Pradeepkiran, 2019). However, the progressive intensification of tilapia farming systems has increased exposure to environmental stressors, deteriorating water quality, and elevated pathogen pressure, all of which compromise fish health and production efficiency (Moreira et al., 2021; Sundström et al., 2014). These constraints frequently result in reduced growth performance, impaired immune competence, and increased mortality, thereby generating significant economic losses. In parallel, increasing regulatory restrictions and public concern regarding antibiotic usage in aquaculture have accelerated the search for sustainable, nutrition-based strategies to enhance fish resilience and productivity.

Nutrition is a primary factor in fish health and physiological performance. Beyond macronutrient supply, adequate provision of micronutrients, particularly vitamins and minerals, is essential for maintaining metabolic homeostasis, supporting antioxidant defense systems, and sustaining immune function (Hassan et al., 2025; Khan et al., 2025; Saras, 2023). Several vitamins act as cofactors in enzymatic pathways involved in energy metabolism, tissue repair, and immune regulation. Deficiencies in key vitamins such as ascorbic acid and α-tocopherol have been associated with growth depression, oxidative stress, and increased susceptibility to infectious diseases in fish (Hassan et al., 2025; Pohlenz & Gatlin, 2014). Moreover, micronutrients contribute to the maintenance of epithelial integrity and activation of innate immune components, including lysozyme activity and phagocytic responses (Pohlenz & Gatlin, 2014). Consequently, multivitamin–mineral premixes are routinely incorporated into aquafeeds to prevent subclinical deficiencies and optimize physiological performance under intensive production conditions.

In addition to micronutrient fortification, dietary supplementation with probiotics has gained substantial attention as an environmentally sustainable strategy for improving fish health and reducing dependency on chemotherapeutics (Amenyogbe, 2023; Hancz, 2022; Mukhtar et al., 2025; Sihag & Sharma, 2012). Probiotics are defined as live microorganisms that, when administered in adequate amounts, confer health benefits to the host. In aquaculture, probiotics have been reported to enhance growth performance, improve feed utilization, modulate gut microbial communities, stimulate innate immune responses (Hill et al., 2014; Ringø et al., 2016; Shanahan, 2010; Wu et al., 2024), and enhance disease resistance (Kaew-on et al., 2016; Panase et al., 2023). Proposed mechanisms include competitive exclusion of pathogenic bacteria, secretion of antimicrobial compounds, production of digestive enzymes, and activation of host immune pathways through gut-associated lymphoid tissues (Ringø et al., 2016; Shanahan, 2010). In Nile tilapia, probiotic supplementation has been shown to improve growth indices and enhance non-specific immune parameters such as respiratory burst activity and serum lysozyme levels (Ringø et al., 2016; Shanahan, 2010; Wu et al., 2024).

Although the individual effects of dietary vitamin–mineral supplementation and probiotic inclusion have been extensively investigated, studies evaluating their combined application within a single functional premix formulation remain limited, particularly in Nile tilapia culture systems. Previous research has demonstrated that dietary supplementation with probiotics such as *Bacillus* spp. and *Lactobacillus* spp. can improve growth performance in Nile tilapia, typically increasing weight gain by approximately 10–25% and reducing feed conversion ratio (FCR) by 5–15% compared with unsupplemented controls (Hai, 2015; Ringø et al., 2016). Similar responses have been reported in other cultured species, including whiteleg shrimp (*Litopenaeus vannamei*), where probiotic supplementation increased final body weight by 12 – 20% (Liu et al., 2009; Kuebutornye et al., 2019; Olmos et al., 2020) while improving survival under bacterial challenge, and in common carp (*Cyprinus carpio*) (Mohammed et al., 2025) where dietary probiotics enhanced weight gain by approximately 15–30% and improved feed utilization (Dawood et al., 2018). Given that micronutrients are critical for maintaining metabolic and antioxidant capacity, while probiotics primarily act through modulation of intestinal homeostasis and immune stimulation, their co-supplementation may produce complementary or synergistic effects. Integrated nutritional strategies targeting both physiological maintenance and gut-mediated immune modulation could therefore provide enhanced protection against stress and disease challenges compared to single-additive approaches (Hill et al., 2014; Ringø et al., 2016). However, empirical evidence supporting such combined formulations under practical rearing conditions remains insufficient.

While improvements in growth performance and health are essential indicators of feed efficacy, their practical adoption by fish farmers ultimately depends on economic viability. Feed accounts for approximately 50–70% of total production costs in intensive Nile tilapia culture, making cost-effectiveness a critical consideration when evaluating functional feed additives. Economic indices such as the benefit–cost ratio (BCR), net profit, and return on investment are increasingly used to determine whether the biological advantages of dietary interventions translate into greater profitability under commercial production conditions. Previous studies have shown that functional feed additives, including probiotics and phytogenic supplements, can improve economic returns by enhancing growth, feed efficiency, and survival, thereby increasing production output relative to feed costs (Dawood et al., 2018; Panase et al., 2023). Nevertheless, studies simultaneously evaluating the biological efficacy and economic feasibility of combined vitamin–mineral and probiotic premixes in Nile tilapia remain scarce.

Therefore, the present study evaluated the effects of a dietary vitamin–mineral premix containing probiotics (Pro Max Plus) on growth performance, feed utilization, and innate immune responses of juvenile Nile tilapia. We hypothesized that co-supplementation would enhance production performance and stimulate non-specific immune parameters. The findings of this study aimed to contribute to the development of evidence-based functional feed strategies that support sustainable and resilient tilapia aquaculture.

2. Materials and methods

2.1 Ethical Statement

All experimental protocols, methods, and feeding regimes were approved by the Institutional Animal Care and Use Committee (IACUC), Faculty of Fisheries Technology and Aquatic Resources, Maejo University, Thailand (Approval No. MACUC 026F/2568; approved on 30 July 2025).

2.2 Experimental Animals and Acclimatization

A total of 135 Nile tilapia with an initial mean body weight of 42.36 ± 3.95 g were transferred to fiberglass holding tanks for a 14-day acclimatization period under controlled laboratory conditions. During this phase, fish were maintained under a natural photoperiod and provided with a basal commercial diet twice daily to apparent satiation. This pre-experimental conditioning was conducted to ensure metabolic homeostasis, minimize handling-induced stress, and facilitate behavioral adaptation to the aquaculture system.

2.3 Experimental Feed Preparation

A commercial floating pellet diet was used as the basal diet for this study. Three dietary treatments were prepared as follows: (1) Control, the basal diet without supplementation; (2) Pro Max, the basal diet supplemented with a vitamin–mineral premix (Pro Max; Groupnet Medicine Co., Ltd., Thailand) at 5 g/kg feed; and (3) Pro Max Plus, the basal diet supplemented with a probiotic-containing vitamin–mineral premix (Pro Max Plus; Groupnet Medicine Co., Ltd., Thailand) at 5 g/kg feed.

The experimental diets were prepared by mechanically homogenizing the respective supplements with the basal diet to ensure uniform distribution of the additives. To improve palatability and enhance the hydrostability of the supplements, the fortified pellets were coated with a 3% gelatin solution. The diets were then dried in a forced-air oven at 55 °C for 24 h until a constant moisture content was achieved. To minimize lipid oxidation and maintain the stability of the supplements during storage, the finished diets were vacuum-packaged and stored at 4 °C throughout the experimental period.

Pro Max consisted of a vitamin–mineral premix, whereas Pro Max Plus contained the same vitamin–mineral formulation with added probiotic microorganisms.

2.4 Experimental Design and Husbandry

The trial was structured according to a completely randomized design (CRD). A total of 135 specimens were randomly allocated into nine glass aquaria (dimensions: 40 x 75 x 47 cm), achieving a standardized stocking density of 15 fish per unit. The experimental framework consisted of three distinct dietary treatments, each conducted in triplicate: Control, basal diet without supplementation; Pro Max, basal diet supplemented with Pro Max at 5 g/kg feed; and Pro Max Plus, basal diet supplemented with Pro Max Plus at 5 g/kg feed.

2.5 Feeding Management and Growth Monitoring

The feeding trial was maintained for a duration of 60 days. Fish were hand-fed their assigned diets twice daily (08:30–09:30 and 16:30–17:30) to apparent satiation. To account for biomass increments

and maintain consistent feeding pressure, the total fish weight in each aquarium was reassessed biweekly, with feed rations recalibrated based on the updated biomass. Quantitative growth performance and feed utilization indices were formally evaluated at 30-day intervals. At each sampling point, all fish were temporarily anesthetized using clove oil (5 ppm) to minimize handling stress during gravimetric and morphometric measurements.

2.6 Evaluation of Growth Performance and Feed Utilization

Over the 60-day experimental period, growth performance was monitored biweekly by randomly sampling 30% of the fish population from each aquarium to record body weight (g) and total length (cm). To ensure nutritional consistency and account for biomass fluctuations, dietary rations were adjusted every 14 days based on the updated mean weight, maintaining a fixed feeding rate of 5% of body weight. Upon the conclusion of the 60-day feeding trial, all remaining fish in each treatment were harvested, counted, and weighed to determine growth parameters.

Growth performance was evaluated using the following equations:

Weight gain (WG, g):

$$WG = W_f - W_i \tag{1}$$

where W_f is the final body weight (g) and W_i is the initial body weight (g).

Length gain (LG, cm):

$$LG = L_f - L_i \tag{2}$$

where L_f is the final total length (cm) and L_i is the initial total length (cm).

Average daily gain (ADG, g/day):

$$ADG = \frac{W_f - W_i}{T} \tag{3}$$

where T is the experimental period (days).

Specific growth rate (SGR, %/day):

$$SGR = \frac{\ln W_f - \ln W_i}{T} \times 100 \tag{4}$$

where $\ln$ denotes the natural logarithm.

Condition factor (CF):

$$CF = \frac{W}{L^3} \times 100 \tag{5}$$

where W is the body weight (g) and L is the total length (cm). The multiplication factor (100) is appropriate when weight is expressed in grams and length in centimeters.

Survival rate (SR, %):

$$SR = \frac{N_f}{N_i} \times 100 \quad (6)$$

where N_i is the initial number of fish and N_f is the final number of surviving fish.

Feed utilization was assessed using the following equations:

Feed intake (FI, g/fish):

$$FI = \frac{\text{Total feed consumed (g)}}{\text{Number of fish}} \quad (7)$$

Average daily feed intake (ADFI, g/fish/day):

$$ADFI = \frac{FI}{T} \quad (8)$$

where T is the duration of the feeding trial (days).

Feed conversion ratio (FCR):

$$FCR = \frac{\text{Total feed consumed (g)}}{\text{Weight gain (g)}} \quad (9)$$

Feed conversion efficiency (FCE, %):

$$FCE = \frac{\text{Weight gain (g)}}{\text{Total feed consumed (g)}} \times 100 \quad (10)$$

Feed efficiency (FE):

$$FE = \frac{\text{Weight gain (g)}}{\text{Total feed consumed (g)}} \quad (11)$$

2.7 Water Quality

Table 1 presents the recorded water quality parameters during the experiment. The temperature, dissolved oxygen, and pH readings were stable across all treatments and within the optimal ranges for tilapia.

Table 1. Water quality parameters during the experimental period

Treatment	Temperature (°C)	Dissolved Oxygen (mg/L)	pH
Control	29 ± 0.00	4.20 ± 0.17	7.50 ± 0.00
Pro Max	29 ± 0.00	4.23 ± 0.17	7.50 ± 0.00
Pro Max Plus	29 ± 0.00	4.20 ± 0.17	7.50 ± 0.00

Note. Control, basal diet without supplementation; Pro Max, basal diet supplemented with a vitamin–mineral premix at 5 g/kg feed; Pro Max Plus, basal diet supplemented with a probiotic-containing vitamin–mineral premix at 5 g/kg feed. Values are presented as mean ± SE.

2.8 Immunological Analysis

2.8.1 Collecting Fish Blood Samples

Blood samples were collected from six randomly selected fish per treatment group. To minimize handling stress, specimens were anesthetized using clove oil (5 ppm) prior to the procedure. Blood (0.7 mL per fish) was drawn from the caudal vein using a 1 mL sterile syringe (0.5 x 25 mm) and transferred into 1.5 mL Eppendorf tubes. To obtain serum, the samples were allowed to clot at room temperature for 1 h, followed by further incubation at 4 °C for 4 h. The clotted blood was then subjected to centrifugation at 10,000 x g for 10 min at 4 °C. The resulting supernatant (serum) was carefully collected and stored at -80 °C for subsequent immunological and biochemical analyses.

2.8.2 Lysozyme Activity Assay

Serum lysozyme activity was determined following a protocol adapted from Chandan et al. (1965). Serum samples were thawed on ice before analysis. Then a suspension of *Micrococcus lysodeikticus* ATCC No. 4698 was prepared at 0.3 mg/mL in 0.1 M citrate-phosphate buffer, pH 5.8. After that, a volume of 25 µL of serum was placed into each well of a 96-well microplate. Then, 175 µL of *Micrococcus lysodeikticus* ATCC No. 4698 suspension was added to each well. Then the mixture was gently mixed to ensure uniform reaction between the serum and bacterial suspension. Then the decrease in turbidity was measured at 540 nm using a microplate reader (Multiskan GO, Thermo Fisher Scientific, Vantaa, Finland). After that absorbance readings were recorded every 30 s for 10 min. Then the lysozyme activity was calculated based on the reduction in absorbance over time, which reflected the lysis of *Micrococcus lysodeikticus* cells. One unit of lysozyme activity was defined as the amount of enzyme causing a decrease in absorbance of 0.001 per min at 540 nm.

2.8.3 Respiratory Burst Activity

Respiratory burst activity of blood leukocytes was determined using the nitro blue tetrazolium (NBT) reduction assay according to Secombes (1990), with minor modifications. Whole blood was collected from the caudal vein into heparinized syringes. Leukocytes were isolated by centrifugation over a Histopaque-1077 density gradient (Sigma-Aldrich, USA) at 400 × g for 30 min at room temperature. The leukocyte layer was carefully collected, washed twice with phosphate-buffered saline (PBS, pH 7.4), and resuspended in PBS. Cell viability was confirmed to be greater than 95% by trypan blue exclusion, and the leukocyte concentration was adjusted to 1×10^6 cells/mL.

Aliquots (100 µL) of the leukocyte suspension were dispensed into 96-well microplates and mixed with an equal volume of 0.2% NBT solution. No exogenous stimulant was added, and respiratory burst activity was assessed under basal conditions. The plates were incubated at room temperature for 2 h. After incubation, the supernatant was discarded, and the cells were fixed with absolute methanol for 5 min. The wells were washed twice with 70% methanol, air-dried, and the intracellular formazan deposits were dissolved by adding 120 µL of 2 M KOH followed by 140 µL of dimethyl sulfoxide (DMSO). The absorbance of the dissolved intracellular formazan was measured at 655 nm using a microplate reader, and respiratory burst activity was expressed as NBT reduction activity (OD655) after correction against the corresponding blank.

2.8.4 Serum Agglutination Titer

The humoral antibody response was quantified using the U-bottom microtiter plate agglutination method described by Yarahmadi et al. (2014). Serum samples underwent twofold serial dilutions (ranging from 1:2 to 1:128) in phosphate-buffered saline (PBS). Subsequently, 50 µL of an *Aeromonas hydrophila* suspension (OD 540 nm = 1.0, approximately 10^7 CFU/mL) was added to each well.

The plates were incubated at room temperature for 24 h. The agglutination titer was recorded as the reciprocal of the highest serum dilution showing visible bacterial clumping.

2.8.5 RNA extraction, cDNA synthesis, and quantitative real-time PCR (qPCR)

Following the 60-day experimental duration, head kidney samples (~0.2 g) were excised from three randomly selected fish per treatment group. Samples were immediately preserved in RNAlater® (Amnion, Cambridgeshire, UK) and stored at −80 °C until RNA extraction. Total RNA was isolated using 1 mL of QIAzol® Lysis Reagent (Qiagen, USA) and further purified using the RNeasy® Mini Kit (Qiagen, Hilden, Germany) in accordance with the manufacturer's instructions. Residual genomic DNA was eliminated by DNase I treatment (Thermo Fisher Scientific, USA). RNA purity and concentration were assessed via absorbance at 260 nm and 280 nm using a Synergy™ H1 Multi-Mode Microplate Reader (BioTek Instruments Inc., USA), while RNA integrity was confirmed by electrophoresis on a 2% agarose gel. First-strand cDNA synthesis was performed using 1 µg of total RNA and the RevertAid™ First-Strand cDNA Synthesis Kit (Thermo Scientific, USA) following the manufacturer's protocol. Synthesized cDNA was treated with RNase H (Invitrogen, USA) at 37 °C for 20 min and stored at −20 °C until use.

Quantitative real-time PCR was carried out on a PCRmax ECO 48 Real-Time PCR System (PCRmax, UK) using Maxima™ SYBR Green/ROX qPCR Master Mix (2×) (Thermo Fisher Scientific, Lithuania). Primer sequences used for amplification are provided in Table 2. β-actin was selected as the reference gene for normalization. Primer efficiency was validated via standard curve analysis using serially diluted cDNA, ensuring correlation coefficients (R^2) > 0.99. A melt curve analysis was performed post-amplification to confirm product specificity. Each qPCR reaction was performed in triplicate in a 20 µL volume, comprising 2 µL of 1:100 diluted cDNA, 10 µL of SYBR Green Master Mix, 1 µL of each primer (1 pmol), and 6 µL of nuclease-free water. The thermal cycling protocol included an initial denaturation at 95 °C for 3 min, followed by 40 cycles of denaturation at 95 °C for 10 s, and annealing/extension at 60 °C for 30 s. *Actin* was used as the housekeeping gene for sample normalization. Relative gene expression levels were quantified using the $2^{-\Delta\Delta Ct}$ method. The Control group (fish receiving the basal diet without supplementation) was used as the calibrator group, and its relative expression level was set to 1.0. Gene expression levels in the Pro Max and Pro Max Plus groups were expressed as fold changes relative to the Control group.

Table 2. Primers used to quantify the relative gene expression

Gene	Primer sequences (5′-3′)	References
TNF-α	F-GCTGGAGGCCAATAAAATCA R-CCTTCGTCAGTCTCCAGCTC	(Kayansamruaj et al., 2014).
IL1-β	F-AAGATGAATTGTGGAGCTGTGTT R-AAAAGCATCGACAGTATGTGAAAT	(Chadzinska et al., 2009).
Actin	F-TGGTGGGTATGGGTCAGAAAG R-TGTTGGCTTTGGGGTTCA	XM_003443127

2.9 Economic Analysis

An economic evaluation was performed to determine the cost-effectiveness of each experimental diet. The total cost per kilogram of feed (Baht/kg) was calculated based on the inclusion levels of each ingredient and their respective market prices at the time of the study. To assess the financial efficiency of the supplements, the economic conversion ratio (ECR), also referred to as the incidence cost, was determined. This parameter represents the feed cost required to produce one kilogram of fish weight

gain. The benefit–cost ratio (BCR), net profit, return on investment (ROI), and profit margin per fish were also calculated to evaluate the economic performance of each dietary treatment.

2.10 Statistical Analysis

All experimental data were subjected to one-way analysis of variance (ANOVA) to determine significant differences among treatment groups. When statistical significance was detected, Tukey's Honest Significant Difference (HSD) post hoc test was employed for multiple comparisons of treatment means. All statistical analyses were conducted using SPSS (version 23.0, IBM Corporation, Armonk, USA) for Windows, with a significance level established at ($p < 0.05$).

3. Results

3.1 Growth performance and survival rate

Dietary supplementation with Pro Max Plus significantly improved the growth performance of Nile tilapia compared with the control and the Pro Max formulation (Table 3). Fish fed the Pro Max Plus diet achieved the highest weight gain (68.80 ± 0.43 g), length gain (6.04 ± 0.34 cm), average daily gain (1.15 ± 0.01 g/day), and specific growth rate (1.85 ± 0.04%/day), all of which were significantly greater than those of the other treatment groups ($p < 0.05$). In contrast, the condition factor did not differ significantly among treatments ($p \geq 0.05$), with values ranging from 1.55 ± 0.10 to 1.60 ± 0.02. Survival rate was also significantly enhanced by Pro Max Plus supplementation, reaching 95.55 ± 2.22%, which was significantly higher than that of the control (86.66 ± 0.00%), while the Pro Max group (91.11 ± 2.22%) showed an intermediate response that was not significantly different from either control or Pro Max Plus.

Table 3. Growth performance and survival rate of Nile tilapia fed different experimental diets

Parameters	control	Pro Max	Pro Max Plus
Weight gain (g)	61.38 ± 1.18^{a}	57.92 ± 0.64^{a}	68.80 ± 0.43^{b}
Length gain (cm)	5.62 ± 0.11^{a}	4.87 ± 0.08^{a}	6.04 ± 0.34^{b}
Average daily gain (g/day)	1.02 ± 0.19^{b}	0.97 ± 0.19^{a}	1.15 ± 0.01^{b}
Specific growth rate (%/day)	1.39 ± 0.03^{a}	1.36 ± 0.02^{a}	1.85 ± 0.04^{b}
Condition factor (K)	1.55 ± 0.10^{a}	1.60 ± 0.02^{a}	1.58 ± 0.14^{a}
Survival rate (%)	86.66 ± 0.00^{a}	91.11 ± 2.22^{ab}	95.55 ± 2.22^{b}

Note. Control, basal diet without supplementation; Pro Max, basal diet supplemented with a vitamin–mineral premix at 5 g/kg feed; Pro Max Plus, basal diet supplemented with a probiotic-containing vitamin–mineral premix at 5 g/kg feed. Values are presented as mean ± SE. Different superscript letters within the same row indicate significant differences among treatments ($p < 0.05$)

3.2 Feed utilization and efficiency parameters

Analysis of feed utilization efficiency revealed that Nile tilapia fed the Pro Max Plus diet achieved the lowest feed conversion ratio (FCR) at 0.80 ± 0.00 (Table 4). This represented a significant improvement ($p < 0.05$) over the control and Pro Max groups, which exhibited FCR values ranging from 1.12 to 1.19. Correspondingly, the Pro Max Plus group cohort demonstrated significantly higher feed conversion efficiency (FCE: 8.36 ± 0.05) and feed efficiency percentage (125.39 ± 0.78) compared to other treatments. Interestingly, despite these superior efficiency markers, the daily feed intake (FI) in the Pro Max Plus group was the lowest (1.37 ± 0.02 g/day), indicating that probiotic supplementation enables more effective biomass conversion with reduced consumption.

3.3 Immune Responses and gene expression

The immunological parameters and gene expression profiles of Nile tilapia fed different experimental feeds over a two-month period showed significant differences among treatments, with the Pro Max Plus group exhibiting an improved immunological profile, as evidenced by enhanced lysozyme activity, respiratory burst response, and agglutinating antibody titers (Figure 1). Lysozyme levels in the fish fed Pro Max Plus were highest at 5.93 U/ml and 3.96 U/ml during the first and second months, respectively, consistently outperforming the control and Pro Max groups ($p < 0.05$). While lysozyme activity diminished across all groups by the second month, the Pro Max Plus group's ability to maintain superior levels suggests a persistent stimulation of the innate immune system. Furthermore, respiratory burst activity increased progressively, reaching a maximum of 0.143 in Pro Max Plus by the end of the study. Notably, fish fed Pro Max Plus showed an enhanced antibody response, with antibody titers reaching 2.00 by month two, whereas titers remained undetectable in the control group.

Furthermore, the relative expression of immune-related genes showed different expression patterns (Figure 2); fish fed Pro Max Plus exhibited the highest expression of Interleukin-1β (IL-1β) at 1.82 (Fig. 2A), whereas Tumor Necrosis Factor-alpha (TNF- α) expression was significantly lower in Pro Max Plus (0.35) compared with the control and Pro Max groups (1.07 and 1.18, respectively) ($p < 0.05$).

Table 4. Feed utilization and efficiency parameters of Nile tilapia fed different experimental diets

Parameters	control	Pro Max	Pro Max Plus
Feed intake (g/fish)	1.58 ± 0.01^{b}	1.61 ± 0.04^{b}	1.37 ± 0.02^{a}
Average daily feed intake (g/fish/day)	0.02 ± 0.00^{a}	0.02 ± 0.00^{a}	0.01 ± 0.00^{a}
Feed conversion ratio	1.12 ± 0.02^{b}	1.19 ± 0.01^{c}	0.80 ± 0.00^{a}
Feed conversion efficiency (%)	5.94 ± 0.11^{a}	5.61 ± 0.06^{a}	8.36 ± 0.05^{b}
Feed efficiency (g)	89.13 ± 1.71^{a}	84.10 ± 0.93^{a}	125.39 ± 0.78^{b}

Note. Control, basal diet without supplementation; Pro Max, basal diet supplemented with a vitamin–mineral premix at 5 g/kg feed; Pro Max Plus, basal diet supplemented with a probiotic-containing vitamin–mineral premix at 5 g/kg feed. Values are presented as mean ± SE. Different superscript letters within the same row indicate significant differences among treatments ($p < 0.05$)

3.4 Economic Sustainability

The financial assessment of Nile tilapia production in this study indicated that the combined supplementation of a multivitamin–mineral complex and probiotics provided the greatest economic benefit (Pro Max Plus), as evidenced by the data in Table 5. Although the Pro Max Plus diet required the highest initial feed cost, with a total feed cost of 43.93 ± 0.00 Baht/kg, this investment was effectively neutralized by enhanced biological efficiency and superior biomass yields. Notably, the Pro Max Plus group had the lowest cost per unit of weight gain (36.69 ± 0.78 Baht/kg), significantly lower than that of the Pro Max group ($p < 0.05$), which received micronutrient fortification in the absence of microbial additives. This economic divergence highlights a critical finding: although micronutrient supplementation is vital for metabolic homeostasis, its economic efficiency remains sub-optimal unless coupled with functional additives that refine gastrointestinal processing and nutrient partitioning.

From a commercial profitability standpoint, the Pro Max Plus group exhibited the most resilient financial profile, generating a significantly higher net profit (32.87 ± 1.49 Baht) and profit margin per fish (2.19 ± 0.10 Baht/fish) compared to both the control and Pro Max treatments ($p < 0.05$). Furthermore, the Pro Max treatment (multivitamin-only) resulted in a diminished benefit–cost ratio (BCR) of 1.25, a figure

significantly lower than the control's 1.72. This suggests that escalating dietary costs through fortification without concurrent improvements in absorption capacity can paradoxically undermine the economic sustainability of aquaculture operations. In contrast, the Pro Max Plus group attained the highest BCR of 1.91.

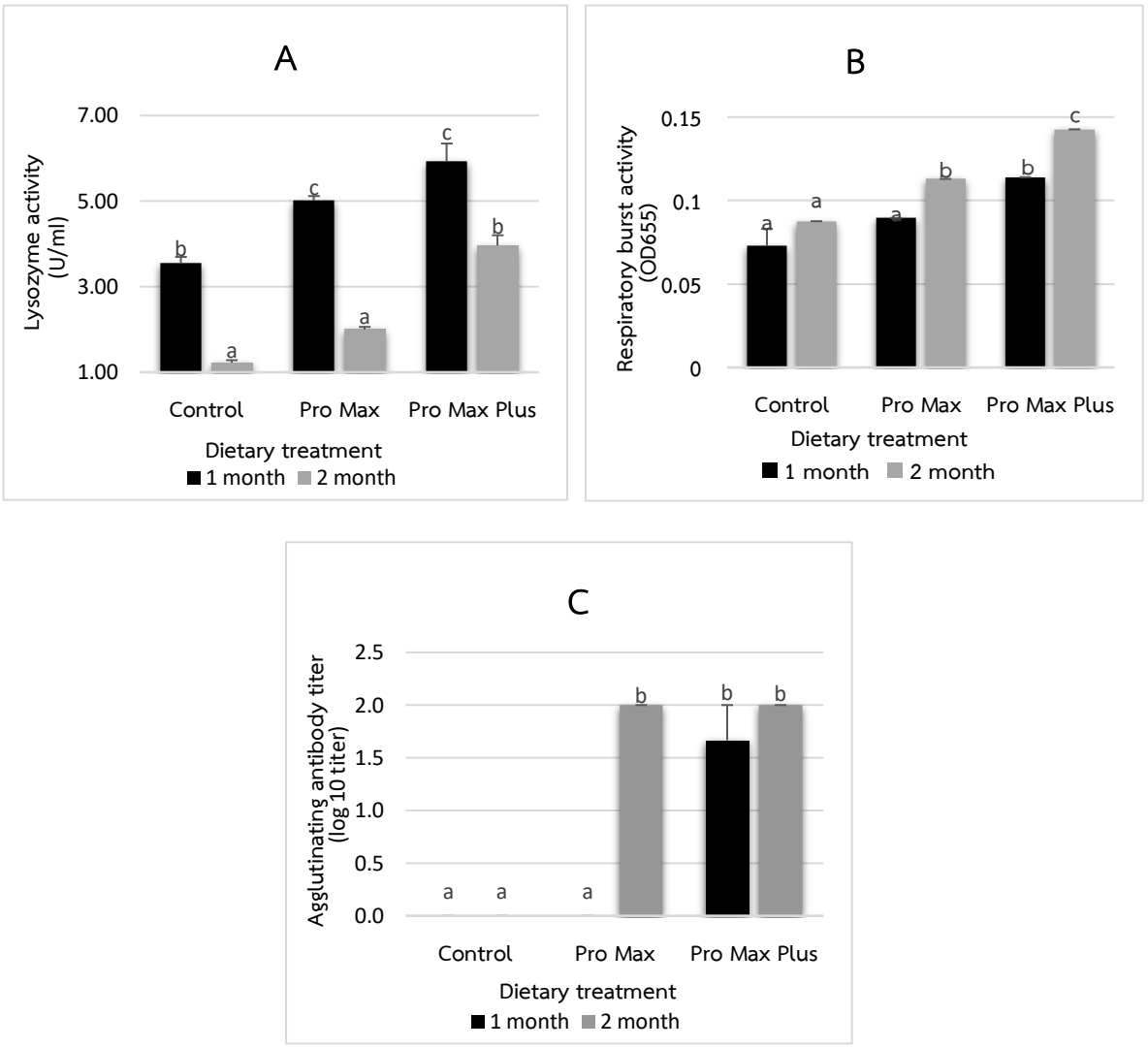


Figure 1. Lysozyme activity (A), respiratory burst activity (B), and agglutinating antibody titer (C) in Nile tilapia fed the Control, Pro Max, and Pro Max Plus diets for one and two months. Values are presented as mean ± SE. Different letters indicate significant differences among dietary treatments at the same sampling time (p <0.05)

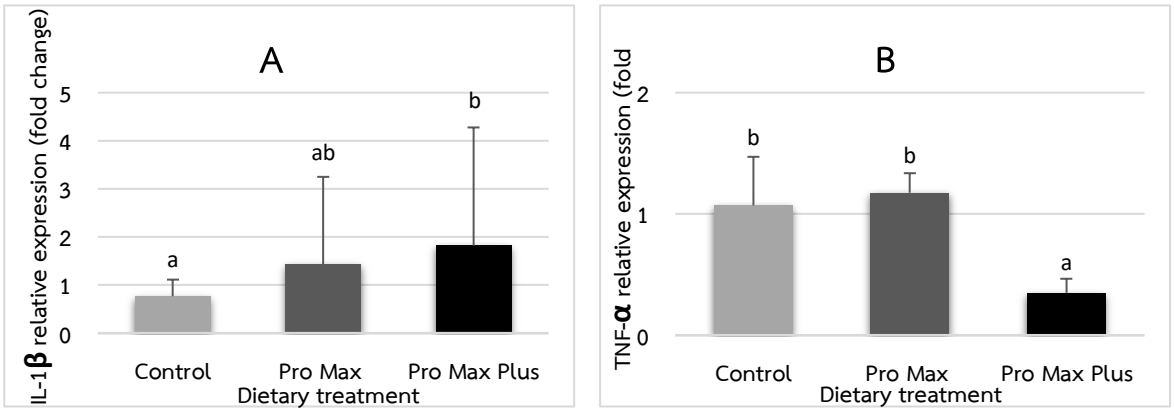


Figure 2. Relative expression of the immune-related genes IL-1β (A) and TNF-α (B) in Nile tilapia fed the Control, Pro Max, and Pro Max Plus diets. Gene expression was normalized to β-actin and calculated using the $2^{-\Delta\Delta Ct}$ method. Values are presented as mean ± SE. Different letters indicate significant differences among dietary treatments ($p < 0.05$)

Table 5. Economic analysis of Nile tilapia fed different experimental diets

Parameters	control	Pro Max	Pro Max Plus
Total cost (Baht/kg diet)	31.50 ± 0.00^{a}	42.93 ± 0.00^{b}	43.93 ± 0.00^{b}
Feeding cost (Baht/kg fish gain)	40.81 ± 0.77^{a}	56.10 ± 1.50^{b}	36.69 ± 0.78^{a}
Benefit-Cost Ratio	1.72 ± 0.03^{b}	1.25 ± 0.03^{a}	1.91 ± 0.04^{c}
Net profit (Baht)	23.31 ± 1.07^{a}	11.06 ± 2.54^{b}	32.87 ± 1.49^{c}
Return on investment (%)	71.65 ± 3.29^{b}	24.95 ± 3.31^{a}	62.51 ± 4.13^{c}
Profit margin per fish (Baht/fish)	1.55 ± 0.74^{b}	0.74 ± 0.98^{a}	2.19 ± 0.10^{c}

Note. Control, basal diet without supplementation; Pro Max, basal diet supplemented with a vitamin–mineral premix at 5 g/kg feed; Pro Max Plus, basal diet supplemented with a probiotic-containing vitamin–mineral premix at 5 g/kg feed. Values are presented as mean ± SE. Different superscript letters within the same row indicate significant differences among treatments ($p < 0.05$). Economic analysis was based on market prices during the experimental period. Supplements were incorporated at 5 g/kg feed (0.5%, w/w). Feeding cost per kg fish gain was calculated based on total feed intake and total weight gain. Revenue was calculated based on a Nile Tilapia selling price of 70 Baht/kg

4. Discussion

4.1 Growth performance and survival rate

The improved growth performance observed in the Pro Max Plus group may be attributed to the complementary effects of probiotics, vitamins, and minerals on nutrient utilization and physiological function. In the present study, fish fed Pro Max Plus achieved a weight gain of 68.80 ± 0.43 g, representing an approximately 12.1% increase over the control group (61.38 ± 1.18 g). These findings are consistent with previous studies demonstrating that probiotic supplementation enhances growth performance in Nile tilapia. For example, Rahayu et al. (2024) reported that dietary probiotic supplementation increased final weight by approximately 12 – 18% and significantly improved feed utilization compared with the control treatment. Similarly, Sahu et al. (2008) observed that probiotic-fed fish exhibited approximately 15 – 20% greater weight gain than unsupplemented fish, which was attributed to improved intestinal microbial balance and enhanced nutrient digestion. These improvements are likely mediated through the ability of probiotics to modulate gut microbiota, increase digestive enzyme activity, and improve nutrient absorption

efficiency. In particular, *Bacillus* spp. have been shown to stimulate endogenous digestive enzymes, including amylase and protease, thereby enhancing feed digestibility and nutrient utilization (Bahaddad et al., 2023; El-Saadony et al., 2014). However, condition factors did not differ significantly among treatments, indicating that Pro Max Plus supplementation did not significantly affect this parameter.

The higher survival rates observed in the Pro Max Plus group may also be associated with improved immune competence and physiological stability. Similar findings have been reported by Ashraf & Shah (2014), who demonstrated that probiotic supplementation increased survival by approximately 8 – 12% under culture conditions. Likewise, Goudarzi et al. (2024) reported significantly higher survival and enhanced disease resistance in probiotic-fed fish compared with untreated controls. These beneficial effects are primarily attributed to competitive exclusion of pathogenic microorganisms, maintenance of intestinal microbial homeostasis, production of antimicrobial metabolites, and stimulation of innate immune responses (Lutgendorff et al., 2008; Van Zyl et al., 2020; Panase et al., 2023). Collectively, these mechanisms reduce physiological stress and improve the resilience of Nile tilapia to environmental and pathogenic challenges, thereby contributing to improved survival during culture.

4.2 Feed utilization and efficiency parameters

The improved feed utilization efficiency in the Pro Max Plus group suggests that probiotic supplementation may enhance nutrient digestion and utilization. The significant reduction in FCR suggests an optimized conversion of dietary nutrients into somatic growth. This improvement may be associated with enhanced nutrient utilization, as previously reported in fish receiving probiotic supplementation (Adeoye et al., 2016; Wang & Ji, 2019; Yang et al., 2025).

The inverse relationship observed between feed intake and growth performance in Pro Max Plus may indicate improved nutrient utilization efficiency. This is consistent with Ramos et al. (2017), who reported that probiotic administration in Nile tilapia promotes intestinal integrity by increasing villi height, thereby expanding the absorptive surface area. Furthermore, vitamins and minerals may have contributed to the improved growth and feed utilization observed in the probiotic-supplemented group. The higher feed efficiency observed in the Pro Max Plus group may reflect improved feed utilization under the experimental conditions.

4.3 Immune responses and gene expression

These findings suggest that the combined supplementation of vitamins, minerals, and probiotics may enhance the immune responses of Nile tilapia. The lysozyme, a key enzyme for degrading Gram-positive bacterial cell walls, is a recognized indicator of heightened disease resistance (Ferraboschi et al., 2021; Saurabh & Sahoo, 2008; Zhydzetski et al., 2024). The augmented respiratory burst and lysozyme activities likely stem from probiotic-driven stimulation of leucocytes, leading to increased phagocytic capacity and reactive oxygen species (ROS) production (Martins et al., 2003; Wang et al., 2018).

Interestingly, the gene expression results suggest a controlled inflammatory response; the upregulation of IL-1β in Pro Max Plus points to an active recruitment of immune cells (Ticinesi et al., 2016), while the downregulation of TNF- α may indicate a mechanism to prevent excessive inflammation, which can be detrimental to host tissues. This is consistent with findings by (Cano-Lozano et al., 2022; Pirarat et al., 2006), who reported that probiotics like *Lactobacillus* spp. can modulate cytokine expression to balance the immune response in Nile tilapia (Panase et al., 2023). The robust development of antibody titers in Pro Max Plus further confirms that this dietary supplement bridges innate and adaptive immunity. Collectively, these results suggest that Pro Max Plus enhanced the immediate defensive enzyme activities while modulating molecular immune response, providing better overall health protection for Nile tilapia.

4.4 Economic Sustainability

The Pro Max Plus diet demonstrated superior economic performance despite its slightly higher feed cost per kilogram, indicating that improvements in biological performance outweighed the additional investment in feed additives. The enhanced economic return was primarily attributable to improved feed utilization and growth performance, which reduced feed expenditure per unit of fish biomass produced. Similar observations have been reported in previous studies evaluating functional feed additives in aquaculture. For example, Dawood et al. (2018) reported that probiotic supplementation in Nile tilapia reduced feed conversion ratio by approximately 10 – 15%, resulting in an increase in net profit of approximately 12–18% compared with the control treatment. Likewise, Hai (2015) summarized several studies demonstrating that probiotic supplementation in freshwater fish generally increased economic returns by 10–25%, primarily through improved growth, higher survival, and reduced feed costs. In whiteleg shrimp (*Litopenaeus vannamei*), dietary probiotics have been shown to improve benefit–cost ratios by approximately 8–20% through enhanced feed efficiency and survival under commercial farming conditions (Newaj-Fyzul et al., 2014). Similar economic benefits have also been reported in common carp and other cultured fish species, where probiotic supplementation improved feed conversion efficiency and increased net production value relative to feed costs (Sharifuzzaman & Austin, 2017).

The present findings are consistent with these reports. Although the probiotic-fortified diet had the highest feed cost, its superior growth performance and feed conversion efficiency resulted in a higher benefit–cost ratio (BCR) and net profit. In the present study, the Pro Max Plus treatment achieved a BCR of 1.91 and a net profit of 32.87 ± 1.49 Baht, both of which were higher than those of the control and Pro Max treatments. The ROI of the Pro Max Plus treatment was 62.51 ± 4.13%. This improvement is likely associated with the complementary actions of probiotics and micronutrients, which enhance digestive enzyme activity, improve nutrient digestibility, promote intestinal microbial balance, and increase nutrient utilization efficiency (Hai, 2015; Newaj-Fyzul et al., 2014). As a result, fish reached marketable size with lower feed input per unit of weight gain, thereby reducing production costs and improving farm profitability.

5. Conclusions and recommendations

5.1 Conclusions

This study demonstrated that dietary supplementation with a probiotic-containing vitamin–mineral premix positively influenced growth performance, feed efficiency, immune responses, and economic returns in Nile tilapia. Among the dietary treatments, the Pro Max Plus formulation produced the most favorable outcomes, including significantly improved weight gain, specific growth rate, feed conversion ratio, and survival performance, indicating enhanced nutrient utilization and production performance.

The probiotic supplementation also contributed to strengthening innate immune function, as reflected by increased lysozyme activity, enhanced respiratory burst responses, and modulation of immune-related gene expression, particularly IL-1β and TNF-α. These findings suggest that probiotic inclusion may improve host defense mechanisms while modulating inflammatory responses in Nile tilapia.

From an economic perspective, although the Pro Max Plus diet involved a relatively higher production cost, improvements in growth performance and survival compensated for this investment, resulting in superior economic efficiency as evidenced by a higher benefit–cost ratio and net return. Therefore, the incorporation of Pro Max Plus into Nile tilapia diets may represent a practical and economically sustainable strategy for improving aquaculture productivity.

These findings support the study objective that probiotic-containing vitamin–mineral supplementation can enhance growth, immunity, and production efficiency in Nile tilapia culture. However, further studies are recommended to investigate the long-term effects of supplementation under commercial farming conditions, optimize dosage levels, and clarify the underlying molecular and microbiome-related mechanisms responsible for the observed improvements in fish health and performance.

5.2 Recommendations

5.2.1 Further studies should be conducted to investigate the long-term effects of this supplementation under actual commercial farming conditions to evaluate its efficacy and consistency across variable environments.

5.2.2 Future research should focus on clarifying the underlying molecular and gut microbiome-related mechanisms responsible for immune stimulation and nutrient utilization, as well as optimizing dosage levels for different growth stages of Nile tilapia.

6. Acknowledgements

This research was supported by a research grant from the Agricultural Research and Academic Promotion Office, Maejo University, fiscal year 2025, with support from the National Research Council of Thailand (NRCT).

7. References

Adeoye, A. A., Yomla, R., Jaramillo-Torres, A., Rodiles, A., Merrifield, D. L., & Davies, S. J. (2016). Combined effects of exogenous enzymes and probiotic on Nile tilapia (*Oreochromis niloticus*) growth, intestinal morphology and microbiome. Aquaculture, 463, 61-70. https://doi.org/10.1016/j.aquaculture.2016.05.028

Amenyogbe, E. (2023). Application of probiotics for sustainable and environment-friendly aquaculture management-A review. Cogent Food and Agriculture, 9(1), 2226425. https://doi.org/10.1080/23311932.2023.2226425

Ashraf, R., & Shah, N. P. (2014). Immune system stimulation by probiotic microorganisms. Critical reviews in food science and nutrition, 54(7), 938-956. https://doi.org/10.1080/10408398.2011.619671

Bahaddad, S. A., Almalki, M. H., Alghamdi, O. A., Sohrab, S. S., Yasir, M., Azhar, E. I., & Chouayekh, H. (2023). Bacillus species as direct-fed microbial antibiotic alternatives for monogastric production. Probiotics and antimicrobial proteins, 15, 1-16. https://doi.org/10.1007/s12602-022-09909-5

Cano-Lozano, J. A., Diaz, L. M. V., Bolivar, J. F. M., Hume, M. E., & Pardo, R. Y. R. (2022). Probiotics in tilapia (*Oreochromis niloticus*) culture: Potential probiotic *Lactococcus lactis* culture conditions. Journal of bioscience and bioengineering, 133(3), 187-194. https://doi.org/10.1016/j.jbiosc.2021.11.004

Chadzinska, M., Savelkoul, H. F., & Verburg-van Kemenade, B .L. (2009). Morphine affects the inflammatory response in carp by impairment of leukocyte migration. Developmental and Comparative Immunology, 33(1), 88-96. https://doi.org/10.1016/j.dci.2008.07.004

Chandan, R. C., Parry Jr, R. M., & Shahani, K. M. (1965). Purification and some properties of bovine milk lysozyme. Biochimica et Biophysica Acta (BBA)-Enzymology and Biological Oxidation, 110(2), 389-398. https://doi.org/10.1016/S0926-6593(65)80046-7

Dawood, M.A., Koshio, S., & Esteban, M.Á. (2018). Beneficial roles of feed additives as immunostimulants in aquaculture: a review. Reviews in Aquaculture, 10(4), 950-974. https://doi.org/10.1111/raq.12209

El-Saadony, M. T., Alagawany, M., Patra, A. K., Kar, I., Tiwari, R., Dawood, M. A., & Abdel-Latif, H. M. (2021). The functionality of probiotics in aquaculture: An overview. Fish and shellfish immunology, 117, 36-52. https://doi.org/10.1016/j.fsi.2021.07.007

Ferraboschi, P., Ciceri, S., and Grisenti, P. (2021). Applications of lysozyme, an innate immune defense factor, as an alternative antibiotic. Antibiotics, 10(12), 1534. https://doi.org/10.3390/antibiotics10121534

Goudarzi, F., Kiani, A., Nami, Y., Shahmohammadi, A., Mohammadalipour, A., Karami, A., & Haghshenas, B. (2024). Potential probiotic *Lactobacillus delbrueckii* subsp. lactis KUMS-Y33 suppresses adipogenesis and promotes osteogenesis in human adipose-derived mesenchymal stem cell. Scientific Reports, 14, 9689. https://doi.org/10.1038/s41598-024-60061-2

Hai, N. V. (2015). The use of probiotics in aquaculture. Journal of applied microbiology, 119(4), 917-935. https://doi.org/10.1111/jam.12886

Hancz, C. (2022). Application of probiotics for environmentally friendly and sustainable aquaculture: a review. Sustainability, 14(22), 15479. https://doi.org/10.3390/su142215479

Hassan, A., Ahmed, I., Reshi, Q.M., & Hassan, P. (2025). Role of fat-soluble vitamins in fish nutrition. In A. A. Editor (Ed.), Aquaculture: Enhancing food security and nutrition (pp. 203–224). Springer Nature. https://doi.org/10.1007/978-3-031-92858-1_10

Hill, C., Guarner, F., Reid, G., Gibson, G.R., Merenstein, D.J., Pot, B., & Sanders, M.E. (2014). The International Scientific Association for Probiotics and Prebiotics consensus statement on the scope and appropriate use of the term probiotic. Nature reviews Gastroenterology and hepatology, 11, 506-514. https://doi:10.1038/nrgastro.2014.66

Kaew-on, S., Areechon, N., & Wanchaitanawong, P. (2016). Effects of *Pediococcus pentosaceus* PKWA-1 and *Bacillus subtilis* BA04 on growth performances, immune responses and disease resistance against *Aeromonas hydrophila* in Nile Tilapia (*Oreochromis niloticus* Linn.). Chiang Mai Journal of Science, 43, 997-1006.

Kayansamruaj, P., Pirarat, N., Hirono, I., & Rodkhum, C. (2014). Increasing of temperature induces pathogenicity of *Streptococcus agalactiae* and the up-regulation of inflammatory related genes in infected Nile tilapia (*Oreochromis niloticus*). Veterinary microbiology, 172(1-2), 265-271. https://doi.org/10.1016/j.vetmic.2014.04.013

Khan, M.A., Zafar, N., & Naz, S. (2025). Nutritional Strategies for Improving Growth and Health in Aquaculture. Aquaculture: Enhancing Food Security and Nutrition, *1*. https://doi.org/10.1007/978-3-031-92858-1_1

Kuebutornye, F. K. A., Abarike, E.D., & Lu, Y. (2019). A review on the application of Bacillus as probiotics in aquaculture, Fish & Shellfish Immunology, 87, 820-828, https://doi.org/10.1016/j.fsi.2019.02.010

Liu, C.H., Chiu, C.S., Ho, P.L., & Wang, S.W. (2009). Improvement in the growth performance of white shrimp, *Litopenaeus vannamei*, by a protease‐producing probiotic, *Bacillus subtilis* E20, from natto, *Journal of Applied Microbiology*, 107(3), 1031–1041, https://doi.org/10.1111/j.1365-2672.2009.04284.x

Lutgendorff, F., Akkermans, L.M., & Soderholm, J.D. (2008). The role of microbiota and probiotics in stress-induced gastrointestinal damage. Current molecular medicine, 8(4), 282-298. https://doi.org/10.2174/156652408784533779

Martins, P. S., Kallas, E.G., Neto, M. C., Dalboni, M. A., Blecher, S., & Salomão, R. (2003). Upregulation of reactive oxygen species generation and phagocytosis, and increased apoptosis in human neutrophils during severe sepsis and septic shock. Shock, 20(3), 208-212. https://doi: 10.1097/01.shk.0000079425.52617.db

Mohammed, E. A. H., Ahmed, A. E. M., Kovács, B., & Pál, K. (2025). The Significance of Probiotics in Aquaculture: A Review of Research Trend and Latest Scientific Findings. Antibiotics, 14(3), 242. https://doi.org/10.3390/antibiotics14030242

Moreira, M., Schrama, D., Farinha, A. P., Cerqueira, M., Raposo de Magalhaes, C., Carrilho, R., & Rodrigues, P. (2021). Fish pathology research and diagnosis in aquaculture of farmed fish; a proteomics perspective. Animals, 11(1): 125. https://doi.org/10.3390/ani11010125

Mukhtar, S., Hussain, S. M., Ali, S., Yilmaz, E., Shahzad, M. M., Munir, M., & Rashid, E. (2025). Promoting sustainable aquaculture: exploring antibiotic alternatives to fight against pathogens. International Aquatic Research, 17(1). https://doi.org/10.22034/iar.2025.2008914.1732

Newaj-Fyzul, A., Al-Harbi, A. H., & Austin, B. (2014). Developments in the use of probiotics for disease control in aquaculture. Aquaculture, 431(1-11). https://doi.org/10.1016/j.aquaculture.2013.08.026

Olmos, J., Acosta, M., & Mendoza, G. (2020). *Bacillus subtilis,* an ideal probiotic bacterium to shrimp and fish aquaculture that increase feed digestibility, prevent microbial diseases, and avoid water pollution. Archives of Microbiology 202, 427–435 https://doi.org/10.1007/s00203-019-01757-2

Panase, A., Thirabunyanon, M., Promya, J., Palic, D., & Chitmanat, C. (2023). Synergistic Effects of Fructooligosaccharide and *Bacillus subtilis* Dietary Supplementation on Growth, Innate Immune Responses, and Protection against *Streptococcus agalactiae* in Juvenile Nile Tilapia (*Oreochromis niloticus*). Chiang Mai Journal of Science, 50(5). https://doi.org/: 10.12982/CMJS.2023.050

Pirarat, N., Kobayashi, T., Katagiri, T., Maita, M., & Endo, M. (2006). Protective effects and mechanisms of a probiotic bacterium *Lactobacillus rhamnosus* against experimental *Edwardsiella tarda* infection in tilapia (*Oreochromis niloticus*). Veterinary immunology and immunopathology, 113(3-4), 339-347. https://doi.org/10.1016/j.vetimm.2006.06.003

Pohlenz, C., & Gatlin III, D. M. (2014). Interrelationships between fish nutrition and health. Aquaculture, 431, 111-117. https://doi.org/10.1016/j.aquaculture.2014.02.008

Pradeepkiran, J. A. (2019). Aquaculture role in global food security with nutritional value: a review. Translational Animal Science, 3(2), 903-910. https://doi.org/10.1093/tas/txz012

Rahayu, S., Amoah, K., Huang, Y., Cai, J., Wang, B., Shija, V. M., & Jiang, M. (2024). Probiotics application in aquaculture: its potential effects, current status in China and future prospects. Frontiers in Marine Science, 11, 1455905. https://doi.org/10.3389/fmars.2024.1455905

Ramos, M. A., Batista, S., Pires, M. A., Silva, A. P., Pereira, L. F., Saavedra, M.J., & Rema, P. (2017). Dietary probiotic supplementation improves growth and the intestinal morphology of Nile tilapia. Animal, 11(8), 1259-1269 https://doi.org/10.1017/S1751731116002792

Ringø, E. Z. Z. V., Zhou, Z., Vecino, J. G., Wadsworth, S., Romero, J., Krogdahl, Å., & Merrifield, D.L. (2016). Effect of dietary components on the gut microbiota of aquatic animals. A never–ending story? Aquaculture nutrition, 22(2), 219-282. https://doi.org/10.1111/anu.12346

Sahu, M. K., Swarnakumar, N. S., Sivakumar, K., Thangaradjou, T., & Kannan, L. (2008). Probiotics in aquaculture: importance and future perspectives. Indian journal of microbiology, 48(3), 299-308. https://doi.org/10.1007/s12088-008-0024-3

Saras, T. (2023). Unlocking the power of vitamins: A comprehensive guide to optimal health. Tiram Media.

Saurabh, S., & Sahoo, P. K. (2008). Lysozyme: an important defence molecule of fish innate immune system. Aquaculture research, 39(3), 223-239. https://doi.org/10.1111/j.1365-2109.2007.01883.x

Secombes, C. J. (1990). Isolation of salmonid macrophages and analysis of their killing activity. Techniques in fish immunology, 1, 137-163.

Shanahan, F. (2010). Probiotics in perspective. Gastroenterology, 139(6), 1808-1812. https://doi: 10.1053/j.gastro.2010.10.025

Sharifuzzaman, S. M., & Austin, B. (2017). Probiotics for disease control in aquaculture. In B. Austin & A. Newaj-Fyzul (Eds.), *Diagnosis and control of diseases of fish and shellfish*. Wiley. https://doi.org/10.1002/9781119152125.ch8

Sihag, R. C., & Sharma, P. (2012). Probiotics: the new ecofriendly alternative measures of disease control for sustainable aquaculture. Journal of Fisheries and Aquatic Science, 7(2), 72-103. https://doi: 10.3923/jfas.2012.72.103

Sundström, J. F., Albihn, A., Boqvist, S., Ljungvall, K., Marstorp, H., Martiin, C., & Magnusson, U. (2014). Future threats to agricultural food production posed by environmental degradation, climate change, and animal and plant diseases–a risk analysis in three economic and climate settings. Food Security, 6(2), 201-215. https://doi.org/10.1007/s12571-014-0331-y

Ticinesi, A., Meschi, T., Lauretani, F., Felis, G., Franchi, F., Pedrolli, C., & Maggio, M. (2016). Nutrition and inflammation in older individuals: focus on vitamin D, n-3 polyunsaturated fatty acids and whey proteins. Nutrients, 8(4), 186.https://doi.org/10.3390/nu8040186

Van Zyl, W. F., Deane, S. M., & Dicks, L. M. (2020). Molecular insights into probiotic mechanisms of action employed against intestinal pathogenic bacteria. Gut microbes, 12(1), 1831339. https://doi.org/10.1080/19490976.2020.1831339

Wang, A. R., Ran, C., Ringø, E., & Zhou, Z. G. (2018). Progress in fish gastrointestinal microbiota research. Reviews in Aquaculture, 10(3), 626-640. https://doi.org/10.1111/raq.12191

Wang, J., & Ji, H. (2019). Influence of probiotics on dietary protein digestion and utilization in the gastrointestinal tract. Current Protein and Peptide Science, 20(2), 125-131. https://doi.org/10.2174/1389203719666180517100339

Wu, S., Pan, M., Zan, Z., Jakovlić, I., Zhao, W., Zou, H., & Wang, G. (2024). Regulation of lipid metabolism by gut microbiota in aquatic animals. Reviews in Aquaculture, 16(1), 34-46.https://doi.org/10.1111/raq.12819

Yang, Y., Kumrungsee, T., Okazaki, Y., Watanabe, T., Inoue, J., Iguchi, T., & Kato, N. (2025). Potential roles of exogenous proteases and lipases as prebiotics. Nutrients, 17(5), 924. https://doi.org/10.3390/nu17050924

Yarahmadi, P., Miandare, H. K., Farahmand, H., Mirvaghefi, A., & Hoseinifar, S.H. (2014). Dietary fermentable fiber upregulated immune related genes expression, increased innate immune response and resistance of rainbow trout (*Oncorhynchus mykiss*) against *Aeromonas hydrophila*. Fish and shellfish immunology, 41(2), 326-331. https://doi.org/10.1016/j.fsi.2014.09.007

Zhydzetski, A., Głowacka-Grzyb, Z., Bukowski, M., Żądło, T., Bonar, E., & Władyka, B. (2024). Agents targeting the bacterial cell wall as tools to combat gram-positive pathogens. Molecules, 29(17), 4065. https://doi.org/10.3390/molecules29174065

การเพิ่มประสิทธิภาพตัวจำแนกการยกเลิกบริการในแพลตฟอร์มวิดีโอออนไลน์แบบมีค่าใช้จ่ายด้วยการผสมผสานโมเดลการเรียนรู้แบบรวม

Optimizing Service Cancellation Classifiers for Subscription-Based Online Video Platforms through Ensemble Learning

จักรินทร์ สันติรัตนภักดี[1*]

Chakkarin Santirattanaphakdi[1*]

[1]สาขาวิชาเทคโนโลยีธุรกิจดิจิทัล คณะบริหารธุรกิจ มหาวิทยาลัยวงษ์ชวลิตกุล จังหวัดนครราชสีมา

[1] Department of Digital Business Technology, Faculty of Business Administration, Vongchavalitkul University, Nakhon Ratchasima Province

[*]Corresponding Author: chakkarin_san@vu.ac.th

Received: June 4, 2026 **Revised:** August 13, 2026 **Accepted:** August 20, 2026

บทคัดย่อ

งานวิจัยนี้มีวัตถุประสงค์เพื่อเพิ่มประสิทธิภาพตัวจำแนกการยกเลิกบริการในแพลตฟอร์มวิดีโอออนไลน์แบบมีค่าใช้จ่าย โดยมุ่งเน้นการบูรณาการข้อมูลพฤติกรรมที่ผู้ใช้รายงานด้วยตนเองผ่านเทคนิคการเรียนรู้ของเครื่องแบบรวม เพื่อลดข้อจำกัดของโมเดลเชิงเดี่ยว และเพิ่มความทนทานในการพยากรณ์บนชุดข้อมูลที่มีความซับซ้อนและไม่สมดุล กระบวนการวิจัยประกอบด้วยการรวบรวมข้อมูลจากผู้ใช้งานจำนวน 10,983 ราย การจัดการปัญหาความไม่สมดุลของคลาสด้วยเทคนิค SMOTE และการคัดเลือกคุณลักษณะแบบสองขั้นตอนด้วยเทคนิค Boruta และ RFE จนได้ 10 ปัจจัยสำคัญ โดยปัจจัยหลักที่มีอิทธิพลต่อการยกเลิกบริการสูงที่สุด 3 อันดับแรก คือ จำนวนช่องที่กดติดตาม (Subscribed) จำนวนเนื้อหาที่รับชม (ContentCount) และระยะเวลาสมาชิก (Period) เมื่อพิจารณาประสิทธิภาพของโมเดล พบว่า LightGBM เป็นโมเดลฐานเชิงเดี่ยวที่มีประสิทธิภาพสูงสุดทั้งก่อนและหลังการปรับแต่งพารามิเตอร์ โดยให้ค่าความถูกต้องเท่ากับ 0.8157 อย่างไรก็ดี เมื่อผสมผสานโมเดลการเรียนรู้แบบรวม พบว่า โมเดลกลุ่ม Voting-based สามารถยกระดับค่าความถูกต้องรวมขึ้นสู่ระดับสูงสุดเท่ากับ 0.8204 ขณะที่โมเดลกลุ่ม Mixed-based ซึ่งประยุกต์ใช้การถดถอยโลจิสติกเป็นโมเดลอภิมานในชั้นตัดสินผลลัพธ์ มีความสามารถในการตรวจจับกลุ่มเสี่ยงได้อย่างครอบคลุมที่สุด ด้วยค่าการเรียกคืน และค่า AUC-ROC สูงสุดเท่ากับ 0.8057 และ 0.8833 ตามลำดับ งานวิจัยนี้จึงเสนอแนวทางการเลือกใช้โมเดลให้สอดคล้องกับกลยุทธ์การรักษาลูกค้า โดยโมเดลกลุ่ม Mixed-based เหมาะสำหรับกลยุทธ์รักษาลูกค้าโดยใช้ต้นทุนต่ำที่ต้องการดักจับกลุ่มเสี่ยงให้ครอบคลุม และโมเดลกลุ่ม Voting-based เหมาะสำหรับกลยุทธ์รักษาลูกค้าแบบใช้ต้นทุนสูงที่ต้องการความแม่นยำในระดับบุคคล เพื่อบริหารจัดการงบประมาณและทรัพยากรทางการตลาดของธุรกิจแพลตฟอร์มสื่อบันเทิงออนไลน์ได้อย่างคุ้มค่าและยั่งยืน

คำสำคัญ: การเพิ่มประสิทธิภาพตัวจำแนก, การยกเลิกบริการ, การเรียนรู้ของเครื่อง, แพลตฟอร์มวิดีโอออนไลน์, โมเดลการเรียนรู้แบบรวม

Abstract

This research aims to optimize service cancellation classifiers for subscription-based online video platforms. It focuses on integrating self-reported user behavior data through ensemble learning techniques to mitigate the limitations of single-base models and enhance predictive robustness on complex and imbalanced datasets. The methodology encompasses data collection from 10,983 users, the use of the Synthetic Minority Over-sampling Technique (SMOTE) to address class imbalance, and a two-stage feature selection process using Boruta and Recursive Feature Elimination (RFE) to identify 10 critical predictors. The three primary determinants with the greatest influence on service cancellation are the number of subscribed channels (Subscribed), the volume of content consumed (ContentCount), and membership duration

(Period). In terms of model performance, LightGBM emerged as the most effective single-base model both before and after hyperparameter tuning, yielding an accuracy of 0.8157. However, after ensemble learning frameworks were incorporated, the voting-based ensemble model increased overall accuracy to a maximum of 0.8204. Meanwhile, the mixed-based ensemble model, which uses logistic regression as the meta-model at the decision layer, demonstrated the most comprehensive ability to identify at-risk users, achieving the highest recall and Area Under the Receiver Operating Characteristic Curve (AUC-ROC) values of 0.8057 and 0.8833, respectively. Consequently, this research proposes a model-selection framework aligned with customer retention strategies: the mixed-based model is best suited to low-cost retention strategies that require comprehensive identification of at-risk users, whereas the voting-based model is appropriate for high-cost retention strategies that require high precision at the individual level, thereby enabling the cost-effective and sustainable management of marketing budgets and resources in the online media and entertainment platform industry.

Keywords: Ensemble learning, Machine learning, Online video platforms, Classifier optimization, Service cancellation

1. Introduction

The media and entertainment industry in Thailand is undergoing a comprehensive transition into the digital era. According to a report by PwC Thailand (2025), the market value is projected to exceed THB 700 billion and continue expanding to THB 788 billion by 2029. This growth is primarily driven by over-the-top (OTT) media services, whose value has increased more than sixfold since 2020. This shift closely aligns with the behavior of Thai consumers who use YouTube as a substitute for traditional linear television. The trend is particularly pronounced among Generation Z, whose daily usage rate reaches 71.35%. Conversely, although Baby Boomers predominantly retain traditional television-viewing habits, their daily engagement with YouTube remains substantial at over 51.6% (Forge et al., 2024). YouTube now functions not merely as an online video repository but also as an initial gateway for discovering personalized content based on individual interests (Lotz, 2022).

Furthermore, nearly half of the respondents had used the platform for more than three years, with an average viewing duration of 1–2 hours per day. Awareness of the premium service was generated predominantly through the platform's internal advertising mechanisms. Nevertheless, attitudes toward advertising and the underlying pricing structure were critical determinants of service adoption. Most respondents identified mid-roll advertisements as the primary source of user dissatisfaction. At the same time, pricing presented a significant barrier, as approximately 46% of consumers perceived the current subscription rates as excessive relative to those of competitors in the streaming market (Sridevi & Gowtham, 2021). Anticipated future price increases further contributed to this reluctance, ultimately causing subscription decisions to stagnate.

In such a volatile landscape, the ability to accurately predict consumer cancellation behavior is critical. Developing advanced predictive models provides a strategic advantage by enabling service providers to move beyond reactive measures toward proactive intervention. By identifying at-risk cohorts with high precision, providers can design more effective and targeted retention campaigns and allocate marketing resources more efficiently to maximize customer lifetime value. Consequently, the literature has increasingly focused on using machine learning and ensemble models to improve service cancellation classification.

Although contemporary research has achieved notable success using standardized public repositories, such as telecommunications churn datasets from the UCI Machine Learning Repository and e-commerce and banking churn collections from Kaggle, reliance on these sources may create a critical gap when models are applied to empirical, self-reported data from real-world users. Although these established benchmarks facilitate algorithmic comparison, they often lack localized context and platform-specific behavioral nuances, such as granular viewing frequencies and transaction-related friction points inherent in contemporary online media ecosystems. Furthermore, single-base models frequently suffer from bias or variance caused by overfitting to static training environments, which ultimately degrades their performance in practical settings. Consequently, these models may lack the flexibility to adapt to the highly dynamic and continually evolving demands of online content consumers and may not comprehensively capture all dimensions of consumer behavior. Online platform service providers must therefore respond to rapidly changing consumer behavior, particularly within premium video-streaming subscription models, where users can terminate their services at any time. This challenge motivates the present research, which focuses on optimizing service cancellation classifiers and analyzing user characteristics specific to premium online video platforms.

In many real-world applications, machine learning datasets are characterized by substantial class imbalance, in which "normal" instances greatly outnumber "abnormal" or "interesting" instances. Standard classification algorithms typically struggle in such scenarios because their objective is to maximize overall accuracy, often resulting in a bias toward the majority class and poor predictive performance for the minority class of interest. To mitigate these challenges, previous studies have explored various resampling approaches, such as random undersampling and random oversampling through replication. Although undersampling can produce a compact, balanced training set, it may discard useful examples that are critical to model generalization. In contrast, random oversampling through simple replication often leads to overfitting because it emphasizes specific, restricted regions of the feature space rather than expanding the decision boundary.

To address class imbalance, previous studies have applied oversampling approaches such as SMOTE to establish more robust decision boundaries. Unlike simple replication, SMOTE operates in the feature space by generating synthetic minority-class examples through interpolation between neighboring instances. This method encourages more general minority-class decision regions, thereby reducing overfitting and enhancing the model's generalization capacity. Consequently, the literature has increasingly combined SMOTE with machine learning and ensemble methods to improve service cancellation classification.

Previous studies have classified service cancellation behavior using various machine learning techniques, ranging from standalone classifiers to complex integrated architectures. Specifically, Maretta & Permai (2021) used boosted trees with SMOTE-Tomek to examine bank churn and found that a standalone LightGBM model achieved an accuracy of 91.40%. By contrast, studies adopting ensemble paradigms have demonstrated substantially enhanced classification performance. Pustokhina et al. (2023) integrated an improved SMOTE method with an optimal weighted extreme learning machine (ISMOTE-OWELM) and achieved 94.00% accuracy. Furthermore, Xu et al. (2021) constructed a two-level stacking model comprising XGBoost and base classifiers, achieving 98.09% accuracy. Manohar et al. (2021) implemented majority voting in the e-commerce sector and achieved 94.00% accuracy, whereas Ramesh et al. (2022) hybridized artificial neural networks with random forests and achieved 90.30% accuracy. Finally, Beeharry & Fokone (2022) developed a flexible two-layer voting ensemble that achieved 76.20% accuracy.

A comparative summary of these predictive methods and their respective performance metrics is presented in Table 1. The comparison shows that, although standalone models are computationally efficient, ensemble and hybrid approaches consistently provide the robustness required for high-accuracy churn classification by mitigating the inherent bias and variance of single-base learners. Thus, ensemble learning is a highly effective strategy, particularly when combined with data balancing and parameter optimization.

Table 1. Summary of past studies on service cancellation and churn prediction

Study	Domain	Methodology	Performance (Accuracy)
Maretta & Permai (2021)	Banking	Standalone (LightGBM)	91.40%
Pustokhina et al. (2023)	Telecom	Hybrid (ISMOTE-OWELM)	94.00%
Xu et al. (2021)	Telecom	Ensemble (Stacking)	98.09%
Manohar et al. (2021)	E-commerce	Ensemble (Voting)	94.00%
Ramesh et al. (2022)	General Churn	Hybrid (ANN-RF)	90.30%
Beeharry & Fokone (2022)	Telecom	Ensemble (Voting)	76.20%

Accordingly, this research applies ensemble learning to optimize service cancellation prediction for premium online video platforms, an industry characterized by highly dynamic data and distinct user behavior patterns that are critical to contemporary digital-business customer retention planning. The principal contributions of this study are as follows: (1) the generation of a novel, domain-specific empirical dataset derived from 10,983 active users of premium online video platforms in Thailand; (2) a systematic comparative evaluation of three distinct ensemble paradigms, tree-based, voting-based, and mixed-based architectures, to identify the most robust predictive frameworks for imbalanced cancellation data; and (3) the proposal of a practical model-selection guideline that aligns specific algorithmic strengths (precision versus recall) with the economic trade-offs of customer retention strategies, distinguishing between low-cost and high-cost interventions.

To address the limitations of single-base models, this study categorizes its integration framework into three distinct paradigms: tree-based, voting-based, and mixed-based ensembles. The selection of these paradigms is theoretically grounded in the principle of ensemble diversity, which seeks to mitigate both bias and variance by combining classifiers with divergent mathematical assumptions. This approach follows the ensemble learning methodologies proposed by Kunapuli (2023), thereby providing a robust predictive framework for identifying the propensity for service cancellation within the dynamic digital media landscape.

The primary objective of this research is to optimize service cancellation classifiers for premium online video platforms by integrating self-reported user behavior data through ensemble learning techniques. This approach is designed to mitigate the limitations inherent in single-base models and enhance predictive robustness when applied to complex and imbalanced datasets. Furthermore, the study aims to accurately identify the propensity for service cancellation to facilitate the development of tailored customer retention strategies, ultimately enabling the cost-effective and sustainable management of marketing budgets and resources within the digital media industry.

2. Materials and methods

The process used to optimize service cancellation classifiers for premium online video platforms through ensemble learning comprises data collection, data preprocessing, feature selection, model development and hyperparameter tuning, model integration using ensemble learning techniques, and performance evaluation, as illustrated in Figure 1.

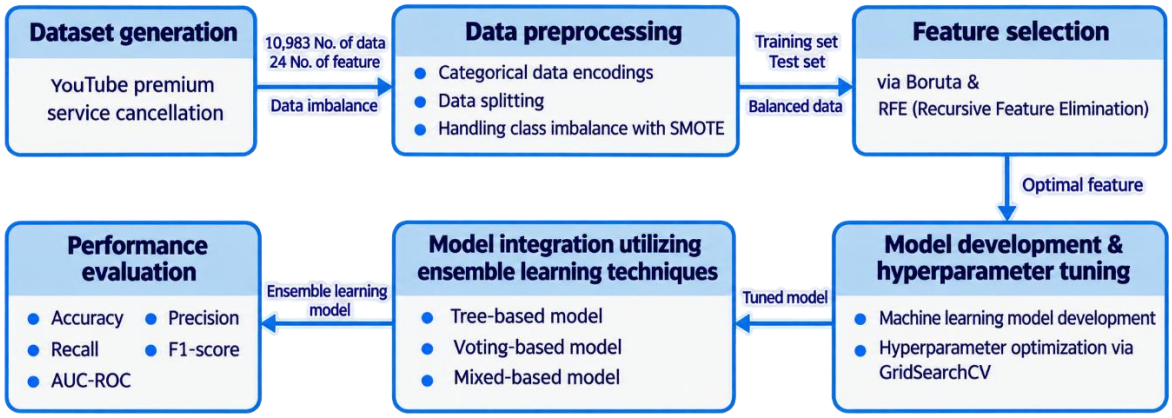


Figure 1. The process for optimizing service cancellation classifiers leveraging ensemble learning

2.1 Data collection

To obtain a representative sample, this research used quota sampling to allocate and control respondent proportions based on baseline characteristics and usage behaviors, supplemented by convenience sampling. Data were collected from users in Bangkok and the surrounding area by distributing electronic research instruments through online channels. This combined approach was used to reduce sampling bias arising from data clustering and to increase diversity across usage contexts. Data collection spanned nine months, from January to September 2025.

All data collection procedures strictly adhered to research ethics frameworks and the Personal Data Protection Act (PDPA). To maintain respondent anonymity, no email addresses or personal identifiers were collected. In accordance with informed-consent protocols, the compiled data were used solely for aggregate statistical analysis within this study, and participants did not consent to the public distribution or secondary use of their raw data by third parties. This rigorous methodology supports the statistical validity of the findings, their generalizability to the target population, and their direct and indirect benefits to the industry.

2.2 Data preprocessing

Data preprocessing was performed to transform the raw data into a suitable format for subsequent analysis. The procedures were as follows:

2.2.1 Categorical data encoding: text-based categorical variables were converted into numerical values using one-hot encoding. This approach was applied specifically to nominal-scale variables to prevent the model from interpreting arbitrary category labels as having an inherent order, thereby preserving the independence of the attributes.

2.2.2 Data splitting: to obtain an unbiased evaluation of model performance and mitigate overfitting, the primary dataset was partitioned into training and test sets at a ratio of 80:20. To prevent data leakage, the test set was retained as a fully independent hold-out set and was excluded from model

development and hyperparameter optimization. Stratified sampling was used to ensure that the target-class distribution in both subsets remained consistent with that of the original dataset.

2.2.3 Handling class imbalance with SMOTE: to reduce potential model bias toward the majority class, the Synthetic Minority Over-sampling Technique (SMOTE) was used. SMOTE generates synthetic instances for the minority class (the "Cancellation" cohort, comprising users who terminated their services) based on the k-nearest neighbors algorithm. This oversampling process was restricted to the training set to prevent data leakage.

2.2.4 Feature normalization: to ensure that independent variables measured on different scales were processed equitably, standardization through z-score normalization was performed. This method converts each raw value into a standard score (z), representing the number of standard deviations by which a data point differs from the mean. Scaling features to a mean of 0 and a standard deviation of 1 prevents algorithms from assigning disproportionate weight to variables with larger numerical ranges, thereby accelerating model convergence and improving statistical stability.

2.3 Feature selection

This research implemented a two-stage feature-selection framework. The first stage used Boruta (Haque, 2023), a wrapper method designed to identify all relevant variables. The algorithm generates shadow features by shuffling the values of the original attributes, thereby establishing a baseline against which the real variables are compared. Statistical testing based on z-scores was performed iteratively until the attributes were designated as confirmed features, indicating a genuine relationship with the dependent variable. In the second stage, the confirmed features were further refined using Recursive Feature Elimination (RFE). This method iteratively removes lower-ranked attributes until only the subset of predictors with the greatest predictive influence remains (Charfaoui, 2021). This two-stage process was used to mitigate overfitting and ensure that the final model retained strong explanatory efficiency.

2.4 Model development and hyperparameter tuning

Following the selection of independent variables associated with service cancellation, the models were developed as follows:

2.4.1 Machine learning model development

Base estimators and meta-estimators were selected from algorithms suitable for classification tasks (Sridhar & Vijayalakshmi, 2021). The models were as follows:

1) Random Forest classifier: utilizing bagging principles, this algorithm constructs an ensemble of randomized decision trees to mitigate overfitting and enhance predictive accuracy through majority voting.

2) Extra Trees classifier: similar to the Random Forest model, this classifier introduces extreme randomization by selecting random splits for features, thereby increasing model diversity and further reducing variance.

3) XGBoost classifier: a high-performance boosting framework that incorporates regularization terms to penalize model complexity, making it suitable as both a base estimator and a meta-estimator.

4) LightGBM classifier: characterized by high computational speed and efficiency on large-scale datasets, this model uses Gradient-based One-Side Sampling (GOSS) to retain instances with large gradients and maintain predictive accuracy.

5) CatBoost classifier: a gradient boosting algorithm optimized for processing categorical attributes automatically, featuring a robust system to prevent overfitting.

6) Support Vector Classifier (SVC): based on maximum-margin hyperplanes that separate classes, this model is effective in complex, high-dimensional spaces.

7) Logistic Regression classifier: a statistical method that predicts binary outcomes using a sigmoid function. It converts model output into a probability score and assigns an instance to the positive class as the probability approaches 1 and to the negative class as it approaches 0.

2.4.2 Hyperparameter optimization via GridSearchCV

To identify the optimal hyperparameter configurations, a grid-search strategy was implemented (Wang, 2022). The approach used a sequential data pipeline in which feature standardization and SMOTE oversampling were performed strictly within each of the 10 training folds during cross-validation. Isolating these preprocessing and resampling steps within the internal training subsets ensured that no information from the validation folds leaked into model training, thereby preserving the integrity of the performance evaluation. Because SMOTE established a 1:1 class distribution, accuracy was used as the primary optimization metric during this phase, as it provides a reliable and stable indicator of overall performance when classes are balanced. This internal cross-validation also served as the validation mechanism: optimal parameters were selected based on average performance across the training folds, while the independent hold-out test set remained excluded from tuning. The final tuned models were subsequently evaluated on this unseen test set to quantify the performance improvement over the baseline models.

2.5 Model integration via ensemble learning

Following hyperparameter optimization of each algorithm, ensemble learning was implemented through a structured combinatorial experiment. The process evaluated different combinations of high-performing standalone models and models with distinct mathematical foundations (e.g., tree-based, linear, and geometric classifiers) to maximize ensemble diversity and reduce correlated errors. The combinations were grouped into three paradigms to identify the most effective synergy among learning mechanisms:

1) Tree-based ensemble model: this approach integrates high-performing algorithms capable of capturing complex, nonlinear relationships in the data. CatBoost, Extra Trees, and Random Forest were used as base estimators, while XGBoost served as the meta-learner (or meta-model), a high-level classifier that learns patterns from the base-level predictions to produce the final classification. A feature-passthrough mechanism also provided the meta-model with direct access to the original independent variables alongside the base-level predictions. This architecture reduces information loss between layers and improves the detection of service cancellation signals.

2) Voting-based ensemble model: based on statistical consensus, this model uses soft voting to improve predictive stability and reliability. It combines algorithms with different mathematical assumptions, principally gradient-boosted trees (LightGBM and XGBoost), a bagging method (Random Forest), and a geometric margin classifier (SVC), to calculate a weighted average of predicted class probabilities. In advanced configurations, this paradigm incorporates nested structures in which high-performing algorithms, such as CatBoost or XGBoost, serve as internal sub-meta-models. These sub-meta-models learn patterns from subsets of learners before the ensemble reaches a final consensus, thereby improving stability in large, dynamic datasets. This consensus-based process reduces variance and overfitting, producing predictions that are more robust than those of an isolated single-base model.

3) Mixed-based ensemble model: designed for architectural flexibility, this paradigm combines algorithms from distinct statistical families. It integrates tree-based ensembles, a geometric framework (SVC), and a linear model (Logistic Regression) to capitalize on their complementary strengths

and offset their structural weaknesses. A meta-estimator coordinates the final outputs using internal cross-validation to construct unbiased meta-features, thereby capturing the complex dimensions of user behavior.

By systematically evaluating these three ensemble strategies, this research establishes a robust framework for predicting service cancellation. The framework is designed to capture multidimensional correlations while maintaining strong generalizability and stable performance under dynamic empirical conditions derived from self-reported behavior.

2.6 Performance evaluation

To assess the ability of the proposed models to identify at-risk cohorts accurately, this research evaluates predictive performance using a comprehensive set of metrics (Manning et al., 2008). These metrics include:

2.6.1 Accuracy: measures the model's overall correctness and represents the proportion of all instances that are correctly predicted, as shown in Equation 1:

$$Accuracy = \frac{TP + TN}{TP + TN + FP + FN} \quad (1)$$

2.6.2 Precision: measures the reliability of positive-class predictions and represents the proportion of instances predicted as positive that are actually positive, as shown in Equation 2:

$$Precision = \frac{TP}{TP + FP} \quad (2)$$

2.6.3 Recall: measures the model's ability to detect actual positive instances and represents the proportion of true positive instances that are correctly identified, as shown in Equation 3:

$$Recall = \frac{TP}{TP + FN} \quad (3)$$

2.6.4 F1-score: the harmonic mean of precision and recall, providing a single measure of the balance between them, as shown in Equation 4:

$$F1 - score = \frac{Precison\ x\ Recall}{Precison + Recall} \quad (4)$$

2.6.5 Area Under the ROC Curve (AUC): evaluates the model's overall ability to discriminate between positive and negative classes across different classification thresholds. The AUC is derived from the Receiver Operating Characteristic (ROC) curve, which plots the True Positive Rate (TPR) against the False Positive Rate (FPR), calculated as shown in Equations 5 and 6, respectively:

$$TPR = \frac{TP}{TP + FN} \quad (5)$$

$$FPR = \frac{FP}{FP + TN} \quad (6)$$

2.7 Data Availability Statement

The dataset generated and analyzed during this study is not publicly available because of privacy constraints and the terms of the informed consent provided by participants. In accordance with the Personal Data Protection Act (PDPA) and applicable research ethics frameworks, respondents were assured

that their data would be used solely for aggregate statistical analysis within the scope of this research. Consequently, the raw data cannot be distributed, thereby ensuring the continued protection of participant anonymity.

3. Results

The service cancellation classifiers were developed and implemented in Python using the Google Colaboratory platform. The detailed results are presented below.

3.1 Data collection results

Following data validation against the research criteria, the final dataset comprised 10,983 records. The dataset was divided into a “non-Cancellation” cohort (n = 7,526) and a “Cancellation” cohort (n = 3,457). In this study, service cancellation (Cancellation) was defined specifically as the actual termination of a subscription by a user during the nine-month period from January to September 2025. To facilitate interpretation of the results, Table 2 provides comprehensive definitions of the variables, including their names, operational definitions, units of measurement, and possible values.

Table 2. Operational definitions and measurements of research variables

Variable Type	Variable	Definition	Possible Values
Numeric (Integer/Continuous)	Age	User's age	Years
	Period	Membership duration	Months
	WatchTime	Daily viewing duration	Hours
	ContentCount	Volume of consumed content	Items
	LoginFrequency	Weekly login frequency	Frequency
	Playlists	Number of playlists created	Count
	Subscribed	Number of subscribed channels	Count
	SupportTickets	Number of support requests	Count
	ServiceChanges	Number of plan changes	Count
	PaymentIssues	Number of billing anomalies	Count
Categorical (Ordinal)	Married	Marital status	Single, Married, Widowed/Divorced
	Contract	Agreement structure	Monthly, Yearly
Categorical (Nominal)	Sex	User's gender	Male, Female
	Place	Primary usage location	Home, Workplace, Transit/Commuting, Public Place
	TopContent	Preferred media format	Audio, Video
	TopViewContent	Preferred content category	Games, Music, News, Sports, Podcasts, Movies & TV Shows, Fashion & Beauty, Education, Horror, Other
	PaymentMethod	Billing channel	Credit Card, Google Play, AIS, TrueMoney
	TypeSubscription	Subscription tier	Personal plan, Family plan, Student plan
	AcquisitionSource	Marketing channel	Advertising, Referrals, Free Trial
	InternetService	Type of connection	Wi-Fi, 4G/5G

Table 2. (Continued)

Variable Type	Variable	Definition	Possible Values
Categorical (Binary)	Child	Presence of children	No, Yes
	TechSupport	Use of technical assistance	No, Yes
	StreamingTV	Use of streaming TV service	No, Yes
	DigitalTV	Use of digital TV service	No, Yes
Target Variable (Binary)	Cancellation	Service termination status	Cancellation, non-Cancellation

A preliminary data analysis was then conducted to examine baseline user characteristics and behavioral patterns by subscription status, as presented in Tables 3 and 4.

Table 3. Average user characteristics by membership status

	non-Cancellation (n=7,526)	Cancellation (n=3,457)	Overall (n=10,983)
Basic characteristics			
1) Age	43.67	43.53	43.61
2) Period	53.09	39.74	47.80
3) WatchTime	5.54	4.84	5.26
4) ContentCount	20.23	13.63	17.61
5) LoginFrequency	15.01	15.35	15.15
6) Playlists	10.07	10.15	10.10
7) Subscribed	42.11	30.07	37.34
8) SupportTickets	2.52	2.51	2.51
9) ServiceChanges	2.26	2.87	2.50
10) PaymentIssues	4.74	5.38	4.99

Table 4. Frequency and percentage distribution of usage behavior by membership status

	non-Cancellation (n=7,526)	Cancellation (n=3,457)	Overall (n=10,983)
1) Sex			
- male	2,933 (64.79%)	1,594 (35.21%)	4,527
- female	4,593 (71.14%)	1,863 (28.86%)	6,456
2) Married			
- single	3,814 (63.32%)	2,209 (36.68%)	6,023
- married	2,382 (79.45%)	616 (20.55%)	2,998
- widowed/divorced	1,330 (67.79%)	632 (32.21%)	1,962
3) Child			
- no	3,711 (61.84%)	2,290 (38.16%)	6,001
- yes	3,815 (76.58%)	1,167 (23.42%)	4,982

Table 4. (Continued)

	non-Cancellation (n=7,526)	Cancellation (n=3,457)	Overall (n=10,983)
4) Place			
- home	3,573 (75.33%)	1,170 (24.67%)	4,743
- workplace	1,885 (69.66%)	821 (30.34%)	2,706
- transit/commuting	951 (54.72%)	787 (45.28%)	1,738
- public place	1,117 (62.19%)	679 (37.81%)	1,796
5) TopContent			
- audio	2,642 (75.10%)	876 (24.90%)	3,518
- video	4,884 (65.43%)	2,581 (34.57%)	7,465
6) TopViewContent			
- games	694 (59.57%)	471 (40.43%)	1,165
- music	1,296 (78.21%)	361 (21.79%)	1,657
- news	1,440 (74.81%)	485 (25.19%)	1,925
- sports	751 (67.72%)	358 (32.28%)	1,109
- podcast	505 (73.40%)	183 (26.60%)	688
- movies & TV shows	482 (64.61%)	264 (35.39%)	746
- fashion & beauty	342 (65.52%)	180 (34.48%)	522
- education	904 (84.57%)	165 (15.43%)	1,069
- horror	621 (58.42%)	442 (41.58%)	1,063
- other	491 (47.26%)	548 (52.74%)	1,039
7) Contract			
- monthly	4,294 (64.80%)	2,333 (35.20%)	6,627
- yearly	3,232 (74.20%)	1,124 (25.80%)	4,356
8) PaymentMethod			
- credit card	2,359 (85.44%)	402 (14.56%)	2,761
- Google Play	1,989 (68.14%)	930 (31.86%)	2,919
- AIS	1,829 (62.59%)	1,093 (37.41%)	2,922
- TrueMoney	1,349 (56.66%)	1,032 (43.34%)	2,381
9) TypeSubscription			
- personal plan	4,498 (67.32%)	2,184 (32.68%)	6,682
- family plan	1,346 (80.21%)	332 (19.79%)	1,678
- student plan	1,682 (64.13%)	941 (35.87%)	2,623
10) AcquisitionSource			
- advertising	2,935 (62.89%)	1,732 (37.11%)	4,667
- referrals	1,467 (89.23%)	177 (10.77%)	1,644
- free trial	3,124 (66.87%)	1,548 (33.13%)	4,672
11) InternetService			
- Wi-Fi	5,694 (74.94%)	1,904 (25.06%)	7,598
- 4G/5G	1,832 (54.12%)	1,553 (45.88%)	3,385

Table 4. (Continued)

	non-Cancellation (n=7,526)	Cancellation (n=3,457)	Overall (n=10,983)
12) TechSupport			
- no	3,385 (55.96%)	2,664 (44.04%)	6,049
- yes	4,141 (83.93%)	793 (16.07%)	4,934
13) StreamingTV			
- no	5,914 (69.17%)	2,636 (30.83%)	8,550
- yes	1,612 (66.26%)	821 (33.74%)	2,433
14) DigitalTV			
- no	2,561 (71.94%)	999 (28.06%)	3,560
- yes	4,965 (66.89%)	2,458 (33.11%)	7,423

Note: Percentages in parentheses are row percentages calculated from the overall count for each behavioral attribute.

Tables 3 and 4 indicate that contract type and payment method are associated with service cancellation. Yearly contracts and credit card payments were associated with lower cancellation rates, whereas monthly plans and mobile billing methods (e.g., Google Play, AIS, and TrueMoney) were associated with higher cancellation rates. Use of technical support and acquisition through referrals were also associated with lower cancellation rates than the corresponding alternatives. In addition, cancellation rates varied by usage environment and content preference: users relying on mobile networks or viewing content while commuting showed higher cancellation rates, as did users who preferred gaming content, whereas users who preferred educational content showed lower cancellation rates. Household characteristics and subscription structure also differed across cancellation groups, with family plans and households with children showing lower cancellation rates.

3.2 Data preprocessing results

Data preprocessing was performed to optimize the data structure for machine learning and improve analytical efficiency. The specific results were as follows:

3.2.1 Categorical data encoding results: binary variables, including Child, TechSupport, StreamingTV, and DigitalTV, were encoded as 0 or 1 to indicate the absence or presence of each attribute. One-hot encoding was applied to multiclass nominal variables, including Sex, Place, TopContent, TopViewContent, PaymentMethod, TypeSubscription, AcquisitionSource, and InternetService, to generate dummy variables and eliminate bias arising from an implied hierarchical order. Ordinal variables, specifically Married and Contract, were mapped to logical sequential values (e.g., 0 = Monthly and 1 = Yearly). The target variable, Cancellation, was coded as 0 for active users and 1 for users who had terminated their services. Quantitative variables, Age, Period, WatchTime, ContentCount, LoginFrequency, Playlists, Subscribed, SupportTickets, ServiceChanges, and PaymentIssues, retained their original continuous structures. The resulting hybrid dataset contained both dummy and quantitative variables and was ready for model processing.

3.2.2 Data splitting results: the complete dataset of 10,983 records was partitioned into training and test sets at an 80:20 ratio. Stratified sampling based on the target variable (Cancellation) was used to preserve the proportional class distribution. The resulting training and test sets comprised 8,786 and 2,197 records, respectively, as shown in Table 5.

Table 5. Data split results (80/20 ratio)

	non-Cancellation class	Cancellation class	Overall
Training set (80%)	6,021	2,765	8,786
Test set (20%)	1,505	692	2,197
Overall	**7,526**	**3,457**	**10,983**

As shown in Table 5, the data-splitting procedure preserved the original proportions of the Cancellation and non-Cancellation cohorts. This preservation supports a statistically reliable evaluation of model performance while reducing the risk of overfitting.

3.2.3 Class imbalance resolution results using SMOTE: the Synthetic Minority Over-sampling Technique (SMOTE) was applied exclusively to the training dataset to address class imbalance, with the Cancellation cohort representing the minority class. The procedure generated 3,256 synthetic instances, increasing the minority-class total to 6,021 records. Consequently, the Cancellation and non-Cancellation classes in the training dataset were balanced at 6,021 records each, as detailed in Table 6.

Table 6. SMOTE resampling results on the training dataset

Training Set	Before SMOTE	After SMOTE
Cancellation	2,765	6,021
non-Cancellation	6,021	6,021
Overall	**8,786**	**12,042**

As indicated in Table 6, the post-oversampling training dataset contains 12,042 records, distributed in an identical 1:1 ratio between the Cancellation and non-Cancellation user cohorts. This balanced distribution facilitates a more robust learning environment, enabling the machine learning models to discern more accurately the defining characteristics and underlying patterns of customers with a high propensity to cancel.

3.2.4 Feature normalization results: because the primary dataset comprised attributes with highly disparate units of measurement, feature scaling was imperative. For instance, for the Age variable, an original value of 64 years was transformed to 1.350025, reflecting a value above the dataset mean; conversely, an age of 28 years was mapped to -1.033662, signifying a value below the mean. Similarly, for the WatchTime feature, an initial value of 8 hours was converted to 1.329073 (reflecting a value above the mean), whereas a value of 1 hour was scaled to -2.066374 (signifying a value below the mean).

Standardizing these features into standard scores (Z-scores) effectively mitigates the risk of variables with larger numerical magnitudes dominating those with inherently smaller scales. A comparative analysis before and after feature scaling demonstrates that the dataset successfully transitioned from its original metrics (e.g., years, hours, or frequencies) to a unitless standardized format. Ultimately, the mean of each quantitative feature was adjusted to approximately 0, with a standard deviation of 1, enabling the models to process the heterogeneously scaled attributes equitably.

3.3 Feature selection results

The specific feature subset influencing service cancellation was identified using a two-stage feature selection framework. The baseline model was configured using a tuned Random Forest algorithm,

with structural complexity controlled by limiting the maximum tree depth to 10 levels and setting the minimum sample split threshold at 10 instances.

In the first stage, the Boruta algorithm was implemented with a 100% strict decision criterion to select only independent variables whose feature importance consistently outperformed that of the best shadow features across all iterations. The statistical significance level (α) was set at 0.05, and the algorithm was executed with a maximum of 100 runs. This rigorous filtering ensured that the confirmed attributes were not products of statistical anomalies but instead had genuine predictive importance for service cancellation.

In the subsequent stage, the variables confirmed by Boruta were subjected to further dimensionality reduction via Recursive Feature Elimination (RFE), with the target selection proportion set at 70% of the input attributes. This process systematically ranked the features and recursively eliminated those with the lowest predictive power to isolate the definitive subset that maximized model accuracy. Under these self-reported constraints, 10 confirmed features successfully passed the two-stage filter, as shown in Table 7. Based on their respective importance scores, these features can be categorized into three distinct clusters according to their impact on the target variable: primary factors, secondary factors, and auxiliary factors.

As indicated in Table 7, the primary factors with the highest predictive influence on service cancellation are Subscribed and ContentCount, which share identical importance scores of 0.1701, followed closely by Period at 0.1666. These findings indicate that the extent of channel subscriptions and the depth of the user-platform relationship are core predictors of retention.

Factors classified within the secondary importance tier consist of PaymentIssues (0.1165), WatchTime (0.1026), and SupportTickets (0.0949). This pattern indicates that user experience metrics are important predictors of immediate cancellation propensity, even among users who otherwise maintain consistent usage frequencies.

Conversely, the cluster of factors exhibiting relatively lower influence includes Contract, Married, TechSupport, and Child. This lower tier indicates that baseline demographic characteristics have less predictive power for consumer behavior than active, real-time behavioral features.

Table 7. Features selection result via Boruta and RFE techniques

Variables	Importance score	Boruta	RFE
1) Subscribed	0.1701		✓
2) ContentCount	0.1701		✓
3) Period	0.1666		✓
4) PaymentIssues	0.1165		✓
5) WatchTime	0.1026		✓
6) SupportTickets	0.0949		✓
7) Contract	0.0565		✓
8) Married	0.0522	✓	✓
9) TechSupport	0.0392	✓	✓
10) Child	0.0315	✓	✓

3.4 Model development and hyperparameter tuning results

3.4.1 Machine learning model development results

Seven distinct machine learning algorithms were evaluated as classifiers within the service cancellation prediction framework, as detailed in Table 8. A granular analysis of the performance metrics indicates that the LightGBM classifier achieved the highest overall baseline accuracy of 0.8157, with an efficient training time of 0.3381 seconds, followed closely by CatBoost at 0.8152 (5.1932 seconds). Meanwhile, the advanced tree-based models, specifically Extra Trees and XGBoost, demonstrated identical accuracy scores of 0.8086, with training times of 1.0677 seconds and 0.4345 seconds, respectively. These models outperformed more traditional algorithms, such as Random Forest (0.7878 accuracy; 1.0281 seconds) and the Support Vector Classifier (SVC), which yielded an accuracy of 0.7704 and encountered a significant computational bottleneck, with the longest training time of 17.6253 seconds.

This performance hierarchy suggests that the underlying structural characteristics of consumer behavioral data align more effectively with the conditional partitioning mechanisms inherent in advanced gradient-boosted tree architectures than with the high-dimensional spatial boundaries established by traditional geometric margin classifiers.

Table 8. Machine learning classifier results

Model	Test accuracy	Train time (seconds)
1) LightGBM	0.8157	0.3381
2) CatBoost	0.8152	5.1932
3) Extra trees	0.8086	1.0677
4) XGBoost	0.8086	0.4345
5) Random forest	0.7878	1.0281
6) SVC	0.7704	17.6253
7) Logistic regression	0.7020	0.0354

An integrated evaluation of prediction accuracy and computational efficiency, as detailed in Table 8, identifies LightGBM as the most structurally optimal model within the experimental framework. Although Logistic Regression demonstrated the lowest training latency (0.0354 seconds), LightGBM showed exceptional computational efficiency among high-performing models, executing the optimization process more than 15 times faster than CatBoost. Conversely, the Support Vector Classifier (SVC) encountered severe computational bottlenecks, exhibiting the longest training time at 17.6253 seconds. However, Logistic Regression yielded the lowest overall accuracy (0.7020) among the tested baseline classifiers.

3.4.2 Hyperparameter optimization results via GridSearchCV

Hyperparameter optimization was performed using a robust sequential data pipeline that integrated feature standardization (Z-score normalization), SMOTE resampling, and the classification algorithms. This framework applied GridSearchCV with a 10-fold cross-validation mechanism to ensure that all preprocessing and oversampling of the minority class ('Cancellation' cohort) were performed exclusively on the training partitions of each fold. This approach effectively eliminated the risk of data leakage from the validation or hold-out sets. The choice of accuracy for hyperparameter selection was justified by the application of SMOTE within the pipeline, which established a balanced 1:1 class distribution and ensured that the tuning process remained unbiased toward the majority class. Furthermore, the performance

reported in this section represents evaluation on the independent test set, which was strictly maintained as hold-out data and remained entirely unseen by the models during the 10-fold cross-validation tuning process. This approach ensured that the reported results accurately reflected the models' true generalization capacity and prevented inflated performance metrics. The detailed results and parameter spaces are presented in Table 9.

As shown in Table 9, both LightGBM and Extra Trees achieved the highest post-tuning accuracy of 0.8157. Notably, the baseline accuracy of LightGBM remained unchanged, suggesting that its default architecture was already highly compatible with this specific dataset structure. Conversely, Extra Trees exhibited an increase in accuracy from 0.8086 to 0.8157 by expanding the forest size (n_estimators) to 200 while permitting unrestricted tree depth (max_depth = None). This configuration enabled the model to construct more comprehensive decision boundaries that captured deeper underlying correlations within the data.

Table 9. Hyperparameter tuning results via GridSearch

Model	Tuned accuracy	Best params selected
1) LightGBM	0.8157	importance_type: 'split'
		learning_rate: 0.01
		n_estimators: 200
		num_leaves: 31
2) Extra trees	0.8157	max_depth: None
		min_samples_split: 5
		n_estimators: 200
3) XGBoost	0.8152	learning_rate: 0.05
		max_depth: 3
		n_estimators: 200
4) Random forest	0.8128	max_depth: None
		min_samples_leaf: 2
		n_estimators: 300
5) CatBoost	0.8109	depth: 4
		iterations: 200
		learning_rate: 0.1
		l2_leaf_reg: 3
6) SVC	0.7643	C: 10
		gamma: 'scale'
7) Logistic regression	0.7020	clf__C: 1
		clf__penalty: 'l2'

As indicated in Table 9, CatBoost and the Support Vector Classifier (SVC) experienced performance degradation, with their accuracy scores dropping from 0.8152 to 0.8109 and from 0.7704 to 0.7643, respectively. For CatBoost, which is natively engineered with symmetric trees and rigorous default regularization properties, restricting the optimization grid to 200 iterations may have prematurely truncated its convergence trajectory toward the global optimum. For the SVC, increasing the regularization parameter (C) to 10 imposed excessively stringent margin separations. In machine learning, C serves as a penalty

parameter that controls the trade-off between achieving a smooth decision boundary and classifying the training points correctly. A higher C value aims for greater accuracy on the training data but may lead to excessive rigidity, which may have induced localized overfitting within the internal cross-validation folds and ultimately reduced generalization to the independent validation data. Importantly, Logistic Regression yielded the lowest accuracy across the cohort. This baseline result provides evidence from the self-reported data that a rigid linear classifier is structurally insufficient for decoding the nonlinear, complex feature interactions inherent in this dataset compared with ensemble-based alternatives.

3.5 Model integration via ensemble learning results

In this phase, a wide range of model combinations were systematically evaluated to determine the optimal synergy among learners. The configurations presented in Table 10 represent the top-tier results derived from this iterative testing process, ranging from 'all-inclusive' configurations to 'selective-high-performance' groups based on their contributions to overall accuracy and class sensitivity. For instance, the top-performing voting-based model was obtained by combining the most robust gradient-boosted trees with a geometric classifier (SVC) to mitigate individual structural biases.

An examination of Table 10 reveals that the evaluated ensemble variants yielded closely competitive accuracy scores. Notably, the voting-based model achieved the highest predictive accuracy of 0.8204. This performance was attained by combining tree-based architectures—specifically LightGBM, XGBoost, and Random Forest—with the Support Vector Classifier (SVC). Without introducing excessive structural complexity, this streamlined configuration maintained statistical balance and effectively minimized the system's cumulative variance.

The next-best-performing configuration was a secondary iteration of the voting-based model that included all individual classifiers and incorporated CatBoost and XGBoost as internal sub-meta-models anchoring the foundational layers. This configuration was closely followed by the mixed-based ensemble variants. In these mixed-based configurations, Logistic Regression was predominantly deployed as the ultimate meta-learner. This choice was justified by its role as a secondary layer that smoothed the stepwise decision boundaries generated by the primary tree-based estimators while equitably calibrating regularization penalties across the predictive distributions.

Table 10. Accuracy comparison of ensemble learning models for service cancellation classification

Ensemble method	Accuracy	LightGBM	CatBoost	Extra trees	XGBoost	Random forest	SVC	Logistic regression
1) Voting-based	0.8204	✓			✓	✓	✓	
2) Voting-based	0.8194	✓	✓ *	✓	✓ *	✓	✓	
2) Mixed-based	0.8194	✓	✓	✓	✓	✓	✓	✓*
3) Mixed-based	0.8190	✓		✓			✓	✓*
3) Voting-based	0.8190	✓	✓		✓		✓	
4) Mixed-based	0.8185	✓	✓	✓	✓	✓		✓*
4) Voting-based	0.8185	✓	✓		✓			

Table 10. (Continued)

Ensemble method	Accuracy	LightGBM	CatBoost	Extra trees	XGBoost	Random forest	SVC	Logistic regression
5) Tree-based	0.8180		✓	✓	✓*	✓		
5) Voting-based	0.8180	✓	✓	✓	✓	✓	✓	
5) Voting-based	0.8180	✓*	✓	✓	✓	✓	✓*	

Note: * denotes the algorithm was designated as the meta-learner or internal sub-meta-model.

It is noteworthy that the tree-based ensemble configuration yielded a lower accuracy of 0.8180, revealing the structural limitations inherent in homogeneous tree architectures. This configuration incorporated CatBoost, Extra Trees, and Random Forest, with XGBoost functioning as the final meta-estimator. Although tree-based models inherently excel at processing tabular data, the absence of statistical or linear classifiers within this ensemble resulted in an overall predictive accuracy lower than that of the mixed-based architectures.

3.6 Performance evaluation results

When deploying predictive models in real-world scenarios, relying solely on accuracy is insufficient. Overall accuracy can be heavily skewed by majority-class performance, thereby masking critical misclassifications within the minority class. To mitigate this bias, this research comprehensively evaluates model performance by incorporating precision, recall, F1-score, and AUC-ROC into the analytical framework, as detailed in Table 11.

Table 11. Performance evaluation of ensemble models using classification metrics

	Ensemble method	Base models	Accuracy	Precision	Recall	F1-score	AUC-ROC
1)	Voting-based	lgbm, xgb, rf, svc	**0.8204**	0.8468	0.7821	0.8131	0.8790
2)	Voting-based	lgbm, cat*, et, xgb*, rf,svc,	0.8194	**0.8472**	0.7792	0.8118	0.8805
	Mixed-based	lgbm, cat, et, xgb, rf, svc, lr*	0.8194	0.8342	0.7972	0.8152	0.8829
3)	Mixed-based	lgbm, et, svc, lr*	0.8190	0.8421	0.7849	0.8125	0.8821
	Voting-based	lgbm, cat, xgb, svc	0.8190	0.8463	0.7792	0.8114	0.8805
4)	Mixed-based	lgbm, cat, et, xgb, rf, lr*	0.8185	0.8267	**0.8057**	**0.8161**	**0.8833**
	Voting-based	lgbm, cat, xgb,	0.8185	0.8469	0.7774	0.8106	0.8823
5)	Tree-based	cat, et, xgb*, rf	0.8180	0.8446	0.7792	0.8106	0.8796
	Voting-based	lgbm, cat, et, xgb, rf, svc	0.8180	0.8418	0.7830	0.8113	0.8811
	Voting-based	lgbm*, cat, et, xgb, rf, svc*	0.8180	0.8418	0.7830	0.8113	0.8761

Note: * denotes the algorithm was designated as the meta-learner or internal sub-meta-model.

Nevertheless, the voting-based ensemble framework consistently demonstrated strong performance. Specifically, the configuration incorporating nested structural overlap achieved the highest precision in the entire experiment, at 0.8472. This model is well suited to enterprises that prioritize predictive precision to minimize false-positive rates, thereby preventing the misallocation of retention resources to low-risk customers who have no genuine intention of cancellation.

Conversely, the mixed-based ensemble variants using a linear meta-estimator (Logistic Regression) exhibited a greater capacity to detect the minority class. By integrating all six baseline classifiers, this architecture yielded the highest recall and AUC-ROC scores across the entire cohort, at 0.8057 and 0.8833, respectively. This profile aligns with practical deployment goals for cost-effective customer retention. Furthermore, although the tree-based ensemble configuration produced a modest accuracy of 0.8180, its capacity to mitigate cumulative error propagation enabled it to achieve a high precision of 0.8446 and an AUC-ROC of 0.8796, maintaining a highly competitive position among the ensemble categories.

4. Discussion

The integrated ensemble framework developed in this research effectively addresses data complexity and class imbalance within the online video streaming ecosystem. Consistent with Wang et al. (2020) and Manohar et al. (2021), the findings based on self-reported data indicate that ensemble architectures systematically outperform standalone classifiers. This is evidenced by the voting-based approach improving the overall performance of the cancellation classification task relative to LightGBM (0.8157), the strongest individual model, and achieving a peak accuracy of 0.8204. This improvement in predictive performance corroborates the findings of Beeharry and Fokone (2022), who successfully deployed flexible voting topologies to mitigate variance within high-volume, dynamic digital datasets.

To counteract highly skewed distributions in which the 'Cancellation' class constitutes the critical minority, the use of SMOTE parallels the resampling paradigms advocated by Maretta & Permai (2021) and Adiputra & Wanchai (2023) to optimize recall and F1-score. Extending this data-level restructuring, the mixed-based ensemble, using Logistic Regression as its meta-estimator, achieved the most comprehensive minority-class identification, with a peak recall of 0.8057. This performance is consistent with the conclusions of Jain et al. (2021) regarding the robust mathematical stability of linear meta-models when mapping complex cancellation probabilities in parallel subscriber-heavy domains.

This predictive performance is further supported by a sophisticated two-stage feature-selection pipeline linking Boruta and Recursive Feature Elimination (RFE), offering a structurally more comprehensive approach than the isolated Information Gain methods of Saheed and Hambali (2021) or the equidistant segmentation of Xu et al. (2021). By identifying the number of subscribed channels (Subscribed) and quantitative viewing frequencies (ContentCount) as the primary predictors of cancellation, the analysis of self-reported data shifts the focus from static demographic profiling toward dynamic, user-centric behavioral streams, mirroring the granular decoding of consumer footprints proposed by Ramesh et al. (2022).

Finally, while this framework achieves refined decision boundaries through systematic hyperparameter tuning with GridSearchCV, alternative methodologies proposed by Fu et al. (2023) and Khoh et al. (2023) favor derivative-free metaheuristics, such as the Nelder-Mead and Powell algorithms, to optimize ensemble weights. Although metaheuristics were not explicitly implemented here, the use of a linear meta-model within the mixed-based ensemble serves as an effective boundary regularizer. This mathematical approach helps bridge the optimization gap, providing comparable predictive refinement without excessive computational overhead.

When translating these multidimensional performance metrics into real-world strategic applications, distinct deployment paradigms emerge:

1) Low-cost retention paradigm: if the organizational strategy focuses on low-cost proactive retention initiatives, such as offering complimentary subscription tiers or monthly discounts, the mixed-based ensemble is the optimal choice. This architecture achieved the highest F1-score of 0.8161 and a

robust recall of 0.8057, identifying over 80% of the actual at-risk target consumers. This high sensitivity may allow the business to execute defensive workflows in a timely and proactive manner.

2) High-cost retention paradigm: in contrast, for high-cost retention campaigns that demand substantial per-unit expenditures, such as dispatching premium physical corporate gifts or deploying dedicated customer success agents for direct outbound calls, the strategy should pivot toward the voting-based ensemble. Its maximum precision of 0.8472 provides precise individual-level verification of critical cancellation propensity, thereby minimizing the financial risks associated with targeting errors.

Additionally, for enterprises requiring real-time screening of service cancellation probability, the integrated ensemble architectures consistently outperformed the independent models. The voting-based ensemble achieved the highest overall accuracy of 0.8204, while the mixed-based ensemble variant achieved the peak AUC-ROC of 0.8833, providing the most stable differentiation of risk signals. These configurations may be integrated into personalized recommender systems to dynamically deliver exclusive content or tailored video streams. By seeking to stimulate user engagement and increase WatchTime, such data-driven interventions may ultimately support a sustainable customer retention and business growth ecosystem.

5. Conclusions

The primary objective of this research was to evaluate and compare three distinct ensemble learning paradigms for service cancellation prediction. Furthermore, the study aimed to establish a model-selection guideline that aligns specific predictive characteristics with the cost structure of customer retention campaigns, ensuring an optimal balance between precision and coverage.

This research provides empirical insights into the predictive modeling of subscription cancellation using self-reported data within a specific empirical context. While the performance improvement achieved through the voting-based ensemble was modest, increasing accuracy from 0.8157 to 0.8204, the results demonstrate the potential of ensemble architectures to refine classification tasks compared with standalone models. The self-reported findings reveal that customer retention is fundamentally governed by user engagement and platform loyalty metrics, with the number of subscribed channels (Subscribed), quantitative content consumption (ContentCount), and membership duration (Period) emerging as the three most influential predictive features for service cancellation. Although long-term engagement remains the primary baseline for retention, technical and operational friction points—specifically transaction anomalies (PaymentIssues) and documented system grievances (SupportTickets)—function as acute secondary predictive factors associated with abrupt, immediate cancellation propensities. Conversely, static demographic features, such as marital status and family composition, exhibit significantly weaker associations with consumer cancellation propensity, thereby possessing substantially lower forecasting utility than real-time, dynamic platform behavioral data. Regarding algorithmic performance, LightGBM stands out as the most structurally optimal standalone estimator, demonstrating a superior baseline accuracy of 0.8157 alongside minimal training latency. However, integrated ensemble architectures consistently outpace independent models, as evidenced by the voting-based ensemble achieving the highest overall accuracy of 0.8204, while the mixed-based ensemble variant—employing Logistic Regression as the ultimate meta-estimator, proves exceptional at minority-class coverage by yielding the highest recall of 0.8057 and an AUC-ROC of 0.8833.

To extend the academic and practical utility of this research, the next phase will focus on developing a "Predictive Risk Assessment Model for Premium Subscription Retention on Online Video

Platforms via Feature Interaction Network Analysis." Building on the self-reported baseline established in this research, future research will comparatively analyze the intricate structural dependencies and correlations among features using network analysis methodologies. By extracting topological weight metrics within the feature interaction network, a specialized computational model will be constructed to dynamically evaluate and recalculate feature importance. Ultimately, this weighted network approach will be synthesized with real-time stream processing architectures to enable instantaneous, multidimensional forecasting of service cancellations, providing streaming platforms with an agile, high-precision instrument for immediate proactive customer retention.

6. References

Adiputra, I. N. M., & Wanchai, P. (2023). Customer churn prediction using weight average ensemble machine learning model. In 2023 20th International Joint Conference on Computer Science and Software Engineering (JCSSE) (pp. 306–311). IEEE. https://doi.org/10.1109/JCSSE58229.2023.10202105

Beeharry, Y., & Fokone, R. T. (2022). Hybrid approach using machine learning algorithms for customers' churn prediction in the telecommunications industry. Concurrency and Computation: Practice and Experience, 34(4), e6627. https://doi.org/10.1002/cpe.6627

Charfaoui, Y. (2021). Feature engineering and feature selection with Python: A practical guide for feature crafting [Online]. Retrieved January 15, 2026, from https://ps.z-library.sk/book/DOgwPe0bOX/feature-engineering-and-feature-selection-with-python-a-practical-guide-for-feature-crafting.html?fbclid=IwY2xjawVeUdlleHRuA2FlbQIxMABwZG9mBWJyaWQRMUJyaXVwcW9BckJzWWNKMVpzcnRjBmFwcF9pZBAyMjIwMzkxNzg4MjAwODkyAAEfnS5LDIDRz-ogSDe8JjJjfWo8QB5_IUd9iNaiFusKIQi4GI1SJD-xdU07QRA_aem_Ypr0RmRJxDVyQn5HCwo4YA

Forge, S., Cave, M., Srinuan, C., Srisaracam, S., Oranop, C., Tambini, D., Treerat, N., Bohlin, E., Chaiwat, T., & Broughton Micova, S. (2024). A study on the future of television broadcast / audio-visual sector in Thailand under a rapidly changing digital evolution (Final report). National Broadcasting and Telecommunications Commission. https://broadcast.nbtc.go.th/data/academic/file/680800000002.pdf

Fu, K., Zheng, G., & Xie, W. (2023). Customer churn prediction for a webcast platform via a voting-based ensemble learning model with Nelder-Mead optimizer. Journal of Intelligent Information Systems, 61, 859–879. https://doi.org/10.1007/s10844-023-00803-2

Haque, M. A. (2023). Feature engineering & selection for explainable models: A Second Course for Data Scientists. Leanpub.

Jain, H., Yadav, G., & Manoov, R. (2020). Churn prediction and retention in banking, telecom and IT sectors using machine learning techniques. In Advances in machine learning and computational intelligence (pp. 137–156). Springer. https://doi.org/10.1007/978-981-15-5243-4_12

Khoh, W. H., Pang, Y. H., Ooi, S. Y., Wang, L. Y. K., & Poh, Q. W. (2023). Predictive churn modeling for sustainable business in the telecommunication industry: Optimized weighted ensemble machine learning. Sustainability, 15(11), 8631. https://doi.org/10.3390/su15118631

Kunapuli, G. (2023). Ensemble methods for machine learning. Manning Publications.

Lotz, A. D. (2022). Netflix and streaming video: The business of subscriber-funded video on demand (1st ed.). Polity Press.

Manning, C. D., Raghavan, P., & Schütze, H. (2008). Introduction to information retrieval. Cambridge University Press.

Manohar, E., Jenifer, P., Sharon Nisha, M., & Benita, B. (2021). A collective data mining approach to predict customer behaviour. In 2021 Third International Conference on Intelligent Communication Technologies and Virtual Mobile Networks (ICICV) (pp. 1–6). IEEE. https://doi.org/10.1109/ICICV50876.2021.9388558

Maretta Sagala, N. T., & Permai, S. D. (2021). Enhanced churn prediction model with boosted trees algorithms in the banking sector. In 2021 International Conference on Data Science and Its Applications (ICoDSA) (pp. 240–245). IEEE. https://doi.org/10.1109/ICoDSA53588.2021.9617503

Pustokhina, I. V., Pustokhin, D. A., Nguyen, P. T., Elhoseny, M., & Shankar, K. (2023). Multi-objective rain optimization algorithm with WELM model for customer churn prediction in telecommunication sector. Complex & Intelligent Systems, 9, 3473–3485. https://doi.org/10.1007/s40747-021-00353-6

PwC Thailand. (2025). PwC: Thai entertainment and media to surpass THB700bn in 2025 despite slowdown [Press release] [Online]. Retrieved January 15, 2026, from https://www.pwc.com/th/en/press-room/press-release/2025/press-release-15-08-25-en.html

Ramesh, P., Emilyn, J. J., & Vijayakumar, V. (2022). Hybrid artificial neural networks using customer churn prediction. Wireless Personal Communications, 124, 1695–1709. https://doi.org/10.1007/s11277-021-09427-7

Saheed, Y. K., & Hambali, M. A. (2021). Customer churn prediction in telecom sector with machine learning and information gain filter feature selection algorithms. In 2021 International Conference on Data Analytics for Business and Industry (ICDABI) (pp. 208–213). IEEE. https://doi.org/10.1109/ICDABI53623.2021.9655792

Sridevi, R., & Gowtham, S. (2021). A comparative study on YouTube viewers perception towards YouTube Premium and non premium service. Utkal Historical Research Journal, 34(30), 72–78. https://www.researchgate.net/publication/353701982

Sridhar, S., & Vijayalakshmi, M. (2021). Machine learning. Oxford University Press.

Wang, J. (2022). Encyclopedia of data science and machine learning. IGI Global.

Wang, X., Huang, L., Huang, H., Li, B., Xia, Z., & Li, J. (2020). An ensemble learning model for short-term passenger flow prediction. Complexity, 6694186. https://doi.org/10.1155/2020/6694186

Xu, T., Ma, Y., & Kim, K. (2021). Telecom churn prediction system based on ensemble learning using feature grouping. Applied Sciences, 11(11), 4742. https://doi.org/10.3390/app11114742

การประยุกต์ใช้การประเมินผลกระทบด้านสุขภาพโดยชุมชนเพื่อการพัฒนาศักยภาพในการรองรับผลกระทบต่อความมั่นคงทางอาหาร ก่อนดำเนินกิจการโรงงานแปรรูปยางพารา พื้นที่ตำบลห้วยยาง อำเภอคอนสาร จังหวัดชัยภูมิ

Application of Community-Based Health Impact Assessment to Build Capacity to Address Impacts on Food Security before the Operation of a Rubber Processing Factory in Huai Yang Subdistrict, Khon San District, Chaiyaphum Province

วลัญช์ชยา เขตบำรุง[1*] และ จิราภรณ์ ประธรรมโย[1]

Valanchaya Ketbumroong[1*] and Jiraphon Pratumyo[1]

[1]คณะสาธารณสุขศาสตร์ มหาวิทยาลัยวงษ์ชวลิตกุล จังหวัดนครราชสีมา

[1]Faculty of Public Health, Vongchavalitkul University, Nakhon Ratchasima Province

*Corresponding Author: valanchaya_ket@vu.ac.th

Received: June 1, 2026 **Revised:** July 29, 2026 **Accepted:** September 15, 2026

บทคัดย่อ

การวิจัยครั้งนี้มีวัตถุประสงค์เพื่อ (1) การประยุกต์ใช้การประเมินผลกระทบด้านสุขภาพโดยชุมชนในการพัฒนาศักยภาพเพื่อรองรับผลกระทบต่อความมั่นคงทางอาหาร ก่อนดำเนินกิจการโรงงานแปรรูปยางพารา และ (2) พัฒนาข้อเสนอเชิงนโยบายต่อองค์กรปกครองส่วนท้องถิ่นและหน่วยงานที่เกี่ยวข้อง โดยใช้รูปแบบวิจัยเชิงปฏิบัติการแบบมีส่วนร่วม กลุ่มตัวอย่าง จาก 19 หมู่บ้าน จำนวน 407 คน ด้วยการสุ่มแบบแบ่งชั้น และเชิงคุณภาพ 20 คน คัดเลือกแบบเจาะจง เก็บข้อมูลด้วยแบบสัมภาษณ์ความมั่นคงทางอาหาร 4 มิติ และการสนทนากลุ่ม ภายใต้กรอบ CHIA 6 ขั้นตอน ดำเนินการระหว่างเดือนพฤษภาคม 2566 ถึงเมษายน 2567 วิเคราะห์ข้อมูลเชิงปริมาณด้วยสถิติเชิงพรรณนา ได้แก่ ร้อยละ ค่าเฉลี่ยและส่วนเบี่ยงเบนมาตรฐาน ข้อมูลเชิงคุณภาพด้วยการวิเคราะห์เนื้อหา ผลการวิจัยพบว่า ระดับความมั่นคงทางอาหารโดยรวมอยู่ในระดับปานกลาง ($\bar{X}$ = 3.67, S.D. = 0.72) เมื่อพิจารณารายมิติ พบว่า มิติการมีอาหารเพียงพอและ มิติการเข้าถึงอาหารอยู่ในระดับสูง ($\bar{X}$ = 3.74, S.D.=0.87), ($\bar{X}$ = 3.76,S.D.=1.27) มิติการใช้ประโยชน์จากอาหาร และมิติเสถียรภาพด้านอาหารอยู่ในระดับปานกลาง($\bar{X}$ = 3.54, S.D.=0.74), ($\bar{X}$ = 3.65,S.D.=1.25) ด้านแนวทางสร้างความมั่นคงทางอาหาร กลยุทธ์ความเข้าใจภายในครอบครัวเป็นจุดแข็งสำคัญของชุมชนอยู่ในระดับสูง ($\bar{X}$ = 3.75, S.D.=0.81) ขณะที่กลยุทธ์การพึ่งพาตนเอง การสนับสนุนทางสังคม การหาอาชีพเสริมการรับมือการเปลี่ยนแปลงภูมิอากาศอยู่ในระดับระดับปานกลาง ($\bar{X}$ = 3.08,S.D.=0.87; $\bar{X}$ = 3.40,S.D.=0.84; $\bar{X}$ = 3.15,S.D.=0.71; $\bar{X}$ = 3.33,S.D.=1.06) นอกจากนี้ ชุมชนคาดว่าจะมีผลกระทบเชิงบวก ได้แก่ การจ้างงานและรายได้ที่เพิ่มขึ้น ส่วนเชิงลบ ได้แก่ มีมลพิษทางน้ำและอากาศ ซึ่งอาจส่งผลต่อความมั่นคงทางอาหารของชุมชน จึงมีข้อเสนอเชิงนโยบาย 4 ด้าน ได้แก่ การจัดการสิ่งแวดล้อมและมลพิษ การสร้างความมั่นคงทางอาหารชุมชน การพัฒนาระบบข้อมูลและการเฝ้าระวัง และการเสริมสร้างความเข้มแข็งของชุมชน ดังนั้น ควรสนับสนุนให้นำข้อเสนอเชิงนโยบาย ไปออกข้อบัญญัติของท้องถิ่นและมีแผนงาน โครงการของหน่วยงานที่เกี่ยวข้องรองรับต่อไป

คำสำคัญ: การประเมินผลกระทบด้านสุขภาพโดยชุมชน, ความมั่นคงทางอาหาร, โรงงานแปรรูปยางพารา, ข้อเสนอเชิงนโยบาย

Abstract

This study aimed to (1) apply community-based health impact assessment (CHIA) to build capacity to address potential impacts on food security prior to the operation of a rubber processing plant, and (2) formulate policy recommendations for local administrative organizations and relevant agencies. A participatory action research design was employed. The sample comprised a quantitative group of 407 participants from 19 villages, selected through stratified random sampling, and a qualitative group of 20 participants selected through purposive sampling. Data were collected using a food security interview questionnaire covering four dimensions and through focus group discussions within a six-step CHIA framework. The study was conducted between May 2023 and April 2024. Quantitative data were analyzed using descriptive statistics, including percentages, means, and standard deviations, while qualitative data were analyzed using content analysis. The results showed that the overall level of food security was moderate ($\bar{X}$ = 3.67, S.D. = 0.72). When considered by dimension, the food availability dimension was at a high level ($\bar{X}$ = 3.74, S.D. = 0.87); the food access dimension was at a high level ($\bar{X}$ = 3.76, S.D. = 1.27); the food utilization dimension was at a moderate level ($\bar{X}$ = 3.54, S.D. = 0.74); and the food stability dimension was at a moderate level ($\bar{X}$ = 3.65, S.D. = 1.25). Regarding strategies for building food security, the family understanding strategy was identified as a key strength of the community, at a high level ($\bar{X}$ = 3.75, S.D. = 0.81), while the self-reliance, social support, supplementary income-generation, and climate change adaptation strategies were all at a moderate level ($\bar{X}$ = 3.08, S.D. = 0.87; $\bar{X}$ = 3.40, S.D. = 0.84; $\bar{X}$ = 3.15, S.D. = 0.71; $\bar{X}$ = 3.33, S.D. = 1.06). In addition, the community anticipated positive impacts, including increased employment and income, and negative impacts, including water and air pollution, which could affect the community's food security. Accordingly, four areas of policy recommendations were proposed: environmental and pollution management, community food security development, information and surveillance system development, and community capacity strengthening. Therefore, the incorporation of these policy recommendations into local ordinances should be supported, along with corresponding plans and projects by relevant agencies.

Keywords: Community health impact assessment, Food security, Rubber processing plant, Policy Recommendations

1. Introduction

Food security is one of the key goals of the United Nations Sustainable Development Goals (SDG 2). The Food and Agriculture Organization of the United Nations (FAO) reported that in 2023, approximately 733 million people worldwide experienced hunger. Food security comprises four core dimensions: food availability, food access, food utilization, and food stability (FAO et al., 2024). Although Thailand is a major food producer and exporter, it continues to face food safety problems arising from chemical residues, farmers' income insecurity, and industrial expansion affecting cultivation areas (World Health Organization (WHO), 2024). Khon San District, Chaiyaphum Province, is an area rich in natural resources and an important eco-tourism destination. However, in 2014, a licence was issued for the establishment of a Category 3 rubber processing factory (machinery exceeding 75 horsepower) in Ban Hin Roi Muen, Dong Bang Subdistrict. Although the plant is located in Dong Bang Subdistrict, Huai Yang Subdistrict, this study's primary site, shares the same watershed and prevailing wind direction, raising public concern about odor, wastewater, air pollution, and the safety of natural food sources. Residents therefore exercised their rights under Section

11 of the National Health Act B.E. 2550 (2007) to conduct this community-based health impact assessment (CHIA).

Health Impact Assessment (HIA) is a participatory learning process that uses evidence from multiple disciplines to assess the impact of policies, plans, or projects on the health and well-being of populations (World Health Organization (WHO), 2022). Thailand's National Health Commission Office (NHCO) has developed a six-step CHIA operational framework, comprising screening, scoping, impact assessment, public review of the draft report, decision-making, and monitoring and evaluation (National Health Commission Office (NHCO), 2021), which enables communities to participate effectively in public policy decision-making (Promthong et al., 2025). Yet research linking CHIA with food security in rural industrial-development contexts, particularly rubber processing plants, remains scarce, and a model for translating findings into area-level policy is still lacking. This gap matters: growing international evidence shows that industrial agglomeration and contamination can measurably affect community health (Pasetto et al., 2024; Qi & Xu, 2024), yet few studies examine the link to household-level food security or how CHIA evidence can be systematically translated into food security policy. This study responds to SDG 2 and SDG 3 by assessing household food security and its link to community health; SDG 11 by developing context-specific policy for an area entering industrial development; and SDG 16 by conducting participatory, multi-stakeholder decision-making throughout CHIA. Although local authorities and the Industrial Estate Authority of Thailand regulate pollution at its source, no systematic mechanism monitors impacts on surrounding communities' food security, and no formal process exists for community participation in assessment and policy recommendation. Participatory action research was therefore adopted, as it allows communities to link empirical evidence directly to policy negotiation with relevant agencies. Accordingly, this research aimed to (1) apply community-based health impact assessment (CHIA) to build capacity to address potential impacts on food security prior to the operation of a rubber processing plant, and (2) develop policy recommendations and key measures for local administrative organizations and relevant agencies to promote public policy development at both the organizational and area levels.

The theoretical foundation draws on Participatory Action Research (PAR), which holds that knowledge creation and social change are most effective when researchers and community members conduct research collaboratively through cycles of planning, action, observation, and reflection (Lewin, 1946); Freire, 1970) concept of conscientization, whereby participatory dialogue enables communities to critically analyze and act on the conditions affecting their lives; and Kemmis & McTaggart (2005) view of PAR as a communicative process creating a public sphere for deliberation. These principles underpin the six-step CHIA process, particularly the scoping and decision-making stages, where community members jointly defined assessment issues and negotiated policy with local government and the plant. To integrate CHIA with food security assessment, this study adopted a systems thinking/socio-ecological perspective (Figure 1): industrial development (plant construction and operation) may lead to environmental changes (water and air pollution), which may affect the four core food security dimensions. CHIA identifies these potential impacts through community participation, generating quantitative and qualitative evidence to inform policy development, with policy outcomes potentially shaping future industrial and environmental conditions.

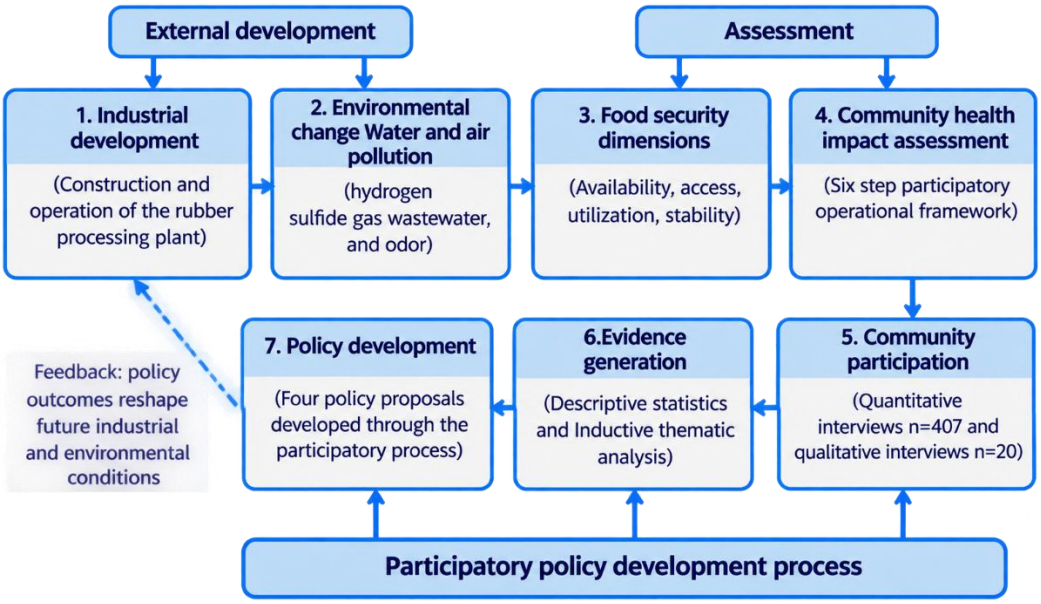


Figure 1. Systems/socio-ecological conceptual framework linking industrial development, environmental change, food security, community health impact assessment (CHIA), community participation, evidence generation, and policy development. The participatory process draws on Lewin (1946), Freire (1970), and Kemmis and McTaggart (2005).

2. Materials and methods

2.1 Research design and study area

This study employed a Participatory Action Research (PAR) design, emphasizing community participation at every stage of the research process. The study was conducted in Huai Yang Subdistrict, Khon San District, Chaiyaphum Province, between May 2023 and April 2024. Participants' rights were protected: the researchers explained the study's objectives, data-collection procedures, and participants' right to join or withdraw from the study at any time. The study was approved by the Human Research Ethics Committee, Nakhon Ratchasima Provincial Public Health Office (Certificate No. NRPH034, approved on 12 April 2023). Participatory action research was selected as the research design because the core research problem was inherently value-laden and context-specific, namely, a prospective assessment of the health and food-security impacts of an industrial plant that had already received construction approval but had not yet begun production. Community members possessed direct experiential knowledge of environmental change, and the ultimate goal was to produce negotiated, area-level policy proposals. This is consistent with Lewin (1946) view of action research as a repeated cycle of fact-finding, action, and reflection. This design allowed the CHIA process itself to serve as both a data-collection tool and a means of building community capacity. This approach was considered more appropriate than a purely quantitative design or qualitative research led solely by researchers, as it enabled residents, local officials, and the plant operator to jointly define the scope of assessment (Step 2: scoping) and jointly negotiate policy measures (Step 5: decision-making), consistent with Kemmis & McTaggart (2005) view of PAR as a communicative process for facilitating public deliberation.

2.2 Population, sample, and sampling method

The sample was divided into two groups: (1) a quantitative group of 407 participants, sampled from the population of Huai Yang Subdistrict's 19 villages using stratified random sampling, with the sample

size determined using Epi Info version 7.2 at a 95% confidence level, an expected frequency of 50%, and a design effect of 1; and (2) a qualitative group of 20 participants, selected through purposive sampling, comprising local administrative officials, community leaders, resident representatives, and academics supporting the CHIA process. Inclusion criteria for the quantitative sample were: being a registered resident of Huai Yang Subdistrict, having resided continuously in the area for at least 6 months, and being willing to participate. The exclusion criterion was not having resided continuously in the area for a full 6 months. For the qualitative group, inclusion criteria were: having a direct role or involvement in at least one step of the CHIA process, and having at least one year of experience related to the rubber processing plant issue or community food security, to ensure that informants had sufficient knowledge and direct experience relevant to the topic under study. The exclusion criterion was being unable to provide in-depth information about the CHIA process or related impacts.

2.3 Research instruments

Data collection instruments comprised two components. (1) The quantitative interview questionnaire measured the four core dimensions of food security (availability, access, utilization, and stability) together with household-level approaches to building food security (self-reliance, social support, family understanding, supplementary income generation, and climate change adaptation). These were rated on a five-point scale (1 = lowest, 5 = highest). The questionnaire also assessed participation in community natural-resource monitoring. For every item, response options were selected to best match each respondent's actual circumstances. Content validity was assessed by three experts using the Index of Item-Objective Congruence (IOC; +1 = consistent, 0 = uncertain, and −1 = not consistent with the objective), yielding a mean IOC of 0.96 (Rovinelli & Hambleton, 1977). Reliability, tested with 30 residents of Dong Bang Subdistrict, was α = 0.83 for the questionnaire as a whole and α = 0.73 for the four core food-security dimensions alone. (2) A semi-structured guide supported three focus group discussions (FGDs) and three key informant interviews (KIIs), involving 20 qualitative participants. Participant composition varied slightly across sessions: business operators did not take part in Session 1, whereas the same group of participants attended both Sessions 2 and 3. The sessions addressed the following topics: food-safety/security regulations (Session 1); joint scoping of the impact assessment (Session 2); and review of the draft community-based health impact assessment (CHIA) report (Session 3). Stakeholder composition by session is summarized in Table 1. Each session lasted approximately two hours. Sessions were audio-recorded (using two recorders, with informed consent from participants) and transcribed verbatim within 24–48 hours using speaker codes; transcripts were checked against the recordings and reviewed by a subset of participants before being placed in secure storage. Trustworthiness was strengthened through triangulation across the three sessions, the questionnaire data, and the key informant interviews (KIIs), the latter of which used a separate interview guide addressing the local definition of food security in Huai Yang Subdistrict, participants' views and experiences regarding the four food-security dimensions, community goals, food-security challenges, and potential solutions.

Table 1. Focus group discussion (FGD) and key informant interview (KII) sessions

Session	Purpose	Approx. N	Key stakeholder groups
1	Review existing food-safety/security plans and regulations	20	Local administrator, chief administrative officer, Public Health & Environment Division, district public health officer, sub-district headman, agricultural officer, community development officers, schools, health-promoting hospital, community enterprise groups, academics
2	Jointly scope the food security impact assessment	20	Local government officials, community leaders, food producers, consumers, business operators, academics
3	Review the draft CHIA report (public review)	20	Local government officials, community leaders, food producers, consumers, business operators, academics

2.4 Community participatory health impact assessment process

The CHIA process followed the six-step framework of the National Health Commission Office (National Health Commission Office, 2022) as follows: Step 1, public screening of the policy; Step 2, public scoping of the study; Step 3, assessing health impacts; Step 4, public review of the draft report; Step 5, influencing the decision-making process; and Step 6, public monitoring and evaluation.

2.5 Data analysis

Quantitative data were analyzed using statistical software to calculate descriptive statistics, including frequencies, percentages, means, and standard deviations. Mean-score interpretation criteria were set as follows: high = 3.68–5.00; moderate = 2.34–3.67; and low = 1.00–2.33. Qualitative data were analyzed using content analysis and summarized into key themes. To strengthen methodological rigor in the qualitative component, data analysis followed an inductive thematic content analysis process. Two researchers independently open-coded the data line by line from transcripts of focus group discussions and key informant interviews. The codes were then compared, discussed, and grouped into candidate themes, with any inconsistencies resolved through consensus. The trustworthiness of the qualitative data was assessed against generally accepted criteria: credibility, supported by data and investigator triangulation (comparing data across village groups, occupational groups, and informant roles, as well as cross-checking against the quantitative analysis results); dependability and confirmability, supported by maintaining an audit trail of coding decisions and analytical memos; and transferability, supported by a detailed description of the study context (Section 2.1). Researcher reflexivity was maintained through regular team debriefing meetings to review and discuss any prior biases or perspectives that may have arisen from the research team's earlier interactions with the community during the initial CHIA screening stage.

2.6 Integration of quantitative and qualitative methods

This study employed a convergent mixed-methods design embedded within the Participatory Action Research (PAR) cycle. Quantitative data (a food security questionnaire covering four core dimensions, n = 407) and qualitative data (focus group discussions and key informant interviews, n = 20) were collected concurrently during CHIA Step 3 (impact assessment) and analyzed separately before being integrated during CHIA Step 4 (public review of the draft report). The quantitative results were first summarized descriptively by dimension and strategy (Tables 3 and 4) and were then presented back to the community and qualitative

participants at the public review forum. The key themes derived from the qualitative content analysis were used to explain, contextualize, and, in some cases, further elaborate on the quantitative patterns. The integration of both strands of data formed the key foundation for the four policy proposals developed during CHIA Step 5 (decision-making), resulting in policy recommendations that were well aligned with the local context. The CHIA/PAR process, including data collection, data integration, and policy development, is illustrated in Figure 2.

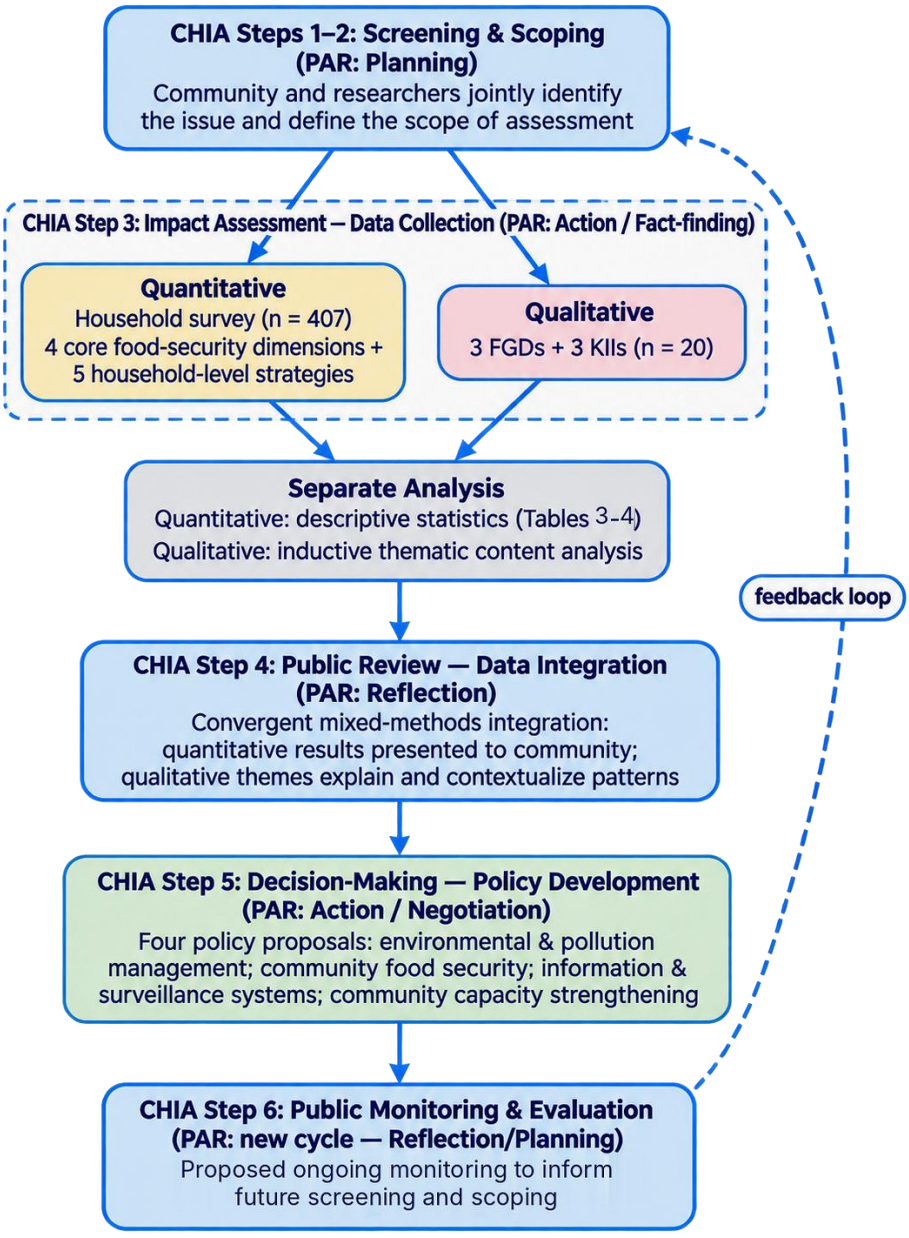


Figure 2. Figure 2. CHIA/PAR process flowchart illustrating the six-step CHIA framework, from screening and scoping (Steps 1–2) through data collection (Step 3), data integration (Step 4), and policy development (Step 5) to monitoring and evaluation (Step 6), aligned with the PAR cycle (planning, action, and reflection).

3. Results

3.1 General characteristics of the sample

Among the 407 participants in the quantitative group, the majority were male (51.4%), with a mean age of 52.9 years (S.D. = 11.2; age range: 15–80 years). The Baby Boomer group (54–72+ years) accounted for the largest proportion (53.1%), followed by Generation X (38–53 years) at 37.3%. Most had completed primary education (54.8%), were married (81.8%), and had lived in the community for more than 20 years (90.7%). Among the 407 participants in the quantitative group, the majority were male (51.4%), with a mean age of 52.9 years (S.D. = 11.2; age range: 15–80 years). The Baby Boomer group (54–72+ years) accounted for the largest proportion (53.1%), followed by Generation X (38–53 years) at 37.3%. Most had completed primary education (54.8%), were married (81.8%), and had lived in the community for more than 20 years (90.7%). General laborers accounted for 45.9% of participants; 73.7% had a total family income exceeding 10,000 THB/month, and 65.8% relied on markets and shops as their main food source. Details are presented in Table 2.

3.2 Food security dimensions

The assessment of food security across the four core dimensions revealed that the overall level was moderate ($\bar{x}$ = 3.67, S.D. = 0.72), as shown in Table 3. The food availability dimension was at a high level ($\bar{x}$ = 3.74, S.D. = 0.87); the food access dimension was at a high level ($\bar{x}$ = 3.76, S.D. = 1.27); the food utilization dimension was at a moderate level ($\bar{x}$ = 3.54, S.D. = 0.74); and the food stability dimension was at a moderate level ($\bar{x}$ = 3.65, S.D. = 1.25). The relatively high standard deviations observed across several dimensions (S.D. ranging from 1.25 to 1.27) reflect considerable variation in food security experiences among households in Huai Yang Subdistrict.

Table 2. General characteristics of respondents (n = 407)

Characteristics	Number	Percentage
Sex		
Male	209	51.4
Female	198	48.6
Age group		
Baby Boomer (54–72+ years)	216	53.1
Generation X (38–53 years)	152	37.3
Generation Y/Z (15–37 years)	39	9.6
Education level		
Primary school	223	54.8
Secondary school	89	21.9
High school/Vocational	57	14.0
Bachelor's degree and above	38	9.3
Marital status: married	333	81.8
Residence > 20 years in community	369	90.7
Family income > 10,000 THB/month	300	73.7

Table 3. Food security dimensions (n = 407)

Dimension	$\bar{x}$	S.D.	Level
1. Food availability	3.74	0.87	High
2. Food access	3.76	1.27	High
3. Food utilization	3.54	0.74	Moderate
4. Food stability	3.65	1.25	Moderate
Overall	3.67	**0.72**	**Moderate**

Note: Score interpretation: High = 3.68–5.00; Moderate = 2.34–3.67; Low = 1.00–2.33

3.3 Strategies for building food security

The assessment of five household food security strategies revealed that the overall level was moderate ($\bar{x}$ = 3.34, S.D. = 0.66). The family understanding strategy was at a high level ($\bar{x}$ = 3.75, S.D. = 0.81). The self-reliance strategy was at a moderate level ($\bar{x}$ = 3.08, S.D. = 0.87), the social support strategy was at a moderate level ($\bar{x}$ = 3.40, S.D. = 0.84), the supplementary income strategy was at a moderate level ($\bar{x}$ = 3.15, S.D. = 0.71), and the climate change adaptation strategy was at a moderate level ($\bar{x}$ = 3.33, S.D. = 1.06), as shown in Table 4.

Table 4. Food security strategy levels (n = 407)

Strategy	$\bar{x}$	S.D.	Level
1. Self-reliance	3.08	0.87	Moderate
2. Social support	3.40	0.84	Moderate
3. Family understanding	3.75	0.81	High
4. Supplementary income	3.15	0.71	Moderate
5. Climate change adaptation	3.33	1.06	Moderate
Overall	**3.34**	**0.66**	**Moderate**

Note: Score interpretation: High = 3.68–5.00; Moderate = 2.34–3.67; Low = 1.00–2.33

3.4 CHIA process outcomes and policy proposals

Results from all six CHIA steps showed that the community expected the rubber processing plant to generate both positive and negative impacts on food security. Expected positive impacts included job creation and supplementary income for community workers (23.1% of respondents) and expanded market channels for rubber farmers. Expected negative impacts included water and air pollution (hydrogen sulfide gas [H_2S] and odor) and threats to biodiversity, rice-field crabs, apple snails, and wild vegetables, which are important natural food sources. These concerns were shared by 94.3% of respondents. Notably, 79.1% agreed with building cooperation among the community, the plant, and government agencies, and residents had already begun natural-resource monitoring.

Inductive content analysis of the qualitative data identified four thematic codes: economic impacts, pollution risks, impacts on natural food sources and biodiversity, and community–plant–government cooperation. These were consistent with and supported the quantitative findings above. The CHIA process also reflected key PAR dynamics: joint learning through focus groups and community forums, consensus-building on impact issues, and policy negotiation between community representatives and local officials. This process further built community capacity, as residents developed water-quality monitoring skills and a network of community leaders emerged to continue addressing environmental health issues.

These outcomes were not derived from descriptive statistics alone; the four policy proposals emerged iteratively through the public review and decision-making steps, in which community representatives examined the quantitative results, discussed underlying causes, and, together with local officials, academic facilitators, and the plant operator, negotiated feasible, context-specific measures: (1) Environmental and pollution management: a local ordinance setting wastewater discharge standards in line with Industrial Estate Authority of Thailand Notification No. 029/2567 (effective 28 May 2024), with water-quality monitoring points along the Huai Yang stream and its six natural water sources, focused on controlling hydrogen sulfide gas (H_2S), the primary pollutant from high-sulfate rubber-industry wastewater; (2) Community food security: a natural food source conservation zone (rice-field crabs, apple snails, wild vegetables) across the Huai Yang watershed (6–10 villages), together with a community seed bank, to guard against contamination from plant effluent; (3) Information and surveillance systems: a community food resource map and early-warning system linked to the database of the subdistrict health-promoting hospital; and (4) Community capacity strengthening: a permanent subdistrict-level CHIA working group, with representatives from all 19 villages, the plant, and Huai Yang Subdistrict Municipality, serving as an ongoing mechanism for negotiation and monitoring, and positioning the area as a subdistrict-level CHIA model for other communities facing industrial development.

Qualitative accounts corroborated these proposals. Participants noted that the plant could ease seasonal unemployment, which currently requires community members to travel outside the area for work, consistent with the 23.1% of respondents who expected increased employment and income. Participants also raised concerns that wind-borne odor and wastewater could affect daily life and nearby agriculture, consistent with the literature identifying H_2S as the primary pollutant from high-sulfate rubber wastewater. One participant described competition over natural resources: “there used to be enough, but people from outside the community collect them to sell.” Most participants supported joint monitoring and clear complaint channels among the community, the plant, and government agencies, consistent with the 79.1% of respondents who agreed with building such cooperation.

4. Discussion

The main finding of this study is that the CHIA process can serve as a concrete “linking mechanism” between household-level food security data and the development of area-level public policy proposals. That is, the results of the food security assessment (four core dimensions) and the community's self-reliance strategy were not merely descriptive outcomes, but were used as an empirical evidence base for formulating all four policy proposals through a participatory process. This discussion is therefore organized in that order, beginning with an interpretation of the observed food security levels, linking them to the role of the CHIA process, and leading to the specificity of the policy proposals within the context of the study area.

This study found that overall food security was at a moderate level ($\bar{x}$ = 3.67), consistent with FAO's food security framework, which states that food security refers not only to having enough food, but also encompasses access, utilization, and stability (FAO et al., 2024). The food access dimension ($\bar{x}$ = 3.76) showed the highest mean because Huai Yang Subdistrict is rich in natural resources, with six natural water sources and diverse community markets, enabling residents to access food from both natural and market sources. However, the food utilization dimension ($\bar{x}$ = 3.54) showed the lowest mean of the four core dimensions. This may reflect the economic vulnerability of smallholder farming households that rely on income from general wage labor (45.9%), which may be affected by labor market fluctuations, particularly

as the industrial sector moves into the area. This finding is consistent with Niederdeppe et al. (2025), who emphasized the importance of health communication and building community awareness to cope with economic and social change.

The community's family understanding strategy showed the highest mean ($\bar{x}$= 3.75), highlighting household cohesion as a key strength in coping with change. By contrast, the self-reliance strategy ($\bar{x}$= 3.08) showed the lowest mean among the five strategies. The community's continued reliance on external income sources may limit self-sufficiency. The arrival of the plant may help create some employment opportunities, but complementary measures are needed to strengthen household self-reliance (World Health Organization (WHO), 2022).

The CHIA process, which applies the principle of participation by residents and all sectors, was found to be effective as a joint forum for data collection, impact analysis, and policy development (National Health Commission Office (NHCO), 2022). In particular, the finding that 79.1% of residents agreed with building cooperation among the community, the plant, and government reflects the community's readiness to work together, which is a key factor in driving public policy (Promthong et al., 2025). The findings of this study are also consistent with Cornish et al. (2023), who noted that PAR is a research process that values communities' experiential knowledge in bringing about sustainable social change, and with approaches to building community power in primary health care through PAR (Mabetha et al., 2023), which similarly emphasize the importance of sustainable collaborative structures between communities and local administrative organizations.

The contribution of this study to knowledge of CHIA lies in demonstrating that the six-step CHIA framework can be effectively integrated with a food security assessment comprising four core dimensions, an approach that has not previously appeared in CHIA studies in Northeastern Thailand. In particular, the development of a community food resource map and a community-based water-quality monitoring system represents a new component that extends the standard CHIA framework and can be applied in other areas where industrial plants are located near communities. This is consistent with the work of Promthong et al. (2025), which confirms CHIA's potential to support area-level policy, particularly in the context of Thai local administrative organizations, which vary widely in geography and culture.

The finding regarding community concern over the plant's potential impact on natural food sources, particularly the risk to water quality in the Huai Yang stream and its six natural water sources, is an important issue requiring urgent management, since these water sources serve as natural food sources (rice-field crabs, apple snails, and wild vegetables) for 6–10 villages, consistent with WHO (2024), which emphasizes that water and food safety are fundamental to community health security. Regarding the use of technology and innovation in community health communication, developing a community early-warning system and a community food resource map would help improve the efficiency of monitoring and responding to food security situations (Olawade et al., 2023).

Nonetheless, these findings should be interpreted critically, not merely to confirm prior research. The consistency with Pasetto et al. (2024) and Qi & Xu (2024) is notable, since those studies, like this one, involved communities located near industrial plants; however, those studies examined contexts where the plants were already in operation, whereas this study conducted the community-based health impact assessment before the plant began production. Moreover, whereas Qi & Xu (2024) found that green industrial agglomeration was generally associated with improved health outcomes, this study instead found predominantly negative community concerns about food-security impacts at the household level. This difference likely reflects context-specific factors in Huai Yang Subdistrict: the rubber processing plant in this

study is a single large Category 3 facility rather than a diverse industrial cluster; the affected population relies directly on nearby natural water sources for food (rather than solely on formal markets); and the community still lacks institutional monitoring capacity compared with the more industrialized contexts examined in those studies. This suggests that the health and food-security impacts of industrial development are not uniform, but are shaped by the type and scale of industry, the community's level of dependence on natural resources, and the strength of local governance and monitoring systems (Pasetto et al., 2024).

The practical implications of these findings extend to multiple stakeholders. For local government agencies, the four policy proposals represent a concrete, negotiated agenda that can be incorporated into local development plans and ordinances. For environmental regulatory agencies, community-based water-quality monitoring highlights the value of integrating citizen-generated data with formal regulatory monitoring, particularly for pollutants such as hydrogen sulfide gas, which are difficult to monitor continuously by other means. For public health practitioners, this study demonstrates a replicable method for linking household-level food security assessment with community-based health impact assessment, applicable to other communities located near industrial plants. For civil society organizations, this study demonstrates that systematic participation throughout every step of CHIA, rather than at a single point of consultation, can translate lived experience into negotiated policy commitments.

This study has several limitations. First, the quantitative assessment was cross-sectional, capturing food security at a single point in time, and therefore cannot support causal inferences about the plant's long-term impacts. Second, the study was conducted in a single subdistrict (Huai Yang) surrounding a single rubber processing plant, which limits the generalizability of the findings to other areas and industry types; transferability to other contexts should be assessed by comparing area conditions (resource dependence, industry type, governance capacity) rather than assumed. Third, because both quantitative and qualitative participants were residents directly affected by and involved in the CHIA process, the findings may carry participation bias toward those most affected by or involved with the plant's impacts, while those less involved or who benefited directly from plant employment may be underrepresented.

5. Conclusions and recommendations

This study demonstrates that the six-step CHIA process can serve as an effective tool for developing area-level public policy proposals. Huai Yang Subdistrict's overall food security level was moderate ($\bar{x}$ = 3.67), with strengths in food access ($\bar{x}$ = 3.76) and the family understanding strategy ($\bar{x}$ = 3.75), but relatively lower scores in food utilization ($\bar{x}$ = 3.54). The community anticipated that once the rubber processing plant began operations, it would generate both positive and negative impacts on food security, and the four policy proposals derived from the CHIA process covered environmental measures, food security, information systems, and community strengthening.

Recommendations: (1) Huai Yang Subdistrict Municipality should incorporate the proposals into its local development plan and ordinances; (2) NHCO should promote this CHIA process as a model for other areas facing industrial development in Northeastern Thailand; (3) the plant's long-term impact on water quality and agricultural yield should be monitored (≥ 3 years); and (4) the relationship between food security and community health status should be studied using chronic-disease and nutritional indicators.

Future research should (1) track food security and water-quality indicators over the long term (≥ 3 years) to build clearer causal evidence; and (2) replicate this CHIA food security integration model in communities near other industry types (e.g., mining, agro-processing) in Northeastern Thailand.

6. Acknowledgements

The research team would like to thank the National Health Commission Office (NHCO) for supporting the research funding and the CHIA implementation process; the Huai Yang Subdistrict Municipality, Khon San District, Chaiyaphum Province; the community leaders of all 19 villages; and all residents who cooperated well in the research. We also thank the faculty members and experts who provided recommendations for the research project, and Vongchavalitkul University for supporting the participation of faculty members in this research project.

7. References

Cornish, F., Breton, N., Moreno-Tabarez, U., Delgado, J., Rua, M., de-Graft Aikins, A., & Hodgetts, D. (2023). Participatory action research. Nature Reviews Methods Primers, 3(1), 34. https://doi.org/10.1038/s43586-023-00214-1

Food and Agriculture Organization of the United Nations (FAO), International Fund for Agricultural Development (IFAD), United Nations Children's Fund (UNICEF), World Food Programme (WFP), & World Health Organization (WHO). (2024). The state of food security and nutrition in the world 2024: Financing to end hunger, food insecurity and malnutrition in all its forms. https://doi.org/10.4060/cd1254en

Freire, P. (1970). Pedagogy of the oppressed (M. B. Ramos, Trans.). Continuum.

Industrial Estate Authority of Thailand. (2024). Notification of the Industrial Estate Authority of Thailand No. 029/2567 regarding general standard for wastewater discharge into the central wastewater treatment system in industrial estates. Government Gazette. https://enviliance.com/regions/southeast-asia/th/report_12094 (in Thai)

Kemmis, S., & McTaggart, R. (2005). Participatory action research: Communicative action and the public sphere. In N. K. Denzin & Y. S. Lincoln (Eds.), The Sage handbook of qualitative research (3rd ed., pp. 559–603). Sage.

Lewin, K. (1946). Action research and minority problems. Journal of Social Issues, 2(4), 34–46. https://doi.org/10.1111/j.1540-4560.1946.tb02295.x

Mabetha, D., Ojewola, T., van der Merwe, M., Mabika, R., Goosen, G., Sigudla, J., Hove, J., Witter, S., & D'Ambruoso, L. (2023). Realising radical potential: Building community power in primary health care through participatory action research. International Journal for Equity in Health, 22, 94. https://doi.org/10.1186/s12939-023-01894-7

National Health Commission Office (NHCO). (2021). Criteria and procedures for health impact assessment from public policies B.E. 2564. NHCO. https://www.nationalhealth.or.th/th/node/3581 (in Thai)

National Health Commission Office (NHCO). (2022). Community health impact assessment guidebook. NHCO. https://www.nationalhealth.or.th (in Thai)

Niederdeppe, J., Boyd, A. D., King, A. J., & Rimal, R. N. (2025). Strategies for effective public health communication in a complex information environment. Annual Review of Public Health, 46, 411–431. https://doi.org/10.1146/annurev-publhealth-071723-120721

Olawade, D. B., Wada, O. J., David-Olawade, A. C., Kunonga, E., Abaire, O., & Ling, J. (2023). Using artificial intelligence to improve public health: A narrative review. Frontiers in Public Health, 11, Article 1196397. https://doi.org/10.3389/fpubh.2023.1196397

Pasetto, R., Zona, A., Marsili, D., Buratti, F. M., Iavarone, I., Soggiu, M. E., & Testai, E. (2024). Promotion of environmental public health and environmental justice in communities affected by large and long lasting industrial contamination: Methods applied and lessons learned from the case study of Porto Torres (Italy). Frontiers in Public Health, 12, Article 1408127. https://doi.org/10.3389/fpubh.2024.1408127

Promthong, N., Thaweesook, S., Sukmak, P., Mongkolsomlit, S., Hengboriboonpong Jaidee, P., & Putthasri, W. (2025). Participatory health impact assessment for health and well-being policy at local level in Thailand. Health Promotion Journal of Australia, 36(3), e70073. https://doi.org/10.1002/hpja.70073

Qi, D., & Xu, W. (2024). The impact of industrial synergistic agglomeration on residents' health levels. Frontiers in Public Health, 12, Article 1410359. https://doi.org/10.3389/fpubh.2024.1410359

Rovinelli, R. J., & Hambleton, R. K. (1977). On the use of content specialists in the assessment of criterion-referenced test item validity. Dutch Journal of Educational Research, 2, 49–60.

World Health Organization (WHO). (2022). Health impact assessment. WHO. https://www.who.int/health-topics/health-impact-assessment

World Health Organization (WHO). (2024). Food safety [Fact sheet]. WHO. https://www.who.int/news-room/fact-sheets/detail/food-safety

ผลของการเตรียมเบื้องต้นด้วยสารละลายแมกนีเซียมซัลเฟตต่อฤทธิ์ต้านอนุมูลอิสระและปริมาณคลอโรฟิลล์ของผำอบแห้ง

Effect of Magnesium Sulfate Solution Pretreatment on Antioxidant Properties and Chlorophyll Content of Dried Wolffia (*Wolffia globosa*)

ปภากร ศรีสอน[1*] พีรรัตน์ ดวงติ๊บ[1] และ กานต์รวี ฮั่นสกุล[1]

Paphakorn Srisorn[1*], Peerarat Doungtip[1] and Kanrawee Hunsakul[1]

[1]คณะวิทยาศาสตร์และเทคโนโลยี มหาวิทยาลัยเทคโนโลยีราชมงคลตะวันออก จังหวัดชลบุรี

[1]Faculty of Science and Technology, Rajamangala University of Technology Tawan-ok, Chonburi Province

*Corresponding Author: paphakorn_sr@rmutto.ac.th

Received: September 28, 2025 **Revised:** August 01 2026 **Accepted:** August 19, 2026

บทคัดย่อ

ผำ (*Wolffia globosa*) ซึ่งเป็นพืชน้ำที่อุดมไปด้วยสารอาหารและมีถิ่นกำเนิดในภูมิภาคเอเชียตะวันออกเฉียงใต้กำลังได้รับความสนใจในฐานะแหล่งโปรตีนและสารออกฤทธิ์ทางชีวภาพที่ยั่งยืน อย่างไรก็ตามกระบวนการแปรรูปหลังการเก็บเกี่ยวมักส่งผลกระทบต่อลักษณะปรากฏและสมบัติเชิงหน้าที่ งานวิจัยนี้จึงมุ่งศึกษาผลของการเตรียมการเบื้องต้น (pretreatment) ด้วยสารละลายแมกนีเซียมซัลเฟต ($MgSO_4$) ที่มีต่อการรักษาสีและสมบัติการต้านอนุมูลอิสระของผำอบแห้ง วิธีการศึกษาทำโดยนำผำสดมาลวกในสารละลาย $MgSO_4$ ที่ระดับความเข้มข้นร้อยละ 0.1, 0.3, 0.5 และ 0.7 (น้ำหนักต่อปริมาตร) ก่อนนำไปอบแห้งภายใต้สภาวะควบคุม จากนั้นทำการประเมินค่าพารามิเตอร์สี ได้แก่ ค่าความสว่าง (L*) ค่าความเป็นสีแดง/เขียว (a*) และค่าความเป็นสีเหลือง/น้ำเงิน (b*) ด้วยเครื่องสเปกโตรโฟโตมิเตอร์ พร้อมทั้งประเมินฤทธิ์การต้านอนุมูลอิสระด้วยวิธี DPPH radical scavenging assay และ FRAP assay ผลการศึกษาพบว่าสิ่งทดลองที่ใช้ความเข้มข้นของสารละลาย $MgSO_4$ ร้อยละ 0.7 (น้ำหนักต่อปริมาตร) จะให้ปริมาณคลอโรฟิลล์รวมสูงสุด (6,147.31 มิลลิกรัมต่อกิโลกรัม) แต่การคงอยู่ของคลอโรฟิลล์นี้ไม่ได้ส่งผลต่อการรักษาสภาพสี การเตรียมการเบื้องต้นด้วย $MgSO_4$ ทำให้ค่าความสว่าง (L*) และความเป็นสีเขียวลดลงอย่างมีนัยสำคัญ (โดยมีค่า a* ติดลบน้อยลงเมื่อเทียบกับสิ่งทดลองควบคุม) ($p < 0.05$) นอกจากนี้กระบวนการดังกล่าวยังทำให้ปริมาณสารประกอบฟีนอลิกทั้งหมดและความสามารถในการต้านอนุมูลอิสระลดลงอย่างมีนัยสำคัญเมื่อเปรียบเทียบกับผำอบแห้งที่ไม่ผ่านการลวก ($p < 0.05$) การค้นพบนี้ชี้ให้เห็นว่าแม้การลวกด้วยสารละลาย $MgSO_4$ จะช่วยปกป้องคลอโรฟิลล์ในระดับเคมี แต่กลับส่งผลเชิงลบต่อลักษณะปรากฏด้านความเป็นสีเขียว ความสว่าง และคุณสมบัติการต้านอนุมูลอิสระ ดังนั้นการนำกระบวนการเตรียมการเบื้องต้นนี้ไปใช้จึงควรประเมินถึงความคุ้มค่าระหว่างการรักษาเสถียรภาพของคลอโรฟิลล์กับการสูญเสียคุณภาพทางด้านสีและสารประกอบเชิงหน้าที่

คำสำคัญ: ผำ, สารละลายแมกนีเซียมซัลเฟต, การรักษาสี, สมบัติการต้านอนุมูลอิสระ, ปริมาณคลอโรฟิลล์

Abstract

Wolffia globosa, a nutrient-dense aquatic plant native to Southeast Asia, has gained attention as a sustainable source of protein and bioactive compounds. However, post-harvest processing often compromises its visual appeal and functional properties. This study investigates the effect of magnesium sulfate ($MgSO_4$) solution pretreatment on color retention and antioxidant properties of dried Wolffia. Fresh Wolffia were blanched in varying concentrations of $MgSO_4$ at 0.1%, 0.3%, 0.5%, and 0.7% w/v and dried under controlled conditions. Color parameters including lightness (L*), redness/greenness (a*), and yellowness/blueness (b*) were measured using a spectrophotometer, while antioxidant activity was assessed via DPPH radical scavenging assay and FRAP assay. Results indicated that while the 0.7% w/v $MgSO_4$ treatment yielded the highest total chlorophyll content (6,147.31 mg/kg), this chemical retention did not

translate to color preservation. $MgSO_4$ pretreatments significantly decreased lightness (L*) and greenness (resulting in less negative a* values compared to the unblanched control) ($p < 0.05$). Furthermore, the pretreatments caused a significant reduction in total phenolic content and antioxidant capacity compared to the control dried Wolffia ($p < 0.05$). These findings suggest that while $MgSO_4$ blanching effectively protects chlorophyll chemically, it negatively impacts the greenness, lightness, and antioxidant properties of dried Wolffia. Therefore, the trade-off between chlorophyll stabilization and the loss of color quality and functional compounds must be carefully evaluated for product applications.

Keywords: Wolffia, Magnesium sulfate solution, Color retention, Antioxidant properties, Chlorophyll content

1. Introduction

Wolffia globosa, commonly known as watermeal, is the smallest flowering plant on Earth and a promising source of plant-based protein, dietary fiber, and bioactive compounds. Indigenous to Southeast Asia, Wolffia has long been consumed in traditional diets and is now gaining global attention as a sustainable ingredient for functional foods and nutraceuticals due to its nutritional composition and potential for human food applications (Appenroth et al., 2018). Its rapid growth rate, minimal land requirement, and high nutritional density position it as a strategic crop for addressing food security and environmental sustainability (Appenroth et al., 2018; Masavang et al., 2022).

Despite its nutritional potential, the commercialization of Wolffia-based products faces challenges related to post-harvest stability, particularly in maintaining visual appeal and bioactivity during drying and storage. Color degradation and loss of antioxidant capacity are common issues that compromise consumer acceptance and functional efficacy (Oliveira et al., 2016). These changes are often driven by enzymatic browning, pigment oxidation, chlorophyll degradation, and structural damage during thermal processing or inappropriate drying conditions, which may reduce nutritional value and bioactive compounds in dried duckweed products (Kaur et al., 2018; Prosridee et al., 2023). Therefore, pretreatment strategies that can improve color retention while minimizing the loss of bioactive compounds are important for the development of dried Wolffia products (Minh et al., 2019).

Magnesium sulfate ($MgSO_4$), a food-safe inorganic salt, has been investigated for its potential role in pigment stabilization, particularly in relation to chlorophyll-containing materials. Mg^{2+} ions are associated with the structural stability of chlorophyll, in which magnesium is located at the center of the porphyrin ring; displacement of this central Mg^{2+} during processing can promote the conversion of chlorophyll to pheophytin, resulting in dull green or brownish discoloration (Bohn et al., 2004). Previous studies have suggested that $MgSO_4$ or salt-assisted blanching can help retain color and chlorophyll content in dried Wolffia, although its effect on antioxidant-related properties may vary depending on processing conditions and the leaching of water-soluble phenolic compounds during blanching (Workneh et al., 2014; Khan et al., 2022; Doungtip et al., 2025).

Although $MgSO_4$ has been reported to contribute to pigment retention, its application as a pretreatment for aquatic plants such as *Wolffia globosa* remains insufficiently clarified, particularly when visual quality and functional properties are evaluated together. In addition, limited information is available on the trade-off between chlorophyll retention and the possible reduction of phenolic content and antioxidant activity caused by blanching. Therefore, this study aimed to evaluate the effects of $MgSO_4$ solution pretreatment at different concentrations on color characteristics, water activity, proximate composition, total phenolic content, antioxidant properties, and chlorophyll content of dried *Wolffia*

globosa. The findings are expected to provide useful information for optimizing pretreatment conditions that balance visual quality and functional properties in dried Wolffia products.

2. Materials and methods

2.1 Preparation of Dried Wolffia

Fresh *Wolffia globosa* samples were collected from Tonkla Bon Din Community Enterprise, Ban Bueng, Chonburi and thoroughly rinsed with distilled water to remove surface impurities. The samples were drained to remove excess surface water before treatment. The study was designed to evaluate one control and four $MgSO_4$ pretreatment conditions. The control consisted of fresh Wolffia that was rinsed and drained without $MgSO_4$ pretreatment, while the treated samples were blanched in $MgSO_4$ solutions at concentrations of 0.1%, 0.3%, 0.5%, and 0.7% (w/v). A fixed sample-to-solution ratio of 500 g of powder / 1 L of solution was used for all treatments. Each treatment involved immersing the samples in the respective $MgSO_4$ solution at 80 °C for 3 min. After blanching, the samples were immediately cooled in cold water (4–8 °C) for 10 min and drained for 30 min to ensure uniform moisture removal before drying. All samples were dried in a hot-air oven at 50 °C for 8 h or until the samples reached a moisture content of 10%. The dried samples were then ground using a laboratory grinder and passed through a 100-mesh sieve. The ground samples were stored in aluminum foil pouches protected from light at 4-8 °C until analysis.

2.2 Percent Yield of Dried Wolffia

The percent yield of dried Wolffia was calculated to determine the mass recovery after pretreatment and drying. The initial fresh weight of each sample was recorded before pretreatment, and the dried sample weight was recorded after hot-air drying. The percent yield was calculated using the following equation:

$$\text{Yield (\%)} = \frac{\text{Dried sample weight}}{\text{Initial fresh weight}} \times 100 \quad (1)$$

2.3 Color Analysis Using the CIE L*a*b* System

Color parameters—Lightness (L*), redness/greenness (a*), and yellowness/blueness (b*), were measured using a spectrophotometer (CM-3500d, Konica Minolta, Japan). Color values were expressed according to the CIE L*a*b* system, where L* represents lightness, a* indicates redness (+a*)/greenness (–a*), and b* indicates yellowness (+b*)/blueness (–b*). Dried Wolffia powder that had passed through a 100-mesh sieve was placed in a flat, opaque sample holder to minimize external light interference and ensure uniform sample presentation. The surface was leveled to minimize shadows or uneven reflection, allowing for consistent instrumental color measurement of the powder samples. Color measurements were performed at 3 different points in triplicate for each treatment, and the results were expressed as mean ± standard deviation.

2.4 Water Activity Analysis

Water activity (a_w) of dried Wolffia samples was measured using a water activity meter (Series 3 TE, Aqua Lab, USA) at temperature, at 25 ± 2 °C. Dried Wolffia powder that had passed through a 100-mesh sieve was placed in the sample cup to an appropriate depth according to the instrument requirements, and measurements were performed in triplicate for each treatment. Values are expressed on a scale from 0 to 1, where 1.0 represents pure water. The results were reported as mean ± standard deviation.

2.5 Chemical Composition Analysis

Moisture, ash, crude protein, crude fat, and crude fiber contents were determined according to the Official Methods of Analysis of AOAC INTERNATIONAL (2023) using AOAC Official Methods 925.10, 923.03, 981.10, 920.39, and 962.09, respectively. Protein content was determined using a nitrogen-to-protein conversion factor of 6.25. Carbohydrate content was calculated by difference as follows:

$$\text{Carbohydrate (\%)} = 100 - [\text{moisture (\%)} + \text{protein (\%)} + \text{fat (\%)} + \text{ash (\%)} + \text{crude fiber (\%)}] \quad (2)$$

All analyses were performed in triplicate, and the results were expressed as mean ± standard deviation.

2.6 Antioxidant Properties

Dried Wolffia powder extract was prepared using a modified method described by Yadav et al. (2024). Briefly, 0.2 g of dried Wolffia powder was extracted with 10 mL of distilled water. The mixture was sonicated at 4 ± 2 °C, frequency of about 120 kHz for 25 min, followed by centrifugation at 9,000 rpm for 15 min at 4 ± 2 °C. The supernatant was collected and used for the analysis of antioxidant properties and total phenolic content. All analyses were performed in triplicate, and the results were expressed as mean ± standard deviation.

2.6.1 DPPH Radical Scavenging Assay

DPPH radical scavenging activity was determined according to Maduwanthi & Marapana (2021), with slight modifications. The extract (0.1 mL) was mixed with 0.02 mM DPPH solution (10%) in ethanol, (1 mL), vortexed, and incubated in the dark for 30 min at room temperature. Absorbance was measured at 517 nm using a spectrophotometer (UVmini-1240, Shimadzu, Japan). Trolox 10 – 100 µg/ml was used to construct the standard curve, and the results were expressed as mg Trolox equivalent/g sample.

2.6.2 Ferric Reducing-Antioxidant Power (FRAP) Assay

FRAP assay was performed according to Kubola & Siriamornpun (2008), with slight modifications. The FRAP reagent was prepared by mixing 300 mM acetate buffer, 20 mM $FeCl_3 \cdot 6H_2O$, and 10 mM TPTZ in 40 mM HCl at a ratio of (ratio, e.g., 10:1:1). The extract (20 µL) was mixed with FRAP reagent (150 µL) and 30 µL of acetate buffer and incubated at 37 °C for 4 min. Absorbance was measured at 593 nm using a spectrophotometer. Ferrous sulfate (0.1–1.0 mM) was used to construct the standard curve, and the results were expressed as µmol Fe(II)/g sample.

2.6.3 Total Phenolic Content

Total phenolic content was determined using a modified Folin–Ciocalteu colorimetric method described by Wolfe et al. (2003). The extract (20 µL) was mixed with 10% of Folin–Ciocalteu reagent (110 µL) and allowed to react for 6 min. Then, 10% of sodium carbonate solution (70 µL) was added, and the mixture was incubated for 30 min at room temperature in the dark. Absorbance was measured at 765 nm using a spectrophotometer. Gallic acid (15–270 µg/ml) was used to construct the standard curve, and the results were expressed as mg gallic acid equivalent/g sample.

2.7 Total Chlorophyll Content

Chlorophyll a, chlorophyll b, and total chlorophyll contents were determined according to Rajput & Patil (2017), with slight modifications. Briefly, 1.0 g of dried Wolffia powder was extracted with 80% acetone under light-protected conditions and centrifuged at 5,000 rpm for 5 min. The supernatant was collected and adjusted to a final volume of 100 mL with 80% acetone. The absorbance of the extract was measured at 645 and 663 nm using a spectrophotometer. All analyses were performed in triplicate. To align

with the reported results, chlorophyll contents were calculated and expressed as milligrams per kilogram (mg/kg) of sample using the following equations:

$$\text{Chlorophyll a (mg/kg)} = [(12.7 \times A663) - (2.69 \times A645)] \times \frac{V}{W} \quad (3)$$

$$\text{Chlorophyll b (mg/kg)} = [(22.9 \times A645) - (4.68 \times A663)] \times \frac{V}{W} \quad (4)$$

$$\text{Total chlorophyll (mg/kg)} = [(20.2 \times A645) + (8.02 \times A663)] \times \frac{V}{W} \quad (5)$$

where

A645 and A663 are the absorbance values measured at 645 and 663 nm, respectively

V is the final volume of the extract (mL)

W is the sample weight (g).

2.8 Statistical Analysis

The experiment was designed using a completely Randomized Design (CRD). Data were expressed as mean ± standard deviation (SD) from triplicate analyses (n = 3), unless otherwise stated. Statistical differences among treatments were analyzed using one-way analysis of variance (ANOVA) at a significance level of $p < 0.05$. Differences among treatment means were further evaluated using Duncan's multiple range test. Statistical analyses were performed using IBM SPSS Statistics version 27.0 (IBM Corp., Armonk, NY, USA).

3. Results

3.1 Percent yield and water activity of dried Wolffia

After drying, the percent yield of dried Wolffia decreased significantly with increasing $MgSO_4$ concentration (Table 1). The untreated dried Wolffia (control) sample showed the highest yield (%) of 3.74 ± 0.05. As the $MgSO_4$ concentration increased from 0.1% to 0.7%, the yield continuously declined from 3.63 ± 0.09 to the lowest value of 3.22 ± 0.02. In contrast, the water activity (a_w) values of all $MgSO_4$-treated samples were significantly higher than that of the untreated sample (0.49 ± 0.01). However, the a_w values did not increase proportionally with the $MgSO_4$ concentration. The highest a_w value was observed in the 0.1% $MgSO_4$ treatment (0.58 ± 0.01). When the $MgSO_4$ concentration increased to 0.3%, 0.5%, and 0.7%, the a_w values decreased slightly to 0.53 ± 0.01, 0.53 ± 0.01, and 0.52 ± 0.01, respectively, but remained higher than the control.

Table 1. Percent yield and water activity (a_w) of dried Wolffia under different $MgSO_4$ blanching concentrations

Treatment	Yield (%)	a_w
Dried Wolffia	3.74 ± 0.05^{a}	0.49 ± 0.01^{c}
$MgSO_4$ 0.1 %	3.63 ± 0.09^{b}	0.58 ± 0.01^{a}
$MgSO_4$ 0.3 %	3.53 ± 0.04^{c}	0.53 ± 0.01^{b}
$MgSO_4$ 0.5 %	3.34 ± 0.02^{d}	0.53 ± 0.01^{b}
$MgSO_4$ 0.7 %	3.22 ± 0.02^{e}	0.52 ± 0.01^{b}

Note: Data are expressed as mean ± standard deviation (n=3). Different superscript letters (a–e) within the same column indicate significant differences ($p < 0.05$).

3.2 Color analysis using CIE L*, a*, b* system of dried Wolffia

After drying, $MgSO_4$ blanching significantly affected the color values of dried Wolffia (Table 2). Compared with the untreated dried Wolffia, all $MgSO_4$-treated samples exhibited significantly lower L* values (ranging from 15.41 ± 0.29 to 16.89 ± 0.33, compared to 21.88 ± 0.18 for the control), indicating reduced lightness and a darker appearance. The b* values also decreased after $MgSO_4$ treatment (from 20.66 ± 0.25 to a range of 14.35–15.14), suggesting a reduction in yellowness**.** For the a* value, all samples remained in the negative range, indicating the presence of green pigment. However, $MgSO_4$-treated samples showed significantly less negative a* values (-3.18 to -4.16) than the untreated control (-5.40). Since all measured a* values were well below zero, this shift must be interpreted strictly as reduced greenness rather than an increase in redness. The visual appearance of the samples shown in Figure 1 is highly consistent with these instrumental color results. As depicted, the untreated dried Wolffia (T1) displays a vibrant, lighter green color, which directly corresponds to its higher L* (lightness), higher b* (yellowness), and more negative a* (stronger greenness) values. In contrast, the $MgSO_4$-treated samples (T2–T5) generally appear visually darker, duller, and less intensely green, accurately reflecting the objective spectrophotometric measurements of reduced lightness, reduced greenness, and reduced yellowness.

Table 2. Color values (L*, a*, and b*) of dried Wolffia under different $MgSO_4$ blanching concentrations

Treatment	Color values		
	L*	a*	b*
Dried Wolffia	21.88±0.18^{a}	-5.40±0.05^{d}	20.66±0.25^{a}
$MgSO_4$ 0.1 %	15.41±0.29^{c}	-3.18±0.04^{a}	15.14±0.23^{b}
$MgSO_4$ 0.3 %	16.89±0.33^{b}	-3.74±0.04^{b}	14.83±0.11^{b}
$MgSO_4$ 0.5 %	16.24±0.09^{b}	-4.16±0.02^{c}	14.35±0.02^{c}
$MgSO_4$ 0.7 %	16.22±0.62^{b}	-4.13±0.08^{c}	14.89±0.29^{b}

Note: Data are expressed as mean ± standard deviation (n=3). Different superscript letters (a–d) within the same column indicate significant differences ($p < 0.05$).



Dried Wolffia | $MgSO_4$ 0.1 % | $MgSO_4$ 0.3 % | $MgSO_4$ 0.5 % | $MgSO_4$ 0.7 %

Figure 1. Appearance of dried Wolffia under different $MgSO_4$ blanching concentrations

3.3 Chemical composition of dried Wolffia

After drying, the proximate composition of dried Wolffia was significantly affected by the $MgSO_4$ blanching treatments (Table 3). It was observed that blanching with higher concentrations of $MgSO_4$ solution resulted in a significant increase in carbohydrate content. The carbohydrate content rose continuously from 50.42 ± 0.01 in the untreated dried Wolffia to the highest value of 55.07 ± 0.03 in the

0.7% $MgSO_4$ treatment. Conversely, increasing the $MgSO_4$ concentration led to a significant decrease in protein content, which declined from 18.49 ± 0.02% in the control to 16.06 ± 0.01 in the 0.7% treatment. Additionally, the ash and crude fiber contents generally decreased at higher $MgSO_4$ concentrations (0.3%–0.5%) compared to the 0.1% treatment, although the crude fiber content exhibited a notable recovery at the 0.7% concentration (11.25 ± 0.02).

Table 3. Proximate composition of dried Wolffia samples under different $MgSO_4$ blanching concentrations.

Treatment	Moisture (%)	Protein (%)	Fat (%)	Ash (%)	Fiber (%)	Carbohydrate (%)
Dried Wolffia	10.45 ± 0.05^{b}	18.49 ± 0.02^{a}	3.92 ± 0.01^{c}	4.91 ± 0.01^{a}	12.16 ± 0.01^{a}	50.07 ± 0.01^{e}
$MgSO_4$ 0.1 %	10.80 ± 0.10^{a}	17.55 ± 0.06^{b}	4.89 ± 0.01^{ab}	4.56 ± 0.01^{b}	11.25 ± 0.02^{b}	61.75 ± 0.05^{d}
$MgSO_4$ 0.3 %	10.35 ± 0.05^{bc}	16.92 ± 0.10^{c}	4.90 ± 0.01^{a}	4.34 ± 0.01^{c}	10.73 ± 0.01^{c}	64.23 ± 0.07^{c}
$MgSO_4$ 0.5 %	10.38 ± 0.02^{bc}	16.50 ± 0.10^{d}	4.81 ± 0.01^{b}	4.30 ± 0.01^{c}	9.61 ± 0.01^{d}	64.96 ± 0.19^{b}
$MgSO_4$ 0.7 %	10.32 ± 0.02^{c}	16.06 ± 0.01^{e}	3.00 ± 0.10^{d}	4.30 ± 0.02^{c}	9.43 ± 0.01^{e}	65.39 ± 0.02^{a}

Note: Data are expressed as mean ± standard deviation (n=3). Different superscript letters (a–e) within the same column indicate significant differences ($p < 0.05$).

3.4 Total phenolic content and antioxidant properties of dried Wolffia

The total phenolic content and antioxidant properties of dried Wolffia samples are presented in Table 4. The untreated dried Wolffia showed the highest total phenolic content (4.25 ± 0.05 mg GAE/g sample) and DPPH radical scavenging activity (4.50 ± 0.18 mg Trolox eq./g sample). $MgSO_4$ blanching generally reduced total phenolic content and DPPH activity compared with the untreated sample. Among the $MgSO_4$-treated samples, the lowest total phenolic content and DPPH activity were observed in the 0.5% $MgSO_4$ treatment, whereas the 0.7% $MgSO_4$ treatment showed slightly higher values than the 0.5% treatment.

For FRAP activity, the untreated dried Wolffia exhibited the highest value (44.73 ± 0.43 μmol Fe(II)/g sample). The 0.1% $MgSO_4$ treatment showed a comparable FRAP value (43.76 ± 0.68 μmol Fe(II)/g sample) and was not significantly different from the untreated sample. However, FRAP values decreased markedly in the 0.3–0.7% $MgSO_4$ treatments, with the lowest value observed in the 0.5% $MgSO_4$ treatment. Overall, $MgSO_4$ blanching, particularly at concentrations of 0.3% and above, was associated with reduced phenolic content and antioxidant activity in dried Wolffia.

Table 4. Total phenolic content and antioxidant properties of dried Wolffia.

Treatment	Total phenolic content (mg GAE/g sample)	Antioxidant activity	
		DPPH (mg Trolox eq./g sample)	FRAP (μmol Fe(II)/g sample)
Dried Wolffia	$4.25\pm.0.05^{a}$	4.50 ± 0.18^{a}	44.73 ± 0.43^{a}
$MgSO_4$ 0.1 %	4.20 ± 0.02^{b}	4.10 ± 0.02^{b}	43.76 ± 0.68^{a}
$MgSO_4$ 0.3 %	2.20 ± 0.02^{c}	1.87 ± 0.10^{c}	19.48 ± 0.74^{b}
$MgSO_4$ 0.5 %	1.40 ± 0.01^{e}	1.02 ± 0.03^{e}	11.91 ± 0.10^{d}
$MgSO_4$ 0.7 %	1.89 ± 0.02^{d}	1.56 ± 0.02^{d}	15.87 ± 0.62^{c}

Note: Data are expressed as mean ± standard deviation (n=3). Different superscript letters (a–e) within the same column indicate significant differences ($p < 0.05$).

3.5 Total chlorophyll content of dried Wolffia

The chlorophyll a, chlorophyll b, and total chlorophyll contents of dried Wolffia samples are shown in Table 5. Overall, $MgSO_4$ blanching treatments significantly enhanced the retention of both chlorophyll fractions compared to the untreated control ($p < 0.05$). In the untreated dried Wolffia, chlorophyll a and chlorophyll b contents were 2,862.05 ± 0.01 mg/kg and 1,172.17 ± 0.02 mg/kg, respectively, resulting in a total chlorophyll content of 4,034.21 ± 0.11 mg/kg. For the $MgSO_4$-treated samples, both chlorophyll a and chlorophyll b levels were consistently higher than those of the control. Across all treatments, chlorophyll a remained the dominant pigment fraction compared to chlorophyll b. The 0.7% $MgSO_4$ treatment demonstrated the most effective pigment preservation, yielding the highest concentrations of chlorophyll a (3,906.66 ± 0.01 mg/kg), chlorophyll b (2,240.65 ± 0.02 mg/kg), and total chlorophyll (6,147.31 ± 0.01 mg/kg). Interestingly, the pigment retention did not follow a simple linear concentration-dependent trend; while the 0.3% $MgSO_4$ treatment showed highly effective retention (chlorophyll a: 3,796.73 ± 0.01 mg/kg; chlorophyll b: 2,109.86 ± 0.02 mg/kg), a significant drop occurred at 0.5% $MgSO_4$ before reaching the maximum peak at 0.7%. These results indicate that $MgSO_4$ blanching, particularly at 0.7%, successfully protects both chlorophyll a and b molecules from degradation during the drying process.

Table 5. Total chlorophyll content of dried Wolffia

Treatment	Chlorophyll a (mg/kg)	Chlorophyll b (mg/kg)	Total chlorophyll (mg/kg)
Dried Wolffia	2862.05±0.01^{e}	1172.17±0.02^{d}	4034.21±0.11^{e}
$MgSO_4$ 0.1 %	3280.77±0.17^{d}	1069.09±0.57^{e}	4349.85±0.05^{d}
$MgSO_4$ 0.3 %	3796.73±0.01^{b}	2109.86±0.02^{b}	5906.59±0.04^{b}
$MgSO_4$ 0.5 %	3315.41±0.01^{c}	1530.41±0.01^{c}	4845.82±0.02^{c}
$MgSO_4$ 0.7 %	3906.66±0.01^{a}	2240.65±0.02^{a}	6147.31±0.01^{a}

Note: Data are expressed as mean ± standard deviation (n=3). Different superscript letters (a–e) within the same column indicate significant differences ($p < 0.05$).

4. Discussion

The application of magnesium sulfate ($MgSO_4$) blanching pretreatments significantly influenced the physicochemical properties, proximate composition, and visual characteristics of dried Wolffia. The observed decrease in percentage yield at higher $MgSO_4$ concentrations could be attributed to the potential loss of dry mass and the leaching of water-soluble compounds into the blanching medium. This leaching mechanism might also explain the alterations in proximate composition; as $MgSO_4$ concentration increased, protein content significantly decreased from 18.49% to 16.06%, while the relative carbohydrate proportion increased continuously from 50.42% to 55.07%. Regarding water activity (aw), all $MgSO_4$-treated samples exhibited higher aw values compared to the unblanched control. A possible explanation for this anomaly is that the combined thermal treatment and ionic stress might have altered the plant tissue structure, potentially facilitating the release of previously bound water into the free water pool. However, within the treated groups, increasing the $MgSO_4$ concentration from 0.1% to 0.7% resulted in a slight progressive decrease in aw, which could reflect a concentration-dependent interaction between the sulfate salt and water molecules (Fomenko et al., 2025).

Despite the physical and compositional alterations, chemical analysis indicated that $MgSO_4$ blanching, particularly at 0.7%, successfully retained higher levels of total chlorophyll compared to the untreated control (Negi & Roy, 2000). It is hypothesized that the presence of exogenous Mg^{2+} ions during thermal processing might help stabilize the chlorophyll structure and reduce its conversion to pheophytin, although further mechanistic studies are required to confirm this direct ionic substitution or protection in Wolffia. Interestingly, this enhanced chemical retention of chlorophyll did not translate to improved visual green coloration. Both instrumental color analysis and visual observations demonstrated that $MgSO_4$-treated samples were significantly darker and less green than the control, as evidenced by decreased lightness (L*) and less negative a* values. This discrepancy between chemical pigment content and visual appearance could possibly be driven by non-enzymatic browning reactions during the extended drying process, or by structural changes that altered surface light reflectance.

Furthermore, a significant trade-off was observed between chlorophyll retention and the preservation of bioactive compounds. The $MgSO_4$-treated dried Wolffia exhibited significantly lower total phenolic content (TPC) and antioxidant activities (DPPH and FRAP) compared to the unblanched control. While blanching is theoretically utilized to inactivate oxidative enzymes, the exposure to 80 °C for 3 mins combined with an osmotic gradient from the salt solution might have facilitated the extensive leaching of water-soluble phenolic compounds into the blanching water (Kim et al., 2013; Pichairat & Mahea, 2014). The magnitude of this leaching loss profoundly outweighed any potential benefits of enzymatic inhibition. Ultimately, while 0.7% $MgSO_4$ pretreatment effectively maximizes chemical chlorophyll concentration, it negatively impacts the overall visual lightness, visual greenness, and functional antioxidant capacity of the final dried product.

5. Conclusions and recommendations

Blanching with magnesium sulfate ($MgSO_4$) solution significantly impacts the quality parameters of dried Wolffia. While the treatment, particularly at 0.7% w/v $MgSO_4$, effectively retains the highest levels of chemically extracted total chlorophyll, this chemical retention does not translate to overall visual color preservation. The $MgSO_4$ pretreatment resulted in dried products that were visually darker and less green compared to the unblanched control. Furthermore, the pretreatment caused a reduction in overall yield and significantly decreased the total phenolic content and antioxidant capacity, likely due to the leaching of water-soluble bioactive compounds. Consequently, the application of $MgSO_4$ blanching presents a clear trade-off between maximizing chemical chlorophyll retention and preserving both visual greenness and functional antioxidant properties. Future studies should explore alternative processing conditions to better balance these quality attributes and conduct sensory evaluations for further product applications.

6. References

AOAC International. (2023). Official Methods of Analysis of AOAC international (22nd ed.). Oxford University Press. https://doi.org/10.1093/ 9780197610145.001.0001

Appenroth, K.- J., Sree, K. S., Bog, M., Ecker, J., Seeliger, C., Böhm, V., Lorkowski, S., Sommer, K., Vetter, W., Tolzin-Banasch, K., Kirmse, R., Leiterer, M., Dawczynski, C., Liebisch, G., & Jahreis, G. (2018). Nutritional value of the duckweed species of the genus Wolffia (Lemnaceae) as human food. Frontiers in Chemistry, 6, 483. https://doi.org/ 10.3389/fchem.2018.00483

Bohn, T., Walczyk, T., Leisibach, S., & Hurrell, R. F. (2004). Chlorophyll-bound magnesium in commonly consumed vegetables and fruits: Relevance to magnesium nutrition. Journal of Food Science, 69(9), 347-350. https://doi.org/10.1111/j.1365-2621.2004.tb09947.x

Doungtip, P., Srisorn, P., & Hunsakul, K. (2025). Effect of salt solution combined with blanching on color retention and antioxidant activity in dried Wolffia (Wolffia arrhiza). Journal of Food Technology, Siam University, 20(1), 32-42. https://li01.tci-thaijo.org/index.php/JFTSU/article/view/265825/180193

Fomenko, E. V., Anshits, N. N., Akimochkina, G. V., Ivanenko, T. Y., Morozov, E. V., Yumashev, V. V., Solovyov, L. A., Shestakov, N. P., & Shabanov, V. F. (2025). Experimental study on rapeseed drying characteristics with magnesium sulfate as solid desiccant. Molecules, 30(17), 3604. https://doi.org/10.3390/molecules30173604

Kaur, N., Aggarwal, P., & Rajput, H. (2018). Effect of different blanching treatments on physicochemical, phytochemical constituents of cabinet dried broccoli. Chemical Science Review and Letters, 7(25), 262-271. https://www.academia.edu/37690771/Effect_of_Different_Blanching_Treatments_on_Physicochemical_Phytochemical_Constituents_of_Cabinet_Dried_Broccoli

Khan, A. A., Syarifah Adilah, M. Y., Mamat, M. H., Yahaya, S. Z., Setumin, S., Ibrahim, M. N., Daud, K., & Abdullah, M. H. (2022). Magnesium sulfate as a potential dye additive for chlorophyll-based organic sensitiser of the dye-sensitised solar cell (DSSC). Spectrochimica Acta Part A: Molecular and Biomolecular Spectroscopy, 274, 121140. https://doi.org/10.1016/j.saa.2022.121140

Kim, M. H., Kim, J. M., & Yoon, K. Y. (2013). Effects of blanching on antioxidant activity and total phenolic content according to type of medicinal plants. Food Science and Biotechnology, 22(3), 817-823. https://link.springer.com/article/10.1007/s10068-013-0150-5

Kubola, J., & Siriamornpun, S. (2008). Phenolic contents and antioxidant activities of bitter gourd (Momordica charantia L.) leaf, stem and fruit fraction extracts in vitro. Food Chemistry, 110(4), 881-890. 10.1016/j.foodchem.2008.02.076

Maduwanthi, S.D.T., & Marapana, R.A.U.J. (2021). Total phenolics, flavonoids and antioxidant activity following simulated gastro-intestinal digestion and dialysis of banana (Musa acuminata, AAB) as affected by induced ripening agents. Food Chemistry, 339, 127909. https://doi.org/10.1016/j.foodchem.2020.127909

Masavang, S., Winckler, P., Tira-Umphon, A., & Phahom, T. (2022). New insights into moisture sorption characteristics, nutritional composition, and antioxidant and morphological properties of dried duckweed [Wolffia arrhiza (L.) Wimm]. Journal of the Science of Food and Agriculture, 102(5), 2135-2143. https://doi.org/10.1002/jsfa.11555

Minh, N. P., Nhi, T. T. Y., Lam, T. D. B., Nhat, P. M., & Phuong, N. T. T. (2019). Effect of blanching and drying on quality of dried papaya fruit. Journal of Pharmaceutical Sciences and Research, 11(3), 1082-1086. https://www.proquest.com/scholarly-journals/effect-blanching-drying-on-quality-dried-papaya/docview/2206964729/se-2

Negi, P., & Roy, S.K. (2000). Effect of blanching and drying methods on β-carotene, ascorbic acid and chlorophyll retention of leafy vegetables. LWT-Food Science and Technology, 33(4), 295-298. https://doi.org/10.1006/fstl.2000.0659

Oliveira, S. M., Brandão, T. R. S., & Silva, C. L. M. (2016). Influence of drying processes and pretreatments on nutritional and bioactive characteristics of dried vegetables: A review. Food Engineering Reviews, 8, 134-163. https://doi.org/10.1007/s12393-015-9124-0

Pichairat, D., & Mahea, N. (2014). Effect of blanching on the phenolic content and antioxidant capacities of some Southern Thai indigenous vegetables. Rajamangala University of Technology Srivijaya Research Journal, 6(2), 36-46. https://www.repository.rmutsv.ac.th/bitstream/handle/123456789/1223/FullText.pdf?sequence=1&isAllowed=y

Prosridee, K., Oonsivilai, R., Tira-aumphon, A., Singthong, J., Oonmetta-aree, J., & Oonsivilai, A. (2023). Optimum aquaculture and drying conditions for Wolffia arrhiza (L.) Wimn. Heliyon, 9(9), e19730. https://doi.org/10.1016/j.heliyon.2023.e19730

Rajput, R., & Patil, R. (2017). The comparative study on spectrophotometric analysis of chlorophyll and carotenoids pigments from non-leguminous fodder crops. International Journal of Innovative Science, Engineering & Technology, 4(7), 140-148. https://www.researchgate.net/publication/322356853_The_Comparative_Study_on_Spectrophotometric_Analysis_of_Chlorophyll_and_Carotenoids_Pigments_from_Non-Leguminous_Fodder_Crops

Wolfe, K., Wu, X., & Liu, R. H. (2003). Antioxidant activity of apple peels. Journal of Agricultural and Food Chemistry, 51(3), 609-614. https://doi.org/10.1021/jf020782a

Workneh, T., Zinash, A., & Woldetsadik, K. (2014). Blanching, salting and sun drying of different pumpkin fruit slices. Journal of Food Science and Technology, 51(11), 3114-3123. https://doi.org/10.1007/s13197-012-0835-4

Yadav, N. K., Patel, A. B., Debbarma, S., Priyadarshini, M. B., & Priyadarshi, H. (2024). Characterization of bioactive metabolites and antioxidant activities in solid and liquid fractions of fresh duckweed (Wolffia globosa) subjected to different cell wall rupture methods. ACS Omega, 9(18), 19940-19955. https://pubs.acs.org/doi/10.1021/acsomega.3c09674

การพัฒนากระบวนการทางชีวภาพสำหรับการผลิต และคุณลักษณะเฉพาะของไฮโดรไลเสตคอลลาเจนเพพไทด์ ที่มีคุณสมบัติต้านอนุมูลอิสระจากกระดูกปลากดคัง

Bioprocess Development for the Production and Characterisation of Hydrolysate Collagen Peptides with Antioxidant Properties from *Hemibagrus wyckioides* Bones

วุฒิศักดิ์ คุณุ[1] พิบูรณ์ เหง้าณี[2] สรพงษ์ ภวสุปรีย์[3] และ สุภาวดี ปาทาธนานนท์[4*]

Wuttisak Kunu[1], Piboon Ngaonee[2], Sorapong Pavasupree[3] and Supawadee Patathananone[4*]

[1]สาขาเทคนิคการสัตวแพทย์และการพยาบาลสัตว์ คณะเทคโนโลยีการเกษตร มหาวิทยาลัยราชภัฏมหาสารคาม จังหวัดมหาสารคาม

[2]คณะทันตแพทยศาสตร์ มหาวิทยาลัยขอนแก่น จังหวัดขอนแก่น

[3]ภาควิชาวิศวกรรมวัสดุและโลหการ คณะวิศวกรรมศาสตร์ มหาวิทยาลัยเทคโนโลยีราชมงคลธัญบุรี จังหวัดปทุมธานี

[4]ภาควิชาเคมี คณะวิทยาศาสตร์และเทคโนโลยี มหาวิทยาลัยเทคโนโลยีราชมงคลธัญบุรี จังหวัดปทุมธานี

[1]Program in Veterinary Technology and Veterinary Nursing, Faculty of Agricultural Technology, Rajabhat Maha Sarakham University, Maha Sarakham Province

[2]Faculty of Dentistry, Khon Kaen University, Khon Kaen Province

[3]Department of Materials and Metallurgical Engineering, Faculty of Engineering, Rajamangala University of Technology Thanyaburi, Pathum Thani Province

[4]Department of Chemistry, Faculty of Science and Technology, Rajamangala University of Technology Thanyaburi, Pathum Thani Province

[*]Corresponding Author: Supawadee_P@rmutt.ac.th

Received: August 3, 2026 **Revised:** October 6, 2026 **Accepted:** October 16, 2026

บทคัดย่อ

ปลากดคัง (*Hemibagrus wyckioides*) เป็นปลาน้ำจืดสายพันธุ์หนึ่งที่นิยมรับประทานในประเทศไทยโดยเฉพาะอย่างยิ่งส่วนของเนื้อปลา อย่างไรก็ตาม กระดูกปลากดคังเป็นวัตถุดิบเหลือทิ้งจากสถานประกอบการณ์ที่มีมูลค่าทางเศรษฐกิจต่ำ การศึกษานี้มีวัตถุประสงค์เพื่อศึกษาเปรียบเทียบวิธีการเตรียมไฮโดรไลเซทคอลลาเจนเพพไท์ในส่วนของร้อยละผลผลิต ร้อยละปริมาณโปรตีนรวม และเพื่อตรวจสอบคุณลักษณะและคุณสมบัติบางประการของไฮโดรไลเซทคอลลาเจนเพพไทด์จากกระดูกปลากดคัง ไฮโดรไลเซทคอลลาเจนเพพไทด์ถูกเตรียมขึ้นภายใต้ 5 สภาวะ ได้แก่ การใช้น้ำปราศจากไอออน (CLG-DI-24h, CLG-DI-48h), การใช้กรดอะซิติก (CLG-AC-24h, CLG-AC-48h), การย่อยด้วยเอนไซม์ปาเปน (CLG-PP-24h), การย่อยด้วยเอนไซม์อัลคาเลส (CLG-ACL-24h), และการใช้เอนไซม์เพพซินในกรดอะซิติก (CLG-ACP-24h, CLG-ACP-48h) ทุกสภาวะถูกบ่มที่อุณหภูมิ 37 °C ตัวอย่างในสภาวะกรดถูกสะเทิน กำจัดเกลือ ด้วยการไดอะไลซีส และทำให้แห้งด้วยเครื่องทำแห้งแช่เยือกแข็ง ตัวอย่างถูกวิเคราะห์หมู่ฟังก์ชันในโครงสร้างด้วยสเปกโทรสโกปีอินฟราเรดแบบฟูเรียร์ทรานสฟอร์มองค์ประกอบของกรดอะมิโนถูกศึกษาด้วยเทคนิคทินเลเยอร์โครมาโทกราฟฟี ร้อยละการส่องผ่านแสงของสารละลายตัวอย่างถูกวิเคราะห์ด้วยสเปคโตรโฟโตมิเตอร์ ซึ่งรวมถึงการประเมินคุณสมบัติการเกิดฟอง (การก่อตัวของฟองและความคงตัวของฟอง) การดูดกลืนแสงอัลตราไวโอเลต (ยูวี) ของสารละลายตัวอย่าง และกิจกรรมการกำจัดอนุมูลอิสระดีพีพีเอช ผลการศึกษาแสดงให้เห็นว่า CLG-ACP-24h มีร้อยละผลผลิตสูงสุด (98.77 ± 0.41%), ในขณะที่ CLG-ACL-24h ตรวจพบปริมาณโปรตีนรวมสูงที่สุด (98.43 ± 4.34%) เมื่อเทียบกับสภาวะการเตรียมอื่นๆ ทั้งหมด ($p < 0.05$) สเปคตรัมของสเปกโทรสโกปีอินฟราเรดแบบฟูเรียร์ทรานสฟอร์มถูกตรวจพบที่ตำแหน่ง 3400–3440 เซนติเมตร$^{-1}$ (เอไมด์ เอ), และ 1640–1655 เซนติเมตร$^{-1}$ (เอไมด์ 1) ซึ่งสอดคล้องกับการสั่นแบบยืดของพันธะ N–H และการสั่นแบบยืดของพันธะ C=O ตามลำดับ กรดอะมิโนที่ระบุได้ในตัวอย่างโดยวิธีโครมาโทกราฟฟีแบบกระดาษ ได้แก่ ไกลซีน โพรลีน และไฮดรอกซีโพรลีน มีค่าการเคลื่อนที่สัมพัทธ์ใกล้เคียงกับกรดอะมิโนมาตรฐาน CLG-AC-24h และ CLG-ACP-24h แสดงร้อยละของการส่องผ่านแสงในน้ำปราศจากไอออน (พีเอช 7.0) ที่ 95.97 ± 3.82, และ 94.80 ± 0.87 ตามลำดับ CLG-AC-24h และ CLG-ACP-24h แสดงคุณลักษณะของการเกิดโฟม โดยมีร้อยละความเสถียรภาพในการเกิดโฟม 100 ± 0.01 ที่ความเข้มข้น 20.0 มิลลิกรัมต่อมิลลิลิตร CLG-AC-24h และ CLG-ACP-24h แสดงค่าการดูดกลืนแสงสูงสุดที่ช่วง 190–230 นาโนเมตร ในขณะที่พบการ

ดูดกลืนแสงเพียงเล็กน้อยที่ช่วง 260–280 นาโนเมตร CLG-AC-24h และ CLG-ACP-24h มีฤทธิ์ต้านอนุมูลดีพีพีเอช เท่ากับ 32.95 ± 7.68 และ 31.03 ± 5.45% ตามลำดับ ผลการวิจัยเหล่านี้ชี้ให้เห็นว่ากระดูกของปลากดคัง ซึ่งเป็นผลพลอยได้จากอุตสาหกรรมอาจเป็นวัตถุดิบทางเลือกสำหรับการเตรียมไฮโดรไลเซทคอลลาเจนเพพไทด์ได้

คำสำคัญ: ปลากดคัง, ชีววัตถุ, การยับยั้ง, อาหารเพื่อสุขภาพ, ความปลอดภัย

Abstract

The Asian red-tail catfish (*Hemibagrus wyckioides*) is a species of freshwater fish that is popular for consumption in Thailand, especially its flesh. However, *H. wyckioides* bones are waste materials from industrial processes with low economic value. This study aimed to compare methods for preparing hydrolysed collagen peptides from *H. wyckioides* bone in terms of yield and total protein content, and to examine their characteristic and functional properties. Hydrolysed collagen peptides were prepared under five conditions: deionised water (CLG-DI-24h and CLG-DI-48h), acetic acid (CLG-AC-24h and CLG-AC-48h), enzymatic digestion with papain (CLG-PP-24h), enzymatic digestion with Alcalase (CLG-ACL-24h), and enzymatic digestion with pepsin in acetic acid (CLG-ACP-24h and CLG-ACP-48h). All conditions were incubated at 37°C. The samples prepared under acidic conditions were neutralised, desalted by dialysis, and then freeze-dried. The samples were characterised for their functional groups by Fourier transform infrared (FTIR) spectroscopy. The amino acid composition was studied using thin-layer chromatography. The percentage transmittance (%T) of the sample solution was analyzed using a spectrophotometer. This included evaluating the foaming properties (foam formation and foam stability), the Ultraviolet (UV) absorption of the sample solutions, and the DPPH radical-scavenging activity. The results showed that CLG-ACP-24h exhibited the highest percentage yield (98.77 ± 0.41%), whereas CLG-ACL-24h exhibited the highest total protein content (98.43 ± 4.34%), among all the preparation conditions ($p < 0.05$). The FTIR spectra showed bands at 3400–3440 cm^{-1} (amide A) and 1640–1655 cm^{-1} (amide I), corresponding to N–H stretching and C=O stretching vibrations, respectively. The amino acids identified in the samples by paper chromatography, namely glycine, proline, and hydroxyproline, exhibited Retention factor (R_f) values similar to those of the standard amino acids. CLG-AC-24h and CLG-ACP-24h showed %T in deionized water (pH 7.0) of 95.97 ± 3.82, and 94.80 ± 0.87, respectively. CLG-AC-24h and CLG-ACP-24h exhibited foaming characteristics with foam stability of 100 ± 0.01% at a concentration of 20.0 mg/mL. CLG-AC-24h and CLG-ACP-24h showed a main absorbance peak at 190–230 nm, whereas only weak absorption was observed at 260–280 nm. CLG-AC-24h and CLG-ACP-24h exhibited DPPH radical scavenging activity of 32.95 ± 7.68 and 31.03 ± 5.45%, respectively. These findings suggest that *H. wyckioides* bone, an industrial by-product, may be an alternative raw material for the preparation of hydrolysate collagen peptides.

Keywords: Red-tailed mystus fish, Biomaterial, Inhibition, Functional food, Safety

1. Introduction

Collagens are the fibrous proteins localized in the extracellular matrix of connective tissue, including vertebrate tendons, cartilage, and bones. They display the physiological function to support the stability of cell structures. There have been reports of several collagens with animal origins, ranging from Type I to XXVIII (Karsdal, 2023). Approximately 30 % of all animal proteins are found to be collagens (Birk & Bruckner, 2005). Collagen type I is the most dominant collagen, with 90% of all collagen types. Collagen's wide-ranging uses in cosmetics, food processing, and biomedical fields are driving strong global

demand. As a result, the market was forecasted to nearly double from US$3.61 billion in 2016 to US$6.63 billion in 2025 (Orel et al., 2021; Wang, 2021). Previously, pigs and cows were considered the primary sources of raw materials used to produce collagen (Ogawa et al., 2004; Orel et al., 2021). However, the use of pigs and cows in collagen production is associated with several concerns: (1) religious restrictions (Islam, Buddhism, Hinduism, and Judaism); (2) the risk of transmitting zoonotic diseases, such as foot-and-mouth disease (FMD), bovine spongiform encephalopathy (BSE), and transmissible spongiform encephalopathy (TSE); and (3) the potential for allergic reactions (Orel et al., 2021; Wang, 2021). Therefore, new sources of collagen are being investigated.

Aquatic animals are an alternative source for gathering collagen. The freshwater and marine organism industries produce a high number of processed byproducts, remarkably the fish processing byproducts such as scales, skin, bones, and fins (Zhang et al., 2011; Chalamaiah et al., 2012; Nguyen & Thai, 2024). These sources are used for the preparation of bioactive peptides, including hydrolysate collagens (Ishak & Sarbon, 2018; Abdo et al., 2023).

Improving the functional properties of proteins can broaden their range of applications. The structure of proteins can be modified through several methods, including physical (heat, high-pressure processing, ultrasound), chemical (acidic, alkaline, or saline), and biological (Jafari et al., 2020; Nguyen & Thai, 2024; Kaya et al., 2025). The preparation of hydrolysed peptides using chemical methods, such as sulfuric acid, causes an unpleasant odour (Kristinsson & Rasco, 2000; Pasupuleti & Demaimay, 2010). Additionally, hydrochloric acid causes the loss of the amino acids tryptophan, cysteine, serine, and methionine (Fountoulakis & Lahm, 1998). Protein breakdown by alkali (alkali hydrolysis) can cause some amino acids to undergo racemisation, converting L-amino acids into D-amino acids, which cannot be utilised by the body. In addition, this process degrades certain amino acids, such as arginine, threonine, and cysteine (Friedman, 1999). Owing to these limitations, chemical preparation methods are not favoured in the food industry. A widely used method is protease hydrolysis, because the enzyme exhibits high substrate specificity and efficiently accelerates the breakdown of peptide bonds (Kadam & Aluko, 2026).

Generally, several process factors must be considered, including the enzyme-to-substrate ratio, reaction duration, pH, and temperature. Therefore, controlling the optimal conditions for protease hydrolysis affects the characteristics of the resulting hydrolysed peptide product (Jafari et al., 2020; Kaya et al., 2025). However, the main limitation of using enzymes is the high cost. Additionally, enzymes can naturally degrade, which can lead to reduced biological activity. One possible solution is a hybrid or integrated approach that combines chemical and biological (enzymatic) methods, which could help address these limitations.

Red-tailed Mystus (*Hemibagrus wyckioides*), or red-tailed catfish, is a fish species in the family Bagridae. The natural freshwater rivers are the habitat of *H. wyckioides*. The original distribution of *H. wyckioides* was found along the Mekong River. With a body length of 130 cm and a weight of 80 kg, the red-tail catfish is the largest member of the Bagridae family (Shao et al., 2021). *H. wyckioides* is a freshwater fish species popular for consumption owing to its weaker fishy and muddy odour, flavourful flesh, and high protein content. Moreover, *H. wyckioides* fish also exhibits strong disease resistance, rapid growth, and ease of domestication, which contribute to its increased economic value (Shao et al., 2021; Zhou et al., 2023). Based on the survey data on aquatic resources in Thailand, compiled by the Fisheries Development Policy and Planning Division (2019) for the year 2019, statistics on freshwater aquaculture production were collected. The data indicate that fish constitute the largest group of aquatic organisms of economic importance, with Nile tilapia and catfish ranking as the top two species. According to the findings, freshwater fish categorised under “other species” accounted for 4.26% of total production. This group generated

economic value amounting to 899,669,000 baht from the total volume of all freshwater aquatic organisms. Among these, the *H. wyckioides* represents a significant contributor to economic value. The total volume of *H. wyckioides* reached 1,403 tonnes, with an aggregate market value of 144,646,000 baht. With the increase in farming, consumer demand, and the expansion of the processing industry, the number of by-products from *H. wyckioides* has also increased (Shao et al., 2021; Zhou et al., 2023).

However, studies on value-added utilisation of by-products from *H. wyckioides* fish remain limited, especially data on the preparation of hydrolysed collagen peptides. Therefore, this study aimed to compare three methods, chemical, biological (enzymatic), and a combination of both, for preparing hydrolysed collagen peptides from *H. wyckioides* bone, and to examine their characteristics and functional properties. The results of this study provide a method for preparing hydrolysed collagen peptides from *H. wyckioides* bone, which possess several important biological and functional properties. These findings may contribute to zero waste in the *H. wyckioides* processing industry and support the value-added utilisation of this by-product.

2. Materials and methods

The experimental protocols used in this study were reviewed and approved by the Research Ethics Committee of Rajamangala University of Technology Thanyaburi (Approval No. RMUTT.SCI.2022.R009).

2.1 Materials and Chemicals

Nhan Tailed Mystus fish entrepreneur in Bangplee district, Samut Prakan province, Thailand, purchased fresh *H. wyckioides* (Figure 1) from a Tantarum fish farm in Bangbao district, Samut Prakan province, Thailand. This farm received the Certificate of Good Aquaculture Practice (GAP) from the Department of Fisheries, Thailand. Glacial acetic acid, *n*-butanol, sodium hydroxide (NaOH), trichloroacetic acid (TCA), and ethanol were obtained from RCI Labscan Limited (Thailand). The standard amino acids and 2,2-diphenyl-1-picrylhydrazyl (DPPH) and alcalase were purchased from HiMedia Laboratories Private Limited (India) and Sigma Aldrich. Standard collagen peptides, Type I and II, were bought from Nippi Peptide FCP-EX-G (Japan) and 10KATE laboratory (Netherlands), respectively. Pepsin (activity, 3000NF) and papain powder were ordered from Xi'an Pincredit Bio-Tech Co., Ltd (China).



Figure 1. Representative of 10 months red-tailed Mystus fish (*H. wyckioides*) from Tantarum fish farm in Bangbao district, Samut Prakan province, Thailand. *H. wyckioides* is approximately 8–10 months of age. The fish average weight of 1-1.2 kilograms each, which is the size at which they are sold to the processing industry and restaurant businesses

2.2 *H. wyckioides* bone preparation

In this research, *H. wyckioides* bones were supported by Nhan Tailed Mystus fish entrepreneur in the amount of 50 kg. The fresh *H. wyckioides* bones were placed in an ice box to be transferred to the laboratory. The bones were cut to the same size (2-5 cm). To remove the earthy odour, *H. wyckioides* bones were weighed, and then placed into the chambers placed/ immersed/ submerged in ice-cold deionized water (DI). The chambers containing *H. wyckioides* bones were sonicated using the 35 kHz normal attitude ultrasonic bath (Sonorex digitec, Bandelin, Germany) at 4 °C, for 5 min, three times. The water was transferred. Next, to remove the musty off-flavors, the bones were washed with 5% v/v of ice-cold acetic acid at a ratio of 1:2 w/v. Then, the containers were sonicated using the same conditions. In the last step, the bones were washed with ice-cold DI water, like the above technique. To enhance collagen purity, non-collagenous proteins were removed using a method adapted from Chuaychan et al., (2015). The deodorised bones of *H. wyckioides* were placed into the chambers containing ice-cold sterile 0.1 M NaOH at 1:10 w/v. The containers were incubated at 4 °C for 2 h and this process was repeated three times. The deproteinised bones were washed with ice-cold sterile DI water to neutral (pH 7.0). The nearly dry bones were homogenised using a homogeniser at 10,000 rpm, 4 °C for 30 seconds. The homogenised bones were equilibrated for use in the next procedure.

2.3 Collagen extraction process

Generally, there are various processes for extracting active peptides from fish waste components, including acid, alkaline, and enzyme extraction under multiple conditions. In this study, collagen-derived peptides from *H. wyckioides* bone were prepared using a method adapted by combining approaches from several previous studies (Naqash & Nazeer, 2011; Jafari et al., 2020; Kaya et al., 2025).

In the initial step**,** the 20 g of homogenate bones (dried weight average 6.22 g) was divided into 8 groups, with 3 replicates per group. For the control group, 200 mL of ice-cold sterile DI water was placed into an extraction chamber and then was shaken at 120 rpm and incubated at 37°C for 24–48 h. The reaction was then terminated by immersing the extraction chambers in boiling water at 100°C for 5 min. The samples were collected and freeze-dried using a lyophiliser (OPERON, South Korea). In addition, 200 mL of 0.5 M sterile acetic acid and 1.0% w/v pepsin in 0.5 M acetic acid were added to the extraction chambers for the chemical and combined chemical-biological methods, respectively. Then, the reactions were incubated and shaken at the same temperature, speed, and duration as described for the control group. However, the reaction in these chambers were stopped by titration with 10% w/v NaOH. The supernatant of these conditions was collected and desalted by a 3.5 kDa cut-off dialysis bag in 6-fold ice-cold sterile double-distilled water for four times. Then, the desalted supernatants of each condition were frozen dry.

Moreover, for the biological method, 1.0% w/v papain and 1.0% w/v alcalase were added to each chamber in the same volume as the above conditions. These extraction chambers were treated under the same conditions as the control group, except that the incubation time was only 24 h. The reactions for the papain and alcalase conditions were terminated by immersing in boiling water at 100°C for 5 min. The supernatant from each condition was collected and dried using lyophilizer. The dried powder of the hydrolysed collagen peptides was weighed to calculate the percentage yield, and the total protein content was determined using the Kjeldahl method (AOAC, 2023). Dry weight, percentage sample recovery, and the total protein contents under all conditions were statistically compared at a significance level of $p < 0.05$.

2.4 Determination of functional groups using Fourier transform infrared spectrum (FTIR)

Functional group analysis of the samples was performed by FTIR according to the standard in-house method specified in the instrument's operating manual. Standard potassium bromide (KBr) was

accurately weighed, finely ground using a mortar and pestle, and oven-dried to remove residual moisture. A mass of 0.1 g of the dried KBr powder was immediately transferred to a desiccator. The powder was then placed into a sample holder and compressed using a hydraulic press at a pressure of 10 MPa for 5 min to form a KBr pellet. The prepared KBr pellet was stored in a desiccator prior to analysis. Approximately 0.001–0.005 g of the dried sample powder was thoroughly mixed with the KBr powder. The resulting mixture was processed following the same procedure as that used for the standard KBr pellet preparation. The sample–KBr pellet was subsequently analysed by Fourier-transform infrared (FTIR) spectroscopy (SPECTRUM ONE, PERKIN ELMER, USA) in the spectral region of 400-4000 cm^{-1} (Yang et al., 2021), with an absolute threshold of 0.0003 and a sensitivity of 37. The percentage transmittance was then recorded.

2.5 Determination of amino acids of digested collagen peptides using Thin-layer chromatography (TLC)

The dried powder of CLG-STD-II, CLG-DI-24h, CLG-AC-24h, and CLG-ACP-24h were collected at 0.01 g and placed into sterile microtubes. Then, 100 µL of 6 M hydrochloric acid (HCl) was added into microtubes, mixed vigorously, and incubated at 100°C for 120 h. The reactions were centrifuged at 3000 rpm for 5 min. The clear supernatant was collected and neutralized for separation by paper chromatography. The 0.01 g of the standard amino acids (glycine, proline, hydroxyproline, lysine, alanine, leucine, and isoleucine) was dissolved in DI to 10 mg/mL. All standard solutions and supernatants of each sample were spotted on the TLC sheet. The stationary phase was placed into the separating chamber that contained the mobile phase (n-butanol: acetic acid: water, 3:1:1). The chamber was closed and incubated until the mobile phase moved to the ending line. The stationary phase was oven to 100°C for 10 min. The 1.0% w/v of ninhydrin in ethanol was sprayed on the stationary phase and oven to 100°C for 10 min. The retention factor (R_f) was analyzed according to the formula below.

$$R_f = X/Y \quad (1)$$

X = The distance ending of sample spot (cm)
Y = The distance ending of the mobile phase (cm)

2.6 Investigation percentage transmittance (%T) of dissolved collagen hydrolysate peptides

The powder of CLG-STD-II, CLG-DI-24h, CLG-AC-24h, and CLG-ACP-24h was placed to tubes and then dissolved by deionized water (DI) and 5.0% w/v trichloroacetic acid (5% w/v TCA) to a concentration of 250 µg/mL. The mixture in each tube was vortexed gently for 5 min. The dissolved samples were measured for % transmittance at the wavelength 600 nm using a UV-Vis spectrophotometer (Thermo Scientific, Sweden).

2.7 UV-Vis Absorption Analysis

The purity of hydrolysate collagen peptides was modified according to a previous report by Zhang et al., (2011). The 0.001g of CLG-STD-II, CLG-DI-24h, CLG-AC-24h, and CLG-ACP-24h powder was dissolved in DI water for 1.0 mg/mL preparation. The solution was placed into a quartz cell to determine the absorbance values at wavelengths of 190–340 nm using the scanning mode of a UV-visible spectrophotometer (FP-8500, JASCO, JAPAN), following a slightly modified method from Kaya et al., (2025). The data was recorded and plotted in the graphs. The wavelength was set to the *X*-axis and paired with the *Y*-axis as the absorbance values.

2.8 Foam formation and foam stability assay

A slightly modified version of the procedure outlined by Naghdi et al., (2023) was used to determine the foaming capacity and stability of the hydrolysed collagen peptides. The dried powder of CLG-STD-II, CLG-DI-24h, CLG-AC-24h, and CLG-ACP-24h was dissolved in DI. The samples were prepared to 5, 10, and 20 mg/mL for 20 mL. The 20 mL of sample solution was investigated, and the pH value was then placed into the 50 mL cylinder. The initial volume (V_i) was recorded. The homogenizer probe was positioned into a cylinder and localized at a height of V_i. The homogenizer was turned on to produce the foaming for 1 min. The volume after homogenization was read and recorded as V_1. The reaction was allowed to stand at room temperature for 30 min, and then the foaming (V_{30}) volume was recorded. Foaming and stability were calculated following the equation below:

$$\text{Foam expansion (\%)} = [(V_1-V_i)/V_i] \times 100 \quad (2)$$

$$\text{Foam stability (\%)} = [(V_{30}-V_i)/(V_1-V_i)] \times 100 \quad (3)$$

2.9 Antioxidant activity assay

This study used a 2,2-diphenyl-1-picrylhydrazyl (DPPH) radical scavenging assay to determine the antioxidant potential of collagen and collagen peptides. This experiment was briefly modified from the previously described one by Patathananone et al., (2019). The DPPH powder was dissolved in ethanol to a concentration of 0.2028 mM. This solution was diluted two-fold using DI water. The 190 μL of 0.1014 mM DPPH solution (0.1014 mM DPPH in 50% v/v ethanol) was subjected to wells of the 96-well plate. A 10 μL aliquot of each sample solution (at an initial concentration of 500 μg/mL) was added to the DPPH solution. The plate was incubated at 37°C in the dark for 30 min. The absorbance values were detected at a wavelength of 515 nm using a microplate reader (EZ-Read 2000, Biochrom, United Kingdom). The percentage of antioxidant activity was evaluated following the formula below.

$$\% \text{ Inhibition} = \frac{[Ab_{515\ control} - blank_{control}] - [Ab_{515test} - blank_{test}] \times 100}{[Ab_{515\ control} - blank_{control}]} \quad (4)$$

2.10 Statistical analysis

The dry weight, percentage yield, total protein contents, percentage transmittance (%T), foam formation, and foam stability of the hydrolysate collagen peptides were calculated and are presented as mean ± SD (n = 3). One-way ANOVA was used to evaluate statistical differences among treatments, and Duncan's Multiple Range Test (DMRT) was applied for post hoc comparisons. Values marked with different superscript letters differ significantly ($p < 0.05$).

3. Results

3.1 Dried weight, yield, and total protein contents

The preparation of hydrolysate collagen peptides derived from the bones of *H. wyckioides* is presented in Figure 2 and Table 1. Three extraction approaches were evaluated: (1) chemical (CLG-AC-24h and CLG-AC-48h); (2) biological (CLG-PP-24h and CLG-ACL-24h), and (3) combined chemical–biological (CLG-ACP-24h and CLG-ACP-48h), with deionised water (CLG-DI-24h and CLG-DI-48h) as the control group.

The physical appearance of the products differed depending on the extraction method. CLG-DI-24h and CLG-ACL-24h appeared as viscous, gelatin-like solids, whereas CLG-PP-24h formed a light cream-coloured powder. Both CLG-AC-24h and CLG-ACP-24h appeared as white powders.

After 24 h of incubation, the dry weights of CLG-AC-24h, CLG-PP-24h, CLG-ACL-24h, and CLG-ACP-24h were 5.88 ± 0.07, 5.58 ± 0.14, 5.16 ± 0.03, and 6.14 ± 0.03 g, respectively, with significant differences observed among the treatments ($p < 0.05$). In addition, CLG-DI-24h and CLG-DI-48h showed dry weights of 4.24 ± 0.09 and 4.74 ± 0.06 g, respectively, which were significantly lower than those of the samples prepared by all three other methods at 24 h ($p < 0.05$). However, CLG-AC-48h and CLG-ACP-48h were found to have dry weights of 1.13 ± 0.02 g and 2.09 ± 0.07 g, respectively, which were significantly lower than those of all the conditions mentioned above ($p < 0.05$).

Moreover, CLG-DI-24h, CLG-DI-48h, CLG-AC-24h, CLG-AC-48, CLG-PP-24h, CLG-ACL-24h, CLG-ACP-24h, and CLG-ACP-48h exhibited the percentage yield (% yield) of 68.22 ± 2, 76.15 ± 1.16, 94.48 ± 1.11, 18.22 ± 1.35, 89.76 ± 2.42, 83.01 ± 0.49, 98.77 ± 0.41, and 33.55 ± 0.41%, respectively. Among all treatments, CLG-ACP-24h showed the highest percentage yield (98.77 ± 0.41%) ($p < 0.05$).

However, the total protein content varied markedly among treatments. CLG-ACL-24h (98.43 ± 4.34%) and CLG-PP-24h (84.20 ± 9.72%) exhibited substantially higher protein content than CLG-AC-24h (32.24 ± 0.19%) and CLG-ACP-24h (33.77 ± 0.03%). The control samples (CLG-DI-24h and CLG-DI-48h) showed the lowest values.



Figure 2. The morphology of protein/peptide products extracted by deionised water, acidic reagents, and protease enzymes. (A) CLG-DI-24h, (B) CLG-AC-24h, (C) CLG-ACL-24h, (D) CLG-PP-24h and (E) CLG-ACP-24h. CLG-DI-24h, CLG-AC-24h, CLG-ACL-24h, CLG-PP-24h, and CLG-ACP-24h are the ID name of hydrolysate collagen peptides that was prepared by 6.22 g of the dried powder homogenate bones, incubated in DI water (A), 0.5 M acetic acid (B), 1.0% w/v alcalase (C), 1.0% w/v papain (D), and 1.0% w/v pepsin in 0.5 M acetic acid (E), respectively. All conditions were shaken at 120-160 rpm, 37°C for 24 h, and frozen dry to powder using lyophilization

Table 1. Dry weight of hydrolysate peptides yield and total proteins in each extracted condition

Conditions	Extracted conditions	ID Names	The dry weight of collagen hydrolysate peptides (g)	Yield (%)	Total proteins (%)
Control	(1) DI	CLG-DI-24h	4.24 ± 0.09^{f}	68.22 ± 2.00^{f}	7.00 ± 3.30^{a}
		CLG-DI-48h	4.74 ± 0.06^{e}	76.15 ± 1.16^{e}	9.56 ± 3.98^{a}
Acidic (Chemical)	(2) 0.5 M acetic acid	CLG-AC-24h	5.88 ± 0.07*^{b}	94.48 ± 1.11^{b}	32.24 ± 0.19^{b}
		CLG-AC-48h	1.13 ± 0.02*^{h}	18.22 ± 1.35^{h}	-
Enzymatic (Biological)	(3) 1.0% w/v papain	CLG-PP-24h	5.58 ± 0.14^{c}	89.76 ± 2.42^{c}	84.20 ± 9.72^{c}
	(4) 1.0% w/v alcalase	CLG-ACL-24h	5.16 ± 0.03^{d}	83.01 ± 0.49^{d}	98.43 ± 4.34^{d}
Enzymatic with acidic (Chemical + Biological)	(5) 1.0% w/v pepsin in 0.5 M acetic acid	CLG-ACP-24h	6.14 ± 0.03*^{a}	98.77 ± 0.41^{a}	33.77 ± 0.03^{b}
		CLG-ACP-48h	2.09 ± 0.07*^{g}	33.55 ± 0.41^{g}	-

Note: The dried weight of hydrolysate collagen peptides, percentage yield, and total proteins are represented as mean ± SD. The statistical differences between groups were analysed using one-way ANOVA. The superscript letters (a-h) showed statistically significant differences at $p < 0.05$. CLG-DI-24h, CLG-DI-48h, CLG-AC-24h, CLG-AC-48h, CLG-PP-24h, CLG-ACL-24h, CLG-ACP-24h, and CLG-ACP-48h are the ID names of hydrolysate collagen peptides. The conditions of each ID name were expressed below:

(1) CLG-DI-24h and CLG-DI-48h: Died weight of homogenate bones (6.22 g) were incubated in DI water, shaked 120-160 rpm at 37°C for 24 and 48 h

(2) CLG-AC-24h and CLG-AC-48h: Died weight of homogenate bones were incubated in 0.5 M acetic acid, shaked 120-160 rpm at 37°C for 24 and 48 h

(3) CLG-PP-24h: Died weight of homogenate bones (6.22 g) were incubated in 1.0% w/v papain, shaked 120-160 rpm at 37°C for 24 h

(4) CLG-ACL-24h: Died weight of homogenate bones (6.22 g) were incubated in 1.0% w/v alcalase, shaked 120-160 rpm at 37°C for 24 h

(5) CLG-ACP-24h and CLG-ACP-48h: Died weight of homogenate bones (6.22 g) were incubated in 1.0% w/v pepsin in 0.5 M acetic acid, shaked 120-160 rpm at 37°C for 24 and 48 h

3.2 FTIR spectra of hydrolysate collagen peptides

The FTIR spectra of STD-CLG-II, CLG-DI-24h, CLG-AC-24h, and CLG-ACP-24h are shown in Figure 3A-D. The results showed that the FTIR spectrum of CLG-STD-II (Figure 3A) exhibited bands at 579, 920, 1027, 1242, 1405, 1653, 2924, and 3402 cm^{-1}. The FTIR spectrum of CLG-DI-24h (Figure 3B) presented bands at 727, 1238, 1465, 1655, 1745, 2925, and 3397 cm^{-1}. The FTIR spectrum of CLG-AC-24h (Figure 3C) exhibited bands at 809, 1020, 1416, 1561, 1646, and 3457 cm^{-1}. Similarly, the FTIR spectrum of CLG-ACP-24h (Figure 3D) showed bands at 809, 1020, 1413, 1561, 1643, 1703, and 3433 cm^{-1}. An IR peak at around 3397-3457 cm^{-1} was found in all three prepared samples and matched the band observed in standard collagen type II (STD-CLG-II). The band appearing at 3400–3440 cm^{-1} has been reported as the amide A band, corresponding to N–H stretching vibrations. The amide I band (1640–1655 cm^{-1}), associated with C=O stretching, was present in all samples. The C–H stretching band at 2924–2933 cm^{-1} was clearly observed in STD-CLG-II and CLG-DI-24h but appeared weaker in CLG-AC-24h and CLG-ACP-24h. In addition, the wavenumber range of 1230–1245 cm^{-1}, associated with C–N and N–H bend, was observed in STD-CLG-II and CLG-DI-24h but was absent from CLG-AC-24h and CLG-ACP-24h.

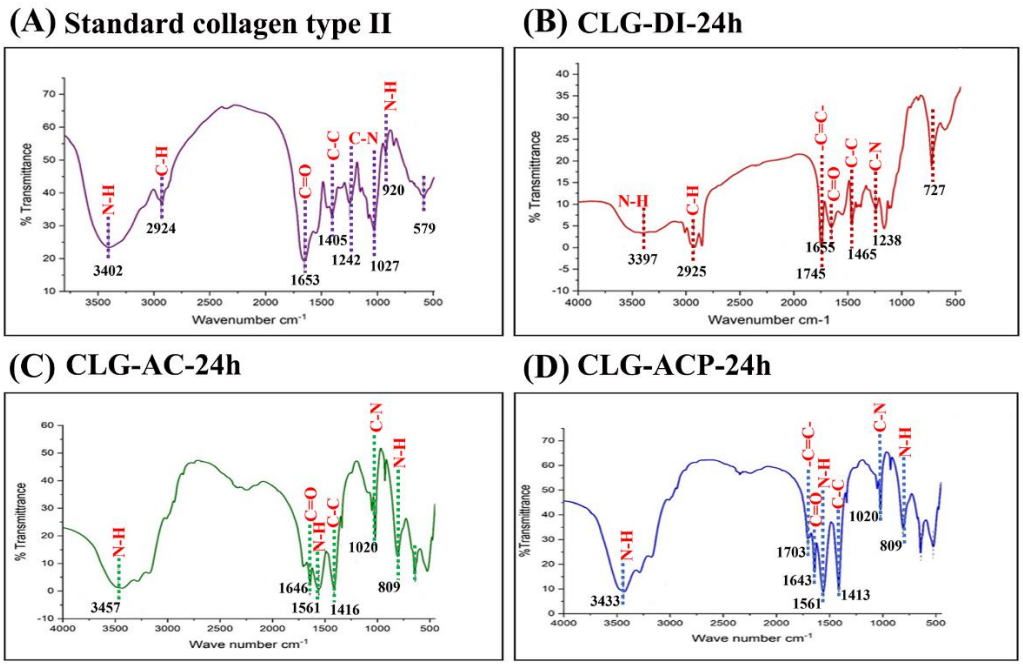


Figure 3. The FTIR spectrum of samples. (A) Standard collagen type II (STD-CLG-II), (B) CLG-DI-24h, (C) CLG-AC-24h, and (D) CLG-ACP-24h. CLG-DI-24h, CLG-AC-24h, and CLG-ACP-24h are the ID names of collagen hydrolysate peptides that were prepared by 6.22 g of the dried powder homogenate bones, incubated in DI water, 0.5 M acetic acid, and 1.0% w/v pepsin, respectively. All conditions were shaken at 120-160 rpm, 37°C for 24 h

3.3 Amino acid composition by thin-layer chromatography

The chromatographic profiles of amino acids separated by thin-layer chromatography (TLC) are presented in Figure 4. In this study, lysine, glycine, hydroxyproline, alanine, proline, isoleucine, and leucine were used as standard amino acids to compare their R_f values with those of the spots found in the hydrolysed collagen peptides prepared from *H. wyckioides* bones. These standard amino acids constitute a major part of the amino acid composition of collagen from various sources and are present in relatively high proportions (Duan et al., 2009). The R_f values of the standard amino acids compared with those of the amino acids in the samples are shown in Table 2. Lysine, glycine, hydroxyproline, alanine, proline, isoleucine, and leucine, exhibited R_f values of 0.22, 0.27, 0.29, 0.38, 0.38, 0.64, and 0.67, respectively. CLG-DI-24h, CLG-AC-24h, and CLG-ACP-24h showed spots with R_f values close to those of several standard amino acids, including glycine, hydroxyproline, proline, alanine, isoleucine, and leucine. However, the analysis in this study was qualitative in nature, providing preliminary data for the subsequent quantitative analysis of amino acid composition using advanced techniques.

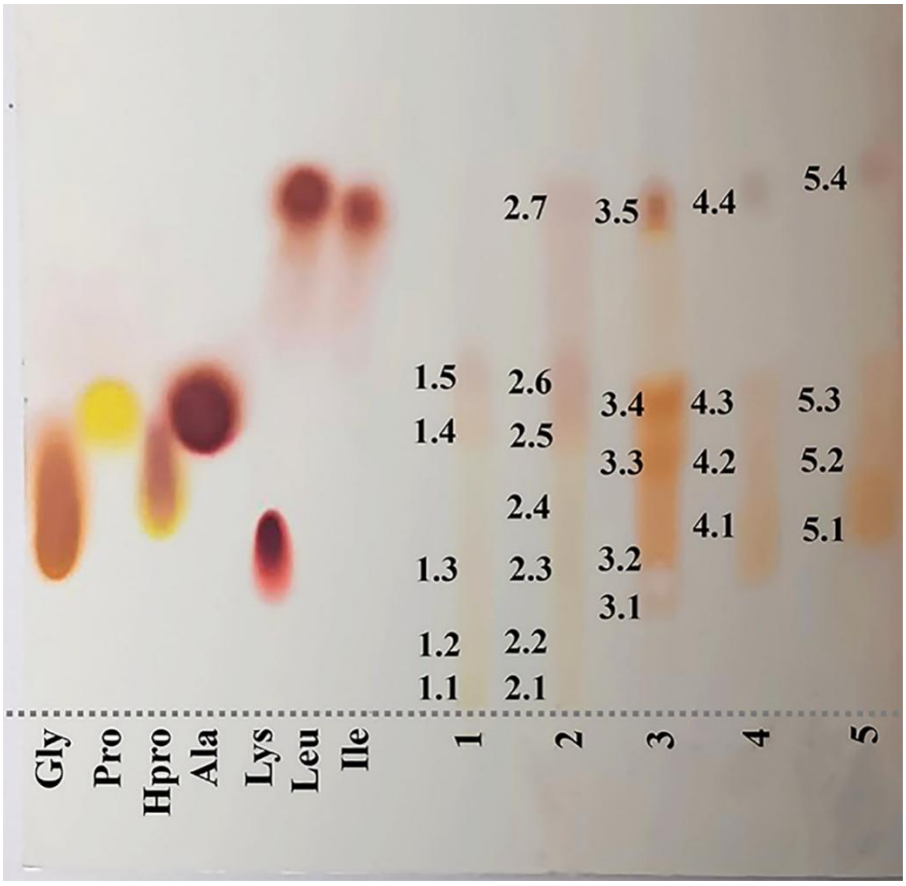


Figure 4. The standard amino acids and samples separated profile on TLC. The standard amino acids are glycine (Gly), proline (Pro), hydroxyproline (Hpro), alanine (Ala), lysine (Lys), leucine (Leu), and Isoleucine (Ile). Lanes 1, 2, 3, 4, and 5 showed the separation profile of acid hydrolysate of standard collagen type I (STD-CLG-I), standard collagen type II (STD-CLG-II), CLG-DI-24h, CLG-AC-24h, and CLG-ACP-24h, respectively. The R_f of each spot number is represented in Table 2

Table 2. Retention factor (R_f) of standard amino acid and the amino acid products from hydrolysate peptides using strong acid reagent

Retention factor (R_f)					
STD amino acids	Collagen Type I	Collagen Type 2	CLG-DI-24h	CLG-AC-24h	CLG-ACP-24h
Lys = 0.22	Spot 1.1 = 0.04	Spot 2.1 = 0.04	Spot 3.1 = 0.15	Spot 4.1 = 0.24	Spot 5.1 = 0.24
Gly = 0.27	Spot 1.2 = 0.10	Spot 2.2 = 0.10	Spot 3.2 = 0.20	Spot 4.2 = 0.32	Spot 5.2 = 0.32
Hpro = 0.29	Spot 1.3 = 0.18	Spot 2.3 = 0.18	Spot 3.3 = 0.32	Spot 4.3 = 0.39	Spot 5.3 = 0.41
Ala = 0.38	Spot 1.4 = 0.37	Spot 2.4 = 0.26	Spot 3.4 = 0.39	Spot 4.4 = 0.64	Spot 5.4 = 0.67
Pro = 0.38	Spot 1.5 = 0.42	Spot 2.5 = 0.29	Spot 3.5 = 0.64		
Ile = 0.64		Spot 2.6 = 0.42			
Leu = 0.67		Spot 2.7 = 0.64			

Note: CLG-DI-24h, CLG-AC-24h, and CLG-ACP-24h are the ID names of hydrolysate collagen peptides that were prepared by 6.22 g of the dried powder homogenate bones, incubated in DI water, 0.5 M acetic acid, and 1.0% w/v pepsin, respectively. All conditions were shaken at 120-160 rpm and 37°C for 24 h.

3.4 Percentage transmittance (%T)

The percentage transmittance data of the hydrolysed collagen peptides and standard collagen type II (STD-CLG-II) in solvents with different pH levels are shown in Figure 5. The results indicated that at 250 μg/mL, STD-CLG-II, CLG-DI-24h, CLG-AC-24h, and CLG-ACP-24h dissolved in deionized (DI) water (pH 7.0) exhibited percentage transmittance (%T) values of 63.90 ± 0.52, 64.37 ± 2.12, 95.97 ± 3.82, and 94.80 ± 0.87, respectively. In addition, when dissolved in an acidic solvent (5% w/v TCA), STD-CLG-II, CLG-DI-24h, CLG-AC-24h, and CLG-ACP-24h exhibited %T values of 58.83 ± 0.81, 82.20 ± 0.72, 97.60 ± 1.42, and 93.63 ± 3.03, respectively. CLG-AC-24h and CLG-ACP-24h exhibited significantly higher %T values than those of STD-CLG-II and CLG-DI-24h ($p < 0.05$). Furthermore, the %T of STD-CLG-II in water was higher than that in the acid solvent, whereas CLG-DI-24h showed a higher %T in the acid solvent than in water; both differences were statistically significant ($p < 0.05$).

3.5 UV–Vis spectrophotometric data

The ultraviolet absorption of the sample solutions was analysed at wavelengths of 190–340 nm to examine the amino acids containing aromatic rings in their side chains, namely phenylalanine, tyrosine, and tryptophan. The results are shown in Figure 6A-F. The results showed that phenylalanine (Figure 6A), tyrosine (Figure 6B), and standard collagen type II (STD-CLG-II) (Figure 6C) had two main absorbance peaks, at 190–230 nm and 260–280 nm. On the other hand, CLG-DI-24h, CLG-AC-24h, and CLG-ACP-24h showed a main absorbance peak at 190–230 nm, with a smaller peak at 260–280 nm. This indicates that the hydrolysed collagen peptides had a low signal from aromatic amino acids.

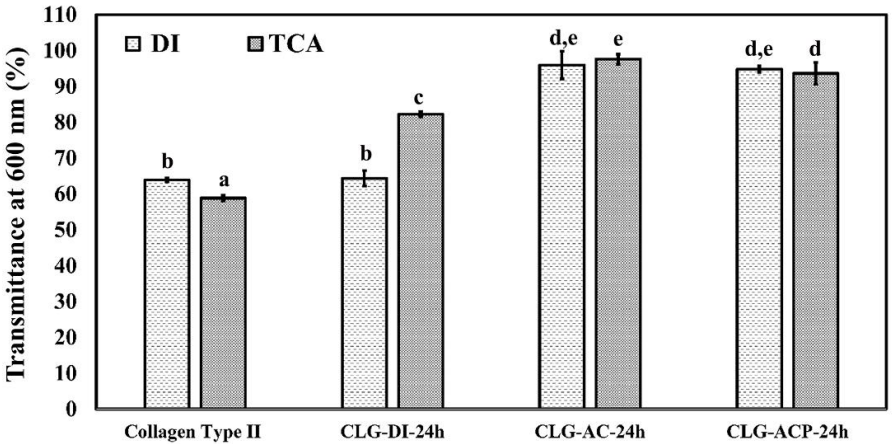


Figure 5. The percentage transmittance (%T) of sample solution that was dissolved in deionised water (DI) and 5.0% w/v trichloroacetic acid (5.0% w/v TCA). The 250 μg/mL was the final concentration of each condition. CLG-DI-24h, CLG-AC-24h, and CLG-ACP-24h are the ID names of collagen hydrolysate peptides that were prepared by 6.22 g of the dried powder homogenate bones, incubated in DI water, 0.5 M acetic acid, and 1.0% w/v pepsin, respectively. All conditions were shaken at 120-160 rpm, 37°C for 24 h. The %T represented as mean ± SD (n = 3). The statistical differences between groups were analysed using one-way ANOVA. The superscript letters (a-e) showed statistically significant differences at $p < 0.05$.

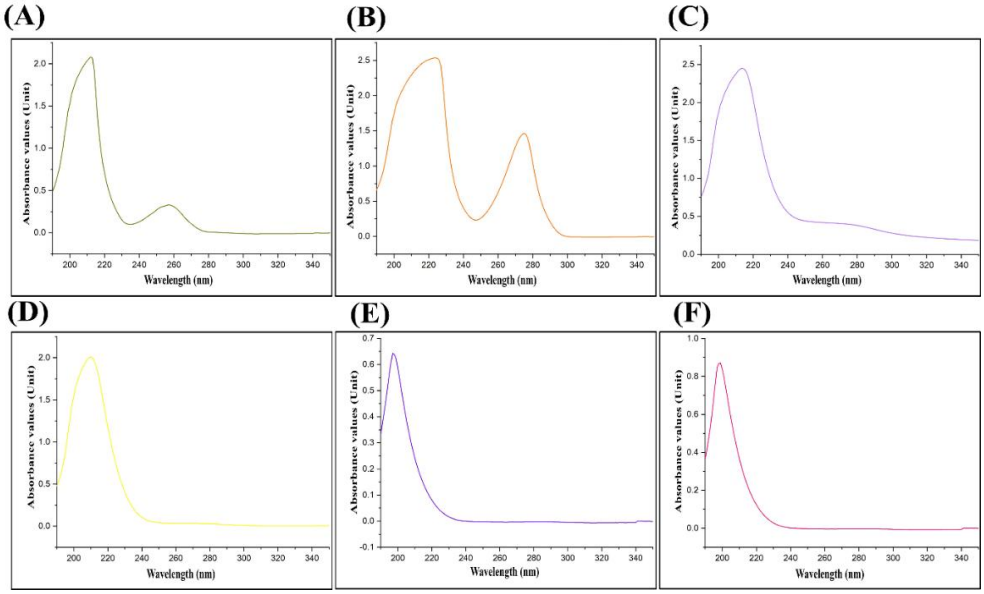


Figure 6. The scanning absorbance values profile of 250 μg/mL sample solutions at UV wavelength 190 - 340 nm. (A) phenylalanine, (B) Tyrosine, (C) Standard collagen type II (STD-CLG-II), (D) CLG-DI-24h, (E) CLG-AC-24h, and (F) CLG-ACP-24h. CLG-DI-24h, CLG-AC-24h, and CLG-ACP-24h are the ID names of hydrolysate collagen peptides that were prepared by 6.22 g of the dried powder homogenate bones, incubated in DI water, 0.5 M acetic acid, and 1.0% w/v pepsin, respectively. All conditions were shaken at 120-160 rpm, 37°C for 24 h.

3.6 Foaming properties

The results of the foam formation test and foam stability are shown in Table 3. The results indicated that STD-CLG-Dipeptides, STD-CLG-II, and CLG-DI-24h showed no foam formation at a concentration of 5.0 mg/mL. In contrast, CLG-AC-24h and CLG-ACP-24h exhibited foam formation of 2.5 ± 0.01% and 12.5 ± 0.02%, respectively, at the same concentration. Foam formation was observed in all samples at concentrations of 10.0 and 20.0 mg/mL. CLG-AC-24h exhibited a foam formation of 20.00 ± 0.03% at 20.0 mg/mL, which was higher than those of all the other tested samples at the same concentration.

STD-CLG-II and CLG-DI-24h exhibited no measurable foam stability at all tested concentrations. At concentrations of 10 and 20 mg/mL, CLG-AC-24h showed foam stability percentages of 75 ± 0.01% and 100 ± 0.01%, respectively. CLG-ACP-24h exhibited foam stability percentages of 40 ± 0.01%, 83 ± 0.05%, and 100 ± 0.01% at 5.0, 10.0, and 20.0 mg/mL, respectively. These results indicated that only CLG-ACP-24h exhibited measurable foam stability at all tested concentrations. CLG-AC-24h and CLG-ACP-24h showed a significant increase in the percentage of foam stability in a concentration-dependent manner.

Table 3 Comparison of foaming and foam stability of hydrolysate collagen peptides in each condition

Samples	Foaming (%)			Foam stability (%)		
	5.0 mg/mL	10.0 mg/mL	20.0 mg/mL	5.0 mg/mL	10.0 mg/mL	20.0 mg/mL
STD-CLG-Dipeptides	ND	2.51 ± 0.01^{a}	12.50 ± 0.01^{a}	ND	ND	60 ± 0.01^{a}
STD-CLG-II	ND	7.50 ± 0.01^{b}	12.51 ± 0.01^{a}	ND	ND	ND
CLG-DI-24h	ND	2.50 ± 0.01^{a}	12.51 ± 0.01^{a}	ND	ND	ND
CLG-AC-24h	2.5 ± 0.01^{a}	12.52 ± 0.01^{c}	20.00 ± 0.03^{c}	ND	75 ± 0.01^{a}	100 ± 0.01^{b}
CLG-ACP-24h	12.5 ± 0.02^{b}	12.51 ± 0.01^{c}	15.00 ± 0.01^{b}	40 ± 0.01^{c}	83 ± 0.05^{b}	100 ± 0.01^{b}

Note: The data were expressed as mean ± SD (n = 3). ND indicates no foam formation, no measurable foam stability, or values below the detection limit. CLG-DI-24h, CLG-AC-24h, and CLG-ACP-24h are the ID names of hydrolysate collagen peptides that were prepared by 6.22 g of the dried powder homogenate bones, incubated in DI water, 0.5 M acetic acid, and 1.0% w/v pepsin, respectively. All conditions were shaken at 120-160 rpm, 37°C for 24 h. The results were analysed using one-way ANOVA followed by Duncan's Multiple Range Test (DMRT). Different superscript letters (a–c) indicate a statistically significant difference ($p < 0.05$).

3.7 Antioxidant activity

The results comparing the DPPH radical-scavenging activity of the standard compounds and the hydrolysed collagen peptides are shown in Table 4. All samples were compared at the same final concentration of 25 µg/mL. L-ascorbic acid, used as a standard antioxidant compound, exhibited the highest DPPH radical-scavenging activity among all tested samples (86.41 ± 0.36%). STD-CLG-Dipeptides, STD-CLG-Tripeptides, STD-CLG-II, CLG-AC-24h and CLG-ACP-24h exhibited DPPH radical-scavenging activities of 33.50 ± 1.16, 28.00 ± 0.94, 44.44 ± 5.26, 2.95 ± 7.68, and 31.03 ± 5.45%, respectively, which were significantly lower than that of L-ascorbic acid ($p < 0.05$). Notably, CLG-AC-24h and CLG-ACP-24h showed DPPH radical-scavenging activities comparable to those of STD-CLG-Dipeptides and STD-CLG-Tripeptides, with no significant differences ($p \geq 0.05$). CLG-AC-48h and CLG-ACP-48h exhibited significantly lower DPPH radical-scavenging activities than those of L-ascorbic acid, STD-CLG-Dipeptides, STD-CLG-Tripeptides, STD-CLG-II, CLG-AC-24h, and CLG-ACP-24h ($p < 0.05$). However, CLG-ACL-24h and CLG-PP-24h showed no detectable DPPH radical-scavenging activity at the tested concentrations.

Table 4. Comparison of DPPH radical-scavenging activity between standard compounds and hydrolysed collagen peptides

Conditions	Samples	DPPH radical scavenging activity (%)
Standard compounds	L-ascorbic acid	86.41± 0.36[d]
	STD-CLG-Dipeptides	33.5 ± 1.16[a]
	STD-CLG-Tripeptides	28 ± 0.94[a]
	STD-CLG-II	44.44 ± 5.26[b]
Control	CLG-DI-24h	19.54 ± 3.52[c]
Acidic (Chemical)	CLG-AC-24h	32.95 ± 7.68[a]
	CLG-AC-48h	0.91 ± 0.02[f]
Enzymatic	CLG-ACL-24h	ND
(Biological)	CLG-PP-24h	ND
Enzymatic with acidic	CLG-ACP-24h	31.03 ± 5.45[a]
(Chemical + Biological)	CLG-ACP-48h	2.82 ± 0.03[e]

Note: ND indicates antioxidant values below the detection limit.
STD-CLG-Dipeptides: Collagen dipeptides of fish skin (Japanese collagen dipeptides).
STD-CLG-Tripeptides: Collagen tripeptides of mammalian skin.
STD-CLG-II: Collagen type II of chicken.
CLG-DI-24h: Homogenate bones were incubated in DI water, shaken at 120-160 rpm at 37°C for 24 h
CLG-AC-24h and CLG-AC-48h: Homogenate bones were incubated in 0.5 M acetic acid, shaken at 120-160 rpm at 37°C for 24 and 48 h
CLG-ACL-24h: Homogenate bones were incubated in 1.0% w/v alcalase, shaken at 120-160 rpm at 37°C for 24 h
CLG-PP-24h: Homogenate bones were incubated in 1.0%w/v papain, shaken at 120-160 rpm at 37°C for 24 h
CLG-ACP-24h and CLG-ACP-48h: Homogenate bones were incubated in 1.0% w/v pepsin in 0.5 M acetic acid, shaken at 120-160 rpm at 37°C for 24 and 48 h.
Different superscript letters (a–f) indicate significant differences among treatment groups ($p < 0.05$).

4. Discussion

Fish processing by-products represent a sustainable and valuable source of bioactive compounds, particularly collagen and its hydrolysates, which have applications in food, pharmaceutical, and biomedical industries (Kaya et al., 2025).

The present study demonstrates that the extraction method significantly influences the yield, composition, and functional properties of collagen hydrolysate peptides derived from *H. wyckioides* bones. Among the tested conditions, the combined chemical–biological method (CLG-ACP-24h) yielded the highest recovery, suggesting a synergistic effect between acid pre-treatment and enzymatic hydrolysis. The total protein content of CLG-AC-24h and CLG-ACP-24h was approximately 32.24 ± 0.19 and 33.77 ± 0.03%, respectively, which were significantly lower than that of CLG-ACL-24h and CLG-PP-24h ($p < 0.05$). One possible explanation for this decrease in total protein content is the dialysis process. In general, the principle of dialysis is to remove small molecules, such as residual salts or acids used during sample preparation, that are smaller than the pore size of the membrane. In this study, CLG-AC-24h and CLG-ACP-24h were subjected to dialysis using a membrane with a molecular weight cut-off (MWCO) of 3.5 kDa. It is possible that low-molecular-weight hydrolysate collagen peptides were also removed during this process. Therefore, the decrease in total protein content may be attributed to the dialysis process described above. One piece of evidence supporting this hypothesis is that CLG-ACL-24h and CLG-PP-24h, which did not undergo dialysis, exhibited a significantly higher percentage of total protein content than those of CLG-AC-24h and CLG-ACP-24h ($p < 0.05$). Similar trends have been reported in other fish collagen studies,

although the magnitude of yield loss may vary depending on enzyme specificity and membrane cut-off thresholds (Jafari et al., 2020; Gaikwad et al., 2024; Kaya et al., 2025). A possible solution is to modify the pore size of the dialysis membrane to achieve a lower molecular weight cut-off (MWCO), which may help reduce yield loss and increase the percentage of total protein content.

FTIR is a technique commonly used in research to analyse the functional groups present in the structure of interested substances, including collagens. According to Li et al., (2004), an unassociated N–H stretching vibration typically appears between 3400 and 3440 cm^{-1}. However, when the N–H group of a peptide participates in hydrogen bonding, this band shifts to a lower wavenumber, generally around 3300 cm^{-1}. In this study, the FTIR spectra of standard collagen type II, CLG-DI-24h, CLG-AC-24h, and CLG-ACP-24h showed a band in the range of 3397–3457 cm^{-1}, corresponding to the position of an unassociated (free) N–H stretching vibration. This result differs from that reported by Duan et al., (2009) for acid-soluble collagen (ASC) prepared from carp (*Cyprinus carpio*) bone, in which the FTIR spectrum showed a band at 3313.85 cm^{-1}, indicating the presence of hydrogen bonding within the collagen structure. In addition, STD-CLG-II and CLG-DI-24h exhibited a C–H stretching band at 2924–2933 cm^{-1}, which was not observed in CLG-AC-24h and CLG-ACP-24h. Muyonga et al., (2004) indicated that this IR band corresponds to the C–H groups of the collagen backbone. The decrease in intensity, or absence, of the C–H stretching band in CLG-AC-24h and CLG-ACP-24h may be associated with the cleavage of bonds within the main collagen chain, resulting in a conformational change into short peptide chains. This, in turn, may account for the band being undetectable or poorly resolved. Similarly, CLG-DI-24h and STD-CLG-II exhibited a band at 1238 and 1242 cm^{-1}, respectively. However, this band was absent in CLG-AC-24h and CLG-ACP-24h. This result is consistent with the report by Kittiphattanabawon et al., (2012), in which high-molecular-weight collagen was shown to exhibit a band at 1230–1245 cm^{-1}. The above findings suggest that CLG-AC-24h and CLG-ACP-24h were converted into hydrolysed collagen peptides through the catalytic mechanism of peptide bond hydrolysis by acid and the enzyme pepsin (Govindharaj et al., 2019; Kaya et al., 2025). Furthermore, the amide I band generally occurs within the range of 1625–1690 cm^{-1}, while the amide II band typically appears within the normal absorption range of 1550–1600 cm^{-1} (Duan et al., 2009). Based on the FTIR spectra, bands were detected at 1653, 1655, 1646, and 1643 cm^{-1} for STD-CLG-II, CLG-DI-24h, CLG-AC-24h, and CLG-ACP-24h, respectively, indicating the position of the amide I band in these samples. More importantly, an amide II band was also detected in CLG-AC-24h and CLG-ACP-24h, both appearing at a similar position of 1561 cm^{-1} (Duan et al., 2009; Jafari et al., 2020).

Fibrillar collagens, such as types I and II, are composed of repeating Gly-X-Y triplets, in which the X and Y positions are frequently occupied by proline and hydroxyproline, respectively (Berillis, 2015). The presence of hydroxyproline is particularly significant as it is unique to collagen and plays a central role in stabilizing the triple helix through hydrogen bonding (He et al., 2019). Analysis of the amino acid composition of collagen from different sources revealed variations in amino acid proportions. The amino acid composition of acid-soluble collagen from calf skin, cod skin, and carp (including carp scale and bone) showed the highest proportion of glycine among all amino acids present. Proline, alanine, and hydroxyproline were detected in decreasing order of proportion, respectively (Duan et al., 2009). In this study, the amino acid groups in the samples were preliminarily examined using paper chromatography. The R_f values of the amino acid spots in collagen type I, collagen type II, CLG-DI-24h, CLG-AC-24h, and CLG-ACP-24h were like those of the standard amino acids glycine, hydroxyproline, proline, alanine, leucine, and isoleucine. This result is consistent with the findings reported by Duan et al., (2009). However,

the amino acid analysis performed in this study was qualitative, serving as preliminary data to guide future quantitative analysis of amino acid composition using more advanced analytical techniques.

The percentage of transmittance of the prepared hydrolysed collagen peptide samples and standard collagen type II (STD-CLG-II) was analysed to assess sample cloudiness in solvents at different pH levels. Generally, collagen is a fibrous protein with a large molecular size and is poorly soluble in water (Nelson & Cox, 2005; Espinales et al., 2023). Consequently, a cloudy appearance is commonly observed when high-molecular-weight collagen is dissolved in water. This effect can pose challenges for product development. The results showed that, in deionized water, CLG-AC-24h and CLG-ACP-24h exhibited percentages of transmittance of 95.97% and 94.80%, respectively, which were higher than those of STD-CLG-II and CLG-DI-24h. A similar trend was observed for the percentage of transmittance of the samples in a solvent with low pH (high acidity). Therefore, acid and enzymatic hydrolysis related to reduced collagen size enhancing the turbidity decrease. This data may support the development of beverages, liquid nutritional, and functional food products in the future.

The foaming capacity and stability of proteins are relevant functional properties for applications in aerated food systems such as ice cream, whipped creams, and meringues (Kittiphattanabawon et al., 2015). The results of this study showed that CLG-AC-24h and CLG-ACP-24h formed foam in a concentration-dependent manner, similar to STD-CLG-Dipeptides and STD-CLG-II. However, the foam formation percentage was relatively low, which might be related to the sample concentration and the molecular size of the protein or peptide (Naghdi et al., 2023). The percentage of foaming stability is related to foam formation and depends on the sample concentration. However, the foam stability of STD-CLG-II was relatively low, which might be due to its solubility behaviour.

UV-Vis spectrophotometric analysis provided additional evidence of the purity of the extracted collagen peptides. The absence of a significant absorbance peak at 260–280 nm in CLG-DI-24h, CLG-AC-24h, and CLG-ACP-24h. The absence of a distinct peak at 260–280 nm suggests a relatively low abundance of aromatic residues or other UV-absorbing components; however, this observation alone does not confirm sample purity.

The DPPH radical scavenging assay revealed that hydrolysate collagen peptides from *H. wyckioides* bones possess moderate antioxidant activity. CLG-AC-24h and CLG-ACP-24h exhibited antioxidant efficacy comparable to standard collagen dipeptides and tripeptides, which are known bioactive fractions. The antioxidant activity of collagen peptides is primarily attributed to specific amino acid sequences—particularly those rich in proline, glycine, and hydroxyproline—which can donate hydrogen atoms to neutralize free radicals (Ngo et al., 2010). However, CLG-ACL-24h and CLG-PP-24h lack antioxidant measurable activity at 500 μg/mL. The antioxidant inactivity of CLG-ACL-24h and CLG-PP-24h might be related to their amino acid sequence and size. Using just one type of protease may result in hydrolysed collagen peptides with a high molecular weight. Thus, only papain or alcalase may still not be suitable for preparing hydrolysate collagen peptide from *H. wyckioides* bone. The large molecular size of the peptides may affect the effectiveness of DPPH radical scavenging. This finding is consistent with the report by Ishak and Sarbon (2018), who demonstrated that hydrolysed peptides with a lower molecular weight exhibited greater antioxidant activity.

Collectively, the findings of this study demonstrate that *H. wyckioides* bone waste is a viable and underutilized source of hydrolysate collagen peptides. The chemical and combined chemical-biological method offers the most favorable balance of yield, foaming stability, and antioxidant activity. The dialysis process can remove salt and small molecules. Thus, this step may decrease the geosmin and 2-MIB, which is critical for consumer acceptance of freshwater fish-derived collagen products. Future research should

focus on: (1) optimization of biological extraction conditions (enzyme concentration, pH, temperature) for improved color and texture; (2) fractionation of active peptides; (3) evaluation bioavailability and safety of hydrolysate collagen peptide in vitro and in vivo and (4) scale-up studies to assess industrial feasibility. The valorization of fish processing by-products, such as bones of *H. wyckioides*, aligns with circular economy principles and contributes to sustainable aquaculture value chains. These data support the classification of the isolated peptides as collagen-derived, reinforcing the suitability of *H. wyckioides* bone waste as a source for collagen peptide production.

5. Conclusions and recommendations

H. wyckioides bones are a collagen source that can be extracted using various conditions (chemical, biological, and combined methods). Among the conditions tested, CLG-ACP-24h produced the highest collagen peptide yield, while CLG-ACL-24h showed the highest total protein content. The FTIR spectrum of the prepared samples showed functional groups like those detected in the standard collagen. CLG-AC-24h and CLG-ACP-24h exhibited foaming properties, and foam stability was concentration-dependent. The percentage of transmittance in water and trifluoroacetic acid was higher than that of collagen type II. The amino acids identified in the sample separated by paper chromatography — glycine, proline, and hydroxyproline, exhibited R_f values close to those of the standard amino acids. Solutions of both samples (CLG-AC-24h and CLG-ACP-24h) exhibited maximum UV absorption at 200–220 nm, similar to that observed for the standard collagen type II solution; however, both samples showed a low UV absorption signal at 280 nm. CLG-AC-24h and CLG-ACP-24h exhibited DPPH radical-scavenging activity that was not significantly different from that of the standard collagen dipeptide solution (CLG-STP-Dipeptides). These findings offer preliminary support for the potential application of fish bone from *H. wyckioides* in the development of collagen-based products.

6. Acknowledgements

This work was supported by Thailand Science, Research, and Innovation Promotion Funding (TSRI).

7. References

Abdo, S., Hou, Y., Al-Dalali, S., Aleryani, H., Shehzads, Q., Asawmahi, O., Shehzad, Q., AL-Fargas, A., Mohammed, B., Lui, X. & Sang, Y. (2023). Modification of marine bioactive peptides: strategy to improve the biological activity, stability, and taste properties. Food and Bioprocess Technology, 17, 1412-1433. https://doi.org/10.1007/s11947-023-03142-w

AOAC, (2023). Nitrogen (Total) in Water: Kjeldahl Method', in Melton Bryant (22nd ed.). Association of Official Analytical Chemists. https://doi.org/10.1093/9780197610145.002.001

Berillis, P. (2015). Marine collagen: extraction and applications. Research Trends in Biochemistry, Molecular Biology and Microbiology, 1, 1-13.

Birk, D. E. & Bruckner, P. (2005). Collagen suprastructures. Topics in Current Chemistry, 247, 185-205. https://doi.org/10.1007/b103823

Chalamaiah, M., Dinesh Kumar, B., Hemalatha, R. & Jythirmayi, T. (2012). Fish protein hydrolysates: Proximate composition, amino acid composition, antioxidant activities and applications: A review. Food Chemistry, 135(4), 3020-3038. https://doi.org/10.1016/j.foodchem.2012.06.100

Chuaychan, S., Benjakul, S. & Kishimura, H. (2015). Characteristics of acid- and pepsin-soluble collagens from scale of seabass (Lates calcarifer). LWT - Food Science and Technology, 63(1), 71-76. https://doi.org/10.1016/j.lwt.2015.03.002

Duan, R., Zhang, J., Du, X., Yao, X. & Konno, K. (2009). Properties of Collagen from skin, scale and bone of Carp (Cyprinus carpio). Food Chemistry, 112(3), 702-706. https://doi.org/10.1016/j.foodchem.2008.06.020

Espinales, C., Romero-Peña, M., Calderón, G., Vergara, K., Ćaceres, P. J. & Castillo, P. (2023). Collagen, protein hydrolysates and chitin from byproducts of fish and shellfish: An overview. Heliyon, 9(4), 1-12. https://doi.org/10.1016/j.heliyon.2023.e14937

Fisheries Development Policy and Planning Division, (2019). Fisheries statistics of Thailand. https://www4.fisheries.go.th/local/file_document/20220324135109_new.pdf.

Fountoulakis, M., & Lahm, H. W. (1998). Hydrolysis and amino acid composition analysis of proteins. Journal of Chromatography A, 826(2), 109–134. https://doi.org/10.1016/S0021-9673(98)00721-3

Friedman, M. (1999). Chemistry, biochemistry, nutrition, and microbiology of lysinoalanine, lanthionine, and histidinoalanine in food and other proteins. Journal of Agricultural and Food Chemistry, 47(4), 1295–1319. https://doi.org/10.1021/jf981000+

Gaikwad, S. & Kim, M. J. (2024). Fish By-Product Collagen Extraction Using Different Methods and Their Application. Marine Drugs, 22(2), 60. https://doi.org/10.3390/md22020060

Govindharaj, M., Roopavath, U. K. & Rath, S. N. (2019). Valorization of discarded Marine eel fish skin for collagen extraction as Ea 3D printable blue biomaterial for tissue engineering. Journal of Cleaner Production, 230, 412-419. https://doi: 10.1016/j.jclepro.2019.05.082

He, L., Mu, C., Shi, J., Zhang, Q., Shi, B. & Lin, W. (2019). Modification of collagen with a natural cross-linker, procyanidin. International Journal of Biological Macromolecules, 48(2), 354-359. https://doi: 10.1016/j.ijbiomac.2010.12.012

Ishak, N. H. & Sarbon, N. M. (2018). A review of protein hydrolysates and bioactive peptides deriving from wastes generated by fish processing. Food Bioprocess Technology, 11(1), 2-16. https://doi.org/10.1007/s11947-017-1940-1

Jafari, H., Lista, A., Siekapen, M. M., Ghaffari-Bohlouli, P., Nie, L., Alimoradi, H. & Shavandi, A. (2020). Fish collagen: extraction, characterisation, and applications for biomaterials engineering. Polymer, 12(10), 1-37. https://doi.org/10.3390/polym12102230

Kadam, D., & Aluko, R. E. (2026). Functional Properties of Enzymatic Food Protein Hydrolysates. Annual review of food science and technology, 17(1), 505–540. https://doi.org/10.1146/annurev-food-053124-013151

Karsdal, M. A. (2023). Biochemistry of collagens, laminins and elastin: Structure, function and biomarkers (3rd ed.). Academic Press.

Kaya, S., Ulusoy, D., Bodur, M. E., Tokmak, O., Yiyit D. S. & Kondolot S. E. (2025). Sustainable Collagen Extraction from Fish Bones: A Green Solution for Waste Management. Hacettepe Journal of Biology and Chemistry, 53(2), 97-106. https://doi.org/10.15671/hjbc.1579144

Kittiphattanabawon, P., Benjakul, S., Sinthusamran, S. & Kishimura, H. (2015). Characteristics of collagen from the skin of clown featherback (Chitala ornata). International Journal of Food Science & Technology, 50(9), 1972–1978. https://doi.org/10.1111/ijfs.12864

Kittiphattanabawon, P., Benjakul, S., Visessanguan, W. & Shahidi, F. (2012). Effect of extraction temperature on functional properties and antioxidative activities of gelatin from shark skin. Food Bioprocess Technology, 5, 2646-2654. https://doi.org/10.1007/s11947-010-0427-0

Kristinsson, H. G., Rasco, B. A. (2000). Fish protein hydrolysate: productivity, biochemical and functional properties. Critical Reviews in Food Science and Nutrition, 40(1), 43-81. https://doi.org/10.1080/10408690091189266

Li, H., Liu, B. L., Gao, L. Z., & Chen, H. L. (2004). Studies on bullfrog skin collagen. Food Chemistry, 84, 65–69. https://doi.org/10.1016/S0308-8146(03)00167-5

Muyonga, J.H., Cole, C. G. B., & Duodu, K.G. (2004). Characterisation of acid soluble collagen from skins of young and adult Nile perch (Lates niloticus). Food Chemistry, 85(1), 81-89. https://doi.org/10.1016/j.foodchem.2003.06.006

Naghdi, S., Lorenzo, J. M., Mirnejad, R., Ahmadvand, M. & Moghaddam, M. M. (2023). Bioactivity evaluation of peptide fractions from bighead carp (Hypophthalmichthys nobilis) using alcalase and hydrolytic enzymes extracted from Oncorhynchus mykiss and their potential to develop the edible coats. Food and Bioprocess Technology, *16*, 1128-1148. https://doi.org/10.1007/s11947-022-02986-y

Naqash, S. Y., & Nazeer, R. A. (2011). Evaluation of bioactive properties of peptide isolated from Exocoetus volitans backbone. International Journal of Food Science and Technology, 46(1), 37–43. https://doi.org/10.1111/j.1365-2621.2010.02443.x

Nelson, D. L. & Cox, M. M. (2005). Lehninger principles of biochemistry (4th ed). Freeman.

Ngo, D. H., Qian, Z. J., Ryu, B., Park, J. W. & Kim, S. K. (2010). In vitro antioxidant activity of a peptide isolated from Nile tilapia (Oreochromis niloticus) scale gelatin in free radical-mediated oxidative systems. Journal of Functional Foods, 2(2), 107-117. https://doi.org/10.1016/j.jff.2010.02.001

Nguyen, T. C., & Thai H. (2024). Review: fish collagen: extraction, characterization and application in wound healing and drug delivery. Vietnam Journal of Science and Technology, 62(1), 1–22. https://doi.org/10.15625/2525-2518/19438

Ogawa, M., Portier, R. J., Moody, M. W., Bell, J., Schexnayder, M. A. & Losso, J. N. (2004). Biochemical properties of bone and scale collagens isolated from the subtropical fish black drum (Pogonia cromis) and sheepshead seabream (Archosargus probatocephalus). Food Chemistry, 88(4), 495-501. https://doi.org/10.1016/j.foodchem.2004.02.006

Orel, B., Giovine, M., & Ilan, M. (2021). On the path to thermo-stable collagen: Culturing the versatile sponge Chondrosia reniformis. Marine Drugs, 19(12), 669. https://doi.org/10.3390/md19120669

Pasupuleti, V. K., & Demaimay, A. (2010). Protein Hydrolysates in Biotechnology. Dordrecht. Springer.

Patathananone, S., Daduang, J., Koraneekij, A. & Li, C. Y. (2019). Tyrosinase inhibitory effect, antioxidant and anticancer activities of bioactive compounds in Ripe Hog Plum (Spondias pinnata) Fruit Extracts. Oriental Journal of Chemistry, 35(3), 916-926. https://doi:10.13005/ojc/350302

Shao, F., Pan, H., Li, P., Ni, L., Xu, Y. & Peng, Z. (2021). Chromosome-level genome assembly of the Asian red-tail catfish (Hemibagrus wyckioides). Frontiers in Genetics, 12,1-7. doi: 10.3389/fgene.2021.747684. https://doi: 10.3389/fgene.2021.747684

Wang, H. (2021). A Review of the Effects of Collagen Treatment in Clinical Studies. Polymers, 13(22), 1-20. https://doi.org/10.3390/polym13223868

Yang, X., Yu, X., Yagoub, A.G.A., Chen, L., Wahia, H., Osae, R., & Zhou, C. (2021). Structure and stability of low molecular weight collagen peptide (prepared from white carp skin) -calcium complex. LWT - Food Science and Technology, 136, 110335. https://doi: 10.1016/j.lwt.2020.110335

Zhang, F., Wang, A., Li, Z., He, S. & Shao, L. (2011). Preparation and characterisation of collagen from freshwater fish scales. Food and Nutrition Sciences, 2(8), 818-823. https://doi.org/10.3390/polym13223868

Zhou, Y. L., Wu, J. J., Gong, G. R., Liu, M., Li, Z., Guo, X. F., Wei, W. Y., Zhang, X. J., Mei, J., Zhou, L., Wang, Z. W. & Gui, J. F. (2023). Barbel regeneration and function divergence in red-tail catfish (*Hemibagrus wyckioides*) based on the chromosome-level genomes and comparative transcriptomes. International Journal of Biological Macromolecules, 232, 1-13. https://doi.org/10.1016/j.ijbiomac.2023.123374

การพัฒนาและประเมินคุณภาพเครื่องดื่มเยลลี่ว่านหางจระเข้ผสมน้ำผลไม้สูตรลดพลังงาน

Development and Quality Evaluation of a Reduced-Energy *Aloe vera* Jelly Beverage Containing Fruit Juice

อมรรัตน์ สีสุกอง[1*] วีรชน ภูหินกอง[1] ฤทธิพันธ์ รุ่งเรือง[1] มณชัย เดชสังกรานนท์[1]
วิสาขา เทียมลม[2] และ ขวัญจิต อิสระสุข[3]

Amornrat Srisukong[1*], Weerachon Phuhinkong[1], Rittipun Rungruang[1], Monchai Dejsungranont[1], Visakha Tiemlom[2] and Khwunjit Itsarasook[3]

[1]คณะวิทยาศาสตร์และเทคโนโลยี มหาวิทยาลัยสวนดุสิต กรุงเทพมหานคร
[2]คณะวิทยาการจัดการ มหาวิทยาลัยสวนดุสิต กรุงเทพมหานคร
[3]คณะวิทยาศาสตร์ มหาวิทยาลัยรามคำแหง กรุงเทพมหานคร
[1]Faculty of Science and Technology, Suan Dusit University, Bangkok
[2]Faculty of Management Sciences, Suan Dusit University, Bangkok
[3]Faculty of Science, Ramkhamhaeng University, Bangkok
Corresponding Author: amornrats@hotmail.com

Received: May 26, 2026 **Revised:** September 21, 2026 **Accepted:** October 20, 2026

บทคัดย่อ

งานวิจัยนี้มีวัตถุประสงค์เพื่อพัฒนาเครื่องดื่มเยลลี่ว่านหางจระเข้ผสมน้ำผลไม้สูตรลดพลังงาน และประเมินสมบัติทางกายภาพและเคมี ความชอบทางประสาทสัมผัส สารออกฤทธิ์ทางชีวภาพ องค์ประกอบทางโภชนาการ และความคงตัวระหว่างการเก็บรักษา โดยศึกษาคุณภาพเบื้องต้นของเจลว่านหางจระเข้สด จากนั้นพัฒนาผลิตภัณฑ์โดยศึกษาผลของอัตราส่วนคาราจีแนนและผงบุก รวมทั้งการใช้ซูคราโลสทดแทนน้ำตาลทรายที่ระดับร้อยละ 0,50 และ 100 ผลการศึกษาพบว่าเจลว่านหางจระเข้สดมีค่า ABTS$^{\bullet+}$ radical scavenging activity ร้อยละ 46.57 ± 3.62 ที่ความเข้มข้นตัวอย่าง 200 mg/mL และค่า FRAP 23.37 ± 0.81 mg TE/100 g fresh weight การศึกษาอัตราส่วนสารก่อเจลพบว่า สูตรที่ใช้คาราจีแนนร้อยละ 0.6 ร่วมกับผงบุกร้อยละ 0.07 ให้คะแนนความชอบด้านรสชาติ เนื้อสัมผัส และความชอบโดยรวมสูงที่สุด เมื่อศึกษาการทดแทนน้ำตาล พบว่าการใช้ซูคราโลสทดแทนน้ำตาลทรายร้อยละ 50 ให้คะแนนความชอบโดยรวมใกล้เคียงสูตรควบคุม พร้อมลดพลังงานของผลิตภัณฑ์จาก 94.52 เป็น 59.72 กิโลแคลอรีต่อ 100 กรัม ผลิตภัณฑ์สูตรที่เหมาะสมมีปริมาณฟีนอลิกรวม 7.18 mg GAE/g sample ปริมาณฟลาโวนอยด์รวม 5.88 mg QE/g sample มีค่า DPPH radical scavenging activity ร้อยละ 34.81 ที่ความเข้มข้นตัวอย่าง 1,000 mg/mL และมีปริมาณอะโลอิน 1.25 mg/kg sample ระหว่างการเก็บรักษาที่อุณหภูมิ 4 ± 2 °C เป็นเวลา 4 สัปดาห์ ผลิตภัณฑ์มีสมบัติทางกายภาพและเคมีค่อนข้างคงตัว ขณะที่จำนวนจุลินทรีย์ทั้งหมด ยีสต์และราโคลิฟอร์ม *Escherichia coli* และ *Staphylococcus aureus* อยู่ในระดับต่ำตลอดการเก็บรักษา โดยสรุปสูตรที่ใช้คาราจีแนนร้อยละ 0.6 ร่วมกับผงบุกร้อยละ 0.07 และทดแทนน้ำตาลทรายด้วยซูคราโลสร้อยละ 50 เป็นสูตรที่เหมาะสมที่สุดในกลุ่มที่ศึกษา โดยสามารถลดพลังงานของผลิตภัณฑ์ ขณะที่ยังคงคะแนนความชอบโดยรวมใกล้เคียงสูตรควบคุม และมีสมบัติทางกายภาพ เคมี และคุณภาพทางจุลชีววิทยาค่อนข้างคงตัวภายใต้การเก็บรักษาแบบแช่เย็นเป็นเวลา 4 สัปดาห์

คำสำคัญ: ว่านหางจระเข้, เครื่องดื่มเยลลี่, ซูคราโลส, การทดแทนน้ำตาลทราย, สารออกฤทธิ์ทางชีวภาพ

Abstract

This study aimed to develop a reduced-energy *Aloe vera* jelly beverage containing fruit juice and to evaluate its physicochemical properties, sensory liking, bioactive compounds, nutritional composition, and storage stability. The effects of carrageenan and konjac powder ratios, together with sucrose

replacement with sucralose at levels of 0, 50, and 100%, were investigated. Fresh *Aloe vera* gel exhibited an ABTS•$^{+}$ radical scavenging activity of 46.57 ± 3.62% at a sample concentration of 200 mg/mL and a FRAP value of 23.37 ± 0.81 mg TE/100 g fresh weight. The formulation containing 0.6% (w/w) carrageenan and 0.07% (w/w) konjac powder achieved the highest scores for taste, texture, and overall liking. Replacing 50% of sucrose with sucralose was considered the most appropriate level among those tested, providing overall liking comparable to the control while reducing the energy content from 94.52 to 59.72 kcal/100 g. The selected formulation contained a total phenolic content of 7.18 mg GAE/g sample, a total flavonoid content of 5.88 mg QE/g sample, DPPH radical scavenging activity of 34.81% at a sample concentration of 1000 mg/mL, and an aloin content of 1.25 mg/kg sample. During refrigerated storage at 4 ± 2 °C for 4 weeks, the product maintained relatively stable physicochemical properties, while total microbial counts, yeasts and molds, coliforms, *Escherichia coli*, and *Staphylococcus aureus* remained at low levels throughout storage. Overall, the formulation containing 0.6% carrageenan and 0.07% konjac powder with 50% sucrose replacement by sucralose was the most appropriate among those tested, reducing the energy content while maintaining overall liking comparable to the control and relatively stable physicochemical and microbiological quality during 4 weeks of refrigerated storage.

Keywords: *Aloe vera*, Jelly beverage, Sucralose, Sucrose replacement, Bioactive compounds

1. Introduction

Aloe vera (*Aloe barbadensis* Mill.) is a succulent plant whose inner gel has been widely utilized in the food, beverage, cosmetic, and pharmaceutical industries. Fresh *Aloe vera* gel consists predominantly of water, accounting for approximately 99% of its composition, but also contains several bioactive constituents, including polysaccharides such as glucomannan and acemannan, phenolic compounds, flavonoids, vitamins, minerals, enzymes, amino acids, and anthraquinone-related compounds (Hamman, 2008; Maan et al., 2018). These constituents have been associated with various biological activities, including antioxidant and anti-inflammatory effects, making *Aloe vera* a potentially useful plant-based ingredient for the development of functional foods and beverages (Sánchez et al., 2020). However, the sensory characteristics of *Aloe vera*, particularly its mild flavor and the possible bitterness associated with residual latex-derived compounds, may limit its palatability when used as a major beverage ingredient. Careful processing is therefore required because the yellow latex located beneath the outer rind contains anthraquinones, particularly aloin, which may adversely affect sensory quality and product safety if not adequately removed (Maan et al., 2018).

The incorporation of fruit juice into *Aloe vera*-based beverages may improve both sensory and physicochemical characteristics. Fruit juice can contribute natural sweetness, characteristic flavor and aroma, color, organic acids, soluble solids, and additional phytochemicals, thereby improving palatability and consumer liking. Previous studies have demonstrated the feasibility of combining *Aloe vera* with fruit-derived ingredients. Mishra and Sangma (2017) developed a ready-to-serve beverage containing *Aloe vera*, sweet lime, amla, and ginger and reported favorable sensory, physicochemical, phytochemical, microbiological, and storage characteristics. Sharma et al. (2022) developed a low-calorie *Aloe vera*-based beverage blended with apricot and aonla juice and showed that fruit blending and partial replacement of sucrose with a high-intensity sweetener could improve sensory quality while reducing energy content. More recently, an *Aloe vera* ready-to-drink beverage containing ginger and lemon was evaluated for sensory, biochemical, microbiological, and refrigerated storage characteristics, further supporting the use of

fruit-derived ingredients in *Aloe vera*-based beverage development. These findings support the incorporation of fruit juice as a practical approach to improving the sensory characteristics and overall quality of *Aloe vera*-based beverages.

Jelly beverages are ready-to-consume products characterized by a soft gel-like texture, and their quality is strongly influenced by the type and concentration of hydrocolloids used. Carrageenan is widely used as a gelling agent in food systems, whereas konjac glucomannan provides water-holding, thickening, and texture-modifying properties. The combination of carrageenan and konjac glucomannan can exhibit synergistic gelation, resulting in improved gel strength, elasticity, and rheological properties (Saha & Bhattacharya, 2010; Li et al., 2024). In addition to texture optimization, reducing sugar and energy content is increasingly important in the development of healthier food products. Sucralose is a high-intensity sweetener approximately 600 times sweeter than sucrose and can therefore be used at substantially lower concentrations. However, sucrose contributes not only sweetness but also flavor balance, mouthfeel, total soluble solids, and textural properties. Consequently, partial or complete replacement of sucrose with sucralose may affect both physicochemical characteristics and consumer liking (Di Monaco et al., 2018).

Although several *Aloe vera*-based beverages containing fruit-derived ingredients have been developed, previous studies have mainly focused on conventional liquid, ready-to-serve, or ready-to-drink beverages. Mishra and Sangma (2017) emphasized formulation, sensory, physicochemical, microbiological, and storage characteristics, whereas Sharma et al. (2022) investigated a reduced-energy fruit-blended *Aloe vera* beverage and sweetener replacement. A recent study by Martinez et al. (2026) integrated *Aloe vera* gel with cashew and acerola juices and evaluated formulation optimization, aloin content, physicochemical properties, and shelf-life behavior, demonstrating increasing interest in more comprehensive evaluation of *Aloe vera*-fruit beverages. Nevertheless, comparatively fewer studies have focused on *Aloe vera*-based jelly beverages containing fruit juice, particularly reduced-energy formulations. Limited information is available on studies integrating gelling-agent formulation, sucrose replacement with sucralose, consumer liking, bioactive compounds, aloin content, nutritional composition, microbiological quality, and refrigerated storage stability within a single *Aloe vera* jelly beverage development framework. Such an integrated evaluation is important because product quality and consumer liking depend simultaneously on gel structure, sweetness, energy content, bioactive composition, residual aloin, microbiological quality, and stability during storage.

In addition to addressing this research gap, the present study aimed to promote the value-added utilization of locally available *Aloe vera*. The fresh *Aloe vera* leaves used in this study were obtained from Homkhajorn Farm, Suan Dusit University, Suphan Buri Campus, Thailand. Developing a value-added food product from this university-grown raw material may provide an additional approach for expanding its utilization beyond fresh plant material. Therefore, this study aimed to develop and evaluate a reduced-energy *Aloe vera* jelly beverage containing fruit juice. The effects of carrageenan–konjac glucomannan formulation and sucrose replacement with sucralose were investigated, followed by evaluation of physicochemical properties, consumer liking, bioactive compounds, aloin content, nutritional composition, microbiological quality, and refrigerated storage stability to identify the optimal formulation among those tested.

2. Materials and methods

2.1 Raw materials and chemicals

Fresh Aloe vera leaves (*Aloe barbadensis* Mill.) were obtained from Homkhajorn Farm, Suan Dusit University, Suphan Buri Campus, Suphan Buri, Thailand. Other ingredients used for product preparation included food-grade carrageenan, konjac powder, fruit juice concentrate, sucrose, citric acid, and malic acid.

Analytical chemicals included 2,2-diphenyl-1-picrylhydrazyl (DPPH; ≥90%, Sigma-Aldrich, St. Louis, MO, USA), ethanol (analytical grade, QRec, New Zealand), Folin–Ciocalteu reagent (Fluka, USA), sodium carbonate (Na_2CO_3; Fluka, USA), gallic acid (Fluka, USA), and Trolox (Sigma-Aldrich, USA).

2.2 Quality analysis of *Aloe vera* gel

The *Aloe vera* gel was characterized for its proximate composition, bioactive compound contents, antioxidant activity, and aloin content prior to product development. Prior to analysis, fresh *Aloe vera* leaves were thoroughly washed with clean water, and the outer green rind was carefully removed to minimize contamination of the inner gel with the yellow latex-containing tissues. The inner gel was separated, washed three times with clean water to remove residual latex and surface mucilage, drained, cut into small pieces, and homogenized to obtain a uniform sample for subsequent analyses. Unless otherwise stated, analytical results for fresh *Aloe vera* gel were expressed on a fresh-weight basis.

2.2.1 Determination of chemical composition

The prepared *Aloe vera* gel was analyzed for proximate composition, including moisture, protein, fat, ash, crude fiber, and carbohydrate contents, according to the AOAC International Official Methods of Analysis (2019).

2.2.2 Determination of total phenolic content

Total phenolic content (TPC) was determined using the Folin–Ciocalteu colorimetric method, modified from Maizura et al. (2011). The homogenized *Aloe vera* gel sample was prepared at approximately 1 g/mL. Briefly, 25 µL of the sample was mixed with 125 µL of 10% (v/v) Folin–Ciocalteu reagent and allowed to react for 4 min at room temperature. Subsequently, 100 µL of 5% (w/v) sodium carbonate solution was added, and the mixture was incubated at room temperature for 30 min. Absorbance was measured at 765 nm using a microplate reader (EZ Read 2000, Biochrom Ltd., UK). All measurements were performed in triplicate. Gallic acid (0.01–0.25 mg/mL) was used to construct the calibration curve, and the results were expressed as mg gallic acid equivalents (GAE)/100 g fresh weight.

2.2.3 Determination of total flavonoid content

Total flavonoid content (TFC) was determined using the aluminium chloride colorimetric method, modified from Itsarasook et al. (2021). The *Aloe vera* gel sample solution was prepared at a concentration of 10 mg/mL. Briefly, 25 µL of the sample solution was mixed with 75 µL of 95% (v/v) ethanol, followed by the addition of 10 µL of 10% (w/v) aluminium chloride solution, 10 µL of 1.0 M potassium acetate, and 140 µL of distilled water in a 96-well microplate. The reaction mixture was incubated in the dark at room temperature for 40 min. Absorbance was measured at 415 nm using a microplate reader (EZ Read 2000, Biochrom Ltd., UK). All measurements were performed in triplicate. Total flavonoid content was calculated from a quercetin calibration curve and expressed as mg quercetin equivalents (QE)/100 g fresh weight.

2.2.4 Determination of antioxidant activity by ABTS assay

Antioxidant activity was evaluated using the ABTS radical cation decolorization assay, as modified from Vongsak et al. (2018). The $ABTS^{\bullet+}$ working solution was prepared by mixing 14 mM ABTS solution with 4.9 mM potassium persulfate solution at a ratio of 1:1 (v/v) and incubating the mixture in the

dark at room temperature for 16–20 h. The resulting ABTS•$^{+}$ solution was diluted with ethanol to obtain an absorbance of 0.70 ± 0.02 at 734 nm.

For the assay, 100 µL of the ABTS•$^{+}$ working solution was mixed with 100 µL of the *Aloe vera* gel sample solution at a concentration of 200 mg/mL. The reaction mixture was vortex-mixed and incubated in the dark at room temperature for 6 min. Absorbance was measured at 734 nm using a microplate reader (EZ Read 2000, Biochrom Ltd., UK). All measurements were performed in triplicate.

ABTS•$^{+}$ radical scavenging activity was calculated using the following equation:

ABTS•$^{+}$ radical scavenging activity (%) = [(Acontrol − Asample) / Acontrol] × 100

where *A*sample is the absorbance of the ABTS•$^{+}$ working solution mixed with the sample, and *A*control is the absorbance of the ABTS•$^{+}$ working solution without the sample. The results were expressed as percentage ABTS•$^{+}$ radical scavenging activity at a sample concentration of 200 mg/mL.

2.2.5 Determination of antioxidant activity by FRAP assay

Ferric reducing antioxidant power (FRAP) was determined using the method of Tananuwong and Tewaruth (2010), with minor modifications. The FRAP reagent was freshly prepared by mixing 300 mM acetate buffer (pH 3.6), 20 mM ferric chloride hexahydrate solution, and 10 mM TPTZ solution prepared in 40 mM HCl at a ratio of 10:1:1 (v/v/v). Subsequently, 190 µL of freshly prepared FRAP reagent was mixed with 10 µL of the *Aloe vera* gel sample solution in a 96-well microplate. The reaction mixture was incubated at 37 °C for 30 min. Absorbance was measured at 593 nm using a microplate reader (EZ Read 2000, Biochrom Ltd., UK).

Trolox was used to construct the calibration curve. FRAP values were calculated from the Trolox calibration curve and expressed as mg Trolox equivalents (TE)/100 g fresh weight. All measurements were performed in triplicate.

2.2.6 Determination of aloin content

Aloin content was determined by the Department of Medical Sciences, Ministry of Public Health, Thailand, using an in-house high-performance liquid chromatography (HPLC) method based on the procedure described by Yamamoto et al. (1985). Results were expressed as milligrams per kilogram of sample (mg/kg).

2.3 Development of *Aloe vera* jelly beverage containing fruit juice

2.3.1 Preparation of *Aloe vera* juice

Fresh *Aloe vera* leaves were washed thoroughly with tap water and cut into approximately 2-cm pieces. The outer green rind was carefully removed to prevent contamination of the inner gel with the yellow latex (aloin-containing exudate). The obtained gel was washed three times with clean water to remove residual latex and mucilage. The gel was then drained, cut into small pieces, homogenized using a blender, and filtered through a fine mesh to obtain *Aloe vera* juice for use as an ingredient in jelly beverage production.

2.3.2 Basic formulation of *Aloe vera* jelly beverage

The *Aloe vera* jelly beverage containing fruit juice was prepared using a basic formulation adapted from Phoonphu (2004), with minor modifications. The formulation consisted of *Aloe vera* juice, white grape juice concentrate (24 °Brix), carrageenan, konjac powder, sweetener, citric acid, and malic acid. White grape juice concentrate (24 °Brix) was selected as the fruit juice source.

Dry ingredients (sweetener, carrageenan, and konjac powder) were first blended to ensure uniform dispersion before being added to the heated *Aloe vera* juice. *Aloe vera* juice was heated to 80–85 °C before the dry ingredients were gradually added under continuous stirring. The mixture was

stirred continuously for 5 min until completely dissolved. White grape juice concentrate was subsequently incorporated, and stirring was continued for 2 min. After cooling to 75–80 °C, citric acid and malic acid were incorporated and mixed until completely dissolved. The resulting mixture was filled into screw-cap pouches, sealed, and allowed to gel at room temperature. The jelly beverage was then stored under refrigerated conditions (4 ± 2 °C).

This basic formulation was used as the starting formulation for investigating the effects of gelling agent ratios and sucrose replacement with sucralose on the quality of the *Aloe vera* jelly beverage.

2.3.3 Determination of the appropriate gelling agent ratio

The effects of carrageenan and konjac glucomannan concentrations on the quality of an *Aloe vera* jelly beverage containing fruit juice were investigated. Carrageenan and konjac glucomannan concentrations were varied between 0.6–0.8% (w/w) and 0.07–0.10% (w/w), respectively, based on the total formulation weight. Four formulations were prepared according to a completely randomized design (CRD), while all other ingredients were kept constant. Each formulation was evaluated for its physicochemical and sensory properties.

Each jelly beverage formulation was analyzed for physicochemical properties. Physical properties included color parameters (L*, a*, and b*), which were measured using a colorimeter (CR-400, Konica Minolta, Osaka, Japan). Total soluble solids (TSS) were determined using a hand refractometer and expressed as °Brix. Chemical properties included pH and titratable acidity (expressed as % citric acid), determined according to AOAC Official Methods (2019). All physicochemical analyses were performed in triplicate.

Consumer sensory evaluation was conducted using a 9-point hedonic scale (1 = dislike extremely; 9 = like extremely). Fifty untrained consumers evaluated the products for color, aroma, taste, texture, and overall liking. The formulation with the highest overall liking score was selected for the subsequent sweetener optimization study.

2.3.4 Determination of the appropriate level of sucrose replacement with sucralose

The *Aloe vera* jelly beverage formulation containing the selected gelling-agent ratio from the previous experiment was used to investigate sucrose replacement with sucralose for the development of a reduced-energy jelly beverage. Three levels of sucrose replacement were evaluated: 0% replacement (control), 50% replacement, and 100% replacement. Because sucralose is a high-intensity sweetener, the amount used in each formulation was calculated based on its relative sweetness compared with sucrose to provide an approximately equivalent level of sweetness. In the 50% replacement formulation, half of the sucrose was retained and the sweetness corresponding to the remaining sucrose was provided by sucralose, whereas in the 100% replacement formulation, sucrose was completely removed and sweetness was provided by sucralose. All other ingredients in the formulation were kept constant.

The three jelly beverage formulations were analyzed for physical quality, including L*, a*, and b* color values and total soluble solids. Chemical and nutritional qualities, including pH, titratable acidity, total energy, energy from fat, carbohydrate, total fat, moisture, protein, and ash, were analyzed according to AOAC International (2019) and the laboratory's in-house methods based on Methods of analysis for nutrition labeling (Sullivan & Carpenter, 1993).

Sensory evaluation was conducted using a randomized complete block design (RCBD), with the jelly beverage formulations as treatments and consumers as blocks. Fifty untrained consumers evaluated all formulations using a 9-point hedonic scale (1 = dislike extremely; 9 = like extremely) for color,

aroma, taste, texture, and overall liking. The appropriate formulation was selected based on overall liking and energy content.

2.3.5 Evaluation of quality changes during storage

The selected formulation was packaged in 150-g screw-cap aluminum foil pouches and stored under refrigerated conditions (4 ± 2 °C) for 4 weeks. Sample were collected at week 0 (initial value) and week 4 to evaluate changes in product quality during refrigerated storage.

Quality changes during storage were evaluated by determining physicochemical, bioactive, and microbiological properties. Physicochemical properties included color (L*, a*, b*), total soluble solids (°Brix), pH, and titratable acidity (% citric acid). Bioactive properties included total phenolic content, total flavonoid content, and DPPH radical scavenging activity. Microbiological quality was evaluated by determining total viable count (TVC), yeasts and molds, coliforms, *Escherichia coli*, and *Staphylococcus aureus*, according to the APHA (2015) and AOAC Official Methods (2019).

2.3.6 Quality analysis of the final product

The selected formulation was analyzed for total phenolic content, total flavonoid content, antioxidant activity, aloin content, and nutritional composition.

2.3.6.1 Total phenolic content

Total phenolic content (TPC) of the final jelly beverage was determined according to the method described in Section 2.2.2. The results were expressed as mg gallic acid equivalents (GAE)/g sample.

2.3.6.2 Total flavonoid content

Total flavonoid content (TFC) of the final jelly beverage was determined according to the method described in Section 2.2.3. The results were expressed as mg quercetin equivalents (QE)/g sample.

2.3.6.3 DPPH radical scavenging activity

Antioxidant activity of the final jelly beverage was evaluated using the DPPH radical scavenging assay following the method of Itsarasook et al. (2021), with minor modifications. A 0.2 mM DPPH solution was prepared in ethanol. The jelly beverage samples were extracted with 70% (v/v) ethanol. In a 96-well microplate, 75 µL of the sample extract was mixed with 150 µL of DPPH solution and incubated in the dark at room temperature for 30 min. Absorbance was measured at 515 nm using a microplate reader (EZ Read 2000, Biochrom Ltd., UK). DPPH radical scavenging activity was calculated using the following equation:

$$\%\ \text{DPPH scavenging} = \frac{Abs_{blank} - Abs_{sample}}{Abs_{blank}} \times 100 \quad (1)$$

where Abs_{sample} is the absorbance of the DPPH solution mixed with the sample extract, and $Abs_{control}$ is the absorbance of the DPPH solution without the sample extract.

The results were expressed as percentage DPPH radical scavenging activity at a sample concentration of 1000 mg/mL.

2.3.6.4 Aloin content

Aloin content in the final jelly beverage was determined by the Department of Medical Sciences, Ministry of Public Health, Thailand, using the same in-house HPLC method described in Section 2.2.6. Results were expressed as mg/kg of sample.

2.3.6.5 Nutritional composition

The selected formulation was submitted to Central Laboratory (Thailand) Co., Ltd., Thailand, for nutritional analysis. Energy, energy from fat, total fat, saturated fat, cholesterol, protein, carbohydrate, dietary fiber, sugars, sodium, calcium, iron, ash, and moisture contents were determined according to AOAC standard methods (AOAC International, 2019) and the laboratory's in-house methods based on Methods of Analysis for Nutrition Labeling (Sullivan & Carpenter, 1993).

2.4 Statistical analysis

Physicochemical and chemical data are presented as mean ± standard deviation (SD) of triplicate analyses. Statistical analyses were performed using IBM SPSS Statistics version 23 (IBM Corp., Armonk, NY, USA). Differences among formulations were analyzed using one-way analysis of variance (ANOVA) followed by Duncan's multiple range test. Statistical significance was considered at $p < 0.05$.

Sensory evaluation was conducted using a randomized complete block design (RCBD), with formulations as treatments and consumers as blocks. Sensory liking scores from 50 untrained consumers using a 9-point hedonic scale were analyzed by ANOVA according to the RCBD. Duncan's multiple range test was used for mean comparison when significant differences were detected ($p < 0.05$).

3. Results

The physicochemical properties, bioactive compounds, antioxidant activity, and product development of the reduced-energy Aloe vera jelly beverage containing fruit juice are presented in this section.

3.1 Chemical composition, bioactive compounds, and antioxidant activity of *Aloe vera* gel

The chemical composition, bioactive compounds, and antioxidant activity of fresh *Aloe vera* gel are summarized in Table 1. Moisture was the predominant component of *Aloe vera* gel, accounting for 99.26%, followed by carbohydrate (0.47%), dietary fiber (0.46%), and ash (0.27%). Protein and fat contents were less than 0.10% and 0.01%, respectively. These findings confirm that *Aloe vera* gel is a high-moisture raw material with low levels of macronutrients, consistent with previous reports.

Regarding bioactive compounds, fresh *Aloe vera* gel contained a total phenolic content of 2.9 ± 0.4 mg GAE/100 g fresh weight and a total flavonoid content of 2.24 ± 0.30 mg QE/100 g fresh weight. Because fresh *Aloe vera* gel had a very high moisture content (99.26%), the relatively low values observed on a fresh-weight basis may partly reflect the high proportion of water in the sample. Therefore, comparison with previous studies reporting phenolic or flavonoid contents on a dry-weight basis should be interpreted with caution. Although the measured total flavonoid content appeared numerically similar to the total phenolic content, these values should not be directly compared quantitatively because the Folin–Ciocalteu and aluminium chloride assays are based on different analytical principles and use different calibration standards, namely gallic acid and quercetin, respectively. Thus, the reported values represent method-dependent estimates of phenolic- and flavonoid-related compounds rather than directly comparable absolute concentrations.

Fresh *Aloe vera* gel exhibited an ABTS•+ radical scavenging activity of 46.57 ± 3.62% at a sample concentration of 200 mg/mL and a FRAP value of 23.37 ± 0.81 mg TE/100 g fresh weight. These results indicate that the fresh gel exhibited measurable antioxidant activity under the assay conditions used. The aloin content of the fresh *Aloe vera* gel was 2.50 mg/kg sample.

Table 1. Chemical composition, bioactive compounds, and antioxidant activity of fresh *Aloe vera* gel

Parameter	Content
Carbohydrate (%)	0.47
Protein (%)	<0.10
Fat (%)	<0.01
Ash (%)	0.27
Dietary fiber (%)	0.46
Moisture (%)	99.26
Total phenolic content (mg GAE/100 g fresh weight)	2.90±0.40
Total flavonoid content (mg QE/100 g fresh weight)	2.24±0.30
ABTS radical scavenging activity (%) at 200 mg/mL	46.57±3.62
Ferric reducing antioxidant power (FRAP) (mg TE/100 g fresh weight)	23.37±0.81
Aloin (mg/kg sample)	2.50

Note: The symbol "<" indicates that the value was below the reporting limit of the analytical method

3.2 Development of *Aloe vera* jelly beverage containing fruit juice

3.2.1 Effect of gelling agent ratio on sensory liking of *Aloe vera* jelly beverage containing fruit juice

Gelling agents play an important role in determining the texture and sensory characteristics of jelly beverages. Table 2 summarizes the sensory evaluation scores of *Aloe vera* jelly beverages prepared with different carrageenan and konjac glucomannan ratios.

Table 2. Sensory evaluation scores of *Aloe vera* jelly beverages with different gelling agent ratios

Attribute	Carrageenan 0.6% + Konjac powder 0.07%	Carrageenan 0.6% + Konjac powder 0.10%	Carrageenan 0.8% + Konjac powder 0.07%	Carrageenan 0.8% + Konjac powder 0.10%
Color ^{ns}	7.22 ± 0.61	7.16 ± 0.62	7.01 ± 0.60	7.00 ± 0.45
Aroma ^{ns}	7.26 ± 0.82	7.02 ± 0.86	7.10 ± 0.91	7.00 ± 0.90
Taste	7.36 ± 0.89^{a}	6.97 ± 0.82^{b}	6.84 ± 0.74^{b}	6.77 ± 0.74^{b}
Texture	7.42 ± 0.83^{a}	6.94 ± 0.74^{b}	6.78 ± 0.68^{b}	6.72 ± 0.67^{b}
Overall liking	7.39 ± 0.86^{a}	7.00 ± 0.69^{b}	6.68 ± 0.69^{c}	6.67 ± 0.59^{c}

Note: Different superscript letters within the same row indicate significant differences ($p < 0.05$); ns indicates no significant difference ($p > 0.05$).

The sensory evaluation scores of *Aloe vera* jelly beverages formulated with different concentrations of carrageenan and konjac glucomannan are shown in Table 2. The results showed that the color and aroma liking scores of the four formulations were not significantly different ($p > 0.05$). The color scores ranged from 7.00 to 7.22, while the aroma scores ranged from 7.00 to 7.26. These findings indicate that variations in carrageenan and konjac glucomannan concentrations did not significantly influence sensory liking of color and aroma ($p > 0.05$).

For taste, texture, and overall liking, the formulation containing 0.6% carrageenan and 0.07% konjac glucomannan received the highest scores, with values of 7.36 ± 0.89, 7.42 ± 0.83, and 7.39 ±

0.86, respectively. These scores were significantly higher ($p < 0.05$) than those of the other formulations. Increasing the concentrations of carrageenan and/or konjac glucomannan generally reduced the liking scores for taste, texture, and overall liking. Therefore, the formulation containing 0.6% carrageenan and 0.07% konjac glucomannan was selected as the optimal gelling agent formulation for further development of the *Aloe vera* jelly beverage.

3.2.2 Effect of carrageenan and konjac glucomannan ratios on the physicochemical properties of *Aloe vera* jelly beverage

Table 3 summarizes the physicochemical properties of *Aloe vera* jelly beverages prepared with different carrageenan and konjac glucomannan ratios. No significant differences ($p > 0.05$) were observed in L* and b* values among the four formulations, with values ranging from 31.07 to 31.57 and from 24.16 to 24.32, respectively. These results suggest that the tested gelling agent concentrations had little influence on the lightness and yellowness of the products. This observation is likely attributable to the identical concentrations of *Aloe vera* juice and white grape juice concentrate, which were the primary contributors to product color.

Table 3. Physicochemical properties of *Aloe vera* jelly beverage with different ratios of gelling agents

Attribute	Carrageenan 0.6% + Konjac powder 0.07%	Carrageenan 0.6% + Konjac powder 0.10%	Carrageenan 0.8% + Konjac powder 0.07%	Carrageenan 0.8% + Konjac powder 0.10%
Color value L* ^{ns}	31.57± 0.42	31.45 ±0.23	31.07± 0.65	31.52 ±0.17
a*	4.14 ±0.06^{a}	4.04 ±0.07^{b}	4.07 ±0.07^{ab}	4.01 ±0.08^{b}
b* ^{ns}	24.16± 0.33	24.25 ±0.37	24.32 ±0.27	24.30 ±0.15
pH	3.43 ±0.06^{b}	3.46 ±0.01^{b}	3.51 ±0.01^{a}	3.53± 0.02^{a}
Titratable acidity (%)	0.70 ±0.01^{a}	0.68 ±0.01^{ab}	0.66 ±0.01^{b}	0.66 ±0.01^{b}
Total soluble solids ns (°Brix) ^{ns}	17.05±0.13	16.67±0.45	16.85±0.12	16.72±0.22

Note: Different superscript letters within the same row indicate significant differences ($p \leq 0.05$); ns indicates no significant difference ($p > 0.05$).

The *a** values differed significantly among formulations ($p < 0.05$). However, the magnitude of the difference was small (4.01–4.14), suggesting only a minor effect of gelling agent ratio on product redness. Therefore, the gelling agent ratio exerted only a minor influence on product redness.

The pH values ranged from 3.43 to 3.53, while titratable acidity ranged from 0.66% to 0.70%. As expected, formulations with lower pH exhibited higher titratable acidity because pH and titratable acidity are inversely related. Total soluble solids (TSS) did not differ significantly ($p > 0.05$) among formulations, with values ranging from 16.67 to 17.05 °Brix. This finding is likely attributable to the constant levels of sucrose and white grape juice concentrate across formulations, whereas only the hydrocolloid concentrations were varied.

3.2.3 Effect of sucrose replacement with sucralose on sensory liking of *Aloe vera* jelly beverage containing fruit juice

The sensory liking scores of *Aloe vera* jelly beverages prepared with different levels of sucrose replacement by sucralose are presented in Table 4. The results showed that the color, aroma, and texture liking scores of the three formulations were not significantly different ($p > 0.05$). The color scores ranged from 7.10 to 7.16, aroma scores ranged from 6.92 to 7.08, and texture scores ranged from 7.24 to

7.36. These findings indicate that sucrose replacement with sucralose at levels of 50% and 100% did not significantly affect sensory liking of color, aroma, and texture.

Table 4. Sensory quality of *Aloe vera* jelly beverages with different levels of sucrose replacement with sucralose

Attribute	Control formulation (0% sucrose replacement)	50% sucrose replacement with sucralose	100% sucrose replacement with sucralose
Color ^{ns}	7.16±0.93	7.10±0.86	7.12±0.75
Aroma ^{ns}	7.08±0.60	7.06±0.71	6.92±0.83
Taste	7.28±0.75^{a}	7.14±0.81^{a}	6.76±0.98^{b}
Texture ^{ns}	7.36±1.01	7.32±0.84	7.24±0.94
Overall liking	7.28±0.83^{a}	7.22±0.81^{ab}	6.90±0.84^{b}

Note: Values are expressed as mean ± SD. Different superscript letters within the same row indicate significant differences ($p \leq 0.05$); ns indicates no significant difference ($p > 0.05$).

For taste, no significant difference ($p > 0.05$) was observed between the control formulation and the formulation with 50% sucrose replacement with sucralose, with mean scores of 7.28 ± 0.75 and 7.14 ± 0.81, respectively. However, complete replacement of sucrose with sucralose significantly reduced the taste score to 6.76 ± 0.98 compared with the other two formulations ($p \leq 0.05$). A similar trend was observed for overall liking, with the formulation containing 100% sucrose replacement receiving the lowest score (6.90 ± 0.84). The overall liking score of the control formulation (7.28 ± 0.83) was significantly higher than that of the 100% replacement formulation, whereas the formulation with 50% sucrose replacement (7.22 ± 0.81) did not differ significantly from either formulation ($p > 0.05$).

Therefore, replacing 50% of sucrose with sucralose was considered the most appropriate level among the formulations tested for developing a reduced-energy *Aloe vera* jelly beverage containing fruit juice, as this formulation maintained taste liking and overall liking comparable to those of the control formulation while allowing a substantial reduction in sucrose content.

3.2.4 Effect of sucrose replacement with sucralose on the physicochemical properties and energy content of Aloe vera jelly beverage

Table 5 summarizes the physicochemical properties and energy content of *Aloe vera* jelly beverages formulated with 0%, 50%, and 100% sucrose replacement with sucralose. No significant differences were observed in L* values among the three formulations ($p > 0.05$), with values ranging from 31.23 to 31.78. These findings indicate that sucrose replacement with sucralose did not markedly affect the lightness of the product. In contrast, significant differences were observed in the a* and b* values among the formulations ($p \leq 0.05$). The formulation with 50% sucrose replacement with sucralose exhibited lower a* and b* values than the control and the formulation with 100% sucrose replacement. These differences may be associated with variations in sucrose concentration and soluble solids within the gel system.

Table 5. Physicochemical properties and nutritional composition of *Aloe vera* jelly beverages with different levels of sucrose replacement with sucralose

Parameter	Control formulation (0% sucrose replacement)	50% sucrose replacement with sucralose	100% sucrose replacement with sucralose
Color (L*) ^{ns}	31.23 ± 0.15	31.28 ± 0.49	31.78 ±0.46
a*	4.28 ±0.16^{a}	4.02 ±0.17^{b}	4.33 ±0.09^{a}
b*	24.26± 0.29^{a}	21.65 ±1.06^{b}	24.28 ±0.45^{a}
pH	3.41 ±0.01^{a}	3.39± 0.01^{b}	3.39 ±0.01^{ab}
Titratable acidity ^{ns} (% citric acid)	0.80 ±0.03	0.86± 0.04	0.89 ±0.08
Total soluble solids (°Brix)	15.9± 0.10^{a}	12.5± 0.10^{b}	8.50± 0.10^{c}
Energy (kcal/100 g)	94.52	59.72	26.00
Energy from fat (kcal/100 g)	0	0	0
Carbohydrate (%)	23.47	14.74	6.28
Total fat (%)	<0.01	<0.01	<0.01
Moisture (%)	76.03	84.75	93.13
Protein (%)	0.17	0.19	0.22
Ash (%)	0.34	0.32	0.37

The pH values ranged from 3.39 to 3.41, indicating only minor variation among the formulations. Although statistically significant differences were detected ($p < 0.05$), the magnitude of these differences was very small. Titratable acidity ranged from 0.80% to 0.89% and did not differ significantly among the formulations ($p > 0.05$). This is likely because identical amounts of citric acid and malic acid were added to all formulations, resulting in comparable acidity.

Total soluble solids (TSS) decreased significantly ($p < 0.05$) as the level of sucrose replacement increased. TSS decreased from 15.90 ± 0.10 °Brix in the control formulation to 12.50 ± 0.10 and 8.50 ± 0.10 °Brix in the formulations with 50% and 100% sucrose replacement with sucralose, respectively. The reduction in TSS was expected because sucrose is a major contributor to soluble solids, whereas sucralose is a high-intensity sweetener used in much smaller quantities. In addition to providing sweetness, sucrose contributes to the flavor, texture, and mouthfeel of food products; therefore, its reduction or complete replacement may alter the overall sensory characteristics of the product (Di Monaco et al., 2018). High-intensity sweeteners may also differ from sucrose in sweetness quality and temporal sensory characteristics, which can influence consumer perception and acceptance (Di Monaco et al., 2014). Consequently, the lower TSS together with the complete removal of sucrose may have contributed to the lower taste and overall liking scores observed for the formulation with 100% sucrose replacement.

Regarding energy content, replacing sucrose with sucralose markedly reduced the energy content of the product. The energy content decreased from 94.52 kcal/100 g in the control formulation to 59.72 and 26.00 kcal/100 g in the formulations containing 50% and 100% sucrose replacement, respectively. This reduction was primarily attributable to the decrease in carbohydrate content because sucrose was progressively replaced with the high-intensity sweetener sucralose.

Carbohydrate content decreased from 23.47% in the control formulation to 14.74% and 6.28% in the formulations with 50% and 100% sucrose replacement, respectively. Energy from fat was 0 kcal/100 g, while total fat remained below 0.01% in all formulations.

Moisture content increased progressively with increasing levels of sucrose replacement, from 76.03% in the control formulation to 84.75% and 93.13% in the formulations with 50% and 100% sucrose replacement, respectively. The increase in moisture content corresponded to the reductions in carbohydrate content and total soluble solids, reflecting the replacement of sucrose with a high-intensity sweetener used at substantially lower concentrations. Considering both sensory liking and energy reduction, the formulation with 50% sucrose replacement with sucralose was selected as the most appropriate reduced-energy *Aloe vera* jelly beverage formulation among those tested for further quality evaluation.

3.3 Quality changes during storage

3.3.1 Changes in physicochemical properties and bioactive compounds during storage

The quality changes of the selected reduced-energy *Aloe vera* jelly beverage during refrigerated storage (4 ± 2 °C) are summarized in Table 6.

Table 6. Changes in physicochemical properties and bioactive compounds of *Aloe vera* jelly beverage during refrigerated storage

Parameter	Week 0	Week 4
Color (L*) ^{ns}	31.55±0.27	31.37±0.23
a* ^{ns}	4.02±0.16	4.03±0.12
b* ^{ns}	22.57±0.20	22.81±0.40
pH ^{ns}	3.42±0.03	3.46±0.02
Titratable acidity ^{ns}	0.77±0.03	0.74±0.04
Total soluble solids (°Brix) ^{ns}	16.8±0.10	16.63±0.15
Total phenolic content (mg GAE/g sample) ^{ns}	7.18±1.63	6.86±0.73
Total flavonoid content (mg QE/g sample) ^{ns}	5.88±1.41	5.04±0.99
DPPH radical scavenging activity (%) at 1,000 mg/mL	34.81±0.60^{a}	32.01±0.07^{b}

Note: Values are expressed as mean ± SD. Different superscript letters within the same row indicate significant differences ($p \leq 0.05$); ns indicates no significant difference ($p > 0.05$).

The absence of significant changes in L*, a*, b*, pH, titratable acidity, and total soluble solids suggests that the selected *Aloe vera* jelly beverage maintained relatively stable physicochemical properties during 4 weeks of refrigerated storage. Although total phenolic and total flavonoid contents showed slight decreases during storage, these changes were not statistically significant, indicating that these bioactive components remained relatively stable over the storage period. In contrast, DPPH radical scavenging activity decreased significantly from 34.81 ± 0.60% to 32.01 ± 0.07% ($p < 0.05$). This reduction may be associated with oxidation or reduced activity of antioxidant constituents during storage, even though the measured total phenolic and flavonoid contents remained relatively stable.

3.3.2 Changes in microbiological quality of *Aloe vera* jelly beverage during storage

The microbiological quality of the selected *Aloe vera* jelly beverage during refrigerated storage is summarized in Table 7. Total viable counts and yeast and mold counts remained below 10 CFU/g throughout storage. Coliforms and *Escherichia coli* remained < 3 MPN/g, while *Staphylococcus aureus* remained <10 CFU/g throughout the storage period.

Table 7. Microbiological quality of *Aloe vera* jelly beverage during refrigerated storage

Microbiological parameter	Week 0	Week 4
Total viable count (CFU/g)	<10	<10
Yeast and mold count (CFU/g)	<10	<10
Coliforms (MPN/g)	<3	<3
Escherichia coli (MPN/g)	<3	<3
Staphylococcus aureus (CFU/g)	<10	<10

These findings indicate that the measured microbiological counts remained low throughout refrigerated storage. The observed microbiological stability may be associated with the low pH of the product (approximately 3.4), together with refrigerated storage and the use of screw-cap aluminum foil pouches, which may have helped minimize external contamination and restrict microbial growth. Overall, the selected *Aloe vera* jelly beverage remained microbiologically stable throughout 4 weeks of refrigerated storage at 4 ± 2 °C.

3.4 Quality characteristics of the final *Aloe vera* jelly beverage formulation

The selected reduced-energy *Aloe vera* jelly beverage containing fruit juice was analyzed for its physicochemical, nutritional, and bioactive characteristics. Table 8 summarizes the physicochemical, nutritional, and bioactive characteristics of the selected formulation. The product contained an energy content of 59.72 kcal/100 g. Carbohydrate was the major macronutrient contributing to the energy content, with a content of 14.74 g/100 g, of which sugars accounted for 12.63 g/100 g. Protein was present at a relatively low level of 0.19 g/100 g, while the moisture content was 84.75 g/100 g, consistent with the high water content characteristic of jelly beverages. The product also contained sodium, calcium, and iron at 75.12, 71.23, and 0.39 mg/100 g, respectively.

Regarding bioactive compounds, the final product contained a total phenolic content of 7.18 mg GAE/g sample and a total flavonoid content of 5.88 mg QE/g sample. DPPH radical scavenging activity was 34.81% at a sample concentration of 1000 mg/mL. These findings indicate that the final product contained measurable levels of phenolic- and flavonoid-related compounds and exhibited DPPH radical scavenging activity under the assay conditions used. The total phenolic content of the final formulation was higher than that measured in fresh *Aloe vera* gel. This difference may be attributed, at least in part, to the contribution of other ingredients in the formulation, particularly white grape juice concentrate, which may provide additional phenolic compounds. However, the individual contribution of each ingredient to the total phenolic content was not determined in the present study; therefore, this interpretation should be considered cautiously.

The aloin content determined by high-performance liquid chromatography (HPLC) was 1.25 mg/kg sample, which was lower than that measured in fresh *Aloe vera* gel. The lower aloin content may be associated with several factors, including removal of the outer leaf tissues, washing and separation of the *Aloe vera* gel from latex-containing tissues, and dilution with other ingredients during product formulation. Because these factors were not evaluated independently, their individual contributions to the reduction in aloin content cannot be determined from the present study.

Overall, the selected formulation had a reduced energy content and contained measurable levels of bioactive compounds and antioxidant activity. These findings describe the nutritional and bioactive characteristics of the selected reduced-energy *Aloe vera* jelly beverage formulation under the conditions evaluated in this study.

Table 8. Nutritional composition, bioactive compounds, antioxidant activity, and aloin content of the selected *Aloe vera* jelly beverage formulation

Parameter	Content
Energy (kcal/100 g)	59.72
Energy from fat (kcal/100 g)	0
Total fat (g/100 g)	<0.01
Saturated fat (g/100 g)	Not detected
Cholesterol (mg/100 g)	Not detected
Protein (g/100 g)	0.19
Carbohydrate (g/100 g)	14.74
Dietary fiber (g/100 g)	0.99
Sugars (g/100 g)	12.63
Sodium (mg/100 g)	75.12
Calcium (mg/100 g)	71.23
Iron (mg/100 g)	0.39
Ash (g/100 g)	0.32
Moisture (g/100 g)	84.75
Total phenolic content (mg GAE/g sample)	7.18
Total flavonoid content (mg QE/g sample)	5.88
DPPH radical scavenging activity (%)at 1000 mg/mL	34.81
Aloin (mg/kg sample)	1.25

Note: "Not detected" indicates that the value was below the detection limit of the analytical method.

4. Discussion

The analysis of fresh *Aloe vera* gel showed that moisture was the predominant component, accounting for 99.26%, whereas protein, fat, carbohydrate, ash, and dietary fiber were present at relatively low levels. This finding is consistent with previous reports indicating that *Aloe vera* gel consists primarily of water, accounting for approximately 99% of its composition, while the remaining solids include polysaccharides, vitamins, minerals, organic acids, enzymes, and phenolic compounds (Hamman, 2008; Maan et al., 2018).

The TPC and TFC values were expressed on a fresh-weight basis because fresh *Aloe vera* gel was used for analysis. Given the very high moisture content of the gel (99.26%), direct comparison with studies reporting results on a dry-weight basis should be interpreted with caution. Although the total phenolic content of fresh *Aloe vera* gel was relatively low, the gel exhibited antioxidant activity as determined by the ABTS and FRAP assays, with an ABTS•+ radical scavenging activity of 46.57 ± 3.62% at a sample concentration of 200 mg/mL and a FRAP value of 23.37 ± 0.81 mg TE/100 g fresh weight. These findings suggest that the observed antioxidant activity may not be associated solely with total phenolic compounds but may also reflect contributions from other bioactive constituents, including flavonoids, polysaccharides, vitamins, and other phytochemicals that may act individually or synergistically. Several flavonoids have been reported in *Aloe vera* and related *Aloe* species, including genistein, isovitexin, isorhamnetin, daidzein, vicenin-2, lucenin-2, and orientin, some of which have been associated with antioxidant and anti-

inflammatory activities (Tizazu & Bekele, 2024). This interpretation is consistent with previous reports indicating that *Aloe vera* contains multiple classes of bioactive compounds with potential antioxidant and anti-inflammatory activities (Sánchez et al., 2020). However, because no correlation analysis between individual bioactive compounds and antioxidant activity was performed in the present study, a direct causal relationship cannot be established.

Aloin was detected in fresh *Aloe vera* gel at 2.50 mg/kg sample, indicating the presence of a low measurable level of latex-derived constituents after gel preparation. Aloin is an anthraquinone glycoside associated with the laxative activity of aloe latex and is predominantly located in the yellow latex layer beneath the leaf rind (Boudreau et al., 2017). Its concentration in *Aloe vera* products can be influenced by raw material preparation and processing, particularly the extent of rind removal, separation of the inner gel from latex-containing tissues, and washing. Therefore, careful removal of the outer leaf tissues, separation of the gel from the yellow latex, and thorough washing are important processing steps for minimizing residual aloin in *Aloe vera*-based food products. From a safety perspective, the European Food Safety Authority has raised concerns regarding hydroxyanthracene derivatives, particularly in relation to prolonged or high-level exposure (EFSA Panel on Food Additives and Nutrient Sources Added to Food, 2018). The aloin concentration observed in the present study should therefore be interpreted in the context of differences in raw material preparation and latex-removal procedures among studies. Direct comparison with regulatory limits should also be made cautiously because applicable criteria may vary according to product category and jurisdiction.

The present study demonstrated that the ratio of carrageenan to konjac glucomannan significantly influenced taste, texture, and overall liking of the *Aloe vera* jelly beverage. The formulation containing 0.6% carrageenan and 0.07% konjac glucomannan received the highest liking scores among the formulations tested. This finding may be explained by the complementary functional properties of the two hydrocolloids, whereby carrageenan contributes to gel formation while konjac glucomannan enhances water binding and modifies gel texture. This observation agrees with previous studies reporting that hydrocolloids can improve the rheological and textural properties of food systems and that interactions between konjac glucomannan and **K**-carrageenan can influence gel strength, elasticity, and overall structural characteristics (Saha & Bhattacharya, 2010; Li et al., 2024). The lower texture and overall liking scores observed at higher hydrocolloid concentrations suggest that excessive gel strength may have negatively affected sensory perception, possibly by producing a firmer, denser, or more adhesive gel structure.

The physicochemical analyses of the jelly beverages formulated with different gelling-agent ratios showed no significant differences in L*, b*, or total soluble solids among the formulations. These findings indicate that variation in the levels of carrageenan and konjac glucomannan within the studied range had little effect on product lightness, yellowness, or soluble solids content. These findings are likely attributable to the relatively small quantities of hydrocolloids used and to the fact that the major ingredients contributing to product color and soluble solids were maintained at constant levels across the formulations.

When sucrose was replaced with sucralose, the formulation with 50% sucrose replacement showed taste and overall liking scores comparable to the control formulation. In contrast, complete replacement of sucrose with sucralose significantly reduced the taste score compared with both the control and 50% replacement formulations, while the overall liking score was significantly lower than that of the control formulation. These findings confirm that sucrose contributes not only sweetness but also flavor balance, mouthfeel, and overall sensory quality. This interpretation is consistent with Di Monaco et al. (2018), who reported that sugar contributes to flavor, texture, and several other quality attributes of food products. Sucralose is a high-intensity sweetener with a sweetness approximately 600 times greater than that of

sucrose and is used at very low concentrations because of its high sweetening potency, thereby reducing sugar and energy contents. However, it cannot fully replace the bulking and sensory functions of sucrose in food systems (U.S. Food and Drug Administration [FDA], n.d.).

The results of the present study are consistent with those of Kanpairo (2018), who reported that 50% sucrose replacement with sucralose in torch ginger gummy jelly resulted in an overall liking score that was not significantly different from that of the control formulation. This suggests that partial sucrose replacement may maintain sensory liking more effectively than complete replacement. Therefore, replacing 50% of sucrose with sucralose may represent an effective strategy for reducing the energy content of jelly products while maintaining liking comparable to that of the control formulation.

Regarding the physicochemical properties and energy content, replacing sucrose with sucralose markedly reduced total soluble solids from 15.90 °Brix in the control formulation to 12.50 and 8.50 °Brix in the formulations with 50% and 100% sucrose replacement, respectively. This reduction was primarily associated with the progressive decrease in sucrose and carbohydrate contents, as sucralose provides sweetness at substantially lower concentrations than sucrose. Consequently, the energy content decreased from 94.52 kcal/100 g in the control formulation to 59.72 and 26.00 kcal/100 g in the formulations with 50% and 100% sucrose replacement, respectively. When overall liking was considered together with energy reduction, the formulation with 50% sucrose replacement was considered the most appropriate among the formulations tested, as it achieved a substantial reduction in energy content while maintaining taste and overall liking comparable to the control formulation.

The final product contained an energy content of 59.72 kcal/100 g and measurable levels of bioactive compounds and antioxidant activity, including a total phenolic content of 7.18 mg GAE/g sample, a total flavonoid content of 5.88 mg QE/g sample, DPPH radical scavenging activity of 34.81% at a sample concentration of 1000 mg/mL, and an aloin content of 1.25 mg/kg sample. The higher total phenolic content of the final product compared with fresh *Aloe vera* gel may be attributed, at least in part, to the contribution of other ingredients in the formulation, particularly white grape juice concentrate, which may provide additional phenolic compounds and other antioxidant-related constituents. However, the present study did not determine the individual contribution of each ingredient to the total phenolic content; therefore, this interpretation should be considered cautiously. The lower aloin content of the final product compared with fresh *Aloe vera* gel may be associated with several factors, including removal of the outer leaf tissues, washing and separation of the *Aloe vera* gel from latex-containing tissues, and dilution with other ingredients during product formulation. Because these factors were not evaluated independently, their individual contributions to the reduction in aloin content cannot be determined from the present study.

DPPH radical scavenging activity was also examined during the preliminary evaluation of fresh *Aloe vera* gel; however, the observed activity was very low, and some calculated inhibition values were negative under the tested conditions. Therefore, antioxidant activity of the fresh gel was primarily interpreted using the ABTS and FRAP assays. In contrast, the final jelly beverage and changes in its antioxidant activity during storage were evaluated using the DPPH assay. Differences in assay mechanisms and sample preparation conditions may have influenced the observed responses. Consequently, antioxidant values obtained from the fresh gel and the final product were interpreted separately and were not directly compared quantitatively. Future studies should apply the same antioxidant assay across experimental stages to improve comparability.

During storage, the selected *Aloe vera* jelly beverage formulation maintained relatively stable physicochemical properties under refrigerated conditions at 4 ± 2 °C for 4 weeks. Color values, pH, titratable acidity, and total soluble solids did not change significantly during storage. The observed stability may be

associated with the combined effects of the acidic pH of the product and refrigerated storage. Although the screw-cap aluminum foil pouch may also have helped limit exposure to light, oxygen, and external contamination, its specific protective effect was not independently evaluated in the present study. Total phenolic and total flavonoid contents showed slight decreases after 4 weeks of storage, although these changes were not statistically significant. In contrast, DPPH radical scavenging activity decreased significantly during storage. This finding suggests that changes in antioxidant activity may have occurred even though the measured total phenolic and flavonoid contents remained statistically unchanged. Such differences may reflect changes in specific antioxidant constituents or their reactivity during storage; however, individual antioxidant compounds were not determined in the present study. The product nevertheless retained measurable levels of bioactive compounds and DPPH radical scavenging activity after 4 weeks of refrigerated storage.

Overall, the results demonstrated that the *Aloe vera* jelly beverage containing fruit juice formulated with 0.6% carrageenan, 0.07% konjac powder, and 50% sucrose replacement with sucralose was the most appropriate formulation among those tested. This formulation reduced energy content while maintaining overall liking comparable to the control and showed relatively stable physicochemical properties and low microbiological counts during 4 weeks of refrigerated storage. The product also contained measurable levels of bioactive compounds and antioxidant activity. However, the present study evaluated storage stability for only 4 weeks and employed untrained consumers for sensory evaluation. Further studies should investigate longer storage periods, consumer liking among target populations, changes in individual bioactive compounds and antioxidant stability during storage, and product performance under conditions relevant to industrial-scale production.

5. Conclusions and recommendations

This study developed a reduced-energy *Aloe vera* jelly beverage containing fruit juice. Fresh *Aloe vera* gel contained 99.26% moisture and relatively low levels of energy-providing nutrients. The gel also contained measurable levels of phenolic compounds, flavonoids, and aloin and exhibited antioxidant activity as determined by the ABTS and FRAP assays.

Among the gelling-agent formulations tested, the formulation containing 0.6% carrageenan and 0.07% konjac powder received the highest liking scores for taste, texture, and overall liking and was therefore selected as the base formulation for further development. When sucrose replacement with sucralose was investigated, replacing 50% of sucrose with sucralose was identified as the most appropriate level among those tested because it maintained taste and overall liking comparable to the control formulation while reducing the energy content from 94.52 to 59.72 kcal/100 g.

The final product contained a total phenolic content of 7.18 mg GAE/g sample, a total flavonoid content of 5.88 mg QE/g sample, DPPH radical scavenging activity of 34.81% at a sample concentration of 1000 mg/mL, and an aloin content of 1.25 mg/kg sample. After 4 weeks of refrigerated storage at 4 ± 2 °C, no significant changes were observed in color values, pH, titratable acidity, or total soluble solids. Total phenolic and total flavonoid contents also remained relatively stable, although DPPH radical scavenging activity decreased significantly during storage. Total viable counts and yeast and mold counts remained below 10 CFU/g, coliforms and *Escherichia coli* remained <3 MPN/g, and *Staphylococcus aureus* remained <10 CFU/g throughout the storage period.

Overall, the formulation containing 0.6% carrageenan, 0.07% konjac powder, and 50% sucrose replacement with sucralose was the most appropriate among those tested. It reduced energy content while

maintaining overall liking comparable to the control and showed relatively stable physicochemical properties and low microbiological counts during 4 weeks of refrigerated storage. Further studies should investigate longer storage periods, changes in individual bioactive compounds and antioxidant stability, consumer liking among target populations, and product performance under conditions relevant to commercial-scale production.

6. Acknowledgement

This research was financially supported by the Fundamental Fund of Suan Dusit University, funded by the Science, Research and Innovation Promotion Fund (TSRI).

7. References

AOAC International. (2019). Official methods of analysis of AOAC International (21st ed.). AOAC International.

Boudreau, M. D., Olson, G. R., Tryndyak, V. P., Bryant, M. S., Felton, R. P., & Beland, F. A. (2017). From the cover: Aloin, a component of the *Aloe vera* plant leaf, induces pathological changes and modulates the composition of microbiota in the large intestines of F344/N male rats. Toxicological Sciences, 158(2), 302–318. https://doi.org/10.1093/toxsci/kfx105

Di Monaco, R., Miele, N. A., Cabisidan, E. K., & Cavella, S. (2018). Strategies to reduce sugars in food. Current Opinion in Food Science, 19, 92–97. https://doi.org/10.1016/j.cofs.2018.03.008

Di Monaco, R., Miele, N. A., Volpe, S., Picone, D., & Cavella, S. (2014). Temporal sweetness profile of MNEI and comparison with commercial sweeteners. Journal of Sensory Studies, 29(6), 385–394. https://doi.org/10.1111/joss.12119

EFSA Panel on Food Additives and Nutrient Sources Added to Food (ANS). (2018). Safety of hydroxyanthracene derivatives for use in food. *EFSA* Journal, 16(1), Article e05090. https://doi.org/10.2903/j.efsa.2018.5090

Hamman, J. H. (2008). Composition and applications of *Aloe vera* leaf gel. Molecules, 13(8), 1599–1616. https://doi.org/10.3390/molecules13081599

Itsarasook, K., Prompamorn, P., Tanghiranrat, J., & Panichakul, T. (2021). Investigation of in vitro antioxidant activity and cytotoxicity on human skin fibroblasts of *Pluchea indica* (L.) Less. leaves extract and development to microemulsion for skin cosmetic product. Asian Journal of Pharmaceutical and Clinical Research, 14(6), 86–93. https://doi.org/10.22159/ajpcr.2021.v14i6.39880

Kanpairo, K. (2018). Effect of different sweeteners on the quality of torch ginger (*Etlingera elatior* (Jack) R.M. Smith) gummy jelly. Burapha Science Journal, 23(2), 944–958. https://scijournal.buu.ac.th/index.php/sci/article/view/1992

Li, Y., Li, K., Guo, Y., Liu, Y., Zhao, G., Qiao, D., Jiang, F., & Zhang, B. (2024). Mechanism for the synergistic gelation of konjac glucomannan and **K**-carrageenan. International Journal of Biological Macromolecules, 277, Article 134423. https://doi.org/10.1016/j.ijbiomac.2024.134423

Maan, A. A., Nazir, A., Khan, M. K. I., Ahmad, T., Zia, R., Murid, M., & Abrar, M. (2018). The therapeutic properties and applications of *Aloe vera*: A review. Journal of Herbal Medicine, 12, 1–10. https://doi.org/10.1016/j.hermed.2018.01.002

Maizura, M., Aminah, A., & Wan Aida, W. M. (2011). Total phenolic content and antioxidant activity of kesum (*Polygonum minus*), ginger (*Zingiber officinale*), and turmeric (*Curcuma longa*) extract. International Food Research Journal, 18(2), 529–534.

Mishra, L. K., & Sangma, D. (2017). Quality attributes, phytochemical profile and storage stability studies of functional ready to serve (RTS) drink made from blend of *Aloe vera*, sweet lime, amla and ginger. Journal of Food Science and Technology, 54(3), 761–769. https://doi.org/10.1007/s13197-017-2516-9

Martinez, J. O., Solano, M. G., Barbas, R. A., & Paternina, G. A. (2026). Healthy drink mixtures with tropical fruits, cashew (*Anacardium occidentale*), acerola (*Malpighia emarginata*), and *Aloe vera* (*Aloe barbadensis* Miller). International Journal of Food Science, 2026, Article 2602574. https://doi.org/10.1155/ijfo/2602574

Saha, D., & Bhattacharya, S. (2010). Hydrocolloids as thickening and gelling agents in food: A critical review. Journal of Food Science and Technology, 47(6), 587–597. https://doi.org/10.1007/s13197-010-0162-6

Sánchez, M., González-Burgos, E., Iglesias, I., & Gómez-Serranillos, M. P. (2020). Pharmacological update properties of *Aloe vera* and its major active constituents. Molecules, 25(6), Article 1324. https://doi.org/10.3390/molecules25061324

Sharma, R., Burang, G., Kumar, S., Sharma, Y. P., & Kumar, V. (2022). Optimization of apricot (*Prunus armeniaca* L.) blended *Aloe vera* (*Aloe barbadensis* M.) based low-calorie beverage functionally enriched with aonla juice (*Phyllanthus emblica* L.). Journal of Food Science and Technology, 59(5), 2013–2024. https://doi.org/10.1007/s13197-021-05216-z

Sullivan, D. M., & Carpenter, D. E. (Eds.). (1993). Methods of analysis for nutrition labeling. AOAC International.

Tananuwong, K., & Tewaruth, W. (2010). Extraction and application of antioxidants from black glutinous rice. LWT - Food Science and Technology, 43(3), 476–481. https://doi.org/10.1016/j.lwt.2009.09.014

Tizazu, A., & Bekele, T. (2024). A review on the medicinal applications of flavonoids from aloe species. European Journal of Medicinal Chemistry Reports, 10, Article 100135. https://doi.org/10.1016/j.ejmcr.2024.100135

U.S. Food and Drug Administration. (n.d.). Aspartame and other sweeteners in food. Retrieved September 21, 2026, from https://www.fda.gov/food/food-additives-petitions/aspartame-and-other-sweeteners-food

Vongsak, B., Kongkiatpaiboon, S., Jaisamut, S., & Konsap, K. (2018). Comparison of active constituents, antioxidant capacity, and α-glucosidase inhibition in *Pluchea indica* leaf extracts at different maturity stages. Food Bioscience, 25, 68–73. https://doi.org/10.1016/j.fbio.2018.08.006

Yamamoto, M., Ishikawa, M., Masui, T., Nakazawa, H., & Kabasawa, Y. (1985). Liquid chromatographic determination of barbaloin (aloin) in foods. Journal of the Association of Official Analytical Chemists, 68(3), 493–494. https://doi.org/10.1093/jaoac/68.3.493

FACULTY OF LIBERAL ARTS AND SCIENCES
SISAKET RAJABHAT UNIVERSITY

319 THAI PHANTHA ROAD, PHO SUB-DISTRICT,
MUEANG DISTRICT, SISAKET PROVINCE, THAILAND 33000
TEL.: +66 9 3327 7215, +66 8 1266 3986

